MASSACHUSETTS INSTITUTE OF TECHNOLOGY

APOLLO

GUIDANCE, NAVIGATION AND CONTROL

Approved: Donald C Fraser Date: 1 April 1970
D. C. FRASER, DIR., CONTROL AND FLIGHT DYNAMICS
APOLLO GUIDANCE AND NAVIGATION PROGRAM

Approved: R.H. Larson Date: 4-3-70
R. A. LARSON, LUMINARY PROJECT MANAGER
APOLLO GUIDANCE AND NAVIGATION PROGRAM

Approved: R.H. Battin Date: 4/3/70
R. H. BATTIN, DIRECTOR, MISSION DEVELOPMENT
APOLLO GUIDANCE AND NAVIGATION PROGRAM

Approved: D.G. Hoag Date: 3 Apr 70
D. G. HOAG, DIRECTOR
APOLLO GUIDANCE AND NAVIGATION PROGRAM

Approved: Ralph R. Ragan Date: 3 Apr 70
R. R. RAGAN, DEPUTY DIRECTOR
CHARLES STARK DRAPER LABORATORY

R-567

GUIDANCE SYSTEM OPERATIONS PLAN FOR MANNED LM EARTH ORBITAL AND LUNAR MISSIONS USING PROGRAM LUMINARY 1C (LM131 REV. 1)

SECTION 3 DIGITAL AUTOPILOT (Rev. 4)

MARCH 1970

MIT CHARLES STARK DRAPER LABORATORY

CAMBRIDGE MASSACHUSETTS 02139

ACKNOWLEDGEMENT

This report was prepared under DSR Project 55-23870, sponsored by the Manned Spacecraft Center of the National Aeronautics and Space Administration through Contract NAS 9-4065 with the Massachusetts Institute of Technology.

R-567

GUIDANCE SYSTEM OPERATIONS PLAN FOR MANNED LM EARTH ORBITAL AND LUNAR MISSIONS USING PROGRAM LUMINARY

SECTION 3 DIGITAL AUTOPILOT

Signatures appearing on this page designate approval of this document by NASA/MSC.

Approved: _____ Date: 11/25/68
Thomas F. Gibson
Asst. Chief, Flight Software Branch
Manned Spacecraft Center, NASA

Approved: _____ Date: 11/25/68
James C. Stokes, Jr.
Chief, Flight Software Branch
Manned Spacecraft Center, NASA

Approved: _____ Date: 11/26/68
Lynwood C. Dunseith
Chief, Flight Support Division
Manned Spacecraft Center, NASA

Date: October 1969

REVISION INDEX COVER SHEET

GUIDANCE SYSTEM OPERATIONS PLAN

GSOP #R-567 Title: For Manned LM Earth Orbital and Lunar Missions Using Program LUMINARY

Section #3 Title: Digital Autopilot (Rev. 3)

Date	Rev.			
12/17/68	0	Revision 0 updated Rev. 1 of Section 3 of the SUNDANCE GSOP (R-557) by incorporating the following NASA/MSC approved changes and became the control document for LUMINARY 1 (Rev. 069).		
		PCR No.	Affected Pages	Title of Change
		140	3.2-6,-7,-20,-21,-22 3.4-2,-26,→ 3.4-37 3.6-14,-15,-16,-17	Incorporate uprated manual RCAH mode for the LM DAP
		141	3.5-3 3.6-10,-17	Reduction of LM DPS gimbal-drive actuator switching frequency
		419	3.2-17 3.6-6,-7,-8,-11,-24	Stage-verify discrete
		420	3.2-19	Rearrangement of extended verbs
		476	3.2-10,-11,-12, -21,-22 3.6-11,-12	FINDCDUW - gimbal drive
		539	3.2-17 3.4-19,-26 3.6-11,-17,-21,-24	Provide option to disable the pitch-roll RCS autopilot
		542	3.2-14,-15 3.6-11,-12,-24	Assure rate command/ attitude hold mode during P66 and P67
		551	None; superseded by PCR 618	Rotational hand controller scaling
		613	3.2-17 3.4-38,-41	Automatic 4-jet translation capability in P12, P70, and P71

Date	Rev.			
12/17/68	0	PCR No.	Affected Pages	Title of Change
		618	3.2-16 3.4-27,-28 3.6-2,-24	Make the DAP rate command a nonlinear function of LM hand-controller deflection.
		637	3.6-2	Delete X-axis override inhibit from R60
June 1969	1	Revision 1 incorporated the following NASA/MSC approved changes and became the control document for LUMINARY 1A.		
		PCR No.	Affected Pages	Title of Change
		701	3.5-2,-4,-5	LM/CSM DAP control law modification
		710	3.2-8 3.4-37	Provide a larger RCS pulse width during the minimum impulse control mode when the CSM is attached
		715	3.3-8,-9,-12,-12A, -31 3.4-19,-20,-21,-22, -23,-24,-25,-26, -45 3.6-10	Docked DAP bending stability
		716	3.1-6,-7,-8 3.2-3,-6,-21 3.3-1 3.4-2,-2A,-2B,-2C, -11,-13,-14,-15, -16,-17,-18,-30, -34,-35,-36,-41, -45 3.6-10,-11,-15,-16, -17	Ascent powered flight RCS control
		717	3.6-8	DAP bias acceleration initialization
		718	3.4-3,-4,-8,-9, -45	Light ascent control with jet failure
		763	3.2-12 3.6-21	Delete requirement for manual rate command mode for the CSM-docked configuration during powered flight

Date	Rev.			
August 1969	2	Revision 2 incorporated the following NASA/MSC approved changes and was published as page additions to GSOP Section 3 (Rev. 1). With these pages added, GSOP Section 3 (Rev. 2) became the control document for both LUMINARY 1A and LUMINARY 1B.		
		PCR No.	Affected Pages	Title of Change
		816	3.2-16a 3.4-13a. 3.6-2a, -22a, -23a	Modify R03 to permit astronaut setting of 1° deadband
		841	xa 3.2-19a, -20a, -21a, -22a 3.7-3a, -4a	PGNCS - derived vehicle attitude rates on FDAI error needles
		842	3.4-15a, -16a, -17a	Modification of criteria (in 1/ACCS routine) used to determine DAP phase-plane parabola intercepts
October 1969	3	Revision 3 incorporated NASA/MSC approved changes as authorized by PCN 1023 as well as document improvement changes, and became the control document for LUMINARY 1C (Rev. 130)		
March 1970	4	Revision 4 incorporates the following NASA/MSC approved changes and becomes the control document for LUMINARY 1C (LM131 Rev. 1)		
		PCR No.	Affected Pages	Title of Change
		988	3.2-14; 3.6-7	AUTO P66
		1031*	(See Below)	Section 3 Rev. 4 GSOP Editorial changes.

*Indicates PCN

NOTE: A solid bar, ▌, in the margin indicates a change in specification authorized by the PCR (PCN*) listed at the bottom of the page. A series of dots, ⋮, indicates a document improvement change as authorized by PCN 1031*.

FOREWORD

The Guidance System Operations Plan (GSOP) assoicated with Program LUMINARY 1C comprises the following six sections, which are published as separate volumes of Instrumentation Laboratory Report R-567.

Section	Title
1	Pre-Launch
2	Data Links
3	Digital Autopilot
4	Operational Modes
5	Guidance Equations
6	Control Data

The present volume (Section 3 of the GSOP) serves as a control document, specifying the lunar-module digital autopilot (LM DAP) design that is delivered in Program LUMINARY 1C (Rev. 130). The autopilot design is unchanged from that delivered in Program LUMINARY 1B (Rev. 116). Therefore, as noted on the Revision Index Cover Sheet, this revision of Section 3 of the GSOP incorporates document-improvement changes only; no NASA/MSC-approved changes are involved. Revisions to this document require NASA approval whenever the changes concerned constitute modifications to the LM DAP design.

The principal contributors to the various subsections that comprise this document are noted at the beginning of each subsection. The autopilot designers who contributed to the extensive review of this document that resulted in the document-improvement changes incorporated herein are Richard D. Goss, J. Edward Jones, George R. Kalan, Donald W. Keene, Robert F. Stengel, and Craig C. Work. Assistance in the preparation of this document for publication was provided by Gardner W. Pope of the Jackson & Moreland Division of United Engineers & Constructors Inc.

TABLE OF CONTENTS

for

SECTION 3

TABLE OF CONTENTS (Cont.)

SUBSECTION 3.1

INTRODUCTION TO THE DIGITAL AUTOPILOT

by

Donald W. Keene and William S. Widnall

3.1.1 Control Requirements

The LM digital autopilot (LM DAP) serves as an integral part of the LM primary guidance, navigation, and control system (PGNCS). It provides automatic and manual attitude and translation control and stabilization of the LM spacecraft for both coasting and powered flight. The LM DAP is designed to control the three spacecraft configurations – LM descent, LM ascent, and CSM-docked – that are depicted in Figs. 3.1-1, 3.1-2, and 3.1-3, respectively.

Control forces and moments are provided by means of the reaction control system (RCS), the descent propulsion system (DPS), and the ascent propulsion system (APS). The RCS employs 16 rocket thrusters mounted in clusters of four on outriggers equally spaced around the LM ascent stage. The DPS utilizes a throttleable, gimbaled engine contained within the vehicle descent stage.. The APS utilizes a fixed, constant-thrust engine installed near the centerline of the ascent stage. Automatic and manual attitude and translation control of the spacecraft is accomplished by ON-OFF command signals supplied to the valves of the RCS thrusters. During powered flight, the LM DAP also supplies command signals to the pitch and roll trim gimbals of the descent engine.

To perform its various control tasks, the LM DAP receives and processes a variety of external and internal inputs, as illustrated in Fig. 3.1-4. These inputs include the following quantities:

1. IMU-CDU measurements of the spacecraft attitude, from which the LM DAP also infers attitude rates and attitude accelerations.
2. Hand-controller signals for providing both manual rotational control and manual translational control.
3. Mode-switch discretes for selecting the autopilot control modes.

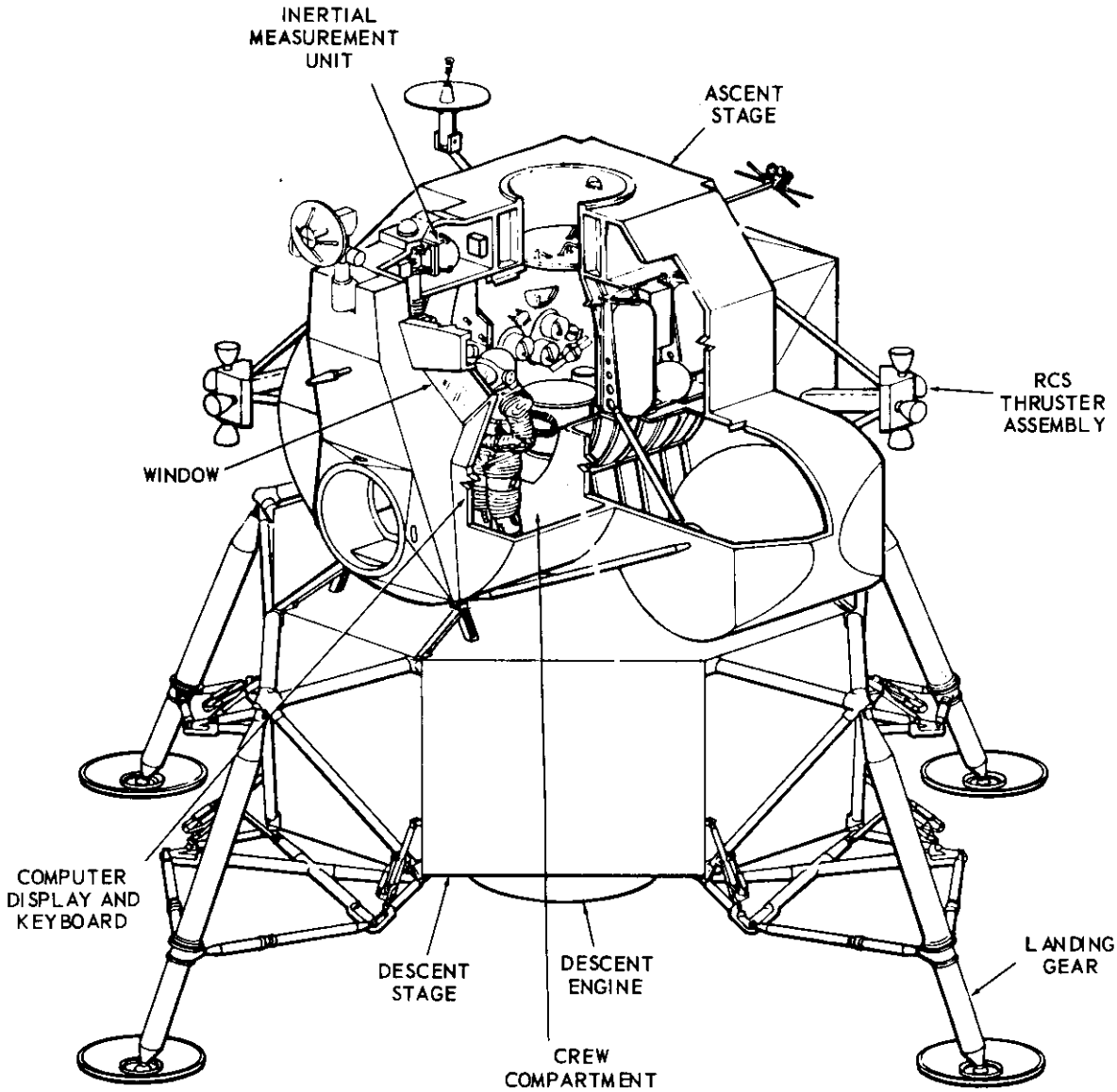

Fig. 3.1-1. The descent configuration of the LM.

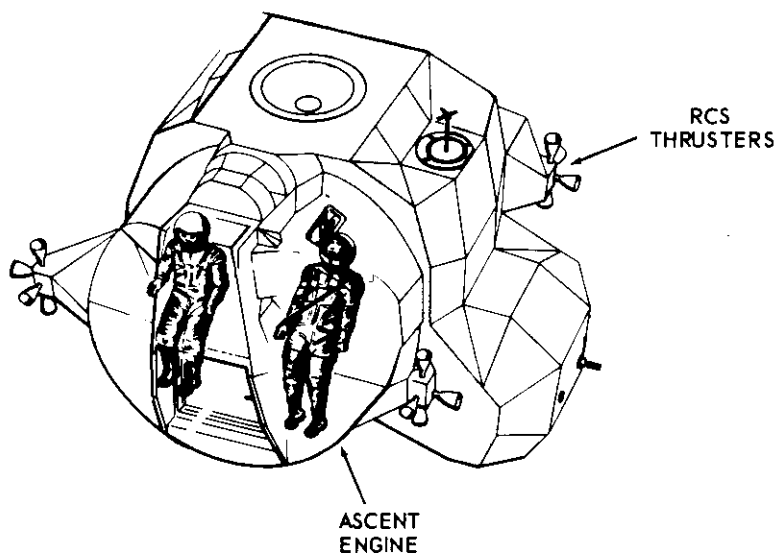

Fig. 3.1-2. The ascent configuration of the LM.

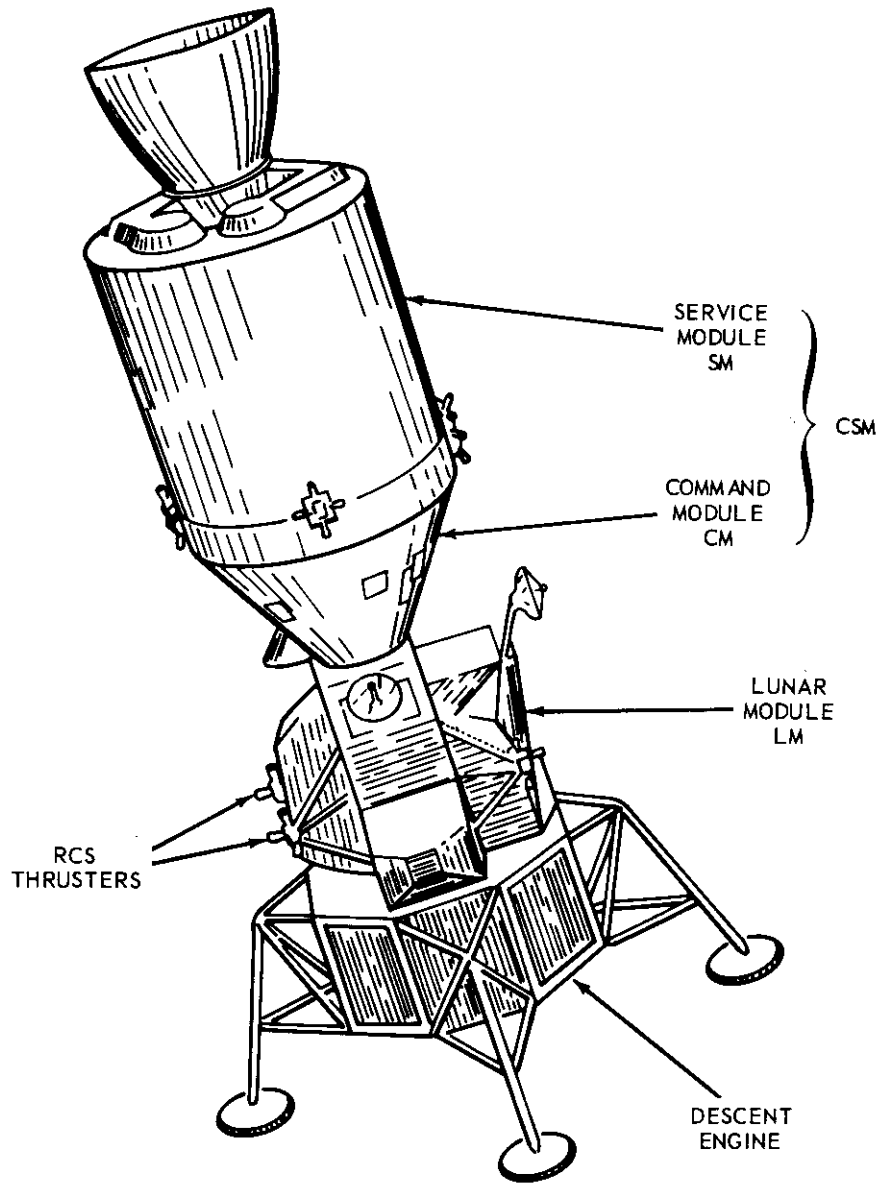

Fig. 3.1-3. The CSM-docked configuration of the LM.

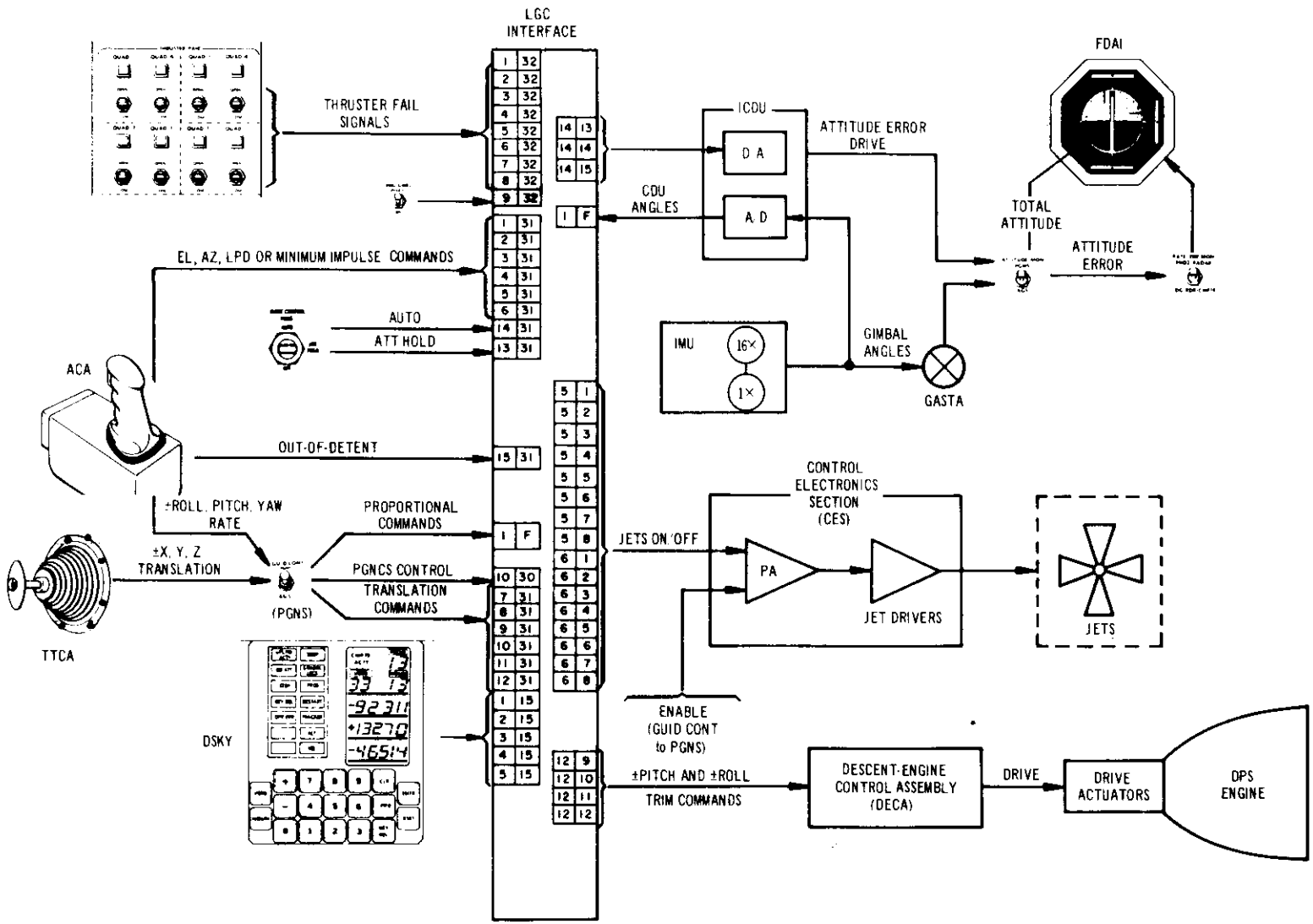

Fig. 3.1-4. LM DAP associated interfaces.

4. Eight thruster-pair disable-switch discretes for modifying the RCS selection logic and optimizing the autopilot performance in the presence of failed jets.

5. Keyboard inputs for specifying autopilot control parameters – such as angular deadbands, maneuver rates, hand-controller functions, and spacecraft mass properties.

6. Internal steering commands for providing automatic attitude control in both coasting and powered flight.

7. An internal discrete for providing automatic ullage prior to main-engine ignition.

8. Internal discretes for switching the autopilot control modes and configurations.

Working in conjunction with the PGNCS guidance equations, the LM DAP provides an integrated guidance, navigation, and control system to perform the complex tasks of the lunar landing mission. Propellant economy, minimization of the number of RCS jet pulses, and operation in the face of detected and undetected jet failures are some of the autopilot design objectives.

Specifications of the requirements for the LM DAP may be found in the following documents:

1. NASA contract NAS 9-4065 (in particular, the MIT Apollo Statement of Work); signed by NASA and MIT.

2. The Contract Technical Specification, PS6000000; signed by NASA and MIT.

3. The Guidance System Operation Plan; written by MIT and approved by NASA.

4. The LM Primary Guidance, Navigation, and Control Subsystem Performance and Interface Specification, LSP-370-3; written by GAEC and approved by NASA.

5. The LM Guidance, Navigation, and Control System Master End Item Specification, PS6015000. (This document includes the interface control documents.) The MEI Specification is signed by NASA and MIT, but as a general rule, no revisions to the ICD's are made without MIT/GAEC joint signatures.

6. Other documents, such as minutes of NASA/MIT LM Autopilot Design Review Meetings.

If there is disagreement between any of these specifications, the conflict is resolved in favor of the higher contractual document (in the order listed above).

3.1.2 LM Axes and Autopilot Control Channels

The major control axes of the LM are shown in Fig. 3.1-5. The descent engine may be gimbaled under LGC control about the pitch (Q) axis and the roll (R) axis. The descent-engine trim-gimbal control laws have been separated into two channels (Q and R). The computation of the proper trim-gimbal drive for each channel is based on independent single-plane control laws.

If the spacecraft center of gravity lies near the geometric center of the 16 RCS jets, then:

a) The eight jets that thrust only in the Y or Z directions produce torques about the P axis only. (These jets are termed the P jets.)

b) Four of the jets that thrust in the ±X direction produce torques about the U axis only. (These jets are termed the U jets.)

c) The other four jets that thrust in the ±X direction produce torques about the V axis only. (These jets are termed the V jets.)

The autopilot design problem associated with the firing of 16 RCS jets is simplified by the use of two logically independent RCS control systems: a P-axis system comprised of the eight P jets and a U- and V-axes system comprised of the 4 U jets and the 4 V jets. In the first system, ±Y and ±Z translational commands are mixed with P rotational requirements. In the second system, ±X translation commands are mixed with rotational commands requiring U and V jets. In each system, rotational requirements are designed to have priority over translation commands. For the purpose of computing U or V rotational torques, the U-V system is further divided into two logically separate channels: a 4-jet U channel and a 4-jet V channel. In the ascent and descent configurations, U-V system control is actually maintained about an auxiliary (nonorthogonal) set of axes called U' and V'. U'-axis control is maintained by firing U jets, and V'-axis control is maintained by firing V jets. The U'-V' system is defined such that U-jet and V-jet firings do not produce coupled accelerations between U' and V' axes. The U' and V' axes are symmetrically skewed from the U and V axes and are constrained by the LM DAP to lie no more than ±15 deg from the U-V system. In the CSM-docked configuration, control is maintained about the U and V axes. Some consequences of the simplified separated-channel design approach are as follows:

- Rotational requirements in one logical system can not take priority over translation commanded in the other system. For example, if a +Z translation command causes a pitch torque larger than the

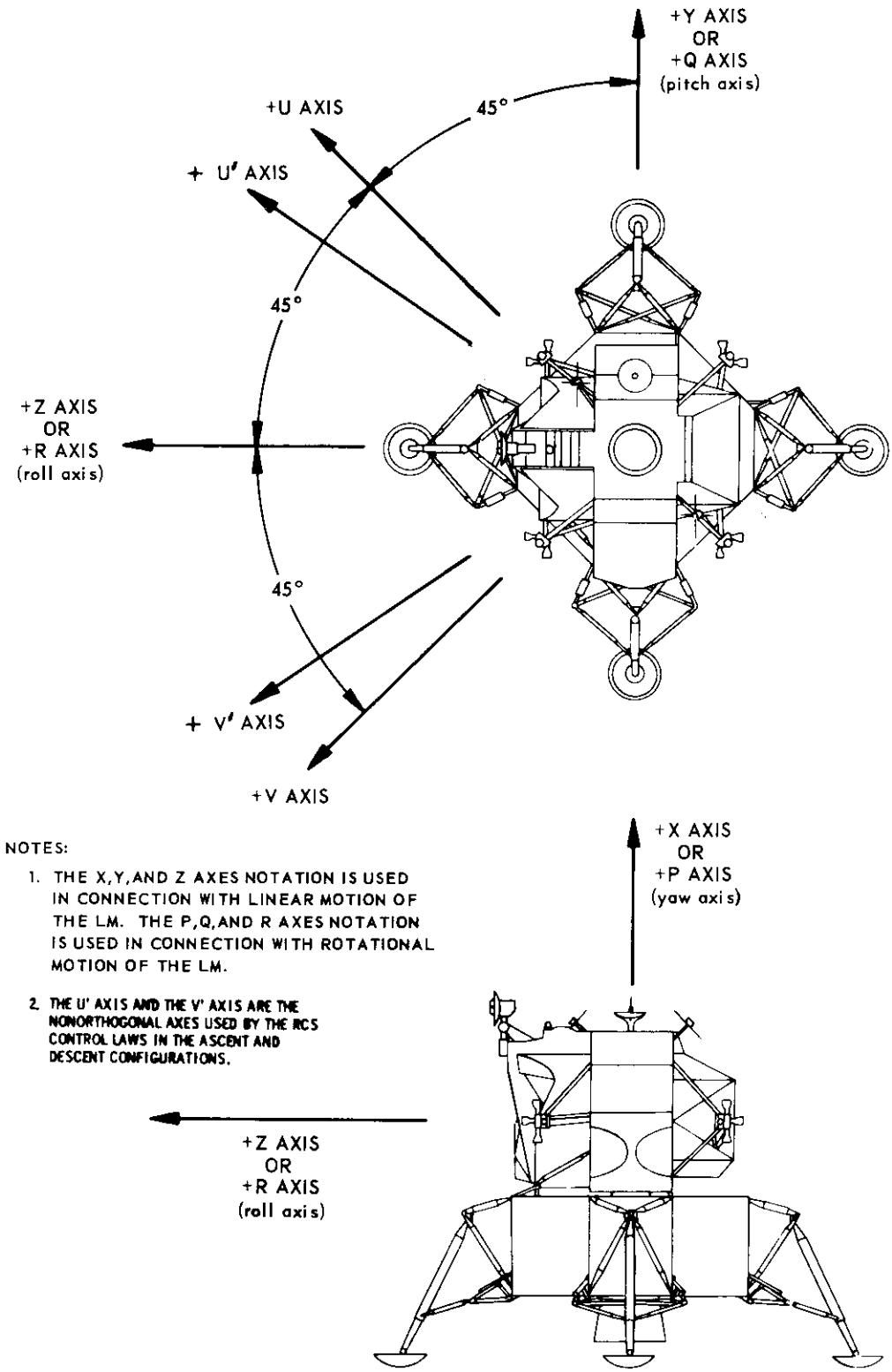

NOTES:

1. THE X,Y,AND Z AXES NOTATION IS USED IN CONNECTION WITH LINEAR MOTION OF THE LM. THE P,Q,AND R AXES NOTATION IS USED IN CONNECTION WITH ROTATIONAL MOTION OF THE LM.
2. THE U' AXIS AND THE V' AXIS ARE THE NONORTHOGONAL AXES USED BY THE RCS CONTROL LAWS IN THE ASCENT AND DESCENT CONFIGURATIONS.

Fig. 3.1-5. The control axes of the LM.

available pitch torque from the U and V jets, then the autopilot will lose pitch attitude control. This condition could occur with the CSM-docked configuration, in which the spacecraft center of gravity lies far away from the geometric center of the 16 RCS jets.

- Torques are generated in what is not necessarily the most efficient manner. For example, in the CSM-docked configuration, the strongest pitch torque can be generated using +Z translation jets in the P-axis system. But the simplified control logic will generate the required pitch impulse using jets in the U-V system.

advantages of the simplified design approach are principally:

- A smaller number of words of fixed memory are required to store the autopilot in the LGC.
- The execution time required for each pass through the autopilot is reduced.

SUBSECTION 3.2

AUTOPILOT CONTROL MODES

by

Donald W. Keene

3.2.1 Introduction

The LM DAP may best be understood by describing its various modes of operation. For the purpose of this discussion, the modes can be divided into two categories: coasting-flight modes and powered-flight modes. In both cases, the LM DAP is capable of performing the following functions:

1. Attitude hold and stabilization.
2. Automatic maneuvering.
3. Manual attitude rate control.
4. Manual X-axis rotational override.
5. Rotational minimum impulse control.
6. Idling.

Manual-translation and automatic-ullage capabilities are provided whenever the LM DAP is not in the idling mode.

To meet the requirements of the two flight regimes and the various space-craft configurations, the LM DAP is altered in accordance with various external and internal control signals and discretes that specify the desired control function. Subsections 3.2.2 and 3.2.3 define the various operating modes of the LM DAP. Subsection 3.2.4 discusses the selection of these modes.

3.2.2 Coasting-Flight Modes

3.2.2.1 Attitude-Hold Mode

In the attitude-hold mode, the LM DAP stabilizes the space-craft attitude about a set of reference CDU angles: θ_{do}, θ_{di}, and θ_{dm} (the desired outer, inner, and middle gimbal angles, respectively). The structure of this mode is shown schematically in Fig. 3.2-1. The LM DAP compares the reference angles with

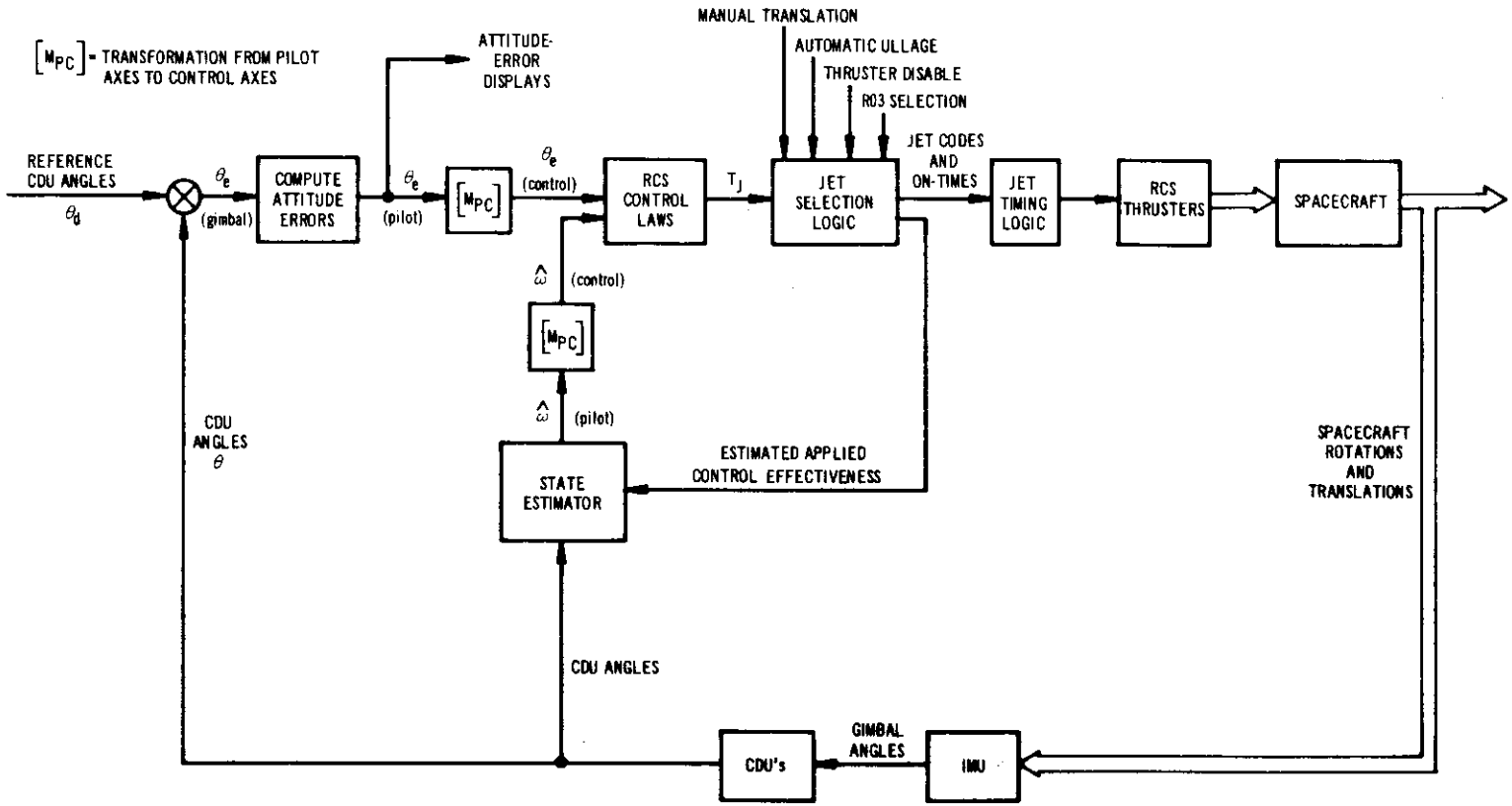

Fig. 3.2-1. Coasting-flight attitude-hold mode.

the CDU angles and computes a set of pilot-axis attitude errors: θ_{eP}, θ_{eQ}, and θ_{eR}. The pilot errors are then resolved into the control axes of the LM DAP as θ_{eP}, $\theta_{eU'}$, and $\theta_{eV'}$ by a nonorthogonal transformation and used as one of two sets of inputs to the RCS control laws. (The RCS control laws are described in Subsection 3.4). The second set of inputs to the RCS control laws consists of a set of estimated spacecraft angular velocities or rates – also resolved into the P, U', and V' axes – which are computed by the state-estimator logic (described in Subsection 3.3). The state-estimator logic infers the spacecraft angular velocities from a combination of CDU measurements and estimates of the applied RCS control effectiveness.

As a function of the attitude errors and attitude-error rates, nonlinear switching logic in the RCS control law (TJETLAW) is employed to generate jet on-times $(TJ)_P$, $(TJ)_U$, and $(TJ)_V$ for each axis. Note that the control about each axis is treated separately and independently. A jet selection logic then combines these rotation commands with the translation commands from the thrust/translation controller assembly (TTCA) or the automatic-ullage discrete and selects the individual jets to be fired. The jet selection logic also incorporates the thruster-disable information and the astronaut options loaded in routine R03 in determining these commands. Vernier timing of the RCS jets is accomplished with the aid of the T6 interrupt structure of the computer. The jet selection logic is described in Subsection 3.4.5.

In the CSM-docked configuration, the LM DAP controls about the orthogonal P, U and V axes using a simplified control law, which is described in Subsection 3.4.3. This law computes on-off rotation commands based upon estimated spacecraft rates and attitude errors. Although vernier jet timing is not employed, the basic structure of the LM DAP remains the same.

3.2.2.2 Automatic Maneuvers

Automatic attitude maneuvers are implemented with exactly the same logic as that used in attitude hold, except for the additional inputs shown in Fig. 3.2-2. One important difference is that the reference angles, θ_d, will, in general, be functions of time. These angles are generated by the steering programs, such as the attitude-maneuver routine shown schematically in Fig. 3.2-2. The steering routine also generates the following quantities to provide smooth and efficient control:

1. $\Delta\theta_{do}$, $\Delta\theta_{di}$, $\Delta\theta_{dm}$ – reference CDU angle increments
2. ω_{dP}, ω_{dQ}, ω_{dR} – desired spacecraft rates
3. β_P, β_Q, β_R – attitude lag angles

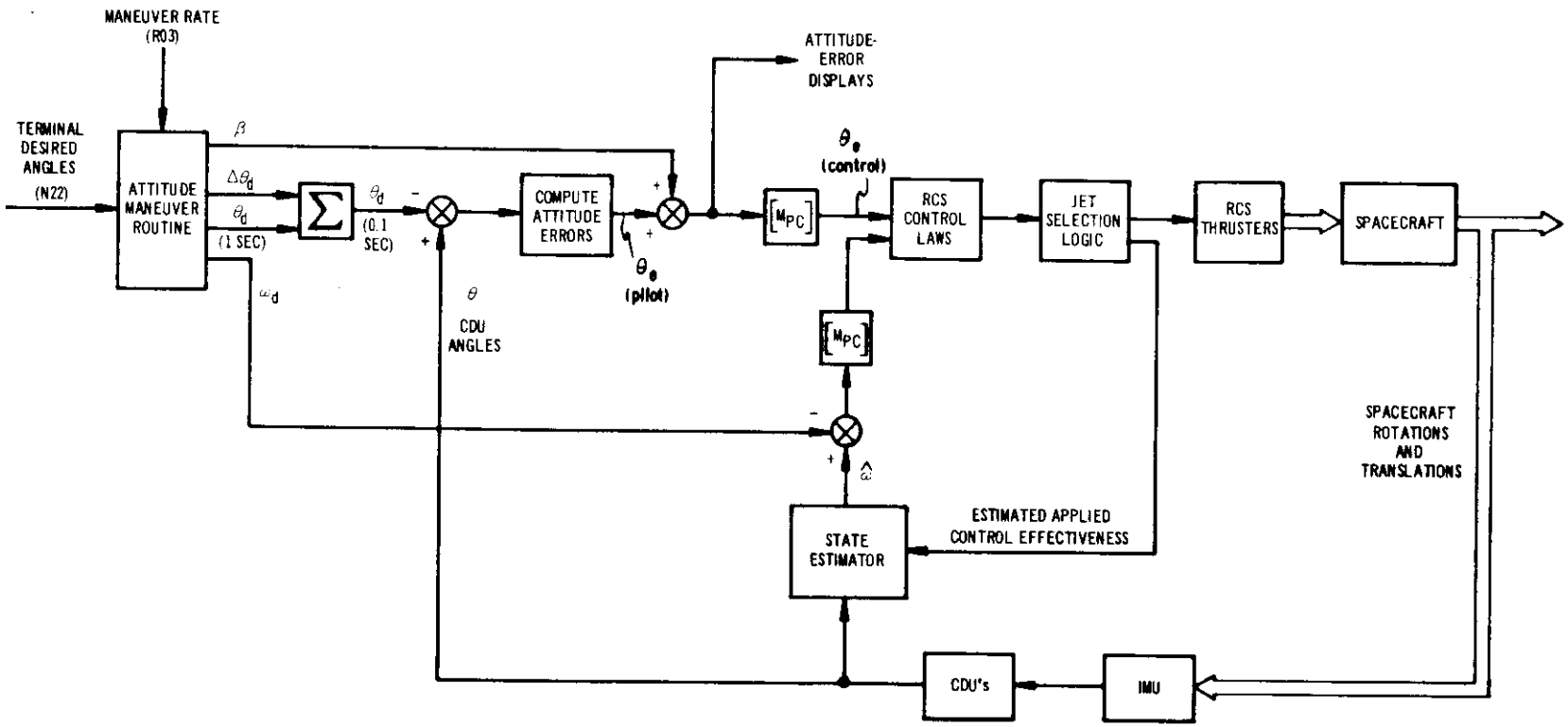

Fig. 3.2-2. Coasting-flight automatic maneuvers.

Since the steering programs generate the desired gimbal angles at an interval (ΔT_c) that is much greater than the LM DAP sample rate (ΔT_s = 0.1 sec), the incremental angles, $\Delta\theta_d$, are provided for smoothing the commands between successive updates. These angles can be computed as

$$\Delta\theta_d(t_n) = [\theta_d(t_{n+1}) - \theta_d(t_n)]\frac{\Delta T_s}{\Delta T_c} \tag{3.2-1}$$

The LM DAP will then perform the following angle additions every 100 millisec:

$$\left.\begin{aligned} \theta_{do}(N) &= \theta_{do}(N-1) + \Delta\theta_{do}(t_n) \\ \theta_{di}(N) &= \theta_{di}(N-1) + \Delta\theta_{di}(t_n) \\ \theta_{dm}(N) &= \theta_{dm}(N-1) + \Delta\theta_{dm}(t_n) \end{aligned}\right\} \tag{3.2-2}$$

The steering programs also compute a set of command spacecraft rates, $\bar{\omega}_d$, that are subtracted from the measured body rates by the LM DAP. The result is used by the RCS control laws. This procedure allows the LM DAP to maneuver the spacecraft smoothly at the required rate. For proper attitude control, the desired gimbal-angle rates should be consistent with $\bar{\omega}_d$. In addition, the steering programs will generate a set of lag angles, $\bar{\beta}$, that are added to the attitude errors to prevent overshoot when starting and stopping an automatic maneuver. The values of β for each axis are given by

$$\left.\begin{aligned} \beta_P &= \omega_{dP}|\omega_{dP}|/2\alpha_P \\ \beta_Q &= \omega_{dQ}|\omega_{dQ}|/2\alpha_Q \\ \beta_R &= \omega_{dR}|\omega_{dR}|/2\alpha_R \end{aligned}\right\} \tag{3.2-3}$$

where α_P, α_Q, and α_R are the magnitudes of the assumed available two-jet accelerations in each axis as computed in the 1/ACCS routine. If these lag angles were not introduced into the attitude command during an automatic maneuver, then the autopilot would have to accelerate to a rate in excess of the desired maneuver rate to catch up with the attitude command, which instantly started moving at the desired maneuver rate. This rate overshoot would waste fuel. In addition, at the end of the maneuver, without the lag angles, the autopilot would command the vehicle to decelerate only when the final attitude was reached; thus, overshooting of the desired attitude would occur and additional fuel expenditure would be required to return the vehicle to the desired attitude.

No limits are imposed on the computed values of these lag angles. Thus, if one attempted to perform an automatic maneuver at the highest selectable maneuver rate of 10 deg/sec with the heaviest CSM-docked configuration (where the two-jet acceleration in pitch is of the order of 0.2 deg/sec^2), the computed lag angle

β_Q would be of the order of 250 deg. This would produce unpredictable results; therefore, the high rate with the CSM-docked configuration should not be selected. (Even with a working autopilot algorithm, this should not be done because of the exorbitant RCS fuel consumption.)

Note that when steering is completed, $\bar{\omega}_d$ and $\overline{\Delta\theta}_d$, as well as $\bar{\beta}$, are reset to zero and, in effect, the LM DAP reverts to attitude hold about the desired gimbal angles.

In the CSM-docked configuration, the basic structure of the mode remains unchanged except for the simplified RCS control logic.

The coasting-flight attitude maneuver routine is specified in detail in Subsection 3.7.

3.2.2.3 Manual Rate Command Mode

In the manual rate command mode, the LM DAP interrogates the hand-controller counters that interface with the proportional rate command signals supplied by the attitude controller assembly (ACA). Based upon the contents of these counters, the LM DAP computes the corresponding rate commands in pilot axes (ω_{cP}, ω_{cQ}, ω_{cR}). The magnitude of each of these commands is a quadratic function of the hand-controller deflection. The LM DAP then compares the rate commands with the estimated spacecraft rates and computes a set of rate errors as shown in Fig. 3.2-3. These errors are transformed into the LM DAP control axes and are used as one set of inputs to the manual rate control laws. The LM DAP also computes a set of body-axis attitude errors, θ_e, by integrating the difference between the command rates and unfiltered measurements of the actual vehicle rates. These rate measurements are made by back-differencing the CDU measurements over a control-sample period and transforming to pilot axes. The attitude errors are then transformed to control axes and used as a second set of inputs to the manual control laws. The manual control logic selects one of two control laws, as discussed in Subsection 3.4.4. (The direct rate mode, which is entered when the change in commanded rate is large and returns control to the pseudo-automatic mode when rate errors have been sufficiently reduced or after four seconds of direct rate control, ignores attitude errors. The pseudo-automatic mode, which is used when the change is small and the direct rate mode is inactive, controls through the LM-alone or CSM-docked phase-plane logic and requires both rate and attitude errors.) Control-law selection occurs in the P, Q, R axes. Control is effected in the P, U', V' axes for the ascent and descent configurations and in the P, U, V axes for the CSM-docked configuration. The control laws compute jet on-times that interface with the jet selection logic. When the hand controller is returned to the center (detent) position, the commands are zeroed and the LM DAP damps the spacecraft rates below a threshold value at which time the LM DAP samples the CDU's, sets the desired attitude to the present attitude, and reverts to attitude hold.

3.2.2.4 X-Axis Override

This mode allows the crew to override automatic control of the X axis (yaw axis) and permit manual yaw rate control, while the automatic steering maintains control of the pitch and roll axes. In this mode, the X axis operates in the attitude-hold mode or the rate command mode as described in Subsections 3.2.2.1 and 3.2.2.3.

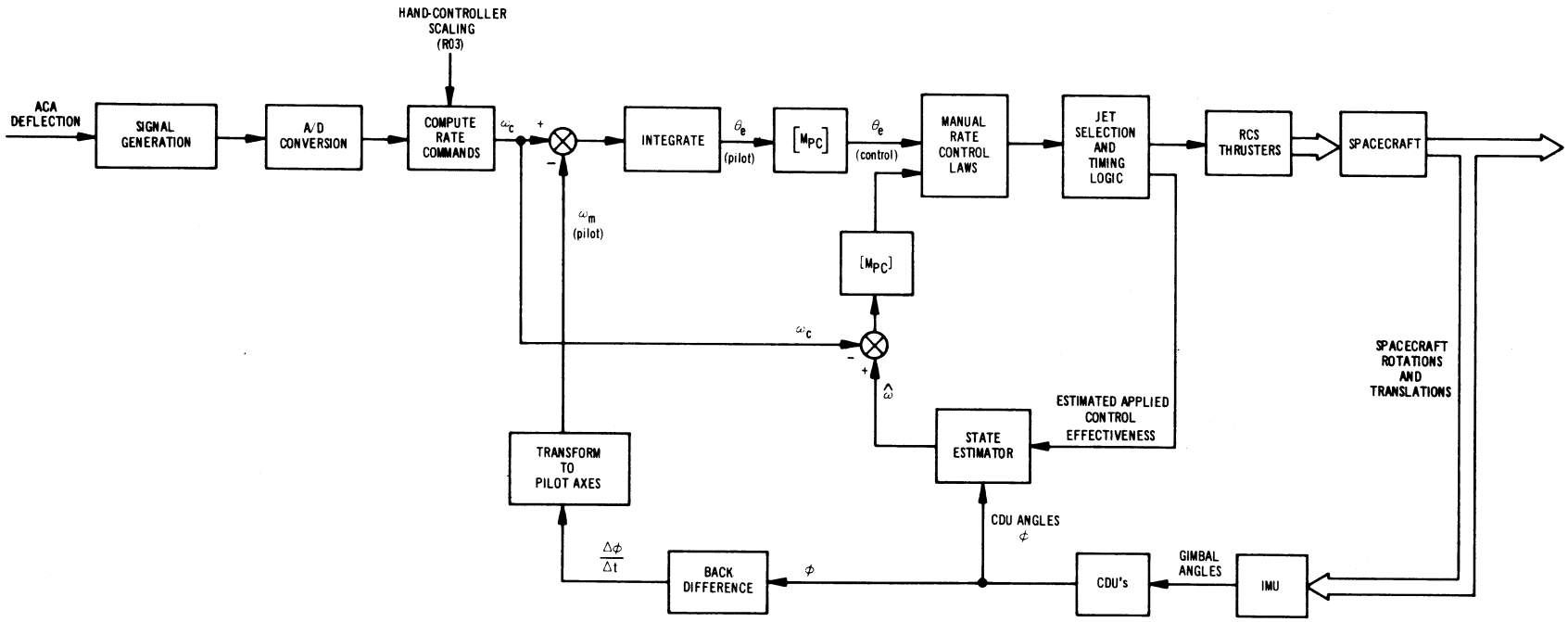

Fig. 3.2-3. Manual rate control logic.

The pitch and roll axes are restricted to the attitude-hold and automatic-maneuvering modes of operation.

X-axis override is available only when the attitude mode control switch is placed in the AUTO position. Its use is further restricted by an internal program discrete as described in Subsection 3.6.

3.2.2.5 Minimum Impulse Mode

Figure 3.2-4 shows the functional elements associated with the minimum impulse mode. In this mode, the LM DAP responds only to hand-controller commands. Each time the ACA is moved from the center (detent) position past the pulse/direct switches of the ACA, a single 14-millisec firing of the RCS jets results about the axes commanded. The ACA must be returned to detent before another firing will be made. If no ACA commands are present, the spacecraft will drift freely.

In the CSM-docked configuration, the duration of minimum-impulse firings is 14 millisec for commands about the P axis and is 60 millisec for commands about the Q and R axes. In all other respects, the minimum impulse mode is identical for the CSM-docked and LM-alone configurations.

3.2.2.6 Autopilot Off Mode

If the attitude mode control switch is placed in the OFF position, the LM DAP will turn off the jets and the gimbal drives and revert to an idle mode in which the DAP will not exercise the automatic control logic nor respond to any inputs. When the mode control switch is returned to either the AUTO position or the ATT HOLD position, the LM DAP will reinitialize and resume active control of the spacecraft.

Similarly, if the guidance select switch is moved from the PGNCS position to the AGS position, the LM DAP will revert to the idle mode. If, however, the PGNCS attitude mode control switch is left in either the AUTO position or the ATT HOLD position, the LM DAP will continue to display attitude errors or DAP-estimated rates on the FDAI attitude-error needles. Since the DAP rate estimator is not executed in the idling mode, the rate display will be useless in this mode.

3.2.3 Powered-Flight Modes

The powered-flight operations of the LM DAP are considerably more complicated than the coasting-flight operations. First of all, the LM DAP - working in conjunction with the outer-loop guidance - must accurately steer the spacecraft to meet the stringent thrust-pointing requirements of all powered-flight phases, including the lunar landing. In addition, the LM DAP must control the gimballing of the descent engine as well as the firing of the RCS jets. The control problem is further aggravated by large angular accelerations induced by engine moment offsets. The LM DAP must compute these accelerations to maintain control of the spacecraft and produce efficient limit-cycle performance. Since the mass properties of the vehicle are continually changing, the LM DAP must also repetitively adjust its gains and control parameters to adapt to the varying conditions of powered flight.

The structure of the LM DAP during powered flight is shown schematically in Fig. 3.2-5. The major additions required for powered-flight operation are the following:

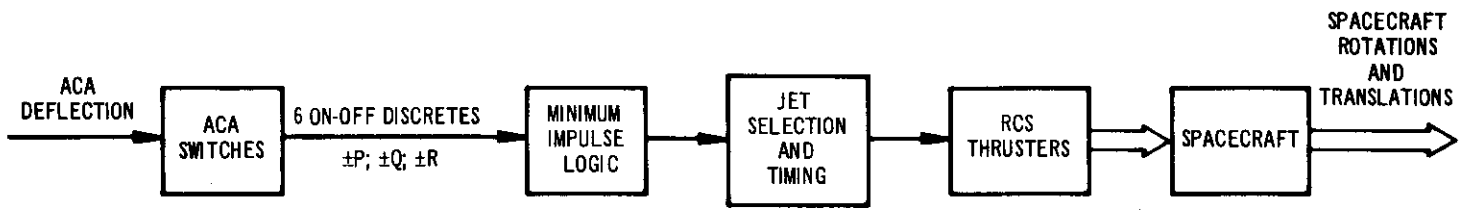

Fig. 3.2-4. Minimum impulse control mode.

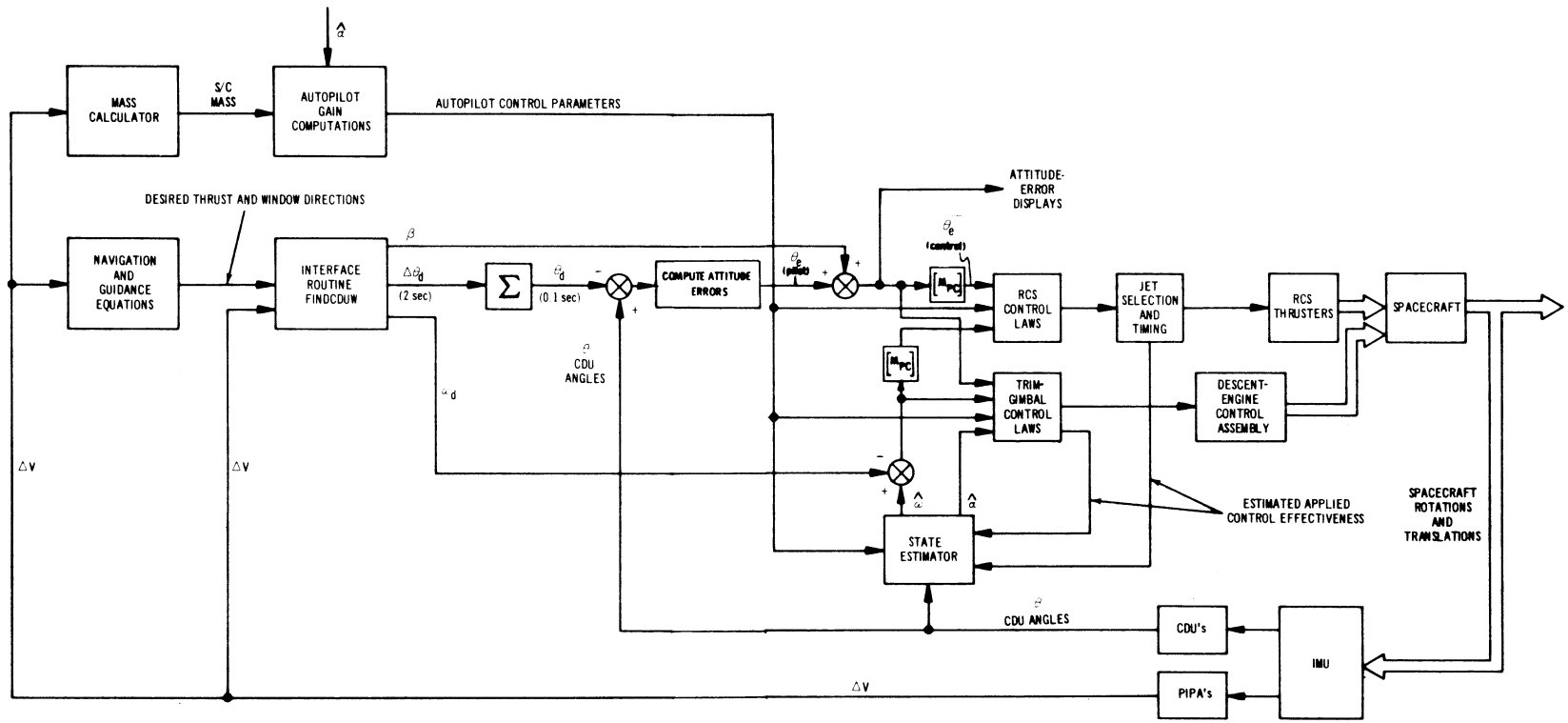

Fig. 3.2-5. Powered-flight automatic control.

1. An integrated guidance and navigation outer loop that interfaces with the LM DAP through a powered-flight steering routine known as FINDCDUW.

   This routine computes the vehicle rotation required to bring the measured thrusting direction into alignment with the desired thrusting direction and to provide window pointing control. A detailed specification of this guidance/control interface routine is given in Section 5 of the GSOP.

2. Control laws for gimballing the descent engine.

   Two control laws are used. The first is a nearly time-optimal attitude control law capable of independent steering of the spacecraft; it is called the GTS attitude control law. The second is a simplified acceleration control law used to null the offset accelerations; it is called the GTS acceleration nulling control law. Both of these control laws are described in Subsection 3.5. The interaction between RCS control, GTS attitude control, and GTS acceleration nulling control is discussed in Subsection 3.6.

3. A mass-monitor-and-control-parameter calculation used to compute a) the switch curves and jet effectiveness for the RCS control laws, and b) the control authority of the trim-gimbal control drives.

   These computations are presented in parts of Subsections 3.3 and 3.4.

4. A derivation of the spacecraft offset angular accelerations, $\hat{a}_Q$ and $\hat{a}_R$, performed by the state estimator.

   These quantities, as well as the estimates of vehicle rates, are required by the RCS control laws and the trim-gimbal control laws. A description of the equations employed to compute $\hat{a}_Q$ and $\hat{a}_R$ is given in Subsection 3.3.

In accordance with this basic structure, the following subsections describe the control modes available in powered flight.

3.2.3.1 Automatic Steering

In the LM-descent configuration, the autopilot is structured as shown in Fig. 3.2-5. Every two seconds the guidance computes a new desired attitude. The interface routine FINDCDUW attempts to deliver the desired attitude by issuing appropriate rotation-rate commands. This provides ramp smoothing of the discontinuous guidance attitude commands. FINDCDUW maintains the same set of interface variables ($\Delta\theta_d$'s, ω_d's, and β's) that are maintained in a coasting-flight maneuver by KALCMANU.

In the CSM-docked configuration, the basic structure remains the same except that the LM-alone RCS control laws are replaced by the simpler CSM-docked RCS control laws.

In ascent, however, the trim-gimbal laws are not employed and the RCS path must assume complete responsibility for providing control of the spacecraft.

3.2.3.2 Attitude Hold

For the LUMINARY program, this mode differs from the automatic steering mode in only two respects:

1. The automatic steering routine, FINDCDUW, does not send commands across the interface.
2. The trim gimbals are used only in the acceleration-nulling mode during LM-alone DPS burns.

3.2.3.3 Manual Rate Control

The manual rate mode for powered flight functions in the same way as for coasting flight (see Subsection 3.2.2.3) except that for the descent configuration the trim-gimbal acceleration-nulling control law will be operative (to the exclusion of the trim-gimbal attitude control law). As in attitude hold, steering commands are not sent across the interface.

In the CSM-docked configuration, there is no requirement to provide manual rate control in powered flight.

3.2.3.4 X-Axis Override

X-axis override functions in a way similar to that described in Subsection 3.2.2.4. The main difference is that manual yaw control will override the automatic steering about the X axis while the powered-flight steering continues to control thrust-axis pointing. In this case, the pitch and roll channels of the LM DAP are structured in the automatic steering mode described in Subsection 3.2.3.1.

3.2.3.5 Minimum Impulse Mode

This mode operates in the same way as described in Subsection 3.2.2.5 except that the trim-gimbal control laws will be operative in the descent and CSM-docked configurations. Care must be taken to prevent inadvertent selection of this mode in powered flight.

3.2.3.6 Off Mode

Operation in this mode is the same as described in Subsection 3.2.2.6 except that the Mode 2 attitude-error displays will reference the output of the powered-flight steering routine.* The guidance and navigation, as well as the control-gain calculations, will continue to function.

*See Subsection 3.2.6 for definition of the modes of operation associated with the attitude-error displays.

3.2.4 Mode Selection

Selection of the LM DAP control modes is shared between astronaut action and program control. Manual selection is governed by the guidance select switch, the attitude mode control switch, and by keyboard entries. Program selection is accomplished by various internal discretes.

Before describing the detail selection of each of the modes, a few general statements can be made. All operating modes (on-modes) of the LM DAP will be available only if the guidance select switch is in the PGNCS position. In the AGS position, the Mode 2 attitude-error displays will be maintained by the LM DAP, provided that the attitude mode control switch is placed in the AUTO or ATT HOLD positions. The selection of all powered-flight modes is governed solely by an internal mission-program control discrete (DRIFTBIT of the DAP control word DAPBOOLS). Use of the trim-gimbal control laws is governed by another internal discrete (USEQRJTS bit in DAPBOOLS)*

The parts played by astronaut action and program control in each of the LM DAP control modes is summarized in the following presentation.

Idling Mode

1. Entered automatically if the guidance select switch is in the AGS position.
2. Entered automatically if the DAP mode control switch is in the OFF position.
3. Entered automatically if the IMU CDU's are not usable. The IMU CDU's are considered to be unusable if any of the following conditions exist:
   a) The IMU is off.
   b) The IMU is in coarse align.
   c) The IMU is performing a CDU zero.
   d) The IMU is in its turn-on sequence.
4. Entered automatically if the 1/ACCS adaptive loop computations have not been completed since the last fresh start or restart.

Coasting-Flight Automatic Maneuver Mode

1. DAP mode control switch must be in the AUTO position.
2. Entered manually via the V49 DSKY entry, which calls the R62 crew-defined automatic maneuver routine.
3. Entered manually via the V89 DSKY entry, which calls the R63 rendezvous final attitude routine.

*For further information on these discretes and other discretes in DAPBOOLS see Subsection 3.6.

4. Entered via the crew DSKY response in:

   a) The P40 DPS program.
   b) The P41 RCS program.
   c) The P42 APS program.
   d) The P63 braking phase program.
   e) The R52 automatic optics positioning routine.
   f) The R61 preferred tracking attitude routine.
   g) The R65 fine preferred tracking attitude routine.

Powered-Flight Automatic Steering Mode

1. PGNCS attitude mode control switch must be in the AUTO position.
2. Automatically selected in:

   a) The P12 powered ascent program.
   b) The P70 DPS abort program.
   c) The P71 APS abort program.
   d) The P63 braking phase program.
   e) The P64 approach phase program.
   f) The P66 Auto landing phase program.
   g) The P40 DPS program.
   h) The P42 APS program.

Attitude Hold Mode

1. Entered automatically in coasting flight when the PGNCS attitude mode control switch is in the AUTO position, the R60 attitude maneuver routine is inactive, and the yaw axis of the ACA hand controller is in the detent position.
2. Entered automatically in coasting flight when the PGNCS attitude mode control switch is in the ATT HOLD position, the ACA hand controller is in the detent position, and the PULSES bit has been reset via the V77 DSKY entry or by the program.
3. Entered automatically in powered flight when the PGNCS attitude mode control switch is in the ATT HOLD position and the ACA hand controller is in the detent position.

[X] Revised LUMINARY 1C
[ ] Added GSOP # R-567 PCR # 988 Rev. 4 Date 3/70

Manual Rate Command Mode

1. DAP mode control switch must be in the ATT HOLD position.
2. ACA hand controller must be moved out of detent.
3. PULSES bit must have been reset. PULSES is reset:
   a) Manually by the crew via the V77 DSKY entry.
   b) Automatically by the ignition sequence of any APS, DPS or RCS burn program.
   c) Automatically by a fresh start.

X-Axis Override Mode

1. DAP mode control switch must be in the AUTO position.
2. ACA hand controller must be out of detent about the yaw axis.
3. XOVINHIB bit must not be set. XOVINHIB is set automatically in:
   a) The P12 powered ascent program between the time of ignition and 12 sec after the radial velocity equals +40 ft/sec.
   b) The P70 DPS abort program and the P71 APS abort program (if the LGC-estimated altitude at initiation is less than 25,000 ft) from initiation to completion of the pitch maneuver to attitude-for-ascent maneuver.
   c) The P63 braking phase program when the LGC-estimated altitude is less than 25,000 ft.
   d) The P64 approach phase program.

Minimum Impulse Command Mode

1. DAP mode control switch must be in the ATT HOLD position.
2. PULSES bit must have been set. PULSES is set:
   a) Manually by the crew via the V76 DSKY entry.
   b) Automatically by the P68 landing confirmation program.

The dependence of mode selection on the position of the mode control switch is summarized in Table 3.2-1.

3.2.5 Parameter Specification

The LM DAP is designed to provide a degree of flexibility in specifying its control parameters. Among those parameters that the astronaut may select are the following:

1. Angular deadbands.
2. Automatic maneuver rates.
3. Rotational-hand-controller scalings.

Table 3.2-1. The positions of the mode control switch required for the various LM DAP control modes.

LM DAP Control Mode		Position of Mode Control Switch		
		AUTO	ATT HOLD	OFF
COASTING FLIGHT	Automatic Maneuvering	X		
	Attitude Hold	X	X	
	Manual Rate Control		X	
	X-axis override	X		
	Minimum Impulse Control		X	
	Off			X
POWERED FLIGHT	Automatic Steering	X		
	Attitude Hold		X	
	Manual Rate Control		X	
	X-axis override	X		
	Minimum Impulse Control		X	
	Off			X

4. Two- or four-jet X axis translation.
5. The fuel system (A or B) for providing two-jet X-axis translation and Q, R minimum impulses in the minimum impulse mode.

The mechanism for making these selections is the LM DAP data-load routine (R03), which is called by V48E. Crew procedures for using R03 are described in Section 4 of the GSOP.

The crew may indicate a preference for a deadband of 5 deg, 1 deg, or 0.3 deg. This preference is honored in the LM-alone configurations unless overridden by an automatic mission-control program. For example, in most powered flight programs, a deadband of 1 deg is actually used. The specification of the automatic override of the crew-selected deadbands is indicated throughout Section 4 of the GSOP. In the CSM-docked configuration, there is no variation in deadband in response to either manual or automatic selection.

The maneuver rates that may be selected by the crew for use by the automatic attitude-maneuver routine are 10 deg/sec, 2 deg/sec, 0.5 deg/sec, or 0.2 deg/sec. It is strongly advised that the crew not select 10 deg/sec in the CSM-docked configuration since the fuel consumption will be enormous because of the large moments of inertia.

Two rotational-hand-controller scalings are available. In the LM-alone configuration, the maximum commanded rates are 20 deg/sec and 4 deg/sec. In the CSM-docked configuration, the scalings are reduced by a factor of ten; that is, the maximum commanded rates are 2 deg/sec and 0.4 deg/sec.

The crew has some fuel-management control over the automatic system. One input via R03 indicates whether two or four jets should be used for X-axis translation (including ullage). If two jets are chosen, the crew may select the two jets in either System A or System B.* However, an indication of a jet failure will override the crew preference and cause selection of a firing policy that does not include a disabled jet. Furthermore, the ascent program P12 and the abort programs P70 and P71 internally set the indicator for four-jet translation.

The crew may elect to disallow use of the RCS jets for attitude control about the Q and R spacecraft axes during any unstaged burn (CSM-docked or LM-alone). This is accomplished by calling up Verb 65 on the DSKY, which serves to set the flag bit SNUFFBIT. The bit may be subsequently cleared by a call to Verb 75. Regardless of when in the mission SNUFFBIT is set, it affects only automatic Q, R-axes attitude control and only applies during a LM-active burn prior to staging. The purpose of this option is to provide a means of avoiding thermal impingement by the RCS jet plumes. However, when SNUFFBIT is set, control of the spacecraft must be maintained entirely by the slow trim gimbal system. If SNUFFBIT is set in the descent configuration when the mode control switch is in the ATT HOLD position, no pitch or roll attitude control will be provided.

Additional interfaces exist that enable the autopilot to a) control spacecraft configurations that differ widely in their dynamical characteristics and b) take into account known failures in the control-system hardware. These interfaces are described in the succeeding paragraphs.

3.2.5.1 Spacecraft Configurations

The vehicle configuration – that is, the ascent LM, the descent LM, or the (descent) LM docked to the CSM – is specified by two software flag bits: CSMDOCKD and APSFLAG. The hardware-controlled stage-verify discrete is not relied upon, or even referred to, in the LUMINARY program; APSFLAG alone is used by both the LM DAP and the other subprograms. The two flags are set in accordance with the crew's input in Routine 3 (R03). However, APSFLAG is also automatically set by mission-oriented routines to indicate staging after a lunar touchdown (P68), after an ascent abort from powered descent (P71), or before an ascent burn (P42). While a transition is being made from one configuration to another, such as during a docking maneuver, it is generally preferable to indicate the lighter configuration in order to avoid overcontrol by the autopilot.

The LM DAP has not been designed to control the configuration in which the LM ascent stage alone is docked to the CSM, and R03 has been coded so as not to accept such an input.

3.2.5.2 Spacecraft Mass Properties

For each spacecraft configuration, the mass properties of the vehicle are subject to large variations. For example, during ascent, the principal moment

*This choice of system also governs the selection of jets for Q, R minimum impulses for the minimum impulse mode.

of inertia about the spacecraft Z axis changes by almost a factor of four. To optimize the performance of the LM DAP under these conditions, the LM DAP must be provided with a simple means of specifying the mass properties of the spacecraft. To this end, R03 incorporates a LM DAP data load of LM mass and CSM mass (N47) from which the LGC can update all its mass-dependent parameters.

During powered flight, the LM mass (and the mass of the combined vehicle when docked) is decremented every two seconds according to the measured velocity change and the assumed main-engine (descent or ascent) specific impulse. The mass-dependent control gains are then recomputed as a function of the decremented mass. Major changes in the mass properties of the vehicle occur during powered flight. By this automatic mass-update method, the LM DAP should maintain reasonable estimates for the critical quantities. Any adjustment to the LGC-computed values must be made via R03. Adjustments to the LGC-stored values for the LM or CSM masses must be made by the astronaut whenever a significant change in mass has occurred that was not reflected in ΔV measured by the powered-flight programs in the LGC. Examples of such changes would be: 1) A significant reduction in APS fuel as a result of cross-feeding to the RCS and firing the RCS in balanced couples, or 2) a reduction in CSM mass due to SM TVC under CMC control. As a general rule, if there is uncertainty in determining the LM mass or the CSM mass, the crew should load a mass slightly smaller than the estimated mass. A mismatch between the value of mass loaded in the LGC and the actual vehicle mass can cause instabilities only if the LGC believes the vehicle is much heavier than it actually is. It should be noted here that the check on the LM-mass value that is described in Subsection 3.6.1.5 will result in a change from the loaded value if that value is not considered to be within the required range. The crew will not be aware of this correction unless they display the mass again.

3.2.5.3 Descent-Engine Gimbal Trim Angles

Another set of quantities that may be specified in R03 are the descent-engine gimbal trim angles (N48). These quantities are provided for alignment of the descent-engine thrust vector through the initial estimated center of gravity of the spacecraft. This initial alignment of the descent engine is required to reduce the attitude transient caused by thrust offsets at ignition. The alignment procedure is complicated by the lack of gimbal-angle indicators and the very slow gimbal drive rates (0.2 deg/sec). The alignment is achieved by first driving each gimbal to its stops (-6 deg) and then returning the gimbals to the trim angles via an open-loop timed drive at a rate of 0.2 deg/sec. This procedure may take up to two minutes for completion.

At the end of the burn, the trim-gimbal drives will be turned off – leaving the engine thrust axis approximately aligned through the center of gravity. This

procedure will avoid the necessity for realigning the gimbals for subsequent ignitions with the same vehicle configuration. On the other hand, if the CSM has docked or separated, then the center of gravity will, in general, have shifted; the alignment drive must be initiated again before reigniting the descent engine.

3.2.5.4 RCS Failure Monitor and Thruster-Pair Disable

The eight thruster-pair disable switches interface with the LGC via bits 1 through 8 of channel 32, as illustrated in Fig. 3.1-4 of Subsection 3.1. The T4RUPT routine monitors these switches once every 480 millisec and informs the LM DAP of any changes in switch position. With this information, the LM DAP will select the best set of jets to use under the combined conditions of rotational commands, translational commands, and disabled jets.

The LM DAP will not attempt to fire disabled jets and will account for the corresponding reduction in control authority by readjusting its control gains. In situations where a conflict arises between rotational commands and translational commands, rotations will assume priority. For further details, the reader should refer to the description of the jet selection logic in Subsection 3.4.5 and the RCS failure monitor in Subsection 3.6.1.

3.2.5.5 Gimbal-Failure Indication

The crew may indicate by setting a panel switch that the descent-engine trim gimbals are unusable. The setting of this switch indicates to the LM DAP that it should stop sending drive signals to the trim gimbal and should attempt to control despite the fixed (hopefully small) moment offset.

3.2.6 FDAI Attitude-Error Meter Displays

Among the myriad of displays that confront the astronaut are those associated with the FDAI. This instrument displays nine quantities concerned with the spacecraft attitude. The ball provides a display of the spacecraft total attitude, which in the PGNCS mode of operation is supplied by the resolvers mounted on the IMU gimbals. The attitude-rate meters are driven from signals generated by the rate-gyro assembly via the control electronics section of the stabilization and control system. The attitude-error meters, which interface with the LGC via the digital-to analog converters of the IMU CDU's, either display one of the two modes of attitude errors computed by the LM DAP or display the DAP-estimated vehicle rates.

The LM DAP generates two types of attitude errors for display on the FDAI error meters. The modes of operation are designated as Mode 1 and Mode 2 and display the following quantities:

1. Mode 1 displays autopilot following errors – selected via the DSKY by V61E.
2. Mode 2 displays total attitude errors with respect to the angles in Noun 22 – selected by V62E.

Mode 1 is provided as a monitor of the LM DAP and of its ability to track steering commands.

Mode 2 is provided to assist the crew in manually maneuvering the spacecraft to the attitude (gimbal angles) specified in N22. The attitude errors with respect to these angles and the current CDU angles are resolved into pilot axes.

These displays are available in all operational modes of the autopilot and are updated every 200 milliseconds. The crew may preset an attitude reference (desired gimbal angles) into N22, but caution is advised since this may interfere with data generated under program control. It is therefore recommended that N22 be loaded for this purpose in P00 only.

Note that N22 represents desired gimbal angles, not ball angles.

Since the conversion from gimbal angles to FDAI ball angles is somewhat complicated, routine 60 will automatically convert the desired gimbal angles in N22 to the required ball angles in N18 to assist the crew in monitoring and performing large spacecraft attitude maneuvers.

In addition to the Mode 1 and Mode 2 displays, the crew may select a display of the DAP-estimated vehicle rates with the DSKY by means of V60E. This rate-display mode provides a much finer scaling and better accuracy than that available on the attitude-rate needles driven by the rate-gyro assembly and can also be used as a backup to the rate-needle drive by the analog autopilot if the rate-gyro assembly fails.

Routine 60 automatically selects the Mode 2 attitude-error display (an equivalent of V62E). Consequently, DAP-estimated rates will be displayed during and after automatic maneuvers only if selected by the crew via V60 after initiation of R60.

3.2.6.1 Mode 1 Display Implementation

The LM DAP computes the autopilot following errors (phase-plane errors) by differencing the actual angles, $\bar{\theta}$, with the DAP reference angles, $\bar{\theta}_d$, and resolving the difference into the pilot axes (P, Q, R); that is,

$$\begin{Bmatrix} \theta_{eP} \\ \theta_{eQ} \\ \theta_{eR} \end{Bmatrix} = \begin{bmatrix} 1 & \sin\theta_m & 0 \\ 0 & \cos\theta_m \cos\theta_o & \sin\theta_o \\ 0 & -\cos\theta_m \sin\theta_o & \cos\theta_o \end{bmatrix} \begin{Bmatrix} \theta_o - \theta_{do} \\ \theta_i - \theta_{di} \\ \theta_m - \theta_{dm} \end{Bmatrix} \qquad (3.2\text{-}4)$$

where

θ_o = outer gimbal angle

θ_i = inner gimbal angle

θ_m = middle gimbal angle

θ_{do} = desired outer gimbal angle

θ_{di} = desired inner gimbal angle

θ_{dm} = desired middle gimbal angle

Note that this gimbal-rate-to-body-rate transformation matrix $[M_{GP}]$ is the same matrix used in the state-estimator logic described in Subsection 3.3 and is updated every 240 millisec by the T4 interrupt program.

In the manual rate command mode, the errors are computed as described in Subsection 3.4.4.

Since Mode 2 attitude-error displays are automatically selected before the computation and display of desired FDAI ball angles in R60, Mode 1 errors will be displayed during and after automatic maneuvers only if selected by the crew via V61 after the appearance of the first R60 ball-angle display.

During automatic maneuvers, the lag-angle terms (β_P, β_Q, β_R) are added to the errors given by Eq. (3.2-4); that is,

$$\left.\begin{aligned} \theta'_{eP} &= \theta_{eP} + \beta_P \\ \theta'_{eQ} &= \theta_{eQ} + \beta_Q \\ \theta'_{eR} &= \theta_{eR} + \beta_R \end{aligned}\right\} \qquad (3.2\text{-}5)$$

and the results are loaded into the IMU-CDU digital-to-analog converters for display on the FDAI attitude-error meters.

Since the LM DAP uses the modified errors, $\bar{\theta}'_e$, in the phase-plane logic and will attempt to null these errors during an automatic maneuver, the effect of the lag-angle additions will not be evident to the astronaut except, perhaps, during the starting and stopping transients.

The LM DAP provides these inputs to the FDAI needles to permit monitoring of its operation in the PGNCS attitude hold, automatic maneuvering, manual rate command, and X-axis override control modes. The errors should not substantially exceed the attitude deadband if the LM DAP is functioning properly. Since the LM DAP controls the spacecraft about either the U' and V' axes or the U and V axes, the effective deadbands about the Q and R axes may be larger than the selected value. In the ascent and descent configurations, the effective deadband about one of the principal axes, Q or R, can be twice the selected value in the limiting case where the U'-V' system is skewed ±15 deg away from the U-V system. In the CSM-docked configuration, the U-V system control permits a Q- or R-axis maximum effective deadband that is larger than the selected deadband by a factor of 1.4.

Since full-scale deflection of the error needles corresponds approximately to 5 degrees of attitude error in the PGNCS mode of operation, the displays may saturate if a wide deadband (θ_{db} = 5 deg) is selected. This effect should not be interpreted as improper operation of the LM DAP.

In powered flight with a large moment offset, the natural limit cycling of the LM DAP may also exceed the full-scale deflection of 5 deg.

In the PGNCS minimum impulse mode, the LM DAP will zero the Mode 1 error displays. In the OFF mode, the LM DAP does not update the displays. If AGS control is selected, however, the DAP will continue to generate the displays, provided that the attitude mode control switch is left in either the AUTO position or the ATT HOLD position.

3.2.6.2 Mode 2 Display Implementation

The total attitude errors displayed are computed as the difference between the contents of Noun 22 (θ_{co}, θ_{ci}, and θ_{cm}) and the measured gimbal angles; that is,

$$\begin{Bmatrix} \theta''_{eP} \\ \theta''_{eQ} \\ \theta''_{eR} \end{Bmatrix} = [M_{GP}] \begin{Bmatrix} \theta_o - \theta_{co} \\ \theta_i - \theta_{ci} \\ \theta_m - \theta_{cm} \end{Bmatrix} \qquad (3.2\text{-}6)$$

At the beginning of coasting-flight automatic maneuvers in R60, the contents of N22 are set to the terminal attitude of the maneuver so that the error needles will indicate angles to be gained to completion of the maneuver. During powered flight, the automatic steering routine (FINDCDUW) will load N22 to indicate the spacecraft attitude commanded by the guidance equations. In general, these commands, which are updated at two-second intervals, will be slowly changing with time. The Mode 2 errors are provided to assist the crew in manually orienting the spacecraft.

It should be noted that N22 also represents the IMU coarse-align angles that are computed when realignment of the platform is being performed (during P52, for example). Preflight check-out of the display interface, performed via V43E, also uses N22 to load the ISS error counters. This test routine requires that the autopilot be turned off.

Mode 2 error displays are selected automatically in R60 for automatic maneuvers and powered flight.

3.2.6.3 Rate-Display Mode Implementation

The vehicle rates displayed are the P, Q, and R components of the vehicle angular velocity as computed by the LM DAP state estimator. These rate displays are supplied in the "fly to" sense, as is the case with the Mode 1 and Mode 2 attitude errors.

The scaling for the rate-display mode is such that full-scale deflection of the FDAI attitude-error needles corresponds to 1.25 deg/sec.

SUBSECTION 3.3

ATTITUDE STATE ESTIMATION

by

George R. Kalan, Edgar M. Oshika and William S. Widnall

3.3.1 Assumed Control Effectiveness*

3.3.1.1 Introduction

The recursive state estimator, the RCS logic, and the trim-gimbal control laws make use, in varying degree, of the assumed control effectiveness of each of the applied control signals that command the RCS jets or the gimbal trim system (GTS). For a given axis, the effectiveness of the RCS control signals is represented by the component of angular acceleration about that axis that can be expected by firing a single jet. This nominal jet-actuated acceleration – termed the "one-jet acceleration" and designated by the symbol α_J – is based on the nominal RCS jet torque, assuming no jet failure or degraded thrust, the center-of-mass at the geometric center of the RCS quadrangle, and no thrust misalignment or plume impingement. Furthermore, it is based upon the assumed moment of inertia about the axis concerned. The jet-acceleration values are first determined for the P, Q, and R axes. The Q and R values are then resolved to obtain the values for either the U' and V' axes or the U and V axes.

The effectiveness of the GTS control signals is represented by the rate of change of angular acceleration (that is, the jerk) due to the rotation of the trim gimbal. This descent-engine jerk – designated by the symbol $\dot{\alpha}_G$ – is calculated as a function of the particular moment of inertia that exists about the trim-gimbal axis concerned, the gimbal rotation rate, and the torque due to deviation of the descent-engine thrust vector from the LM center of gravity.

The computation of these control-effector gains is carried out in the 1/ACCS routine, which is called every two seconds during powered flight. (See Subsection

*By George R. Kalan and Edgar M. Oshika.

3.6.1 for a discussion of when 1/ACCS is called and of its other functions, which include the limiting of the value of the LM mass.) These gains depend only upon the configuration – CSM-docked, LM-alone in ascent, or LM-alone in descent – and the moments of inertia, the engine thrust, and the location of the vehicle center of gravity. These latter quantities are calculated as functions of only the LM mass – and the CSM mass for the CSM-docked case – and the measured linear acceleration.

3.3.1.2 Calculations for the LM-Alone Case

Jet-Acceleration Calculations

For the LM-alone case, each of the P-, Q-, and R-axis one-jet accelerations, α_J, is calculated directly as a function of mass. For a given axis, the desired function of mass is the ratio of the nominal RCS jet torque, T, that is associated with the particular axis concerned to the LM moment of inertia, I, about that axis; that is,

$$\alpha_J = \frac{T}{I} \tag{3.3-1}$$

It is approximated by a hyperbola of the form

$$\alpha_J = f(m) = \frac{a}{m + c} + b \tag{3.3-2}$$

where m is the mass of the LM and a, b, and c are constants.

A separate set of these three constants is used for each axis. Thus, nine constants are required to specify the one-jet accelerations about the P, Q, and R axes. One set of nine constants is used for the descent configuration of the LM, while another set of nine constants is used for the ascent configuration. The 18 constants associated with the jet-acceleration calculations are given in Table 3.3-1. Plots of the computed ascent and descent jet accelerations are shown in Figs. 3.3-1 and 3.3-2.

Descent-Engine Jerk Calculations

For the LM-alone case, the jerk calculations associated with the rotations of the two trim gimbals about the Q and R axes, respectively, employ the hyperbolic form given by Eq. (3.3-2) to establish another function of mass. One function serves for both the Q-axis jerk calculations and the R-axis jerk calculations. This function, which is the distance L between the descent-engine pivot and the center of gravity of the LM, thus requires an additional separate set of three constants a, b, and c (see Table 3.3-1). A plot of L computed as a function of the LM mass is shown in Fig. 3.3-3.

Table 3.3-1. The constants used in connection with the generalized hyperbolic equation.

Identification of Constants by Use		Values
For Use in the Jet-Acceleration Calculations Associated with the LM Ascent Configuration	P axis	a = 0.0065443852 b = 0.000032 c = -0.006923
	Q axis	a = 0.0035784354 b = 0.162862 c = 0.002588
	R axis	a = 0.0056946631 b = 0.009312 c = -0.023608
For Use in the Jet-Acceleration Calculations Associated with the LM Descent Configuration	P axis	a = 0.0059347674 b = 0.002989 c = 0.008721
	Q axis	a = 0.0014979264 b = 0.018791 c = -0.068163
	R axis	a = 0.0010451889 b = 0.021345 c = -0.066027
For Use in the Descent-Engine Moment-Arm Calculation		a = 0.0410511917 b = 0.155044 c = -0.025233

The following scaling is employed in connection with these constants:

1) The mass m is scaled at 2^{16} kg.

2) For jet accelerations, which are scaled at $\pi/4$ rad/sec^2,
   a is scaled at $(\pi/4)\ 2^{16}$ kg rad/sec^2
   b is scaled at $\pi/4$ rad/sec^2 and
   c is scaled at 2^{16} kg.

3) For jerk accelerations, in which the distance L is scaled at 8 ft,
   a is scaled at $8(2^{16})$ft kg,
   b is scaled at 8 ft, and
   c is scaled at 2^{16} kg.

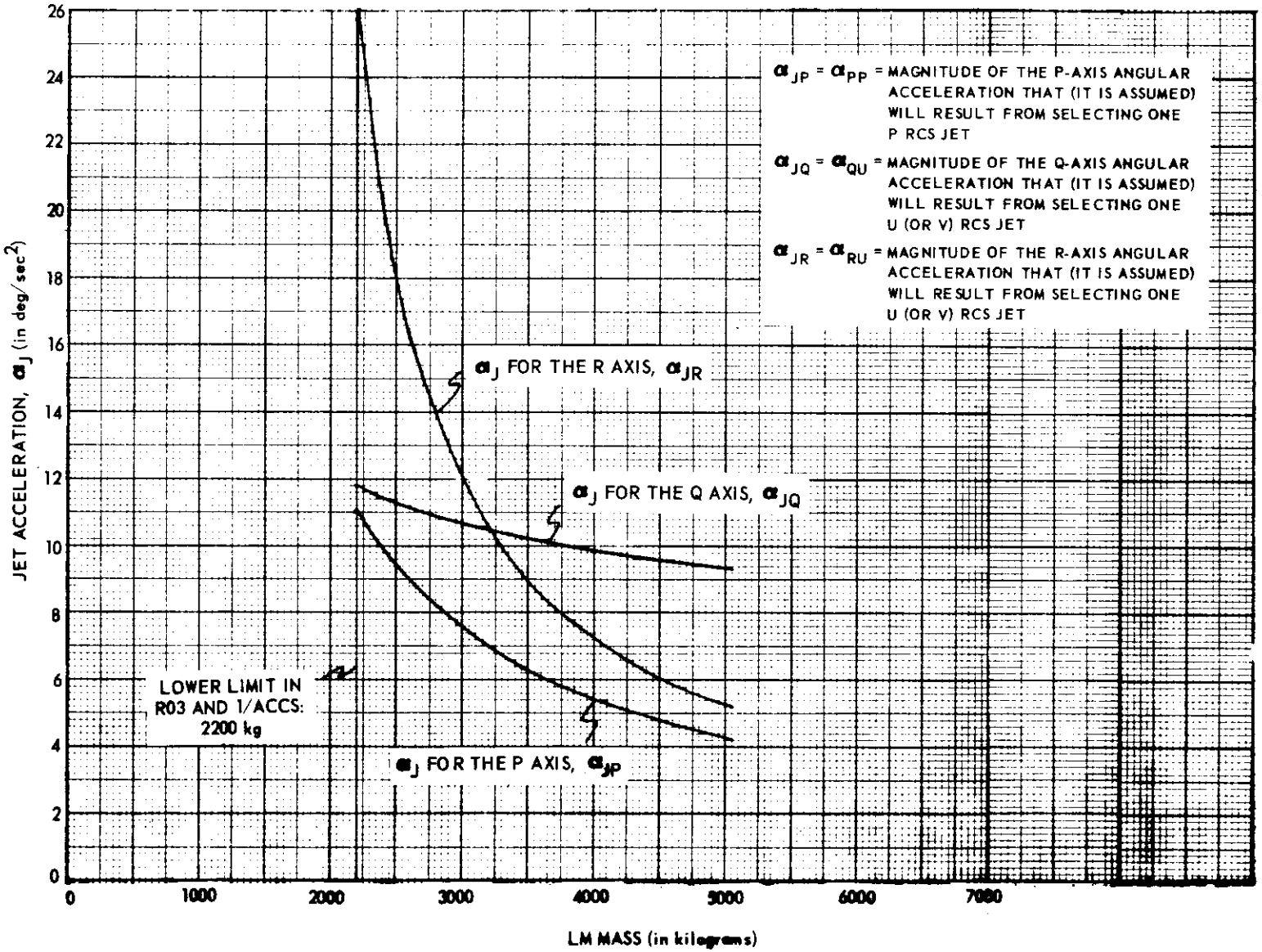

Fig. 3.3-1. The computed jet acceleration, α_J, for the ascent configuration in the LM-alone case.

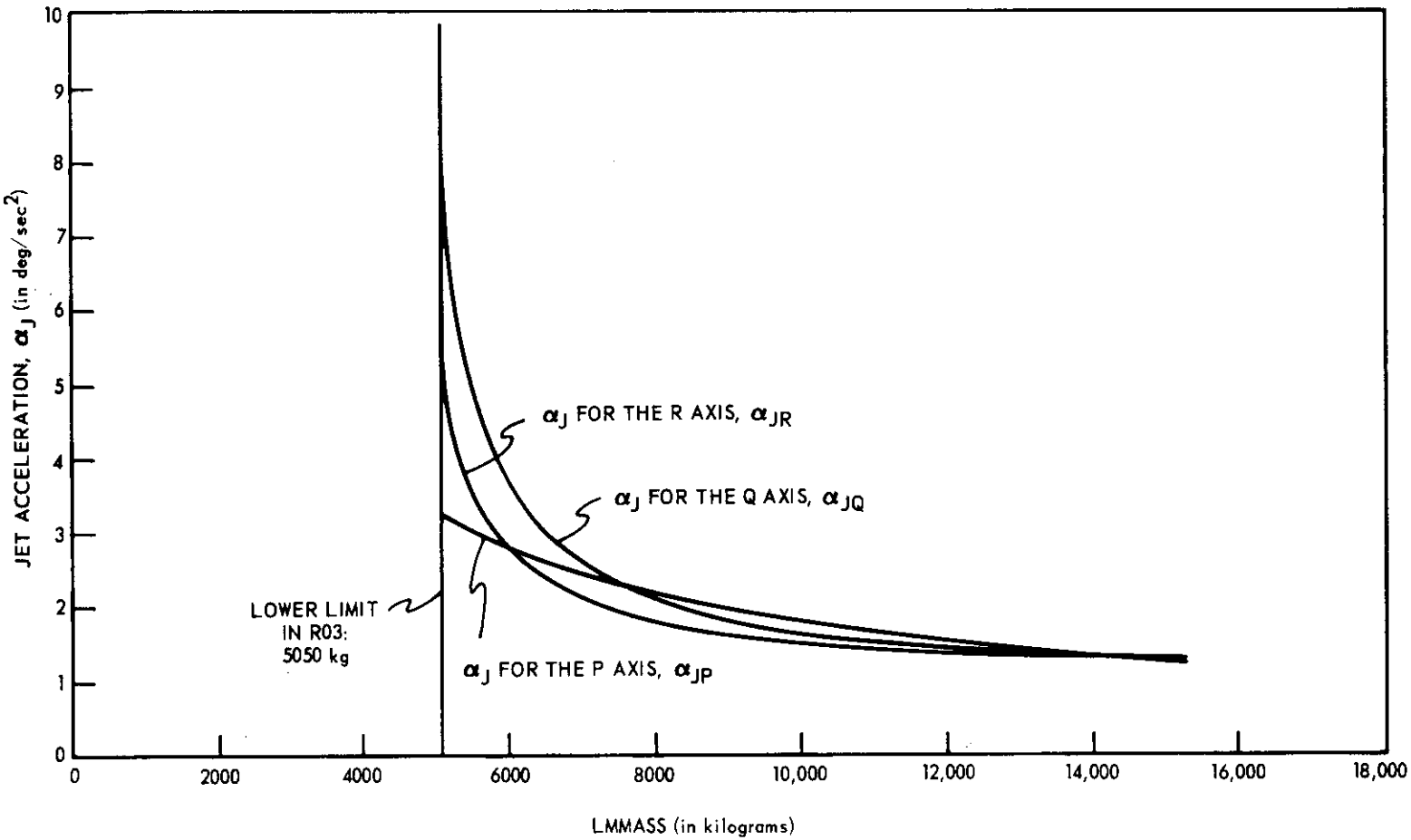

Fig. 3.3-2. The computed jet acceleration, α_J, for the descent configuration in the LM-alone case.

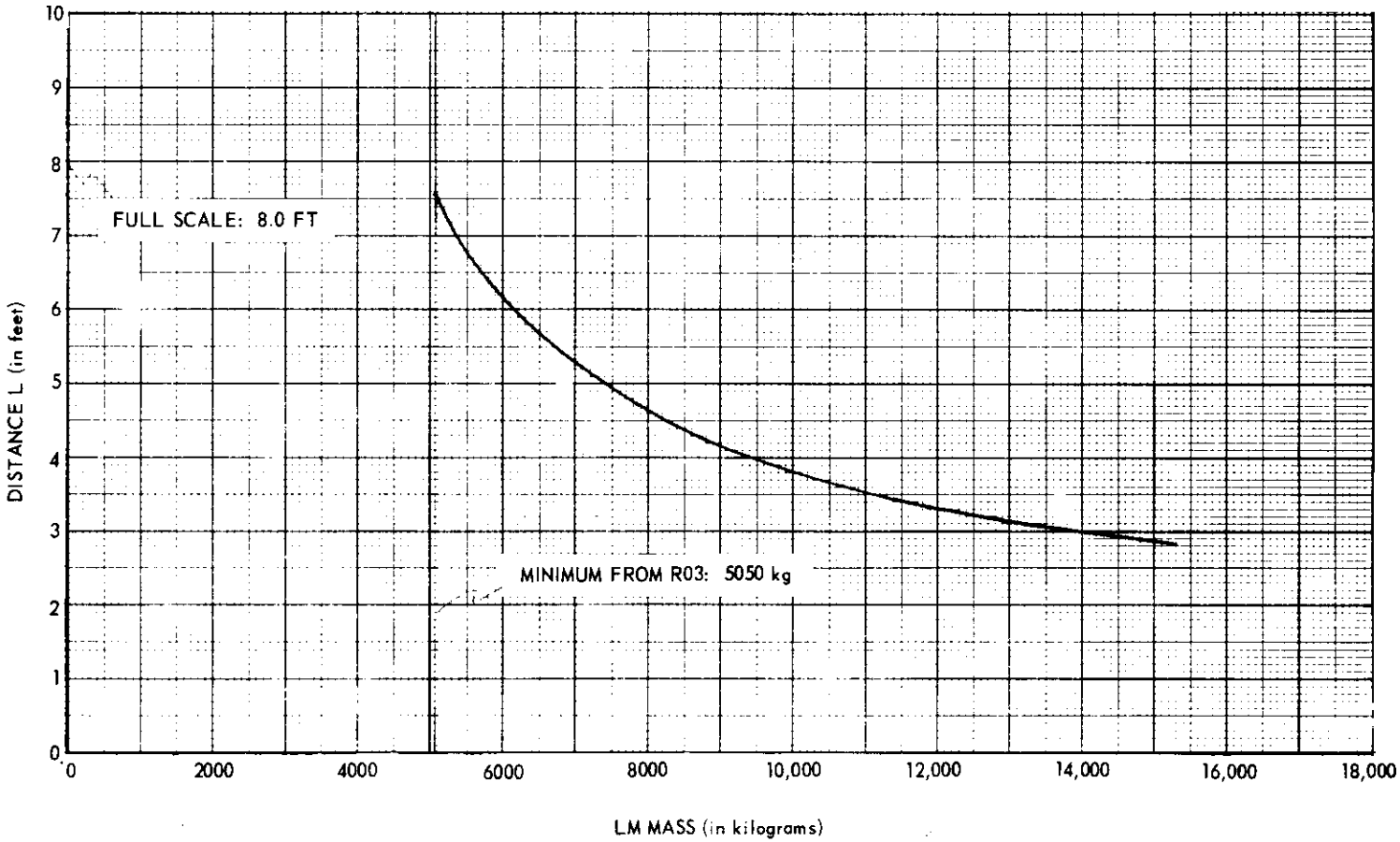

Fig. 3.3-3. The computed hinge-pin-to-center-of-gravity distance, L, in the LM-alone case.

From the foregoing discussion of the jet-acceleration and jerk calculations, it is apparent that a total of 21 separate constants must be stored for use in connection with the hyperbolic relationship given by Eq. (3.3-2). The constants used are based on the data for a manned LM as specified in Reference 1.* The scaling employed in connection with the constants a, b, and c is indicated at the bottom of Table 3.3-1.

For each trim-gimbal axis, the jerk – which is represented by the symbol $\dot{\alpha}_G$ – is calculated by means of the relationship

$$\dot{\alpha}_G = \frac{d}{dt}\left(\frac{FL \sin \delta}{I}\right) \simeq \frac{FL}{I}\,\dot{\delta} \qquad (3.3\text{-}3)$$

where

F = the computed descent-engine thrust

L = the distance from the hinge pin of the descent-engine bell to the center of gravity of the LM

I = the pitch or roll moment of inertia of the LM

δ = the angle between the descent-engine thrust vector and the vector $\overline{L}$ from the descent-engine hinge pin to the LM center of gravity

The quantities F, L, and I are assumed to be constant over the two-second sampling interval employed, and δ is assumed to be a small angle. The thrust F is the product of the estimated mass of the LM and the measured linear acceleration of the LM. The distance L is obtained by use of the hyperbolic fit just described and is therefore a function of the mass of the LM. The moments of inertia I for the Q and R axes are obtained by means of the relationship

$$I = \frac{T}{\alpha_J} \qquad (3.3\text{-}4)$$

where T is the nominal RCS jet torque (500 ft-lb for the P axis; 550 ft-lb for the Q and R axes) and α_J is the one-jet acceleration that has been computed for that axis. The rate of change of the angle δ is assumed to be constant and is set equal to the nominal engine-gimbal rate of 0.2 deg/sec.

3.3.1.3 Calculations for the CSM-Docked Case

For the CSM-docked case, the P, Q, and R jet-acceleration calculations and the Q and R descent-engine jerk calculations require equations that differ considerably from those employed for the LM-alone case. This results from the

*See the list of references at the end of Subsection 3.3.

fact that, for the CSM-docked case, jet acceleration and descent-engine jerk are functions of two separate masses – the CSM mass and the LM mass – instead of only one.

To simplify the computations for the CSM-docked configuration, symmetry about the X axis is assumed. This means that a single, average value may be used for both the Q axis and the R axis. No appreciable errors are introduced by this simplification. The computation of the mass properties for the Q and R axes of the CSM-docked configuration is thus reduced to the calculation of two parameters: (1) the moment of inertia about the Q and R axes, and (2) the distance from the descent-engine pivot to the center of gravity of the vehicle. As in the LM-alone case, these computations are performed every two seconds during powered flight, directly following the updates of the (total LM/CSM) mass and the linear acceleration.

The two parameters for the Q and R axes can be represented with sufficient accuracy by means of second-order polynomials of two variables – the CSM mass and the LM mass. If x and y are used to represent the CSM mass and the LM mass, respectively, then the polynomials are of the following form:

$$L\dot{\delta} = a_1x^2 + b_1y^2 + c_1xy + d_1x + e_1y + f_1 \qquad (3.3\text{-}5)$$

$$I = a_2x^2 + b_2y^2 + c_2xy + d_2x + e_2y + f_2 \qquad (3.3\text{-}6)$$

where

L = the distance from the hinge pin of the descent-engine bell to the center of gravity of the CSM-docked configuration

$\dot{\delta}$ = the gimbal rate of the descent engine = 0.2 deg/sec

I = the average moment of inertia of the CSM-docked configuration

$$= (1/2)(I_Q + I_R) \qquad (3.3\text{-}7)$$

I_Q = the moment of inertia of the CSM-docked configuration about the Q axis

I_R = the moment of inertia of the CSM-docked configuration about the R axis

The constant coefficients used for calculating the functions given by Eqs. (3.3-5) and (3.3-6) are listed in Table 3.3-2. The scaling employed in connection with these coefficients is indicated at the bottom of the table. Plots of the computed center-of-gravity distance, L, and the average moment of inertia, I, as functions of the total mass (CSM mass plus LM mass) are shown in Figs. 3.3-4 and 3.3-5, respectively.

Table 3.3-2. The constant coefficients used in connection with the generalized second-order polynomials of two variables.

Coefficients for the center-of-gravity polynomial	Coefficients for the moment-of-inertia polynomial
$a_1 = -0.37142$	$a_2 = -0.03709$
$b_1 = 0.75704$	$b_2 = -0.17670$
$c_1 = 0.20096$	$c_2 = 0.19518$
$d_1 = 0.41179$	$d_2 = 0.02569$
$e_1 = -0.63117$	$e_2 = 0.06974$
$f_1 = 0.13564$	$f_2 = -0.00529$

The following scaling is employed in connection with these coefficients:

1) The quantity $L\dot{\delta}$ is scaled at 4π rad-cm/sec
2) The average moment of inertia, I, is scaled at 2^{38} kg-cm^2.
3) Both x and y are scaled at 2^{16} kg.

The Q-axis or R-axis jet acceleration and the descent-engine jerk are determined from the following equations:

$$\text{Q- or R-axis one-jet acceleration} = \alpha_{JQ} = \alpha_{JR} = \frac{T}{I} \qquad (3.3\text{-}8)$$

$$\text{jerk due to engine-gimbal rotation} = \dot{\alpha}_G \cong \frac{FL}{I}\dot{\delta} \qquad (3.3\text{-}9)$$

where the torque T is 500 ft-lb and the other quantities are as already defined in connection with the calculations for the LM-alone case.

The average moments of inertia, I, and the center-of-gravity distances, L, used to determine the coefficients were derived from References 1 and 2. A number of mass combinations were selected and the coefficients were chosen so as to obtain a least-square-error fit of the polynomials to the corresponding moments of inertia and center-of-gravity distances.

The P-axis one-jet acceleration, α_{JP}, is computed as a hyperbolic function of mass in the following equation:

$$\text{P-axis one-jet acceleration} = \alpha_{JP} = \frac{K}{m} \qquad (3.3\text{-}9A)$$

where

m = total mass in kg

$K = 21.5 \times 10^3$ (kg)(deg/sec^2)

Figure 3.3-5A illustrates the P-axis one-jet acceleration, α_{JP}, computed as a function of the total mass in accordance with this equation. Additional discussion of the P-axis control-authority computation for the CSM-docked configuration is provided in Reference 3 at the end of this subsection.

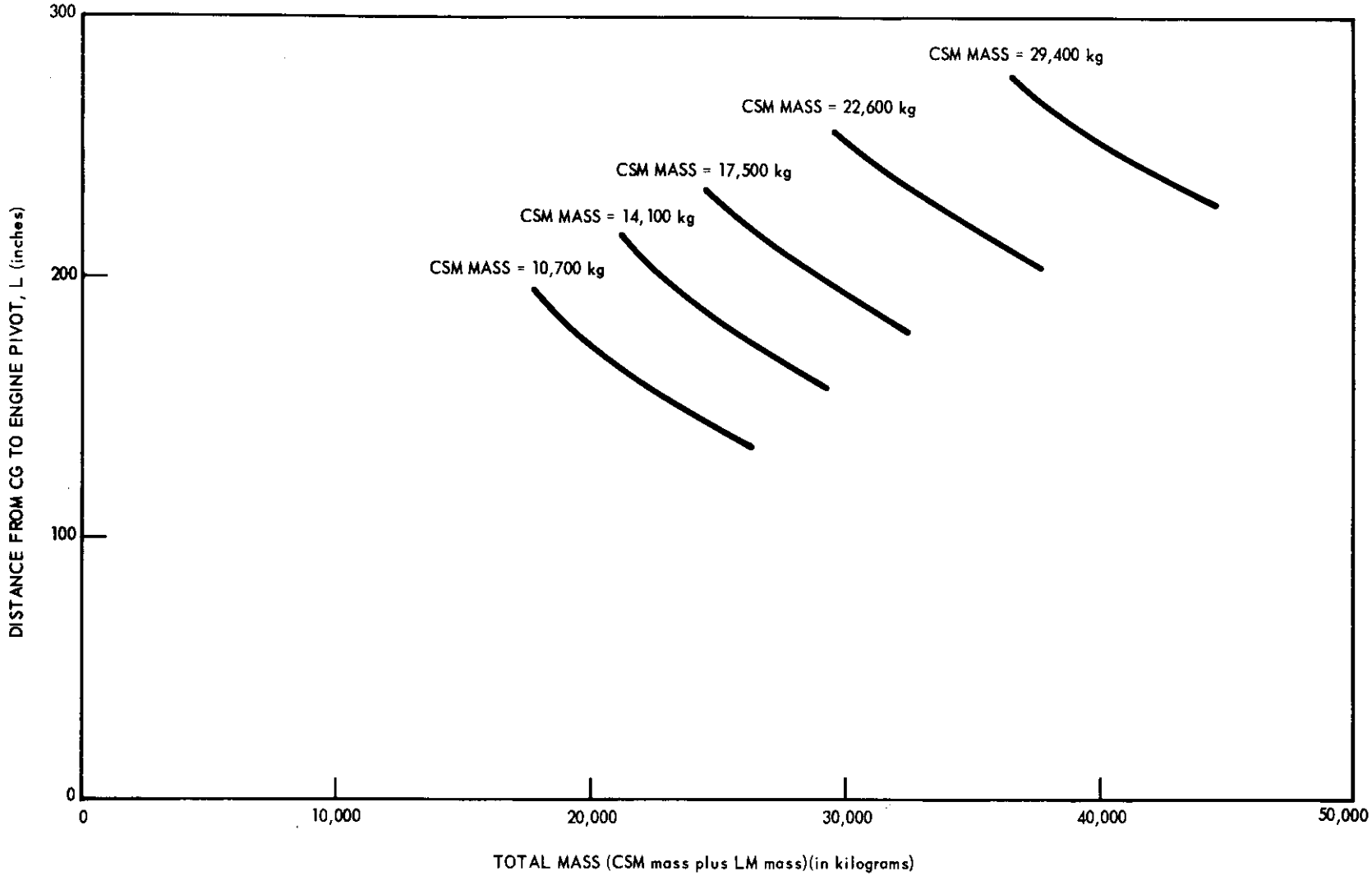

Fig. 3.3-4. The computed hinge-pin-to-center-of-gravity distance, L, in the CSM-docked case.

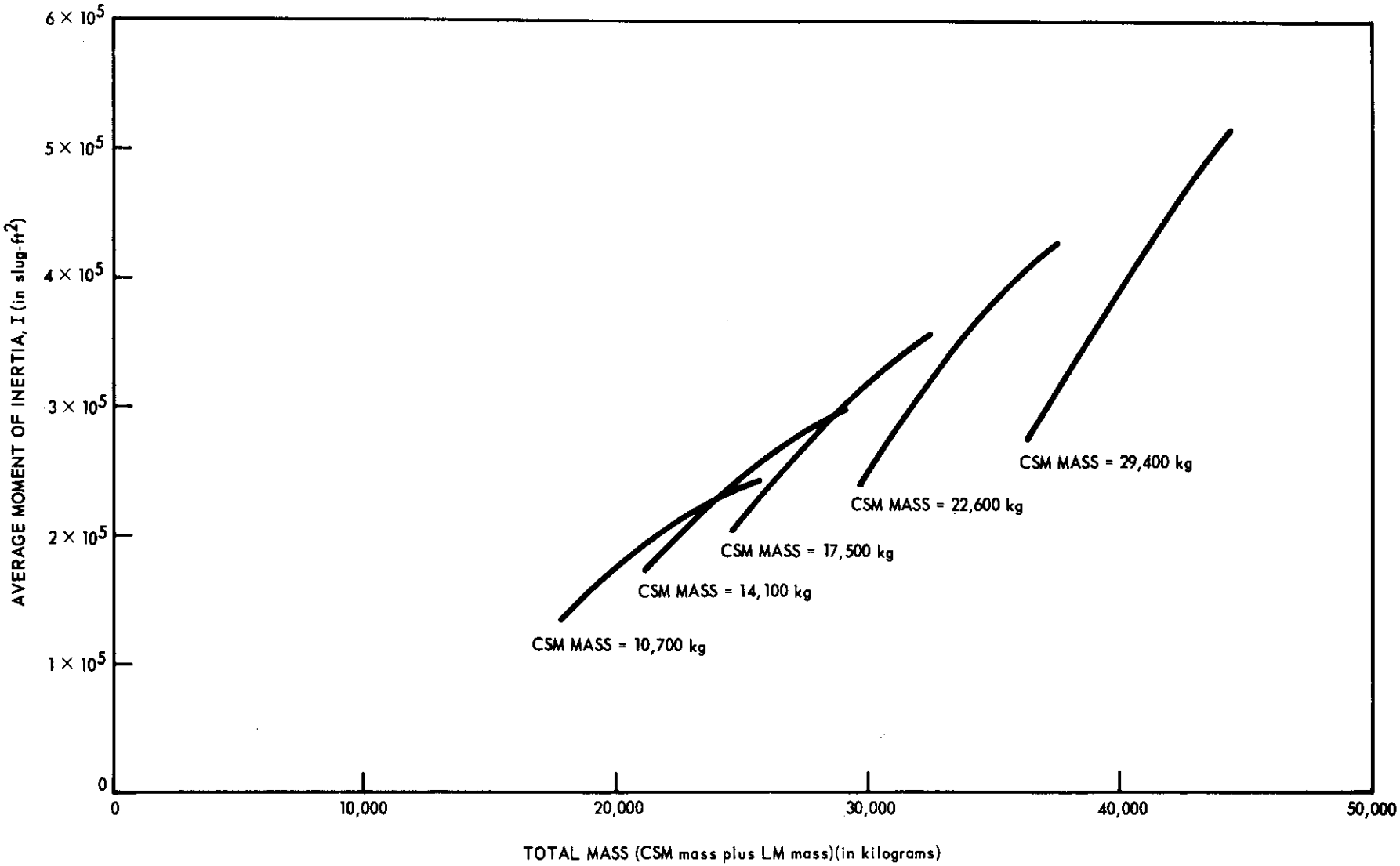

Fig. 3.3-5. The computed average moment of inertia, I, in the CSM-docked case.

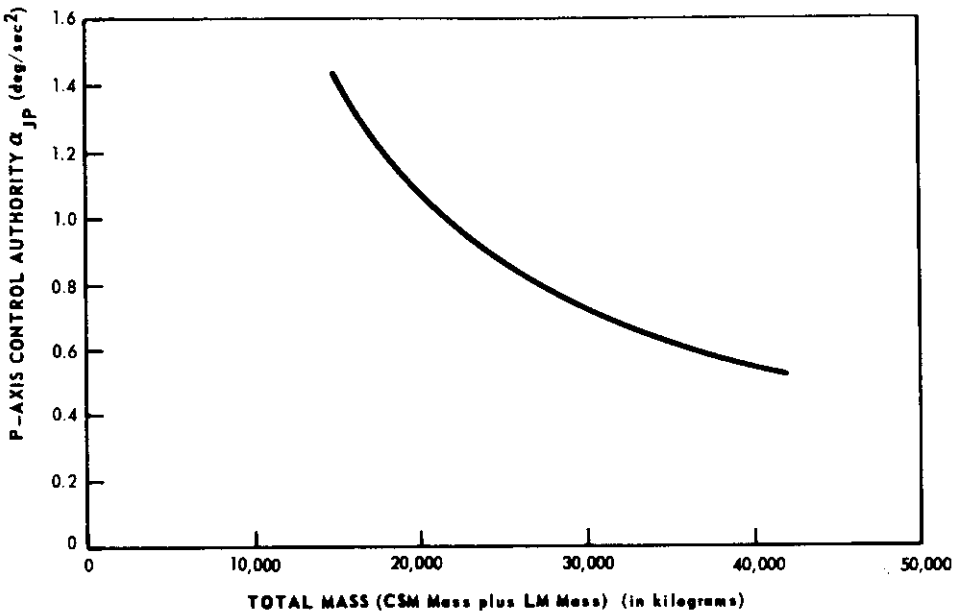

Fig. 3.3-5A. The computed P-axis control authority, α_{JP}, for the CSM-docked configuration.

3.3.2 The Recursive State Estimator*

3.3.2.1 General Discussion

The basic measurements of the vehicle state available to the LM DAP are the gimbal angles of the inertial measurement unit (IMU) as read by the electronic coupling data units (CDU's). For effective control, one must derive an estimate of the angular velocity of the vehicle. Furthermore, one must estimate any bias offset acceleration so that efficient RCS switch curves can be chosen in ascent powered flight or so that the trim gimbal may be used to steer and null the bias acceleration in descent powered flight. To separate any bias angular acceleration due to the main engine from the angular acceleration due to RCS jet firings, the state estimator needs additional inputs from the control laws containing the jet-firing information. Including jet-firing information as well as trim-gimbal-activity information gives an added benefit: the basic attitude inputs may be filtered as required, without necessarily introducing large lags into the estimates of angular velocity and bias angular acceleration.

A basic structure for combining internal estimates of state changes due to jet firings or trim-gimbal activity with external measurements of attitude is suggested by Kalman filter theory. A highly simplified single-plane model for the LM is given by

$$\left.\begin{aligned} \dot{\theta} &= \omega \\ \dot{\omega} &= \alpha + u_J \\ \dot{\alpha} &= u_G + n_{CG} \end{aligned}\right\} \qquad (3.3\text{-}10)$$

*By William S. Widnall.

where θ is the attitude, ω is the angular velocity, $\boldsymbol{\alpha}$ is the bias angular acceleration that results from the misalignment of the thrust vector with the LM center of gravity, u_J is the angular acceleration due to RCS jets, u_G is the rate-of-change of angular acceleration due to gimballing the descent engine, and n_{CG} is the rate-of-change of angular acceleration due to the center of gravity moving, the nozzle eroding, or other effects. The quantities u_J and u_G are control outputs from the guidance computer; n_{CG} is considered to be a process disturbance. These differential equations ignore many important aspects of the vehicle dynamics – such as propellant slosh, structural bending, jet-thrust lags, or trim-gimbal lags. By sampling the CDU's, the computer obtains a noisy measurement θ_m of the attitude θ; that is,

$$\theta_m = \theta + n_{CDU} \tag{3.3-11}$$

Some sources of the measurement noise, n_{CDU}, are high-frequency bending modes or vibration, the tracking-error angles of the CDU, and the quantization of the measurement when encoded into the computer.

The recursive state estimator for this stochastic process, from Kalman filter theory, has the following structure. Given the estimate of the state $\hat{\theta}$, $\hat{\omega}$, and $\hat{\boldsymbol{\alpha}}$ at sample instant t_{n-1} and given the known time history of u_J and u_G between t_{n-1} and t_n, the estimate of the state at sample time t_n in the absence of a measurement is obtained by integrating the differential equation of the vehicle, that is, Eq. (3.3-10). With no knowledge of the disturbance n_{CG}, a zero value is assumed. The GTS control laws usually change the drive u_G only at the control-sample instants; u_G is therefore assumed constant during the period from t_{n-1} to t_n (neglecting any variations in the control effectiveness, FLR/I). The RCS control laws will apply acceleration u_J at t_{n-1} and this will be held for a duration t_J, at which time the rotation jets are commanded off. The duration t_J as used in the state estimator is necessarily less than or equal to the basic control-sample period, T, of the LM DAP – where T is equal to $t_n - t_{n-1}$. The angular acceleration while the jets are firing is constant (neglecting any variations in the control effectiveness FL/I).

Consistent with these assumptions, Eq. (3.3-10) can be integrated explicitly. This yields the extrapolated estimated state θ', ω', and $\boldsymbol{\alpha}'$ before incorporation of the measurement:

$$\left.\begin{aligned}
\theta'(n) &= \hat{\theta}(n-1) + \hat{\omega}(n-1)T + \hat{\boldsymbol{\alpha}}(n-1)\frac{T^2}{2} + u_G\frac{T^3}{6} + u_J t_J\left(T - \frac{t_J}{2}\right) \\
\omega'(n) &= \hat{\omega}(n-1) + \hat{\boldsymbol{\alpha}}(n-1)T + u_G\frac{T^2}{2} + u_J t_J \\
\boldsymbol{\alpha}'(n) &= \hat{\boldsymbol{\alpha}}(n-1) + u_G T
\end{aligned}\right\} \tag{3.3-12}$$

The predicted attitude, θ', is then compared with the measured attitude, θ_m, and corrections to the estimated state are made that are proportional to the difference; that is,

$$\left.\begin{aligned} \hat{\theta}(n) &= \theta'(n) + K_\theta [\theta_m(n) - \theta'(n)] \\ \hat{\omega}(n) &= \omega'(n) + K_\omega \frac{1}{T} [\theta_m(n) - \theta'(n)] \\ \hat{\alpha}(n) &= \alpha'(n) + K_\alpha \frac{1}{T^2} [\theta_m(n) - \theta'(n)] \end{aligned}\right\} \qquad (3.3\text{-}13)$$

Kalman's theory provides recursive computations for determining theoretically optimal weights K_θ, K_ω, and K_α. In general, these weights are time-varying as functions of the number of sample periods that have elapsed since filter initialization. Required inputs to the gain-determination computations would include the uncertainty of the initial state estimate of the vehicle, the statistics of the vehicle disturbance, n_{CG}, and the statistics of the measurement noise, n_{CDU}. Unfortunately, one rarely has reasonable numerical values for the required statistical inputs. Furthermore, the assumption that the vehicle is governed exactly by the differential equation (3.3-10) is often very wrong. For example, the control effectiveness, u_J, assumed for the reaction jets is wrong if a jet has failed undetected. Therefore, it is bad practice in this application to use gains generated literally according to Kalman's theory. Rather, K_θ, K_ω, and K_α are determined by direct engineering considerations.

A most noticeable departure from Kalman theory is desirable because of the non-Gaussian nature of the measurement noise. The electronic CDU's are nonlinear tracking servos. If a gimbal angle is changing at a rate higher than 4.4 deg/sec, the angles read into the computer would have a time variation as shown in Fig. 3.3-6. The CDU samples the tracking-error angle 800 times per second and selects zero rate, low rate, or high rate, depending on the magnitude of the tracking error. If the error is less than about 0.008 deg, zero rate is selected. If the error is greater than 0.008 deg but less than 0.11 deg, the low rate of 4.4 deg/sec is selected. If the error is greater than 0.11 deg, the high rate of 70 deg/sec is selected. The magnitude of the penetration back into the low-rate region shown in Fig. 3.3-6 is a maximum of 70 deg/sec times 1/800 sec or about 0.09 deg. Thus, the CDU angle encoded into the computer for moderate angular velocities of the vehicle will contain a high-frequency noise having a peak-to-peak amplitude of about 0.09 deg.

Since the distribution of this noise is not Gaussian but rectangular, the noise may be rejected by a nonlinear filter logic. If the predicted vehicle attitude,

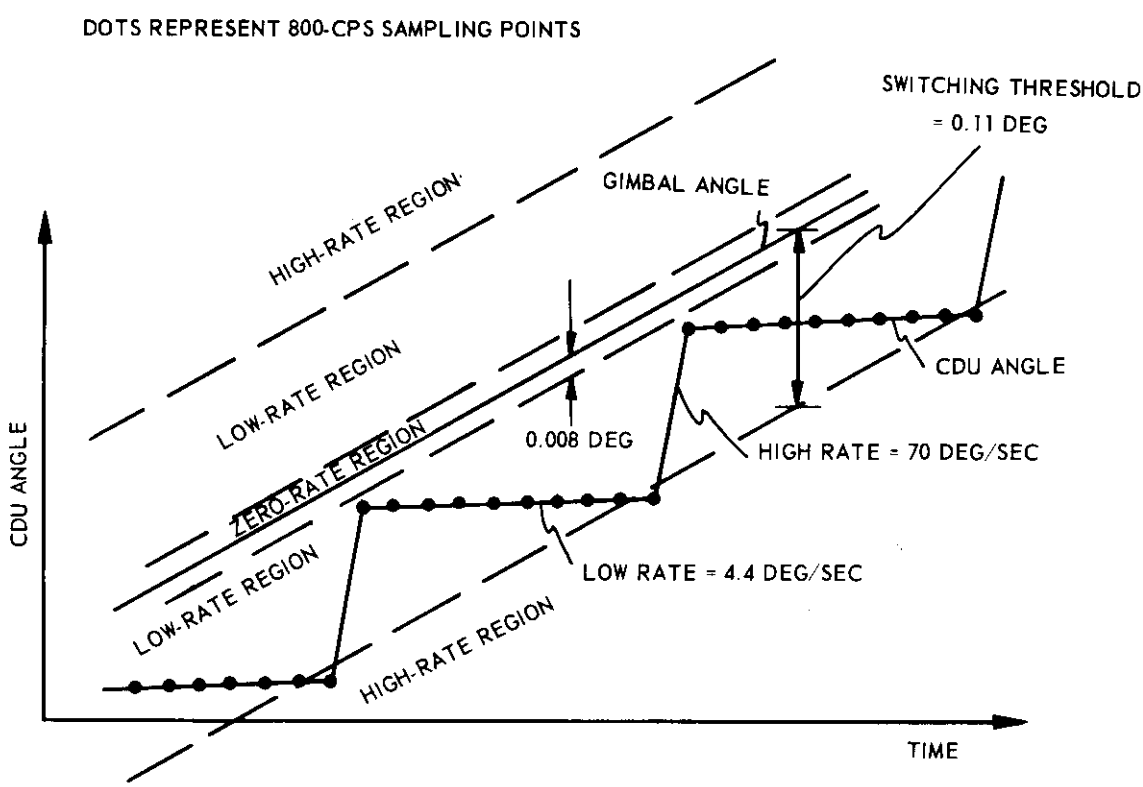

Fig. 3.3-6. CDU dynamics.

$\theta'(n)$, is within some threshold θ_{max} of the measured CDU angle $\theta_m(n)$, then the filter gains are set to zero. That is, the measurement is not incorporated into the state estimate. If, on the other hand, the error relative to the measurement of the predicted attitude exceeds the threshold, then nonzero gains are used to correct the state estimate. The proper numerical value for the threshold θ_{max} is somewhat larger than the expected peak-to-peak fluctuation in the CDU measurement.

The nonlinear threshold logic successfully rejects the low-level measurement noise. It is not necessary to include additional smoothing into the equation estimating attitude. Hence, whenever the threshold is exceeded, an attitude-filter gain, K_θ, of unity is selected. The filter gains chosen for the rate and acceleration estimates when the threshold is exceeded are functions of the number of sample periods, n_t, that have elapsed since the threshold was last exceeded. The functional form permits selection of appropriate time constants for the rate and acceleration estimates by choosing appropriate parameters N_ω and N_α. The functional form is given below in Eq. (3.3-14).

a) If $|\theta_m - \theta'| \leq \theta_{max}$, then

$$K_\theta = 0, \quad K_\omega = 0, \quad K_\alpha = 0$$

b) If $|\theta_m - \theta'| > \theta_{max}$, then

$$K_\theta = 1$$

$$K_\omega = \frac{1}{n_t + N_\omega}$$

$$K_\alpha = \frac{1}{n_t + N_\omega + N_\alpha} K_\omega \qquad (3.3\text{-}14)$$

The resulting modified Kalman filter given by Eqs. (3.3-12), (3.3-14), and (3.3-13) is, with minor differences, the angular state estimator implemented in the LM DAP. The actual calculations programmed in the LM DAP are given in the next subsection. The choice of the critical parameters θ_{max}, N_ω, and N_α is discussed in Subsection 3.3.2.3.

3.3.2.2 Estimator Calculations

The sequence of steps which must be programmed to implement the recursive state estimator is summarized in Fig. 3.3-7. The symbols used in this subsection for the variables in the state estimator are listed in Table 3.3-3. If there exists in the computer program assembly an explicit name for the variable, this tag is also listed. The input and output variables of the state estimator are indicated in Fig. 3.3-8.

Assumed Rate Change Due to RCS Firings

Given the signed firing durations (t_P, t_U, and t_V), the number of RCS jets selected (n_P, n_U, and n_V), and the assumed available angular accelerations (α_{PP}, α_{QU}, and α_{RU}), the estimated changes in the P, Q, and R angular velocities due to RCS jets selected during the last control-sample period are

$$\Delta\omega_P = \alpha_{PP} t_P n_P$$

$$\Delta\omega_Q = \alpha_{QU}(t_U n_U - t_V n_V)$$

$$\Delta\omega_R = \alpha_{RU}(t_U n_U + t_V n_V) \qquad (3.3\text{-}15)$$

The resolution of the U and V control torques into Q and R components has the above simple form because the two coordinate systems differ by 45 deg. The accuracy of the computed rate change depends on the accuracy of the following assumptions:

- P jets cause no Q or R accelerations.

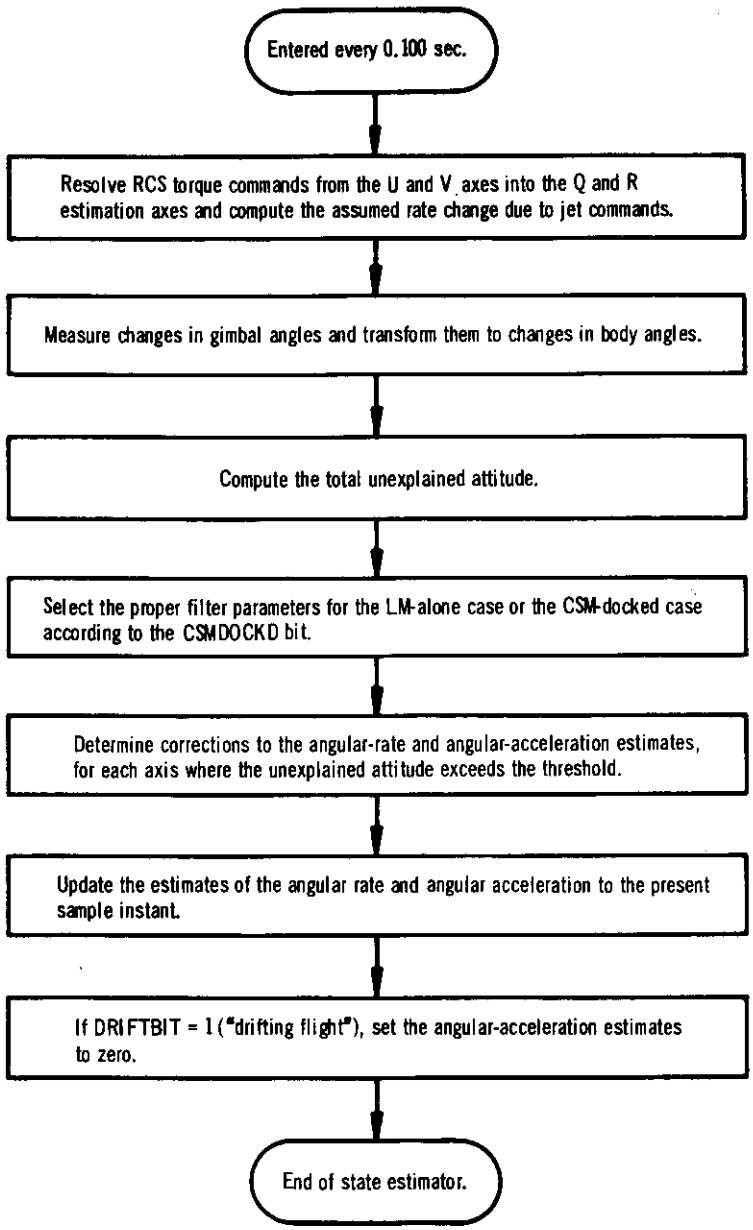

Fig. 3.3-7. Sequence of steps in the recursive state estimator.

- Q and R jets cause no P accelerations.
- The principal axes of inertia lie along the X, Y, and Z spacecraft axes.
- The RCS on-delays and off-delays may be neglected.
- There are no undetected RCS jet failures.
- Each RCS jet produces an effective thrust of 100 lb.
- Jet impulse is proportional to the duration of the electrical on-signal.

Table 3.3-3. State-estimator variables.

(Sheet 1 of 2)

Engineering Notation	Coding Tag	Definition
t_P t_U t_V	TJP TJU TJV	The signed firing durations of the RCS jets commanded during the last control-sample period for the P, U, and V axes. $0 \leq t \leq 0.100$ sec. A negative firing duration implies that negatively torquing jets were selected.
n_P n_U n_V	NO. PJETS NO. UJETS NO. VJETS	The number of RCS jets which were selected for the last control-sample period to provide torquing about the P, U, and V axes.
α_{PP}	1JACC	Magnitude of the P-axis angular acceleration which (it is assumed) will result from selecting one P RCS jet.
α_{QU} α_{RU}	1JACCQ 1JACCR	Magnitudes of the Q-axis and R-axis angular accelerations which (it is assumed) will result from selecting one U (or V) RCS jet.
$\Delta\omega_P$ $\Delta\omega_Q$ $\Delta\omega_R$	JETRATE JETRATEQ JETRATER	Estimated change in the P, Q, and R angular velocities due to RCS jets selected during the last control-sample period.
$\Delta\alpha_Q$ $\Delta\alpha_R$	____* ____	Estimated change in the Q and R bias angular accelerations due to descent-engine trim-gimbal control during the last control-sample period.
u_Q u_R	____ ____	Trim-gimbal drive signals (-1, 0, +1) for the Q and R channels.
$\dot{\alpha}_Q$ $\dot{\alpha}_R$	ACCDOTQ ACCDOTR	Magnitudes of the Q-axis and R-axis rates of change of angular acceleration which (it is assumed) will result from commanding Q and R trim-gimbal drives.
$\dot{\alpha}_Q u_Q$ $\dot{\alpha}_R u_R$	QACCDOT RACCDOT	Signed Q-axis and R-axis rates of change of angular acceleration commanded during the last control-sample period.
T	____	The autopilot control sample interval, 0.100 sec.

*The presence of a dash means that there is no explicit coding tag employed for this quantity. Rather, the quantity is just used temporarily and then destroyed.

Table 3.3-3. State-estimator variables.

(Sheet 2 of 2)

Engineering Notation	Coding Tag	Definition
θ_O	CDUX	CDU measurements of the outer, inner, and middle gimbal angles.
θ_I	CDUY	
θ_M	CDUZ	
θ_P	TRAPEDP	Total unexplained attitude, as incremental body angles.
θ_Q	TRAPEDQ	
θ_R	TRAPEDR	
K_ω	____	Rate gain.
K_{α}	____	Acceleration gain.
θ_{max}	TRAPSIZE	Measurement incorporation threshold.
N_ω	____	Constants used in computing K_ω and K_{α}. Approximately the rate and acceleration time constants as multiples of T.
N_{α}	____	
n_P	____	Number of sample periods that have elapsed since the P, Q, and R estimates of attitude exceeded the threshold.
n_Q	____	
n_R	____	
$n_P + N_\omega$	NPTRAPS	Threshold counter variables in the LM DAP.
$n_Q + N_\omega$	NQTRAPS	
$n_R + N_\omega$	NRTRAPS	
$\delta\omega_P$	____	Corrections to the P, Q, and R estimated angular velocities, due to the attitude measurements.
$\delta\omega_Q$	____	
$\delta\omega_R$	____	
$\delta\alpha_Q$	____	Corrections to the Q and R estimated bias accelerations, due to the attitude measurements.
$\delta\alpha_R$	____	
ω_P	OMEGAP	Estimated P, Q, and R components of the vehicle angular velocity.
ω_Q	OMEGAQ	
ω_R	OMEGAR	
α_Q	AOSQ	Estimated Q and R components of the vehicle bias angular acceleration.
α_R	AOSR	

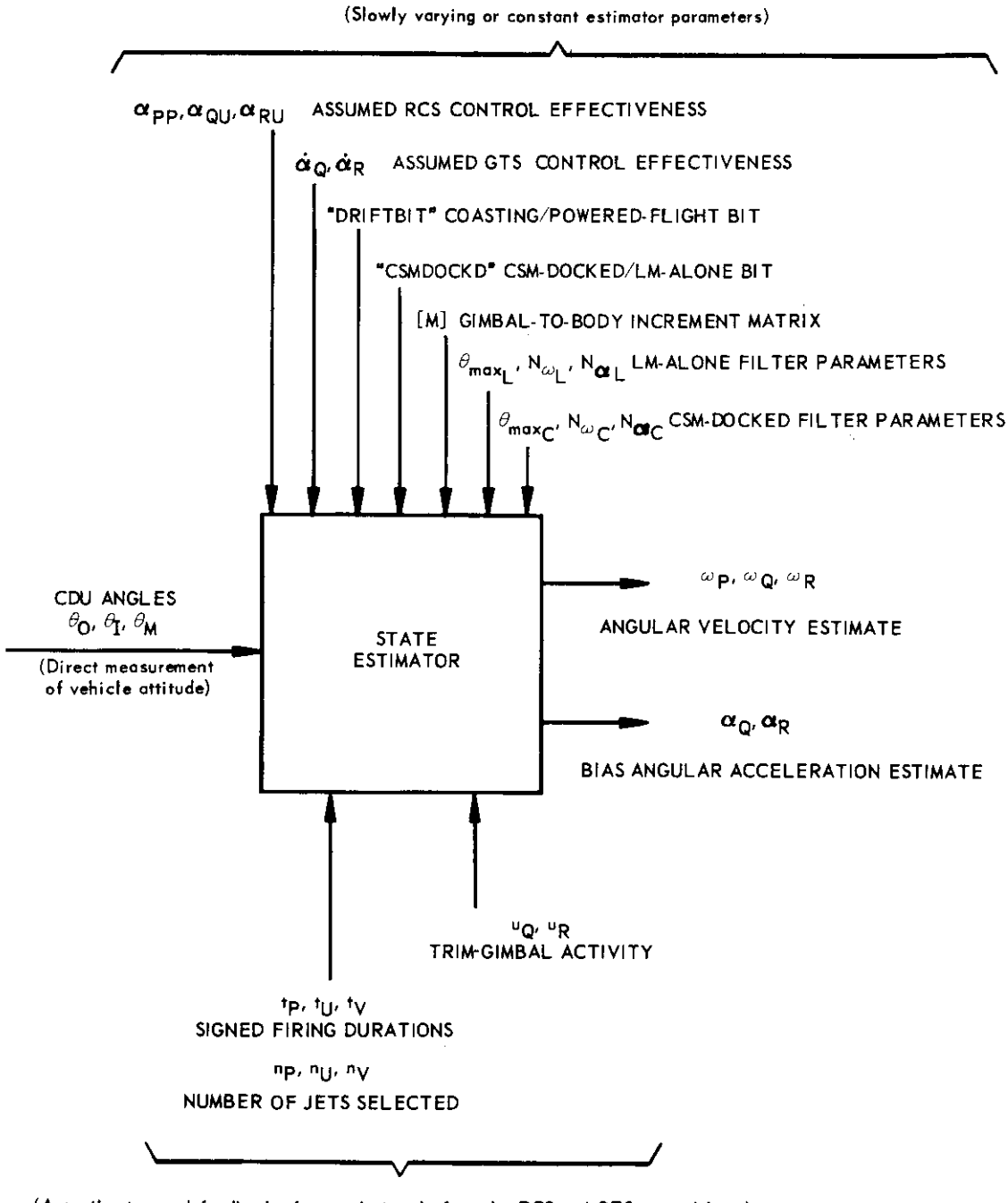

Fig. 3.3-8. Input and output variables of the state estimator.

The last two assumptions are known to be inaccurate, but the effect on the performance of the LM DAP is generally favorable. The thrust of the jets is somewhat lower than 100 lb. In addition, jet impingement forces on the descent-stage jet-plume deflectors change the effective thrust for +X thrusting jets. The specific impulse of jets for short pulses is lower than the specific impulse for long pulses. As a result, the impulse delivered falls below that predicted by the proportional assumption. In general, these assumptions cause the assumed rate change to be somewhat larger than the actual rate change. This is desirable for RCS control as it causes the control laws to "fire short" rather than "fire long". In the case of an undetected jet-off failure, the error introduced also leads to a "fire short" control policy.

Assumed Acceleration Change Due to Trim-Gimbal Commands

Given the trim-gimbal drive signals u_Q and u_R, and given the assumed available rates of change of angular acceleration $\dot{\alpha}_Q$ and $\dot{\alpha}_R$, the estimated changes in the Q and R bias angular accelerations due to trim-gimbal activity in the last control-sample period are

$$\left.\begin{aligned} \Delta\alpha_Q &= \dot{\alpha}_Q T u_Q \\ \Delta\alpha_R &= \dot{\alpha}_R T u_R \end{aligned}\right\} \qquad (3.3\text{-}16)$$

The underlying assumptions are as follows:

- Again, the principal axes of inertia lie along the X, Y, and Z spacecraft axes, so there is no cross-coupling.
- The trim-gimbal drives are started or stopped at the control-sample instants only.
- Gimbal on or off transients may be neglected.

Measured Change in Attitude

The CDU angles θ_O, θ_I, and θ_M observed during the last execution of the estimator computations have been remembered. The present CDU angles are observed, and the change in CDU readings is transformed to a change in body angles, as follows:

$$\begin{bmatrix} \Delta\theta_P \\ \Delta\theta_Q \\ \Delta\theta_R \end{bmatrix} = \begin{bmatrix} 1 & M_{PI} & 0 \\ 0 & M_{QI} & M_{QM} \\ 0 & M_{RI} & M_{RM} \end{bmatrix} \begin{bmatrix} \theta_O(n) - \theta_O(n-1) \\ \theta_I(n) - \theta_I(n-1) \\ \theta_M(n) - \theta_M(n-1) \end{bmatrix} \qquad (3.3\text{-}17)$$

The elements of the gimbal-rate to body-rate transformation matrix M are computed as a function of the observed CDU angles every 0.240 sec under the control of the Time-4 clock interrupt to be

$$M_{PI} = \sin(\theta_M)$$
$$M_{QI} = \cos(\theta_M)\cos(\theta_O)$$
$$M_{QM} = \sin(\theta_O)$$
$$M_{RI} = -\cos(\theta_M)\sin(\theta_O)$$
$$M_{RM} = \cos(\theta_O)$$

Total Unexplained Attitude

The difference between the measured change in attitude and the predicted change in attitude is accumulated to form the total unexplained attitude; that is,

$$\left.\begin{aligned}
\theta_P(n) &= \theta_P(n-1) + \Delta\theta_P - \left[\omega_P(n-1)T + \Delta\omega_P \frac{T}{2}\right] \\
\theta_Q(n) &= \theta_Q(n-1) + \Delta\theta_Q - \left[\omega_Q(n-1)T + \alpha_Q(n-1)\frac{T^2}{2} + \Delta\omega_Q \frac{T}{2}\right] \\
\theta_R(n) &= \theta_R(n-1) + \Delta\theta_R - \left[\omega_R(n-1)T + \alpha_R(n-1)\frac{T^2}{2} + \Delta\omega_R \frac{T}{2}\right]
\end{aligned}\right\} \quad (3.3\text{-}18)$$

Counters are incremented which indicate the number of control-sample periods that have elapsed since each channel of the estimator exceeded the threshold; that is,

$$n_P(n) = n_P(n-1) + 1, \qquad n_Q(n) = n_Q(n-1) + 1, \qquad n_R(n) = n_R(n-1) + 1 \quad (3.3\text{-}19)$$

A comparison of Eq. (3.3-18) with Eq. (3.3-12) shows that the predicted angle change due to gimbal drive is not included and the angle change due to jet firings is approximated by a simpler term. The effect of these approximations is considered to be small.

Rate and Acceleration Corrections

If the total unexplained attitude in any channel exceeds the threshold θ_{max}, then corrections are computed for the angular rate and bias angular acceleration estimates. The critical parameters defining the threshold and the time constants of the rate and acceleration estimates are stored in pad-loaded erasable. There are two sets of parameters: one for the CSM-docked case and one for the LM-alone case. The vehicle configuration assumed by the state estimator is determined by the bit CSMDOCKD of DAPBOOLS.

If CSMDOCKD = 1, then

$$\theta_{max} = \theta_{max_C}, \qquad N_\omega = N_{\omega_C}, \qquad N_\alpha = N_{\alpha_C}$$

If CSMDOCKD = 0, then

$$\theta_{max} = \theta_{max_L}, \qquad N_\omega = N_{\omega_L}, \qquad N_\alpha = N_{\alpha_L} \tag{3.3-20}$$

The P channel of the estimator includes the following computations:

If $|\theta_P(n)| \leq \theta_{max}$, then

$$\delta\omega_P = 0$$

If $|\theta_P(n)| > \theta_{max}$, then

$$K_\omega = \frac{1}{n_P + N_\omega}$$

$$\delta\omega_P = K_\omega \frac{1}{T} \theta_P(n)$$

$$\theta_P(n) = 0, \qquad n_P = 0 \tag{3.3-21}$$

The Q channel is similar, with the addition of the computation of the correction to the bias acceleration estimate.

If $|\theta_Q(n)| \leq \theta_{max}$, then

$$\delta\omega_Q = 0, \qquad \delta\alpha_Q = 0$$

If $|\theta_Q(n)| > \theta_{max}$, then

$$K_\omega = \frac{1}{n_Q + N_\omega}$$

$$K_\alpha = \frac{1}{n_Q + N_\omega + N_\alpha} K_\omega$$

$$\delta\omega_Q = K_\omega \frac{1}{T} \theta_Q(n)$$

$$\delta\alpha_Q = K_\alpha \frac{1}{T^2} \theta_Q(n)$$

$$\theta_Q(n) = 0, \qquad n_Q = 0 \tag{3.3-22}$$

The R channel is similar to the Q channel.

If $|\theta_R(n)| \leq \theta_{max}$, then

$$\delta\omega_R = 0, \qquad \delta\boldsymbol{\alpha}_R = 0$$

If $|\theta_R(n)| > \theta_{max}$, then

$$K_\omega = \frac{1}{n_R + N_\omega}$$

$$K_{\boldsymbol{\alpha}} = \frac{1}{n_R + N_\omega + N_{\boldsymbol{\alpha}}} K_\omega$$

$$\delta\omega_R = K_\omega \frac{1}{T} \theta_R(n)$$

$$\delta\boldsymbol{\alpha}_R = K_{\boldsymbol{\alpha}} \frac{1}{T^2} \theta_R(n)$$

$$\theta_R(n) = 0, \qquad n_R = 0$$

(3.3-23)

Rate and Acceleration Updates

The estimates of angular rate and bias angular acceleration are then updated to the present sample instant, including the incorporation of the corrections.

$$\omega_P(n) = \omega_P(n-1) + \Delta\omega_P + \delta\omega_P$$

$$\omega_Q(n) = \omega_Q(n-1) + \alpha_Q(n-1)T + \Delta\omega_Q + \delta\omega_Q$$

$$\omega_R(n) = \omega_R(n-1) + \alpha_R(n-1)T + \Delta\omega_R + \delta\omega_R$$

(3.3-24)

$$\boldsymbol{\alpha}_Q(n) = \boldsymbol{\alpha}_Q(n-1) + \Delta\boldsymbol{\alpha}_Q + \delta\boldsymbol{\alpha}_Q$$

$$\boldsymbol{\alpha}_R(n) = \boldsymbol{\alpha}_R(n-1) + \Delta\boldsymbol{\alpha}_R + \delta\boldsymbol{\alpha}_R$$

(3.3-25)

A comparison of Eq. (3.3-24) with Eq. (3.3-12) shows that the estimated rate change due to trim-gimbal activity in the last control-sample period has been omitted. The numerical importance of this omitted term is small.

Euler's equation for the angular acceleration of a spinning body, in body coordinates, is

$$\dot{\underline{\omega}} = I^{-1}[\underline{\tau} - \underline{\omega} \times I\underline{\omega}]$$

A comparison of Eq. (3.3-24) with Euler's equation shows that second-order terms in angular rate have been ignored.

Note from Eq. (3.3-25) that the P component of bias angular acceleration is assumed to be zero and is therefore not estimated. In periods of drifting flight,

it is assumed that the Q and R components of bias angular acceleration are also zero. A drifting- or powered-flight condition is assumed by the state estimator according to the bit DRIFTBIT of DAPBOOLS. Accordingly, the final step in the state estimator is:

$$\left.\begin{array}{l}\text{If DRIFTBIT = 1, then} \\ \qquad \alpha_Q(n) = 0, \qquad \alpha_R(n) = 0\end{array}\right\} \qquad (3.3\text{-}26)$$

The estimate of angular velocity is implemented in the LGC scaled for a maximum possible value of 45 deg/sec. To ensure that the LM DAP will correctly attempt to damp a high tumbling rate, the computations of angular velocity are checked for overflow. A computation which causes overflow is reset to the properly signed maximum value.

3.3.2.3 Selection of Critical Filter Parameters

The dynamic characteristics of the state estimator are dominated by three critical parameters: 1) the threshold θ_{max} for measurement incorporation, 2) the rate gain constant, N_ω, and 3) the acceleration gain constant, N_α. There are two independent sets of these three parameters: one for the CSM-docked case and the other for the LM-alone case. These six parameters must be specified as part of the erasable memory load provided for the computer. The six values required in the erasable load are stated in Table 3.3-4.

For both the LM-alone case and the CSM-docked case, the threshold for measurement incorporation has been set at 0.14 deg. The threshold is set to reject CDU measurement noise as well as small-amplitude vibration or bending. The peak-to-peak CDU measurement noise is about 0.09 deg (discussed previously in Subsection 3.3.2.1). The threshold setting of 0.14 deg satisfactorily rejects the CDU noise with some additional margin for spacecraft vibration and bending.

Table 3.3-4. State estimator erasable load.

Parameter	LGC Tag	Numerical Value
$-\theta_{max_C}$	DKTRAP	$77001_8 = -510_{10}$ (0.14 deg scaled at 4.5 deg)
N_{ω_C}	DKOMEGAN	$00012_8 = 10_{10}$ (the integer 10)
N_{α_C}	DKKAOSN	$00074_8 = 60_{10}$ (the integer 60)
$-\theta_{max_L}$	LMTRAP	$77001_8 = -510_{10}$ (0.14 deg scaled at 4.5 deg)
N_{ω_L}	LMOMEGAN	$00000_8 = 0_{10}$ (the integer 0)
N_{α_L}	LMKAOSN	$00074_8 = 60_{10}$ (the integer 60)

The proper choice for the rate gain constants N_{ω_L} and N_{ω_C} and the acceleration gain constants N_{α_L} and N_{α_C} is best understood by an analysis of the state estimator as a frequency-domain filter. In the presence of a sufficiently large unmodeled disturbance such as fuel slosh, or bending, or an undetected jet on-failure, the unexplained attitude θ will exceed the threshold θ_{max} every control-sample period. The computed rate gain K_ω and acceleration gain K_α take on constant values.

$$\left.\begin{aligned} K_\omega &= \frac{1}{1+N_\omega} = \begin{cases} 1 \text{ for the LM-alone case} \\ \frac{1}{11} \text{ for the CSM-docked case} \end{cases} \\ K_\alpha &= \frac{1}{1+N_\omega+N_\alpha}K_\omega = \begin{cases} \frac{1}{61} \text{ for the LM-alone case} \\ \frac{1}{71}\times\frac{1}{11} \text{ for the CSM-docked case} \end{cases} \end{aligned}\right\} \quad (3.3\text{-}27)$$

With constant values for the rate and acceleration gains, the estimator is governed by a set of constant-coefficient linear difference equations. One may therefore apply the standard techniques of frequency-domain analysis; namely, one may compute the Z-transform.

In a single-plane analysis, the transmission of the estimator from attitude measurement θ_m to rate estimate $\hat{\omega}$ and acceleration estimate $\hat{\alpha}$ is governed by Eqs. (3.3-12) and (3.3-13). One may compute the Z transform of this set of equations. The result (for $K_\theta = 1$) is

$$\left.\begin{aligned} \frac{\hat{\omega}}{\theta_m}(z) &= \frac{\left(z-1+\frac{K_\alpha}{K_\omega}\right)(z-1)\frac{K_\omega}{T}}{z^2+\left(-2+K_\omega+\frac{K_\alpha}{2}\right)z+\left(1-K_\omega+\frac{K_\alpha}{2}\right)} \\ \frac{\hat{\alpha}}{\theta_m}(z) &= \frac{(z-1)^2\frac{K_\alpha}{T^2}}{z^2+\left(-2+K_\omega+\frac{K_\alpha}{2}\right)z+\left(1-K_\omega+\frac{K_\alpha}{2}\right)} \end{aligned}\right\} \quad (3.3\text{-}28)$$

These transforms apply to the Q and R channels of the estimator in powered flight (when DRIFTBIT = 0). The P channel of the estimator always assumes zero bias acceleration, as do the Q and R channels in drifting flight (when DRIFTBIT = 1). For these cases, the Z-transform of the rate estimate is simply

$$\frac{\hat{\omega}}{\theta_m}(z) = \frac{(z-1)\frac{K_\omega}{T}}{z-1+K_\omega} \quad (3.3\text{-}29)$$

One may compute the transmission of the filter to a sinusoidal input by evaluating the Z-transform with $z = e^{j2\pi fT}$. A plot of the estimate of rate alone, based on Eq. (3.3-29), is given in Fig. 3.3-9.

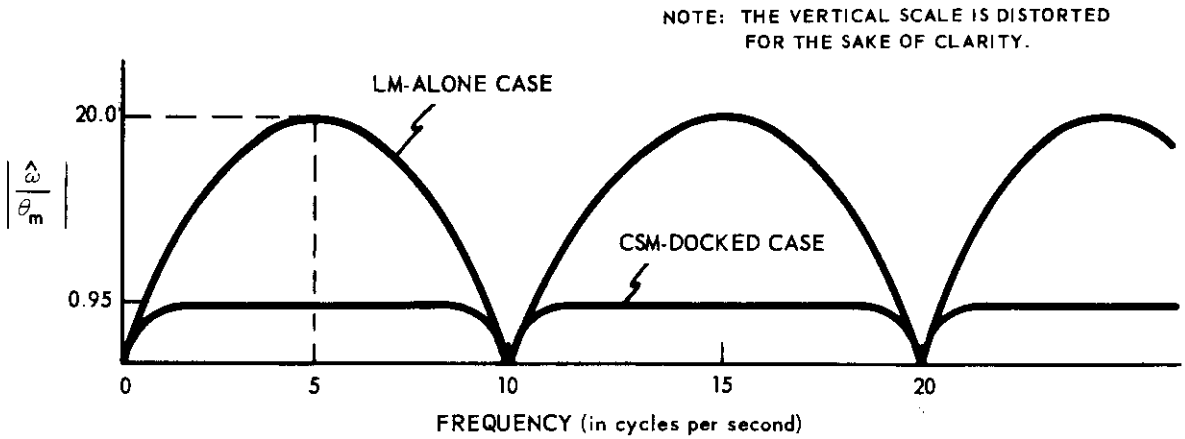

Fig. 3.3-9. Magnitude of the rate-filter frequency response when estimating rate alone.

Assuming that the nonlinear threshold logic successfully rejects the noise and vibration, one wishes to set the rate gain as high as possible to obtain fast, accurate tracking of the vehicle angular velocity. A slow rate filter can have serious errors in the presence of unmodelled angular accelerations. It can be shown that for a steady unmodelled acceleration, α, the steady error in the rate estimate at the control-sample instant is

$$\omega - \hat{\omega} = \left(\frac{T}{K_\omega} - \frac{T}{2}\right)\alpha \qquad (3.3\text{-}30)$$

For a light ascent vehicle with one jet failed-on undetected, α could be 20 deg/sec^2. With a low rate gain of, for example, $K_\omega = 0.1$, the rate-estimation error would be 19 deg/sec. With the large rate gain of $K_\omega = 1.0$, the rate-estimation error is only 1 deg/sec.

However, the high rate gain can not be used in the CSM-docked configuration because of possible bending-mode instabilities. Figure 3.3-9 shows that for a bending oscillation measured at the navigation base as having an amplitude of 1 deg, for the rate gain $K_\omega = 1$ the estimated angular velocity may be as large as 20 deg/sec. This level of rate estimate would far exceed the threshold of the CSM-docked RCS logic, so RCS firings would be commanded. The lag in the estimate of about 0.050 sec combined with the effective lag of about 0.100 sec in the control law, due to re-evaluating the jet firing state only every 0.200 sec (Q and R channels, powered flight) cause the applied jet torques to reinforce the angular velocity, rather than oppose the angular velocity. That is, for the

high rate gain, there could be a phase instability. Therefore, for the CSM-docked configuration, the low rate gain of $K_\omega = 1/11$ is used. Figure 3.3-9 shows that for a bending oscillation of 1-deg amplitude, the estimated angular velocity will be less than 1 deg/sec. This level of estimated rate activity is not sufficient to break out of the RCS control law drift zone, so there will not be jet firings strongly correlated with the bending activity.* That is, for the low rate gain, the LM DAP is gain-stabilized. The cost of gain-stabilizing the docked bending modes is that the effective time constant of the rate filter has been lengthened to 1.1 sec. Equation (3.3-30) shows to what extent the rate estimator is more susceptible to unmodelled steady accelerations. However, for the CSM-docked configuration, where the vehicle is so much heavier, the possible values of acceleration, α, are proportionately reduced. Hence, the slower rate estimate should not introduce difficulties.

The Z-transforms for the rate and acceleration estimates (Q or R channel in powered flight) are given in Eq. (3.3-28). One may check the stability of the filter by examining the roots of the denominator. For the LM-alone case ($K_\omega = 1$, $K_\alpha = 1/61$), the roots are located at about $z = 1 - (1/61)$ and $z = 1/122$. Since both roots lie inside the unit circle, the filter is stable. The behavior of the acceleration estimate is dominated by the root near $z = 1$. This gives the acceleration estimate a time constant of 6.1 sec. In the rate estimate, the zero at $z = 1 - (1/61)$ essentially cancels one pole. Thus, the behavior of the rate estimate is very similar to that of the first-order filter for the drifting-flight case.

For the CSM-docked case [$K_\omega = 1/11$, $K_\alpha = (1/71) \times (1/11)$], the roots of the denominator are located at about $z = 1 - 0.074$ and $z = 1 - 0.017$. Again, the filter is stable. The dominant time constant of the acceleration estimate is now 5.9 sec. The dominant time constant of the rate estimate is 1.3 sec.

The transmission of the acceleration estimate to a sinusoidal input is shown in Fig. 3.3-10.

The proper choice of the acceleration gain is a balance between the need to heavily filter unwanted disturbances such as slosh and bending and the need to have reasonable transient control. Various gains for the control laws are computed every two seconds (in a subroutine called 1/ACCS) according to the present estimate of bias angular acceleration. If the bias-acceleration estimator followed sinusoidal disturbances such as bending or propellant slosh, the resulting fluctu-

*Simulations indicated that the use of low filter gains did not prevent bending-mode instabilities in the presence of large unmodeled disturbing accelerations during coasting flight. Consequently, jet-inhibition logic was added to the CSM-docked autopilot to reduce the probability of exciting and sustaining bending oscillations (see Subsection 3.4.3). Although this bending-stability improvement may allow the use of higher CSM-docked filter gains, the old low gains will be retained until the performance and stability with higher gains has been thoroughly tested and evaluated.

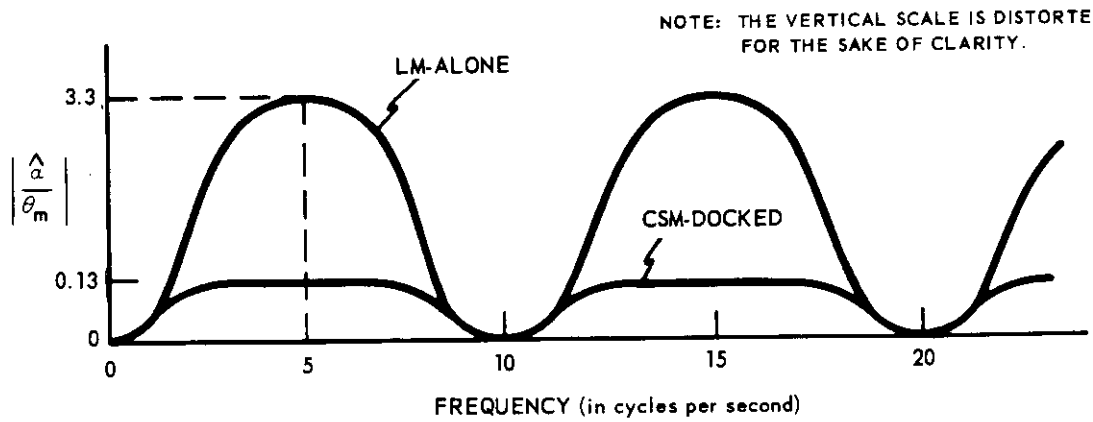

Fig. 3.3-10. Magnitude of the acceleration-filter frequency response.

ations in the autopilot gains would produce unpredictable performance. If, on the other hand, the acceleration-estimate time constant was too great, there would be a prolonged transient in ascent powered flight characterized by inefficient jet firings while the bias-acceleration estimate reached steady-state. In descent powered flight, with the propellant shifting between tanks, the bias-acceleration estimate would be noticeably lagging the actual acceleration. With the trim gimbal following steering commands or servoing to the estimated null-acceleration position, the steady-state lagging trim-gimbal angle would cause unnecessary jet firings.

The values of filter gains selected appear to satisfy the various requirements. Figure 3.3-10 shows that, for a sinusoidal disturbance of 1-deg amplitude, the error in the bias-acceleration estimate for the LM-alone case will not exceed 3.3 deg/sec^2 and for the CSM-docked case will not exceed 0.13 deg/sec^2. Propellant slosh modes, with frequencies usually of the order of 0.5 cycles per second, will induce errors well below these maxima. Testing of the ascent powered flight indicates an acceptable start transient with an offset center of gravity. Testing of descent powered flight with initial propellant unbalance indicates only a few extra kilograms of RCS fuel are consumed in opposing the torque due to the lagging trim gimbal.

It is important to note the behavior of the acceleration estimate with jet failures. Given that there is a fixed bias angular acceleration, and assuming that the closed-loop autopilot is successfully maintaining attitude control, then the average rate must be zero. The average attitude is a constant. The average estimates of rate and acceleration must be constant. The average change in bias acceleration due to trim-gimbal activity will be zero. Using equations developed earlier (but interpreting the symbols as representing average values rather than instantaneous values), with $\alpha(n) = \alpha(n-1)$ and $\Delta\alpha = 0$, Eq. (3.3-25) shows that the average correction $\delta\alpha$ must be zero. But if $\delta\alpha = 0$, Eq. (3.3-23) shows that the rate correction $\delta\omega$ will also be zero. With $\omega(n) = \omega(n-1)$ and $\delta\omega = 0$, Eq. (3.3-24) shows that the average estimated bias angular acceleration must be related to the average assumed rate change due to firing RCS jets as follows:

$$\langle \hat{\alpha} \rangle T = - \langle \Delta \hat{\omega} \rangle \qquad (3.3\text{-}31)$$

With a fixed bias angular acceleration, α, and the autopilot successfully maintaining attitude control, the average actual rate change due to RCS jet firings must balance the rate change due to the offset acceleration; that is,

$$\alpha T = - \langle \Delta \omega \rangle \qquad (3.3\text{-}32)$$

But if one jet of the two-jet torque pair is failed-off undetected, the moment offset is balanced by firing the remaining jet twice as long. The value assumed in the estimator for control effectiveness is the two-jet value. This value times the longer firing duration leads to computed assumed rate changes which are, on the average, double the actual rate changes. This leads to an average value for the estimated bias acceleration which is double the actual bias acceleration.

The steady-state behavior noted for the acceleration estimate is independent of the numerical values for the rate and acceleration gains. Fortunately, there is no error in the sign of the estimate – only in the magnitude. Thus, a simple acceleration nulling control law will still seek the center of gravity properly in the presence of jets failed-off undetected.

REFERENCES FOR SUBSECTION 3.3

1. "LM-3 Mass Properties," given in GN & C Data Submittal Form No. MSC-S-52, dated 2 October 1967. [Identical with: Owen E. Maynard, "Transmittal of LM-3 Mass Properties Data," NASA MSC memo PM3/M-215/67, October 6, 1967.]

2. "CM-103 and LM-3 (Separate and Combined) Mass Properties," given in GN & C Data Submittal Form No. MSC-S-59, dated November 14, 1967.

3. Kalan, G. R., P-Axis Control Authority Computation for the CSM-Docked Configuration, Spacecraft Autopilot Development Memorandum No. 17-69, Instrumentation Laboratory, Massachusetts Institute of Technology, Cambridge, Massachusetts, March 26, 1969.

SUBSECTION 3.4

THE RCS CONTROL LAWS

by

Richard D. Goss, Lowell Hull, George R. Kalan, Donald W. Keene,
Edgar M. Oshika, and Robert F. Stengel*

The LM DAP must determine which of the 16 RCS (reaction control system) jets are to be fired, and for what durations, in order to maintain attitude control and to provide translation. The rotational and translational demands are determined separately. The requirements for rotational impulses are computed in various RCS control laws, depending on the vehicle configuration, the autopilot mode selected, the guidance or manual commands, and the estimated angular state. The translation-acceleration requirements are given directly by the guidance or manual commands. No translational firing times are computed; a requirement is taken to exist for as long as the command exists and ends when the command is found to have been removed. Additional logic merges the required rotational impulses with the commanded translation acceleration to select the appropriate jets.

An "automatic control law" is employed whenever the primary guidance, navigation, and control system of the LM – rather than the LM astronaut – is commanding the orientation of the spacecraft. There are two distinct automatic control laws, one for each of the two following cases:

1. The case when the LM is operating alone, that is, when it is not docked to the CSM. (For convenience, this case is referred to herein as the "LM-alone case".)
2. The case when the LM and the CSM are docked. (For convenience, this case is referred to herein as the "CSM-docked case".)

The automatic control law for the LM-alone case is discussed in Subsection 3.4.2; that for the CSM-docked case is discussed in Subsection 3.4.3.

*The authorship of specific portions of Subsection 3.4 is indicated by appropriate footnotes.

When the LM astronaut is directly exercising attitude control of the spacecraft a manual control law is used. The RCS control laws for the rate command, X-axis override, and minimum impulse modes are discussed in Subsection 3.4.4.

The computation of TJET, the required duration of rotational-torque jet firing, is the primary topic discussed in Subsections 3.4.2 through 3.4.4. Subsection 3.4.5 then discusses the jet select logic whereby the LM DAP selects particular jets to accomplish the required rotation and translation – taking into account any disabled jets.

3.4.1 Nonorthogonal Axis System for the RCS Control Laws*

There are two sets of control axes that must be considered when applying the RCS control laws. The first of these is the orthogonal P, U, V system. The P axis is coincident with the vehicle X axis, and the U and V axes (the "diagonal axes") pass through the RCS jet quads. These axes correspond to the nominal torque directions that result from firing individual RCS jets. For simplicity in the jet select logic, a decision was made to design the control laws such that the P jets, the U jets, and the V jets could be commanded independently of each other. In general, however, a U jet produces an angular acceleration not only about the U axis but also (a coupled component) about the V axis. A similar situation exists for a V jet. If the coupled components are not explicitly considered, then some degradation in control will result. The existence of the coupling problem motivated the selection of the nonorthogonal P, U', V' control-axis system that is used in the LM DAP. The U'-V' axes of this system are described in Fig. 3.4-A. In this system, a U jet will produce a component of acceleration about the U' axis and no component of acceleration about the V' axis. Similarly, a V jet will produce a component of acceleration about the V' axis and no component of acceleration about the U' axis. Changes that are to be made in the vehicle attitude state are determined in the P, U', V' system.

A constraint that has been imposed on the U'-V' system in the LM DAP is that it is not allowed to deviate from the U-V system by more than 15 deg. If larger deviations were allowed, excessively large vehicle angles and rates could result about one of the principal axes, Q or R. In particular, if the U'-V' axes are skewed by an angle δ away from the U-V axes and phase-plane angular excursions about the U' and V' axes are controlled to lie within an angle $\pm$ DB, then corresponding angular excursions about one of the principal axes can be as large as $DB/\cos(45^\circ + |\delta|)$. The 15-deg limitation allows a maximum gain of 2 between U'-V' excursions and Q-R excursions.

---

* By Richard D Goss.

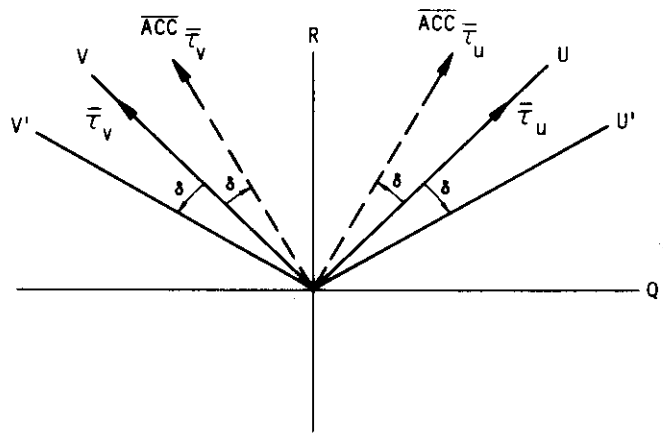

$$\cos\delta = \frac{(I_Q + I_R)}{\sqrt{2(I_Q^2 + I_R^2)}} \qquad \sin\delta = \frac{(I_Q - I_R)}{\sqrt{2(I_Q^2 + I_R^2)}}$$

$\bar{\tau}_U$ = TORQUE ABOUT THE U AXIS

$\bar{\tau}_V$ = TORQUE ABOUT THE V AXIS

$\overline{ACC}\,\bar{\tau}_U$ = ACCELERATION PRODUCED BY $\bar{\tau}_U$

$\overline{ACC}\,\bar{\tau}_V$ = ACCELERATION PRODUCED BY $\bar{\tau}_V$

Fig. 3.4-A. The U'–V' axes of the nonorthogonal axis system for the RCS control laws.

3.4.1.1 Nonorthogonal Transformation from the Q-R System to the U'-V' System

The transformation in the LM DAP that is used whenever any quantities E_Q, E_R are to be transformed from the Q-R system to the U'-V' system is given by the equations

$$E_{U'} = - \text{COEFFQ } E_Q + \text{COEFFR } E_R$$

$$E_{V'} = \text{COEFFQ } E_Q + \text{COEFFR } E_R$$

(The transformation is done in the ROT-TOUV section of the program.) The coefficients COEFFQ and COEFFR are determined in the LM DAP by the procedure illustrated in the flow chart of Fig. 3.4-B. The equations are an approximation of the exact solution, which requires the time-consuming computation of a square root. (The approximation produces a maximum error of approximately 1%). The computation of COEFFQ and COEFFR is made in the 1/ACCS routine, which in powered flight is executed every two seconds. Immediately after the computation of COEFFQ and COEFFR, the one-jet control acceleration 1JACCU' is computed. 1JACCU' is used as the one-jet control acceleration for both the U' and V' axes. The equation for this acceleration is also given in Fig. 3.4-B.

A detailed discussion of the nonorthogonal axis system for the LM DAP is provided in Reference 4.

3.4.2 The RCS Control Law for Automatic Control in the LM-Alone Case*

For automatic control in the LM-alone case, the LM DAP must repetitively provide the RCS thrusting time required for each of the three RCS control axes. Specifically, this means that, for a given axis, the LM DAP must compute the jet burning time, TJET, that will produce a limit cycle (within specified error-angle deadbands) of the LM's actual attitude and attitude rate about a desired LM attitude and attitude rate. This action is carried out in accordance with an RCS control law termed TJETLAW.

3.4.2.1 The General Nature of TJETLAW

In order to apply TJETLAW, an angular error – error rate phase plane is defined for each of the RCS control axes, P, U', and V'. The angular error, E, is the difference between the actual and desired attitudes of the LM for a given LM axis; the error rate, $\dot{E}$, is the derivative of E with respect to time and is identical with the rate error, that is, the difference between the actual (estimated) and commanded rates, as long as the commanded rate is the derivative of the commanded attitude. On the basis of the components of the vehicle state in each of the three control-axis phase planes, TJETLAW computes a jet burning time for each axis. In accordance with these jet burning times, the P-, U-, and V-axis jets are turned on and off independently of one another.

*By Richard D. Goss.

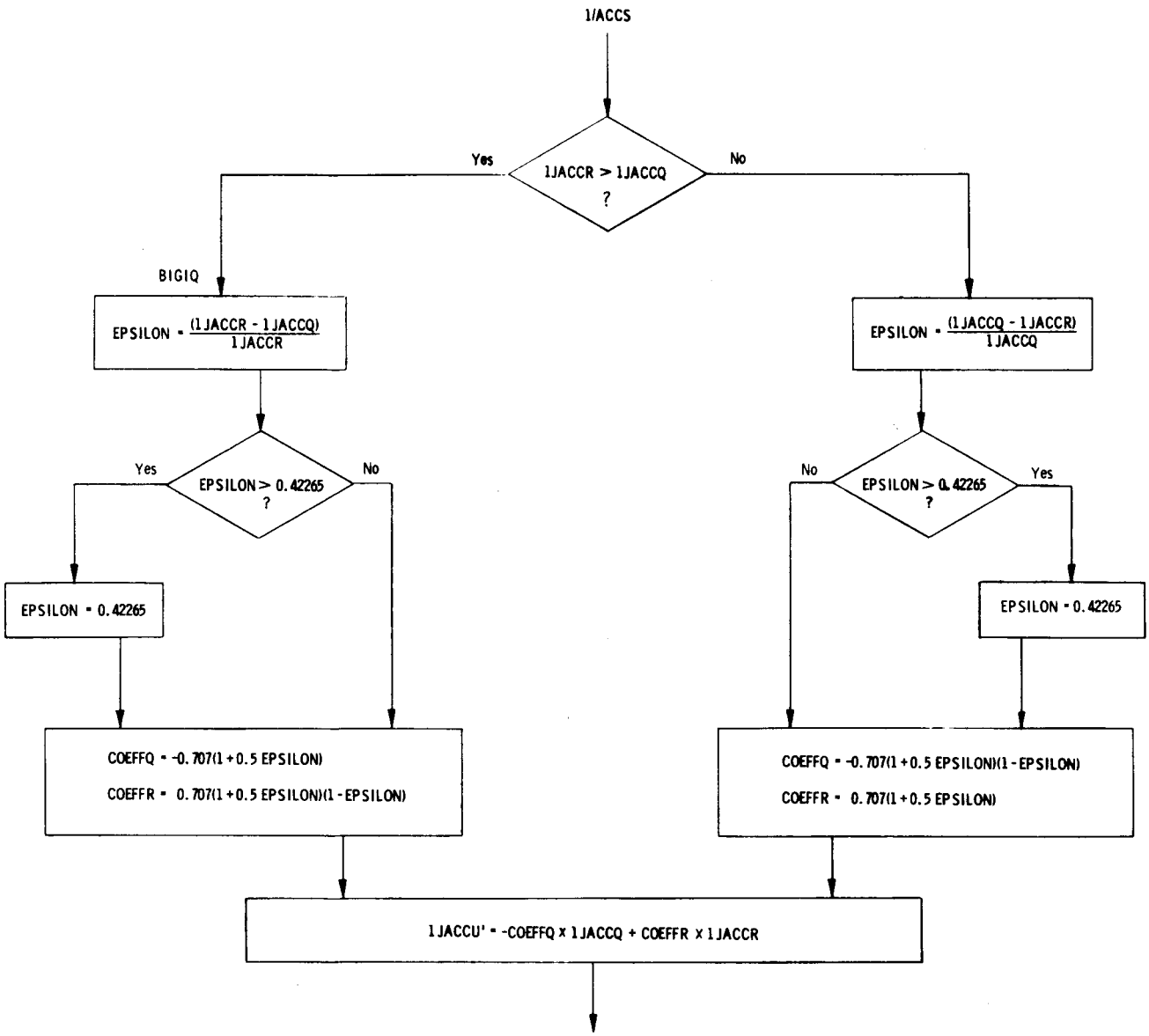

Fig. 3.4-B. Flow chart for the computation of nonorthogonal transformation coefficients.

For a given axis, the time between computations of TJET may be either 0.100 sec or 0.200 sec. The 0.200-sec interval results whenever a "skip" of the TJET computation has been requested. A skip request is made for an axis whenever TJET has been determined to be less than 0.150 sec but not zero. If TJET is either zero or greater than 0.150 sec, no skip is requested and a new computation of TJET is made in 0.100 sec. If TJET is computed to be greater than 0.150 sec, the jets are turned on "open-loop" (that is, no turn-off time is specified).

The control logic used to determine TJET can be described by dividing the angular error – error rate phase plane into zones. Figures 3.4-1 through 3.4-4 illustrate the four phase-plane configurations used by TJETLAW to compute TJET and the corresponding sets of zones.

The configuration shown in Fig. 3.4-1 is used whenever the magnitude of E exceeds 11.25 deg or whenever the magnitude of $\dot{E}$ exceeds 5.625 deg/sec. In this case, a form of TJETLAW called ROUGHLAW is employed. Whenever neither of these limits are exceeded, a form of TJETLAW called FINELAW is employed. This latter law uses the appropriate configuration from Figs. 3.4-2 through 3.4-4 – in accordance with the particular type of flight in which the LM is engaged. The use of ROUGHLAW for large values of E and $\dot{E}$ allows single-precision arithmetic to be used by the LM guidance computer (LGC) in computing TJET for all values of E and $\dot{E}$.

The following discussion describes the two forms of TJETLAW.

3.4.2.2 Description of ROUGHLAW

As shown by Fig. 3.4-1, the phase-plane configuration associated with ROUGHLAW is divided into zones A through D. This division is made for both the upper and lower half-planes. For simplicity, only the upper-half-plane case is described here. (TJET is computed in the same way for the corresponding zones of the lower half-plane.)

Table 3.4-1 sets forth the basis for computing TJET when the LM's state lies in each of the four zones of the upper half-plane of Fig. 3.4-1. The associated flow chart for ROUGHLAW is shown in Fig. 3.4-5. As noted in Fig. 3.4-5, TJET is first computed as a positive number. The ROUGHLAW program then attaches a sign to TJET that conveys the required rotational sense of the LM. Note that, as indicated in Fig. 3.4-1, if TJET is computed to be less than 20 millisec, it is set equal to zero. This is done in order to avoid firing short pulses, which are wasteful of fuel. The ROUGHLAW maneuver rate of 6.5 deg/sec is sufficiently high to assure that attitude control will be maintained in the lightest ascent configuration in the presence of a jet on-failure.[2]

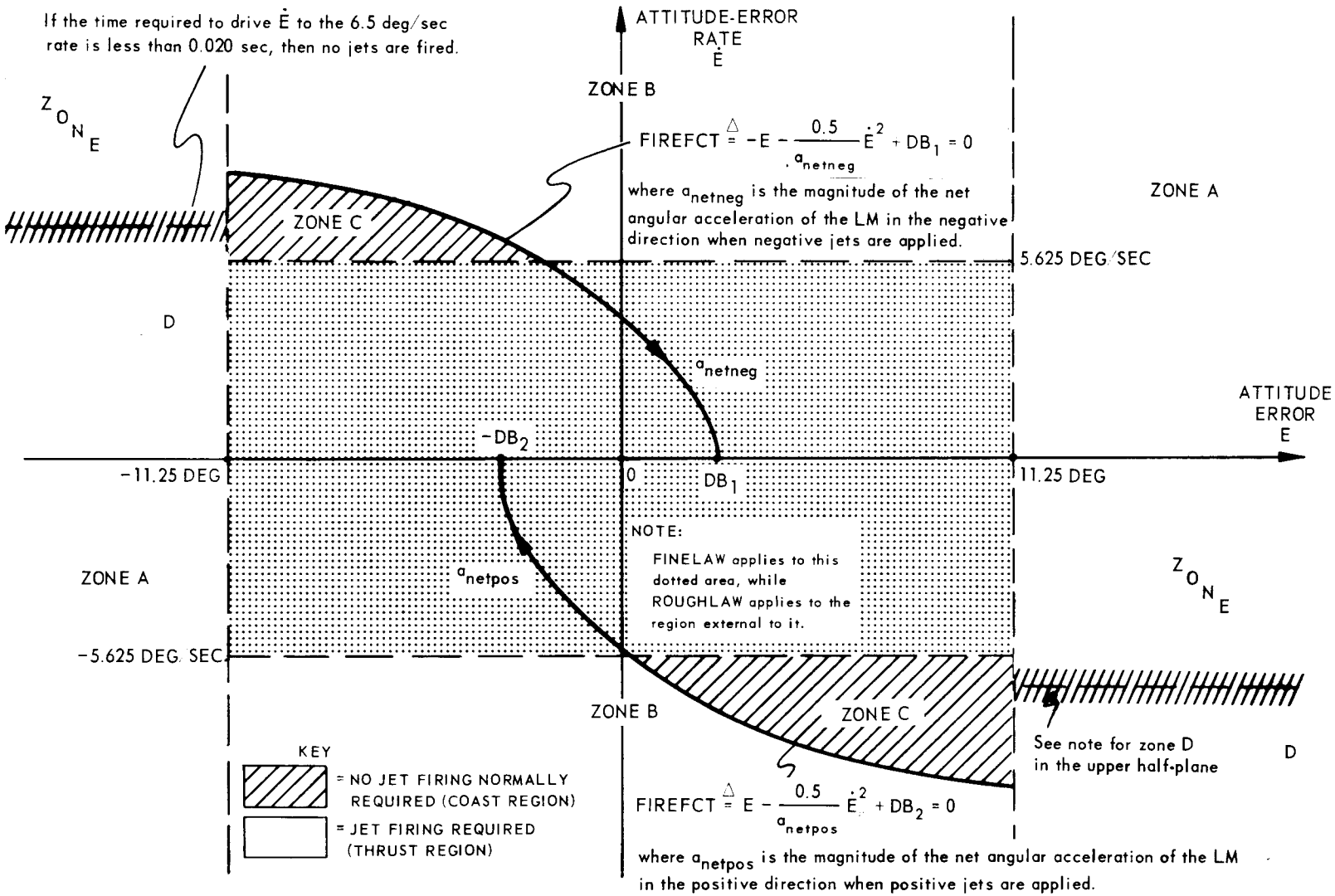

NOTES:

1. ROUGHLAW uses the FIREFCT function as defined for the half-plane (upper or lower) in which the LM's state is located.
2. DB_1 and DB_2 are set in accordance with Table 3.4-4, which is discussed subsequently in connection with the 1 ACCS routine.
3. The ROUGHLAW phase plane applies to both drifting flight and powered flight.

Fig. 3.4-1. The ROUGHLAW phase plane.

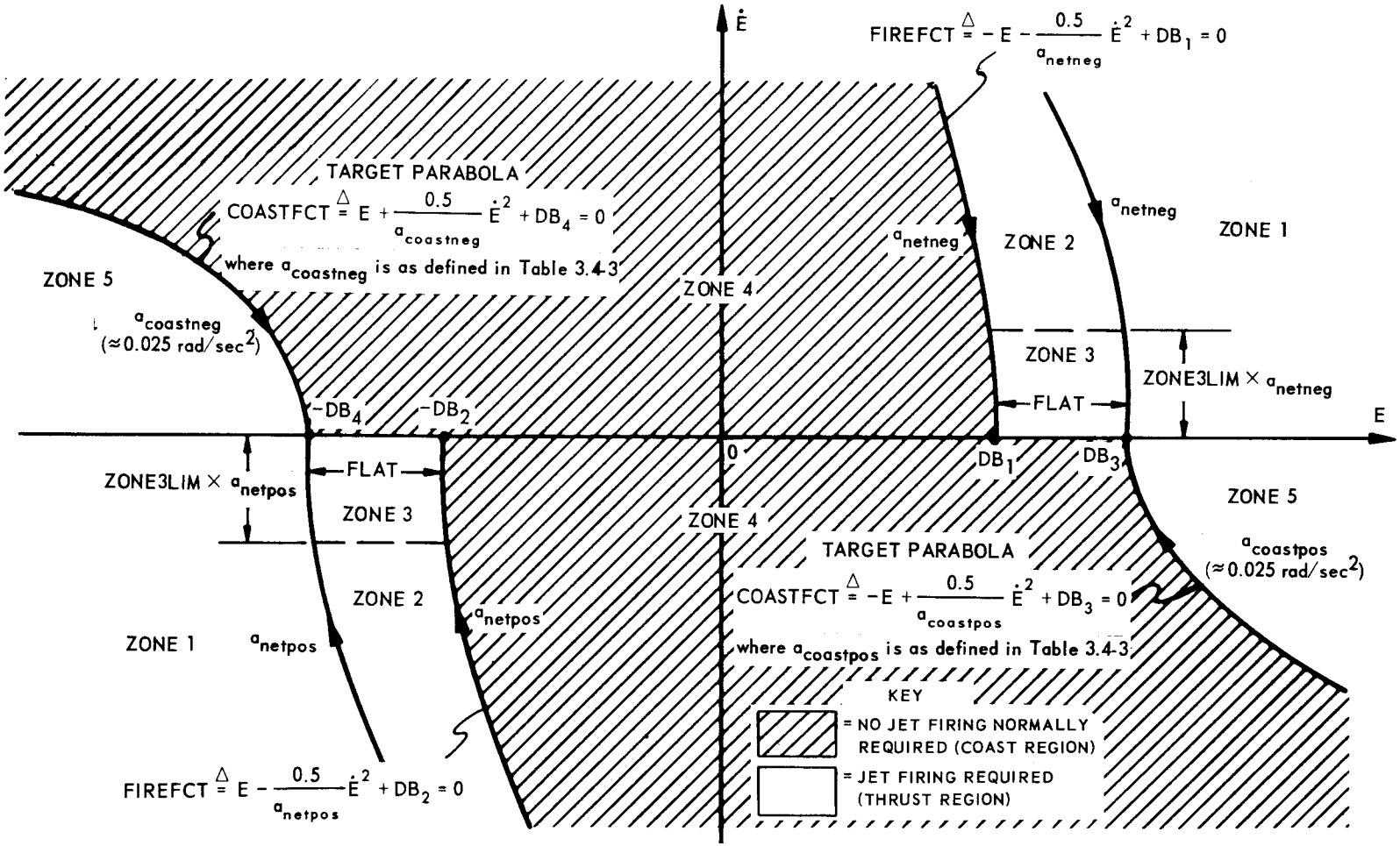

NOTES:

1. FINELAW uses the FIREFCT and COASTFCT functions as defined for the half-plane (upper or lower) in which the LM's state is located.
2. No torquing is commanded about the control axis if the LM's state is in a coast region unless the jets are already on and are driving the state to intersect the E axis between $-DB_2$ and DB_1.
3. DB_1, DB_2, DB_3, DB_4, and FLAT are set in accordance with Table 3.4-4, which is discussed subsequently in connection with the 1/ACCS routine. a_{netneg} and a_{netpos} are equal to the jet acceleration (ref. Table 3.4-3) since the offset acceleration is equal to zero for drifting flight. In the 1/ACCS routine, ZONE3LIM is set equal to 0.0175 sec for drifting flight and is set equal to zero for powered flight.

Fig. 3.4-2. The FINELAW phase plane when the LM is in drifting flight.

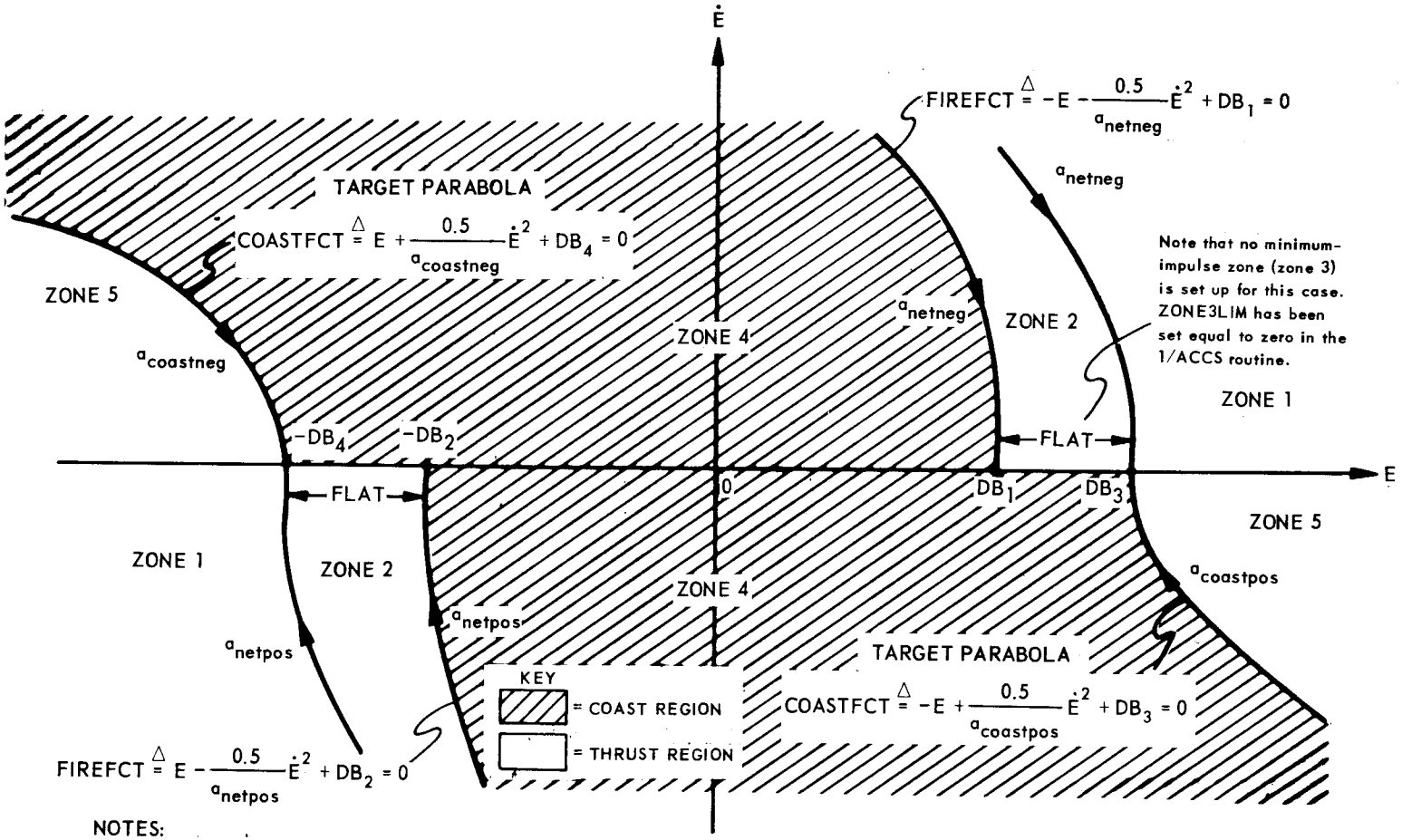

NOTES:

1. DB_1, DB_2, DB_3, DB_4, and FLAT are set as in drifting flight. a_{netneg} and a_{netpos} are computed in accordance with the definitions of Table 3.4-3 and, in general, are not equal – as they are in drifting flight. Similarly, $a_{coastneg}$ and $a_{coastpos}$ are not necessarily equal. ZONE3LIM is zero.
2. Notes 1 and 2 of Fig. 3.4-2 for the drifting-flight case apply for this case also.

Fig. 3.4-3. The FINELAW phase plane when the use of the GTS attitude control law is allowed during powered descent.

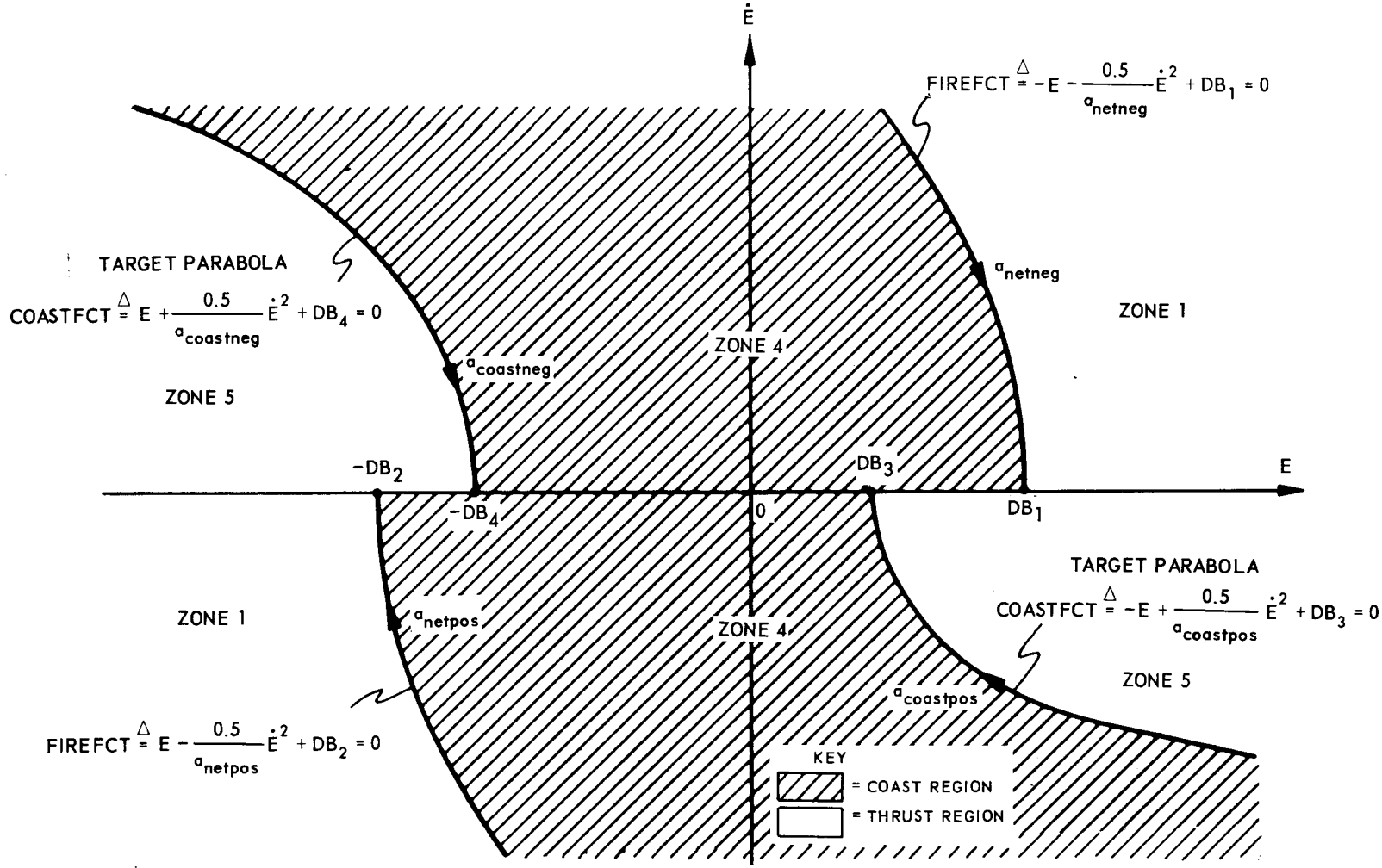

NOTES:

1. FINELAW uses the FIREFCT and COASTFCT functions as defined for the half-plane (upper or lower) in which the LM's state is located.
2. No torquing is commanded about the control axis if the LM's state is in a coast region unless the jets are already on and are driving the state to intersect a target parabola.
3. DB_1 through DB_4 are set in accordance with Table 3.4-4, which is discussed subsequently in connection with the 1/ACCS routine. The relative positions of the switching curves shown here are not representative.

Fig. 3.4-4. The FINELAW phase plane when the LM is in powered ascent or when the use of the GTS attitude control law is prohibited during powered descent.

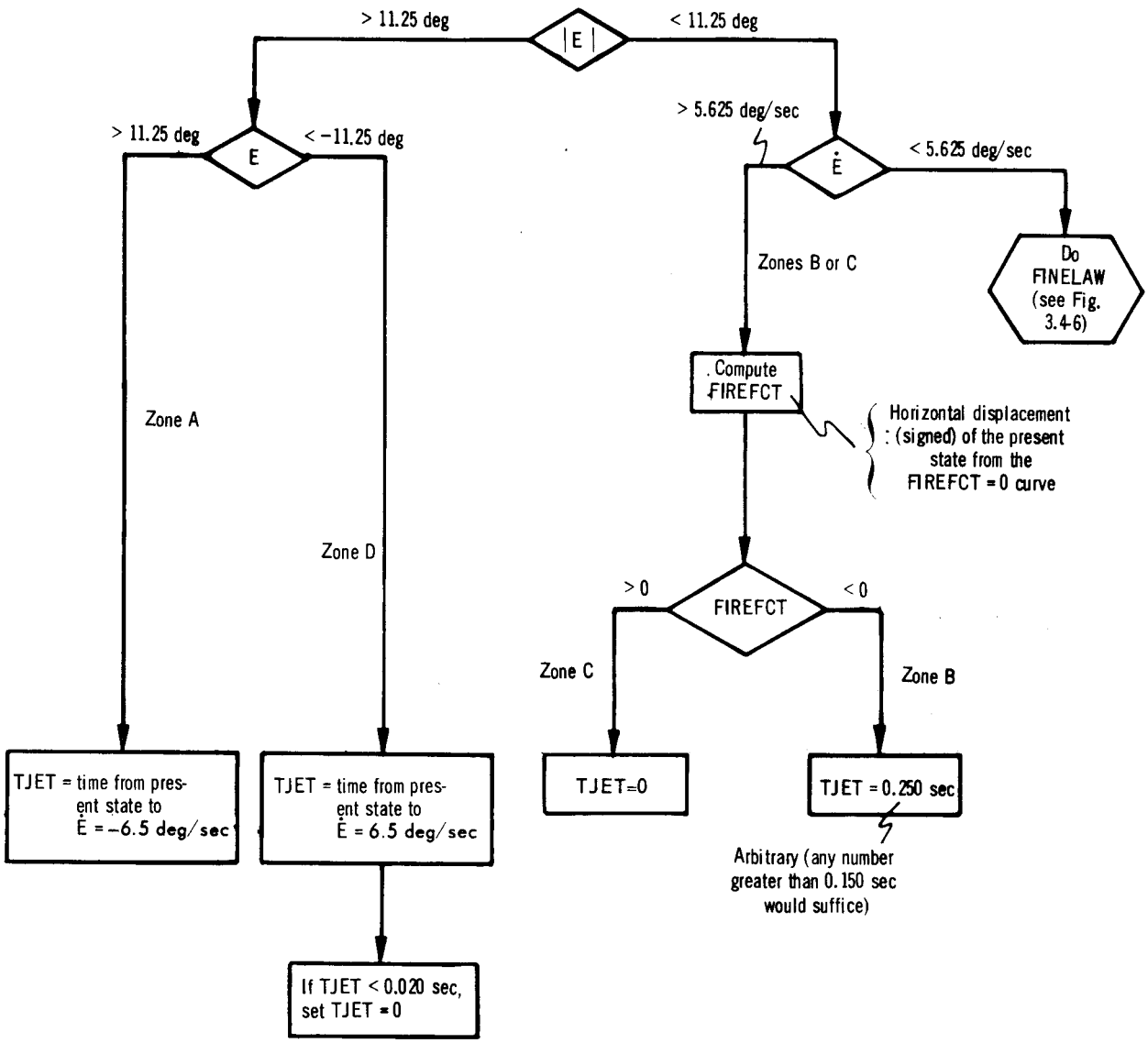

NOTES:

1. It is assumed that $\dot{E}$ is greater than zero in this flow chart. TJET is computed in the same way for the corresponding zones of the lower half-plane (see Fig. 3.4-1).
2. In the above logic, TJET is computed as a positive number. In the ROUGHLAW program, a sign is then applied to TJET that conveys the required rotational sense of the LM.

Fig. 3.4-5. The flow chart for ROUGHLAW.

Table 3.4-1. The basis of computing TJET in the upper half-plane of the ROUGHLAW phase plane.

Location of the LM's State	Basis of Computing TJET
Zone A	TJET is the time required to drive $\dot{E}$ to -6.5 deg/sec.
Zone B	TJET is set equal to 0.250 sec, that is, a "large" value.
Zone C	TJET is set equal to zero; that is, no jets are turned on.
Zone D	TJET is the time required to drive $\dot{E}$ to +6.5 deg/sec.

3.4.2.3 Description of FINELAW

As noted in Subsection 3.4.2.1, there are three phase planes that are associated with the FINELAW form of TJETLAW. One of these applies when the LM is in drifting flight (that is, flight in which the LM is not being powered by either of the main engines), while the other two apply to powered flight. These three phase planes are discussed in the following paragraphs.

FINELAW for Drifting Flight

As shown by Fig. 3.4-2, the phase plane for drifting flight of the LM is divided into zones 1 through 5. Table 3.4-2 sets forth the basis for computing TJET when the LM's state lies in each of these five zones.

FINELAW for Powered Flight

As already noted, there are two phase planes that can be used for powered flight. Their application is based on the following considerations:

1. Whenever the use of the GTS attitude control law is allowed during powered descent, the phase plane of Fig. 3.4-3 is used.
2. During powered ascent or whenever the use of the GTS attitude control law is prohibited during powered descent, the phase plane of Fig. 3.4-4 is used.

The use of the GTS attitude control law can be permitted only by the TIMEGMBL routine. TIMEGMBL is a routine that commands the trim gimbal to drive toward the null position (that is, to put the thrust vector through the vehicle center of gravity). The criterion for entering the TIMEGMBL routine is described in Subsection 3.6.2. After determining the Q- and R-axis gimbal drive times, TIMEGMBL sets a flag, ALLOWGTS, to indicate whether or not use of the GTS attitude control law is permitted. The use of the GTS attitude control law is permitted only if both computed drive times are less than 2 sec and the gimbals are usable.

In the case for which Fig. 3.4-3 applies, TJET is computed in the same way as for drifting flight – with the exception that zone 3 has been eliminated. This logic allows an efficient interface between the RCS and the trim-gimbal control system. In particular, it allows $\dot{E}$ to be reduced to a very small value before the trim-gimbal attitude control law is applied.

Table 3.4-2. The basis of computing TJET in the FINELAW phase plane for drifting flight.

Location of the LM's State	Basis of Computing TJET
Zone 1*	TJET is the time required to drive the LM's state to a "target parabola".
Zone 2**	TJET is the time required to drive the LM's error rate to zero.
Zone 3**	TJET is set so small that the jet select logic will fire a one-jet minimum impulse.
Zone 4	TJET is set to zero unless the jets for the axis concerned are already on and are driving the LM's state to intersect the E axis between $-DB_2$ and DB_1.***
Zone 5*	TJET is the time required to drive the LM's state to a "target parabola".

*In zones 1 and 5, whenever TJETLAW requires the computation of the time required to drive the LM's state to a target parabola, the exact solution involves the computation of a square root. In order to avoid this time-consuming computation in the LGC, an approximation is used. The procedure employed (see Reference 1 for details) involves extrapolating the LM's state to determine in which range of time TJET lies; these intervals are described subsequently in Fig. 3.4-6. The quantity COASTFCT is equal to zero for states on the target parabola. At one end of the interval in which the actual TJET lies, COASTFCT is positive; at the other end, it is negative. By linearly interpolating on COASTFCT, a time is estimated at which COASTFCT is zero. The value of TJET computed in this way will always be smaller than the exact value of TJET. The maximum error that can be incurred is 12.5 millisec.

**Zones 2 and 3 allow the RCS to acquire a minimum-impulse limit cycle.

***The purpose of allowing the jets to remain on in zone 4 is to avoid "chattering" between the coast and thrust regions. Chattering would occur if the magnitude of the net angular acceleration (see definition in Table 3.4-3) were underestimated (as a result, for example, of a too-high estimate of inertia).

In the case for which Fig. 3.4-4 applies, TJET is computed as follows (note that zones 2 and 3 of the drifting-flight case have been eliminated):

1. In zones 1 and 5, TJET is computed as in the case of drifting flight; that is, TJET is the time required to drive the LM's state to a target parabola.

2. In zone 4, TJET is set to zero unless the jets for the axis concerned are already on and are driving the LM's state to intersect a target parabola. (As in the case of zone 4 in Figs. 3.4-2 and 3.4-3, the purpose of allowing the jets to remain on is to avoid chattering between the coast and thrust regions.)

Flow Chart for FINELAW

Figure 3.4-6 shows a flow chart for FINELAW that combines the drifting-flight and powered-flight cases. As in the case of ROUGHLAW, once TJET has been computed a sign is attached to TJET that conveys the required rotational sense of the LM. It should be noted that if either the zone 1 path or the zone 5 path of the flow chart is used for the axis under consideration and TJET is computed to be less than 20 millisec then TJET is set equal to zero. This results in a hysteresis in the coast boundary. The advantage of this procedure is that it eliminates short pulses, which – as noted earlier – are wasteful of fuel.

3.4.2.4 Inputs Required by TJETLAW

The following input information is required for each of the three RCS control axes (that is, P, U', and V') prior to employing TJETLAW:

1. The state of the LM in the phase plane – that is, the values of E and $\dot{E}$.
2. The constants that determine the shape and position of the phase-plane parabolas.
3. The preference for balanced or unbalanced (that is, 2- or 1-jet) firings about the U and V axes.

Each of these three types of input information is discussed in the following paragraphs.

The quantities E and $\dot{E}$ are determined at 0.100-sec intervals. The attitude error, E, of the LM about a given axis is computed as a function of the difference between each of the actual CDU angles and the corresponding desired CDU angle. These differences are resolved to produce the attitude error, E, about each of the three axes concerned, that is, the P, U', and V' axes. The attitude-error rate, $\dot{E}$, of the LM about a given axis is computed as the difference between the vehicle's angular rate, ω, about the given axis and the specified desired rate about that axis, ω_d. The rate ω for the P axis is provided directly by the state estimator. The rates for the U' and V' axes are obtained by resolving the Q and R rates derived by the state estimator. The resolution of E and $\dot{E}$ into the U'-V' system is done in the ROT-TOUV section of the program.

The constants that determine the shape and position of the phase-plane parabolas are determined in the "1/ACCS" routine (see Subsection 3.6.1). This routine

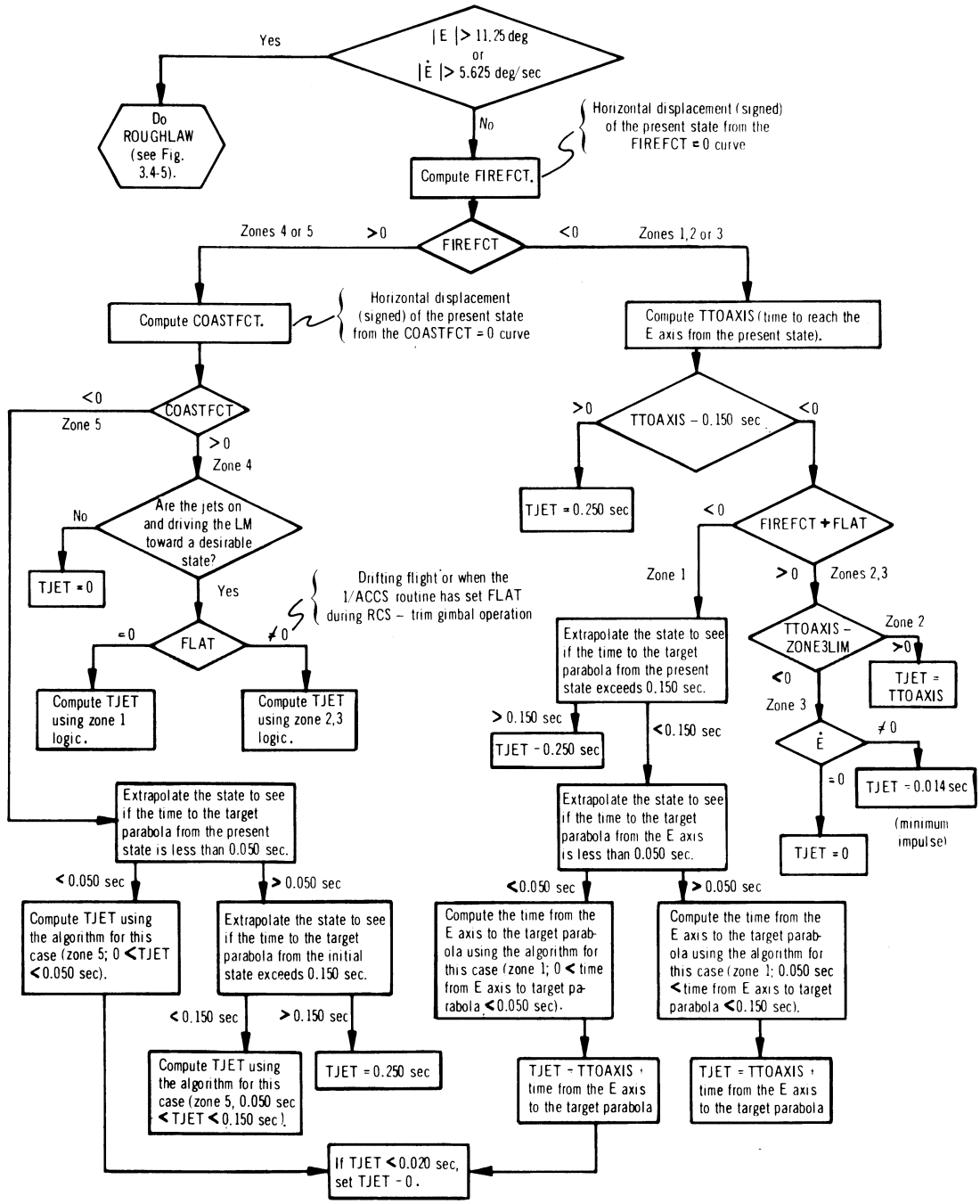

NOTES:

1. The choice of TJET = 0.250 sec for cases when TJET > 0.150 sec is an arbitrary one. Any value greater than 0.150 sec would suffice.
2. In the above logic, TJET is computed as a positive number. In the FINELAW program, a sign is subsequently applied to TJET to convey the required rotational sense.

Fig. 3.4-6. The flow chart for FINELAW.

is executed every two seconds during powered flight, whenever a fresh start or a restart occurs, when a DAP data load is made in R03, and during drifting flight when the deadband is set. The routine computes the functions of acceleration and deadband required by TJETLAW. Table 3.4-3 shows the quantities computed in the 1/ACCS routine. These quantities are computed for the P, U', and V' axes. For the P axis, all quantities that are a function of the number of jets used are computed on the assumption that two jets are used. For the U' and V' axes, these quantities are normally computed for both the one-jet case and the two-jet case. If, for a given direction of rotation about the U' or V' axes, one jet is not sufficient to produce a net angular acceleration greater than $\pi/128$ rad/sec^2, then all functions for that direction are computed under the assumption that two jets are used. On the other hand, if one of the jets used for rotating in a given sense has been disabled, all the functions for that direction are one-jet values.

The criteria used in the 1/ACCS routine to determine the parameters, DB_1 through DB_4, that establish the positions of the phase-plane parabolas are described in Table 3.4-4. The phase-plane parabolas are positioned so as to yield a small average steady-state attitude error during powered flight. Figures 3.4-7 through 3.4-9 give three examples of the way in which the phase-plane parabolas are positioned. In Table 3.4-4 and Figs. 3.4-7 through 3.4-9, all of the intercepts are defined as being proportional to the deadband DB. It should be noted that the proportionality constants are dependent on the value of the offset acceleration, AOS. As indicated in Table 3.4-4, DB is not set by the LM DAP but is selected instead by the mission programs (see Section 4 of R-567) and the LM astronaut. It is expected that DB will be either 1 deg or 0.3 deg for powered flight. For drifting flight, DB will be either 0.3 deg, 1 deg, or 5 deg, depending upon settings by the mission programs and the LM astronaut.

The desirability of employing 1-jet firings about the U and V axes is conveyed to TJETLAW by two flag words that indicate, respectively, 1) whether an X-axis translational sense is called for, and 2) whether a single jet produces a net acceleration greater than the lowest acceptable value. When single-jet firings are not preferred, TJETLAW always calls for balanced couples.

3.4.2.5 Criteria for the Number of Jets to be Used

In discussing the number of jets to be used, it is convenient to treat the U and V axes separately from the P axis.

U and V Axes

Normally, for the U and V axes, a single jet is used during powered ascent and when X-axis translation is desired. For all other cases, a two-jet couple is used. For any of the following conditions, however, a two-jet couple is mandatory – even for powered ascent and for X-axis translation:

Table 3.4-3. The functions computed in the 1/ACCS routine (for each axis) for use in the TJETLAW program.

	Function	Comment
1)	$1/a_{netneg}$	For the U' and V' axes, this function is normally computed for both one jet and two jets. For the P axis, it is computed only for the two-jet case.
2)	$1/a_{netpos}$	(same comment as for item 1)
3)	$1/a_{coastneg}$	
4)	$1/a_{coastpos}$	
5)	$-1/\left(a_{netneg} + \frac{a^2_{netneg}}{a_{coastpos}}\right)$	(same comment as for item 1)
6)	$-1/\left(a_{netpos} + \frac{a^2_{netpos}}{a_{coastneg}}\right)$	(same comment as for item 1)
7)	DB_1	See Table 3.4-4
8)	DB_2	
9)	DB_3	
10)	DB_4	
11)	$DB_1 - DB_3 + FLAT$	
12)	$DB_2 - DB_4 + FLAT$	
13)	ZONE3LIM	

Notes

1. The quantities a_{netpos}, a_{netneg}, $a_{coastpos}$, and $a_{coastneg}$ are each positive and limited to a minimum value of $a_{min} \triangleq \pi/128$ rad/sec^2 ≈ 1.4 deg/sec^2.
2. a_{netpos} is the net angular acceleration in the positive direction when positive jets are applied; that is, it is equal to the jet acceleration plus the offset acceleration. If, for the U' and V' axes, a_{netpos} is computed by the 1/ACCS routine to be negative or less than a_{min} for the 1-jet case, then this information is made available to the TJETLAW program to alert it to the fact that two jets will be required if positive rotation is desired. (No such considerations apply to the P axis inasmuch as, for the P axis, a_{netpos} is computed for the two-jet case only, which always yields a value of a_{netpos} that is greater than a_{min}.)
3. a_{netneg} is the net angular acceleration in the negative direction when negative jets are applied; that is, it is equal to the jet acceleration minus the offset acceleration. If, for the U' and V' axes, a_{netneg} is computed to be negative or less than a_{min} for the one-jet case, then this information is made available to the TJETLAW program to alert it to the fact that two jets will be required if negative rotation is desired. (As in the case of a_{netpos}, no such considerations apply to the P axis.)
4. $a_{coastpos}$ and $a_{coastneg}$ are the jets-off angular accelerations that determine the shapes of the target parabolas in the lower and upper half planes, respectively. They are respectively equal to the offset acceleration and the negative of the offset acceleration, with the restriction that each is limited to a minimum of a_{min}. Since the offset acceleration is assumed to be zero for the P axis, both $a_{coastpos}$ and $a_{coastneg}$ are always set equal to a_{min} for the P axis. If $a_{coastpos}$ or $a_{coastneg}$ is determined to be greater than a_{min}, it is then increased by a factor of 9/8. This steepens the target parabola and reduces the probability of crossing the target parabola from the coast region of the phase plane.
5. ZONE3LIM is set equal to 0.0175 sec for drifting flight and is set equal to zero for powered flight.

Table 3.4-4. The criteria used in the 1/ACCS routine to determine the intercepts of the phase-plane parabolas.

Define

$a_{min} = \pi/128$ rad/sec$^2 \approx 0.025$ rad/sec$^2 \approx 1.4$ deg/sec^2

AOS = offset (disturbing) acceleration

For Powered Flight (except when use of the GTS attitude control law is allowed during powered descent; see Fig. 3.4-4):

FLAT = 0 and:

a) If AOS > a_{min},

$DB_1 = (1 - 0.08889|AOS|)DB$, $DB_2 = 2DB$, $DB_3 = -0.75DB$, $DB_4 = 2DB$

b) If AOS < $-a_{min}$,

$DB_1 = 2DB$, $DB_2 = (1 - 0.08889|AOS|)DB$, $DB_3 = 2DB$, $DB_4 = -0.75DB$

c) If a_{min} > AOS > 0.1 deg/sec^2,

$DB_1 = DB$, $DB_2 = DB$, $DB_3 = 0.5\ DB$, $DB_4 = DB$

d) If -0.1 deg/sec^2 > AOS > $-a_{min}$,

$DB_1 = DB$, $DB_2 = DB$, $DB_3 = DB$, $DB_4 = 0.5DB$

e) If 0.1 deg/sec^2 > AOS > -0.1 deg/sec^2,

$DB_1 = DB_2 = DB_3 = DB_4 = DB$

For Drifting Flight (and when use of the GTS attitude control law is permitted during powered descent; see Fig. 3.4-3):

$DB_1 = DB_2 = DB$, $DB_4 = DB_3 = DB + FLAT$, and

FLAT = 0.8 deg

Notes: 1. This table is applicable to both ROUGHLAW and FINELAW.

2. In a) and b) above, |AOS| is assumed to be expressed in deg/sec^2. It is limited to 16.875 deg/sec^2 for these computations. This prevents DB_1 or DB_2 from becoming less than -0.5DB.

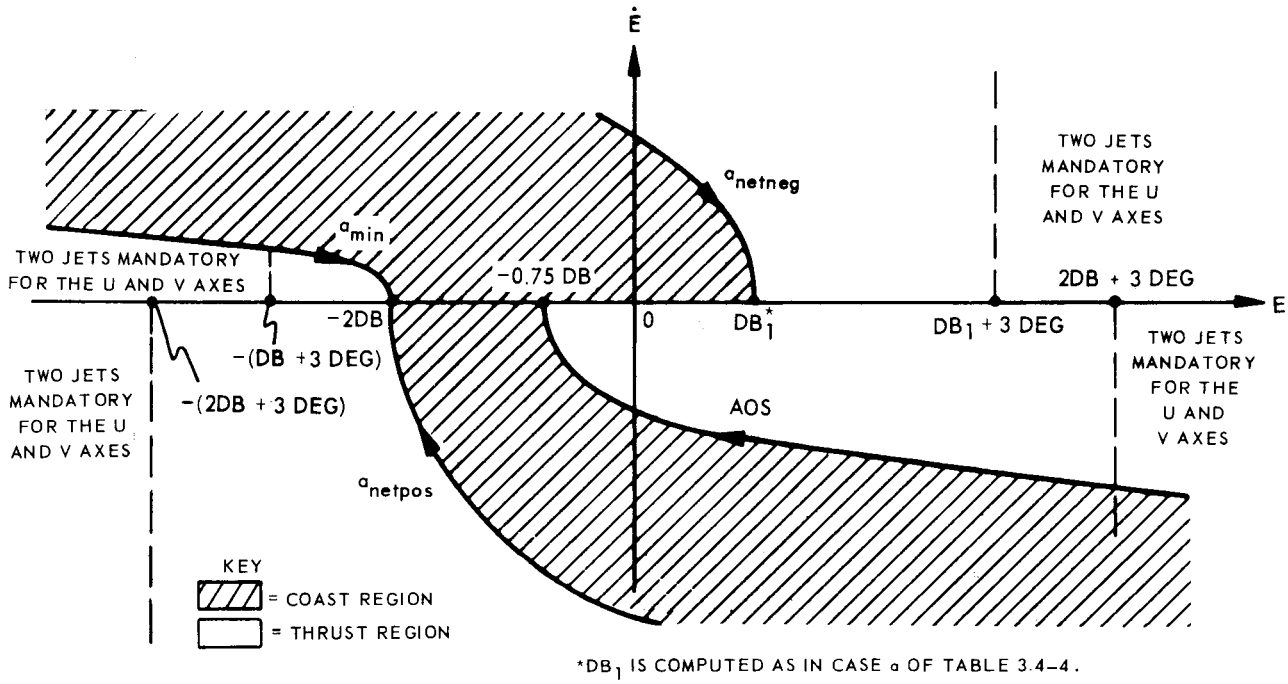

Fig. 3.4-7. The powered-flight phase plane for AOS > a_{min}.

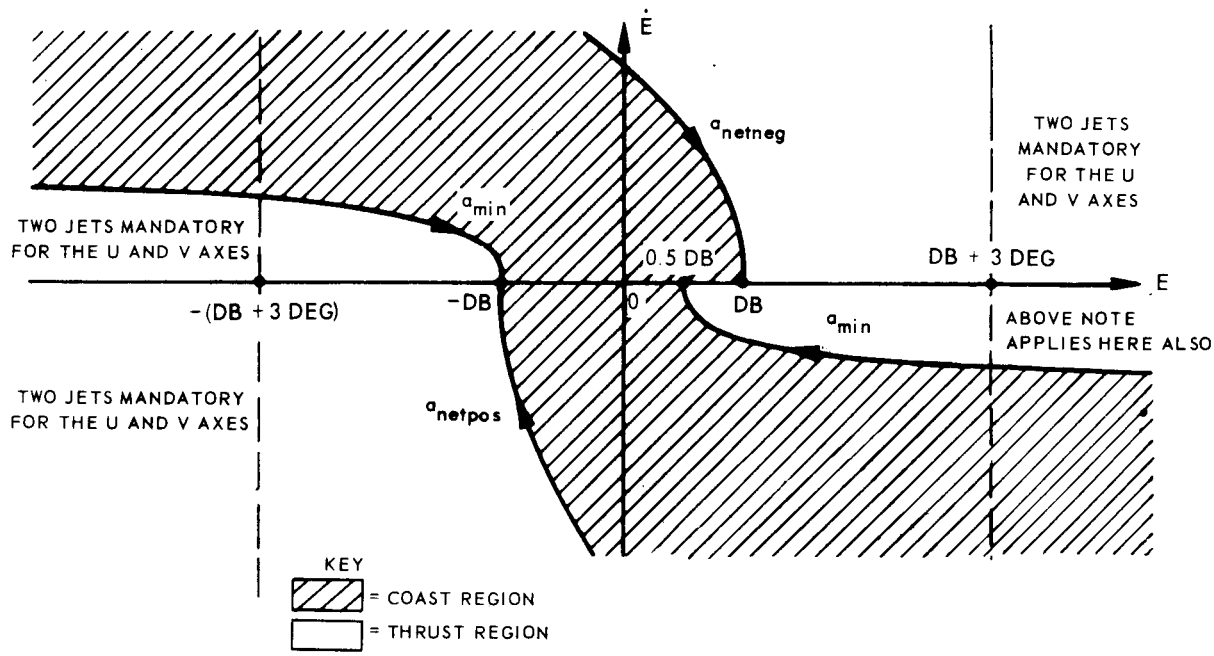

Fig. 3.4-8. The powered-flight phase plane for a_{min} > AOS > 0.1 deg/sec^2.

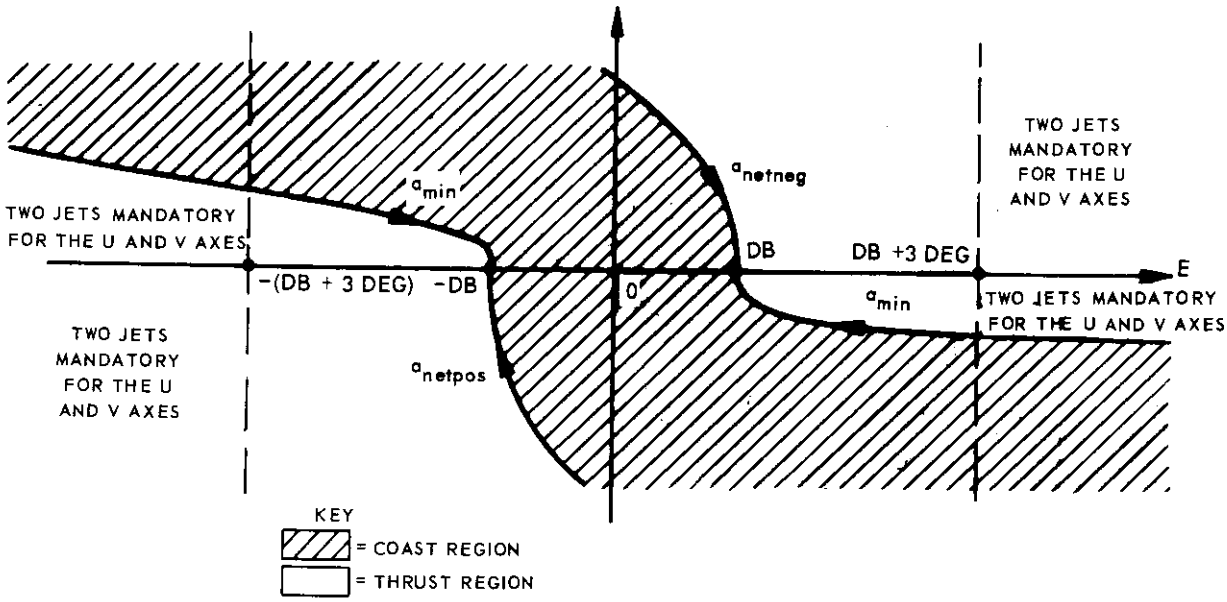

Fig. 3.4-9. The powered-flight phase plane for 0.1 deg/sec^2 > AOS > -0.1 deg/sec.^{2}

1. If the use of ROUGHLAW is required.
2. If FINELAW is being employed and if the magnitude of E exceeds DB_1 by more than 3 deg for upper-half-plane cases or exceeds DB_2 by more than 3 deg for lower-half plane cases (see Figs. 3.4-7 through 3.4-9 for example).
3. If, for the particular required rotational sense of the LM that is determined by TJETLAW, one jet is not sufficient to produce a net angular acceleration greater than $\pi/128$ rad/sec.^{2}

However, a single jet is always employed when a minimum-impulse firing is called for, so that the applied torque may be as small as possible. In the absence of X-axis translation or ullage, the selection of the jet to be used is determined in a semi-random manner (from the low bit of the LGC clock, channel 4) to achieve alternation.

P Axis

For the P axis, the computation of TJET is always made on the basis of two jets. Four jets will actually be employed, however, if – after TJET has been computed – either of the following conditions is found to exist:

1. The use of ROUGHLAW was employed in the computation of TJET and TJET is greater than 0.150 sec.
2. The use of FINELAW was employed in the computation of TJET, the LM state is located in zone 1 and more than 4 deg from the FIREFCT = 0 curve, and TJET is greater than 0.150 sec.

When four jets are decided upon, they are fired for a full 0.1 sec, after which time the control is re-evaluated.

3.4.3 The RCS Control Law for Automatic Control in the CSM-Docked Case*

3.4.3.1 General Considerations

For automatic control in the CSM-docked case, the LM DAP must repetitively provide the RCS thrusting commands for each of the three RCS control axes.** That is, the LM DAP must perform the same basic function in the CSM-docked case that it does in the LM-alone case. It was, however, found desirable to use separate control logic when docked because the control logic employed in the LM-alone case depends on an assumed response of the LM (that is, it depends on a presumed moment of inertia of the LM). Inasmuch as the moment of inertia of the fully loaded CSM-docked configuration differs by two orders of magnitude from that of the lightest LM-alone configuration (that of LM ascent) and because the single-precision arithmetic used in the LM-alone case in order to save computation time cannot handle a two-orders-of-magnitude range, the logic used in the LM-alone case is unsuitable for the CSM-docked case. Accordingly, separate, specialized logic is employed for the CSM-docked case. This logic is considerably simplified from that of the LM-alone case for the reasons given in the ensuing discussion.

The following subsections describe the design guidelines followed, and the mechanization employed, in connection with the simplified and specialized LM DAP used for automatic control in the CSM-docked case. For convenience, this version of the LM DAP is referred to herein as the CSM-docked autopilot, and the version used for the LM-alone case is referred to as the LM-alone autopilot.

3.4.3.2 Design Guidelines

No written specifications exist for the CSM-docked case. (This is in contrast to the situation that exists for the LM-alone case, where GAEC has provided a performance and interface specification.) However, an undocumented agreement does exist between MSC and MIT to the effect that the CSM-docked autopilot shall provide an emergency capability for use in an abnormal situation where the service module cannot be employed to perform required thrusting. Therefore, because the CSM-docked autopilot is a backup autopilot, and because the available computer memory of the LM guidance computer is limited, the design of this autopilot stresses simplicity rather than performance. In particular:

1. RCS fuel usage is assumed to be not critical. Hence, the CSM-docked autopilot does not compute exact jet burning times (as does the LM-alone autopilot). Rather, jets are turned on or off only at the control-sample instants and are left on or off for the full sampling period.

---

*By George R. Kalan and Edgar M. Oshika.

**For the CSM-docked case, the U' and V' axes are set coincident with the U and V axes, respectively. This is a consequence of the assumption (see Subsection 3.3.1.3) that an average moment of inertia is used for both the Q and R axes. When the Q and R inertias are equal, the U'-V' system is equivalent to the U-V system.

2. The number of jet firings is also assumed to be not critical. Hence, simple, piecewise linear control logic is employed (rather than the parabolic control logic used by the LM-alone autopilot).

Within the framework of these guidelines, an RCS control law was designed for the CSM-docked autopilot that possesses the following capabilities:

1. Enable the RCS to perform automatic attitude hold and automatic attitude change at a slow rate during drifting flight.
2. Enable the RCS to perform automatic attitude control during powered flight. Specifically, the RCS would be used to control thrusting maneuvers, using assistance from the descent engine under the control of the trim-gimbal control system. However, in order to avoid excessive RCS impingement on the CM and LM during DPS burns — a problem that came to light after the design was completed — the crew was given the capability of inhibiting RCS control about the U and V axes during CSM-docked DPS burns. This inhibition is imposed by the execution of Verb 65 and is removed by Verb 75. Note that this special check is made only during powered flight although the bit, SNUFFBIT, that indicates it may be set and cleared at any time.
3. Provide RCS automatic control during drifting flight or powered flight in such a way that the RCS jet activity has only a very small probability of exciting the bending modes in excess of the docking-tunnel loads criteria.

3.4.3.3 Mechanization Employed

The design of the CSM-docked autopilot is represented by the phase plane shown in Fig. 3-4.10, which applies to both drifting flight and powered flight. In order to compress and simplify the logic of the CSM-docked case, straight-line segments were chosen for all decision lines. Further, it was decided to use the same phase-plane logic for all three RCS control axes: P, U, and V. Still further simplification was obtained by making the end result of the logic an on-off signal that could be interpreted as a jet burning time, TJET, by the same jet select logic employed for the LM-alone case in such a way that the jets are either turned on or left off for at least one control-sample period. Since — for the CSM-docked case — the RCS sample period is 0.100 sec for all axes in drifting flight but is changed to 0.200 sec for the U and V axes in powered flight, the minimum pulse width may be either 0.100 sec or 0.200 sec for the U and V axes. These minimum values are acceptable for the CSM-docked case because the moment of inertia of the CSM-docked configuration is large and the response is slow.

The two rate limits indicated on the phase-plane plot of Fig. 3.4-10 are provided in order to prevent the attainment of high attitude-error rates, $\dot{E}$. The jets can never be fired in such a way as to increase the attitude-error rate beyond the inner rate limit (that is, the one with the lower magnitude). The inner rate limit is chosen on the basis of the range of moments of inertia of the CSM-docked configuration that can be expected. This rate limit is made sufficiently high to achieve a reasonably fast response (for this heavy vehicle). With the rate limit

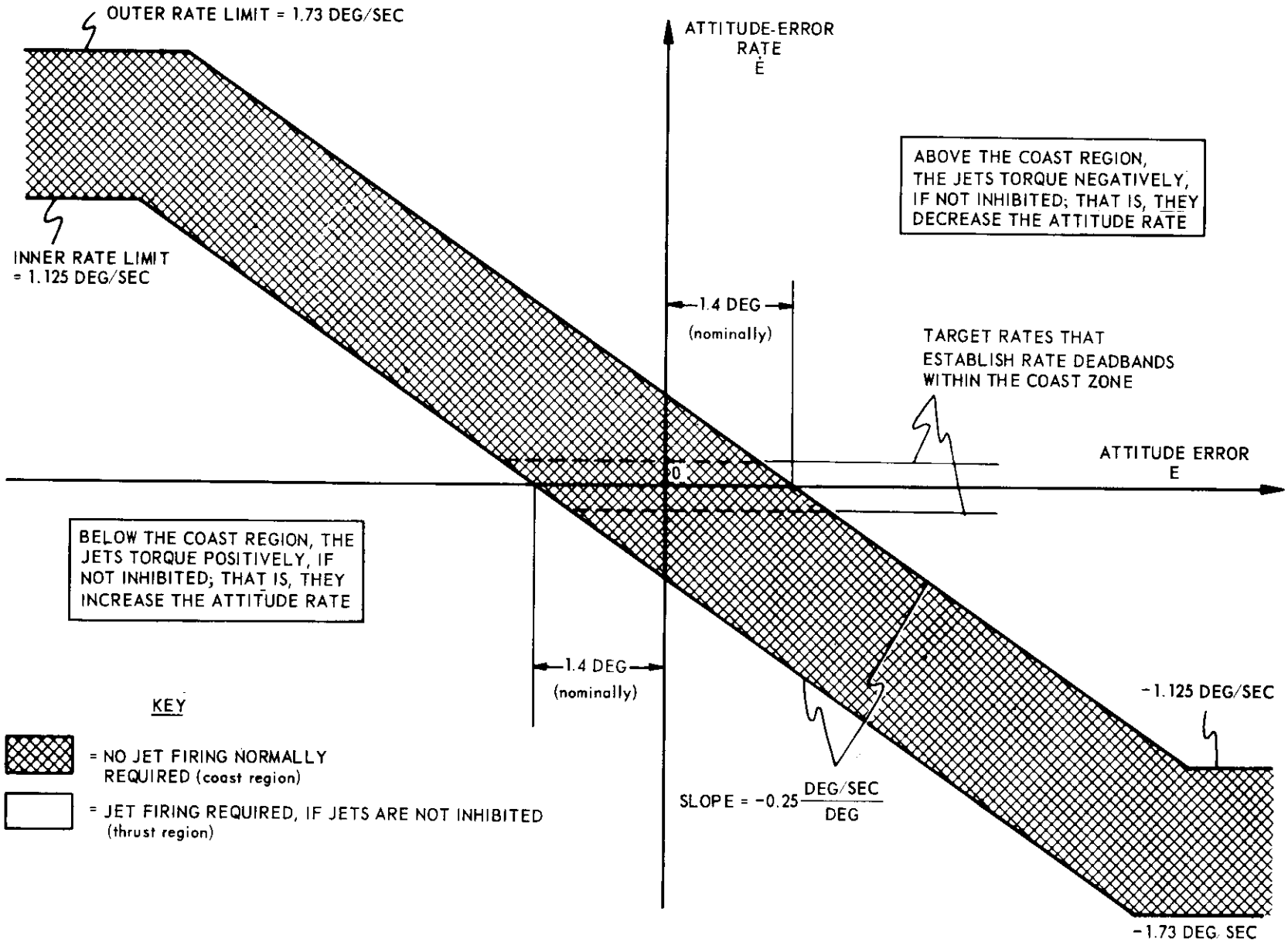

Fig. 3.4-10. The phase plane for the CSM-docked case.

chosen (1.125 deg/sec), the parabolic trajectory (constant-acceleration path*) of the heaviest CSM-docked configuration will have no overshoot of the rate deadband before it falls into a limit cycle (see Fig. 3.4-11). This choice implicitly assumes that the width of the dead zone, which is a pad-loaded parameter, will not be less than the currently anticipated value of 2.8 degrees.

In conjunction with the inner rate limit, the outer rate limit establishes coast-zone bands at large magnitudes of the attitude error, E, as shown in Fig. 3.4-10. Should a trajectory of the CSM-docked configuration intersect an inner rate limit, the arrangement employed would prevent the subsequent path of the configuration's state from hunting about this limit – as it would if this were the sole rate limit involved. The magnitude of the outer rate limit is set sufficiently larger than the magnitude of the inner rate limit that the slow response of the CSM-docked configuration prevents its state from jumping between the two rate limits.

The magnitude of the target rate within the coast zone determines the steady-state limit cycle. In powered flight, when a significant offset acceleration is to be expected, the target rate is set to 0.1 deg/sec. In drifting flight, it is made zero so that the slowest possible limit cycle consistent with a 0.1-sec minimum impulse may be achieved.

In addition to the phase-plane logic of Fig. 3.4-10, the CSM-docked autopilot contains jet-inhibition logic to reduce the frequency of jet firings. This reduces the probability of exciting large bending-mode oscillations with RCS jet activity. If RCS jets for a given axis are on when the phase-plane logic for that axis calls for a torque reversal or commands the jets off, the inhibition logic terminates the jet firings and prohibits subsequent jet firings about that axis for a predetermined time interval. In all other situations, the inhibition logic allows the implementation of commands determined by the phase-plane logic. Jet firings can be inhibited for 0.4 sec about the P axis and for 1.0 sec about the U and V axes. A more detailed description of the design principles used to improve bending stability and of the inhibition logic is included in Reference 3 listed at the end of this subsection.

The automatic RCS control logic of the CSM-docked autopilot can be described with the aid of the flow chart shown in Fig. 3.4-11A. Although the operation of the logic for each RCS control axis is complely independent of that for each of the other control axes, the structure of the logic is common to all three axes. For a given axis, the logic first checks the jet firing time [TJP, TJU, or TJV – represented by the symbol TJP(U,V)] used on the last DAP pass, in order to determine the current state of the jets. The temporary flagword OLDSENSE is then set to +1, -1, or 0 to indicate whether the jets are firing up (to cause rotation in a positive sense about the axis under consideration), down (to cause rotation in a negative sense about the axis under consideration), or not firing.

*Any phase-plane path followed by the state (E, $\dot{E}$) over which the acceleration, $\ddot{E}$, remains constant is a parabola.

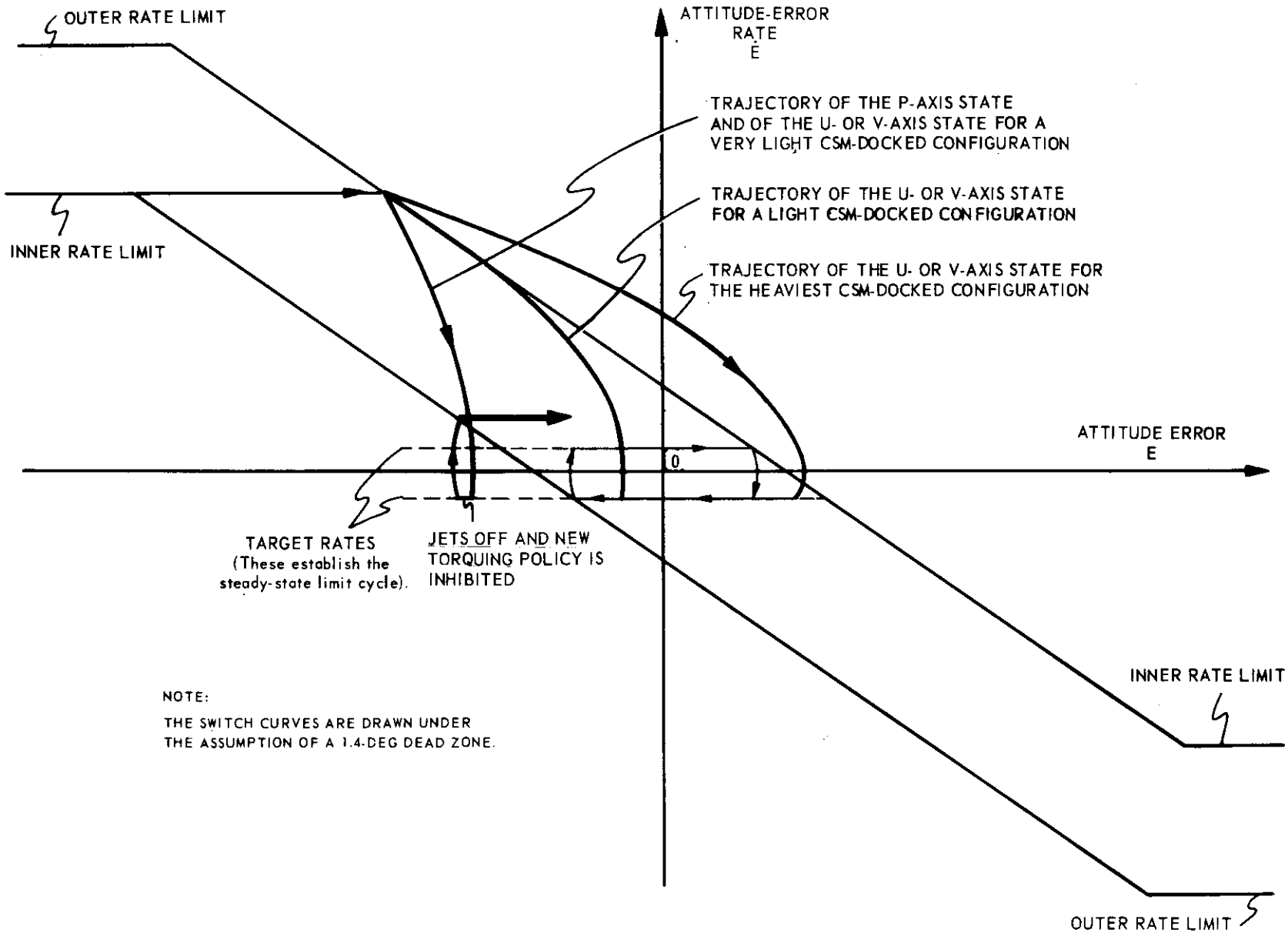

Fig. 3.4-11. Typical error-state trajectories of the CSM-docked configuration.

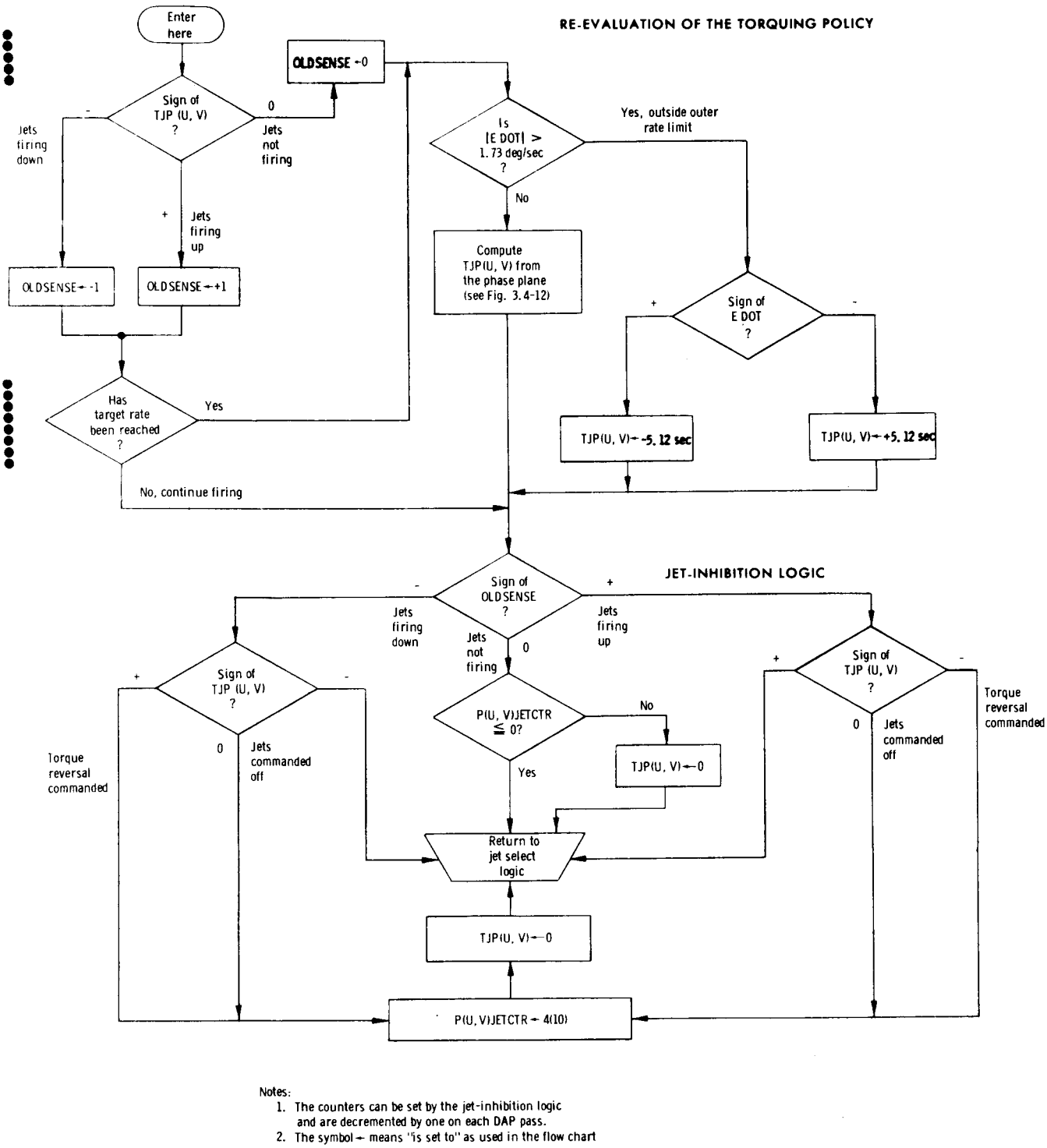

Notes:
1. The counters can be set by the jet-inhibition logic and are decremented by one on each DAP pass.
2. The symbol ← means "is set to" as used in the flow chart

Fig. 3.4–11A. The automatic RCS control logic for the CSM–docked configuration.

If the jets are currently firing, the logic checks the vehicle error rate to determine whether or not the target rate has been reached. If the target rate has not been reached, the re-evaluation of the torquing policy is bypassed. If the target rate has been reached, the DAP returns to the logical path that is followed when the jets are not firing, to re-evaluate the torquing policy.

In the re-evaluation of the torquing policy, a check is first made to determine if the error-rate magnitude, $|EDOT|$, exceeds the outer rate limit of 1.73 deg/sec. If the outer rate limit is exceeded, the jet firing time is set to ± 5.12 sec (signed so as to reduce the error rate), and the jet-inhibition logic is entered. When the outer rate limit is not exceeded, the control policy represented by Fig. 3.4-12 is used to determine the jet firing time. If the state lies in the coast region, the jet firing time is set to zero. If the state lies outside the coast region, the jet firing time is set to ± 5.12 sec.

After the jet firing time has been determined, the DAP enters the jet-inhibition logic. The jet-inhibition logic first checks the current state of the jets previously stored in OLDSENSE. If the jets are firing, the sign of the command about to be implemented is compared with the sense of the current jet firing. If the command calls for a firing of jets that are currently on, it is not altered by the jet-inhibition logic. However, if the jets are about to be commanded off, or on in the direction opposing the jets that are currently firing, the inhibition logic zeroes the jet firing time to turn off the jets during the current DAP pass and sets a counter to a value of 4 or 10 to inhibit jet firings for four DAP passes (0.4 sec) about the P axis or for ten DAP passes (1.0 sec) about the U or V axes. Each of the three counters involved is decremented by one at the beginning of each DAP pass.

If the jets are off, the inhibition logic checks the sign of the counter. If the counter has been decremented to a value less than or equal to zero, indicating that the most recent inhibition period has ended, then the command is not altered by the jet-inhibition logic. If the counter contains a value greater than zero, however, the jet firing time is set to zero to prevent the jets from firing on the current DAP pass.

Typical phase-plane trajectories of the CSM-docked configuration are illustrated in Fig. 3.4-11. The fine solid lines represent the steady-state limit cycle. Typical trajectories for large attitude errors are represented by the heavy solid lines. Note that for rotational jet firings about the P axis (or about the U and V axes for a very light CSM-docked configuration) the logic, which continues a firing until the target rate is reached, causes the phase-plane trajectory to travel not only through the coast region but also into the reverse torquing zone. The firing is eventually terminated, and the reverse firing is commanded after expiration of the inhibition period. This situation is aggravated with initial conditions in excess of

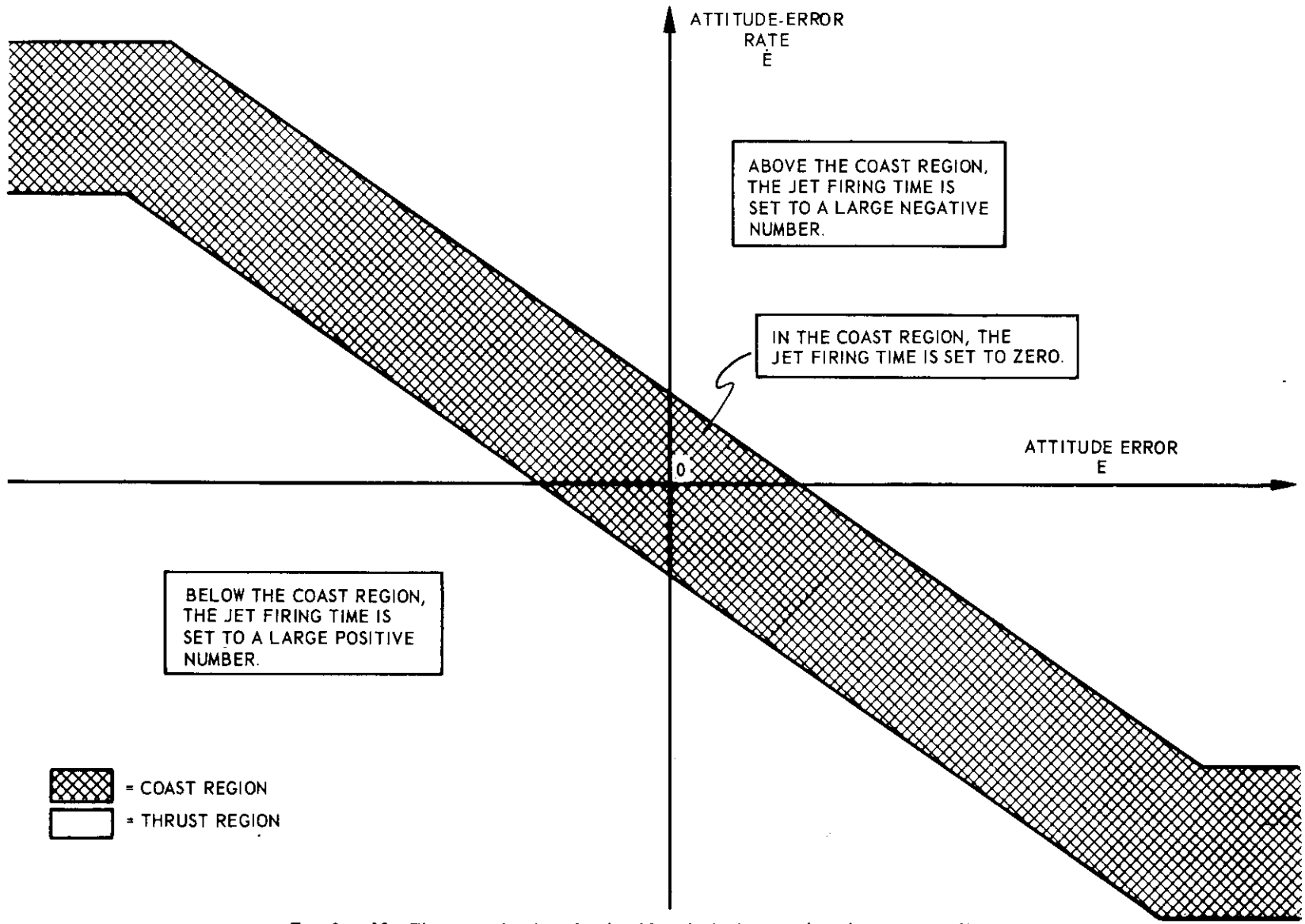

Fig. 3.4–12. The control policy for the CSM–docked case when the jets are off or the target rate has been reached.

the outer rate boundary at a large attitude error. However, according to the design guidelines, this performance is acceptable.

Another interesting (but unimportant) operational characteristic of the CSM-docked autopilot is the termination of continuous RCS rotational jet firings that have failed to torque the vehicle to the target rate within 5.12 sec. This behavior is due to the fact that the jet firing time is set to 5.12 sec when the firing is initiated and is decremented by 100 millisec on each DAP pass until the target rate is reached. Before the target rate is reached, the torquing policy is not re-evaluated and the jet firing time is not re-initialized. Consequently, if the target rate has not been attained after a 5.12-sec period of continuous torquing, the jet firing time reaches zero and the firing is terminated. This characteristic will normally never be seen in closed-loop operation because the required firing durations rarely reach 5.12 sec. However, in open-loop testing, such as polarity testing on the ground, this characteristic may be observed.

Note: Figures 3.4-13 and 3.4-14 were deleted in Rev. 1.

3.4.4 The RCS Control Laws for Manual Attitude Control*

Manual attitude control is exercised by means of one of three different control options: a) manual rate control, b) X-axis override, or c) minimum impulse control. For each option, a different control law is used.

The manual rate command modes employ two distinct control laws. These are known as the direct rate control law and the pseudo-automatic control law. Direct rate control is employed whenever the rate-command change (during 0.1 sec) exceeds a threshold level known as the "breakout level". This law computes jet-on times based upon rate-error information only. It is designed to provide fast response to changes in ACA commands and to null the rate errors without overshoot. This law is also utilized to damp the spacecraft rates below a threshold value (the "target deadband") before returning to attitude hold when the ACA is released.

The pseudo-automatic control law computes jet commands based upon both rate-error and attitude-error information. In this mode of operation, manual control is exercised through the TJETLAW phase-plane logic in the LM-alone configuration or through the simplified RCS control law in the CSM-docked configuration. Use of this law in effect forces the average rate error to be nulled, giving "tighter" control of the vehicle in the presence of disturbing accelerations and preventing attitude drift about axes that are not being commanded. With the

*By Donald W. Keene and Robert F. Stengel

pseudo-automatic control law, it is possible to achieve precise rate control and to obtain commanded rates as small as the quantization level of the ACA. Use of the automatic phase-plane logic allows efficient control to be maintained in any configuration – including the CSM-docked configuration. Because of the relatively large rate and error deadbands used in the phase-plane logic, small spurious changes in the commanded rates are effectively filtered by the logic. A small sustained change in the rate command will, however, be honored as soon as the phase point exceeds the deadbands of the switching logic. The delay in responding to these small commands is a function of the attitude deadband used. For tighter control in the coasting flight, the narrow angular-deadband selection is recommended. If, however, the commands over 0.1 sec exceed the breakout level, control is returned to the direct rate logic, and the response is almost immediate.

As indicated in Subsection 3.2 (Autopilot Control Modes), the manual rate control is considered to be in effect only when the astronaut is actually generating commands with his attitude controller assembly (ACA) and during the rate-damping phase after the astronaut has released the ACA prior to resumption of attitude hold. For three-axis manual control, the mode control switch must be in ATT HOLD.

Manual control for X-axis override is discussed in Subsection 3.4.4.2. The minimum impulse mode is discussed in Subsection 3.4.4.3.

3.4.4.1 Implementation of the Rate Command Mode

In the rate command mode, the LM DAP interrogates the rotational-hand-controller counters (LGC counters 42, 43, and 44), which interface with the proportional signals supplied by the ACA. The LM DAP interprets the counts obtained from counters 42, 43, and 44 as rate commands about the vehicle pilot axes in the order Q, P, and R, respectively. The command rate, ω_c, is computed as a quadratic function of the contents of these counters according to the formula

$$\omega_c = 0.00045335\delta(|\delta| + 10.5)\omega_{max}$$

where

δ = contents of counters 42, 43, and 44

ω_{max} = maximum commanded rate

The function ω_c/ω_{max} is plotted in Fig. 3.4-15. For the LM-alone case, a maximum count of 42 for full-scale deflection of the ACA (to the nominal soft-stop position) about an axis corresponds to a rate command of either 20 deg/sec or 4 deg/sec, depending on the hand-controller scaling selected in routine R03. For the CSM-docked configuration, the controller sensitivity is reduced by a factor of ten, thus giving maximum commanded rates of 2 deg/sec and 0.4 deg/sec, respectively.

The actual implementation of the control logic is somewhat complicated and may best be understood by reference to the flow graphs presented in Figs. 3.4-16 and 3.4-17. Additional flow graphs may be found in Fig. 3.6-5 of Subsection 3.6, which shows the overall structure of automatic and manual mode selection. For the purposes of this discussion, the logic may be divided into two parts: the P-axis manual control logic and the Q, R-axes manual control logic. In fact, the control of the P axis has been made logically independent of the Q, R axes to permit the use of the X-axis override function, which provides manual control of the P axis during automatic steering of the Q, R axes.

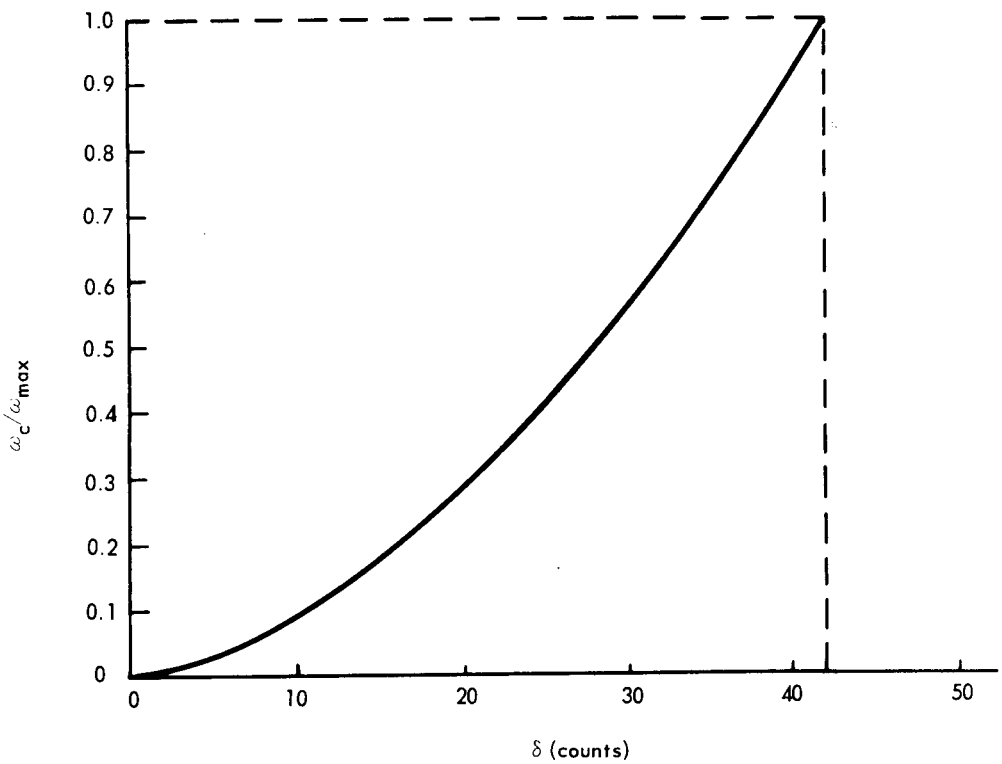

NOTE:

$$\frac{\omega_c}{\omega_{max}} = 0.00045335\delta(|\delta| + 10.5)$$

where

ω_c = command rate

ω_{max} = maximum commanded rate

δ = contents of counters 42, 43, and 44

Fig. 3.4-15. LM rotational-hand-controller quadratic scaling.

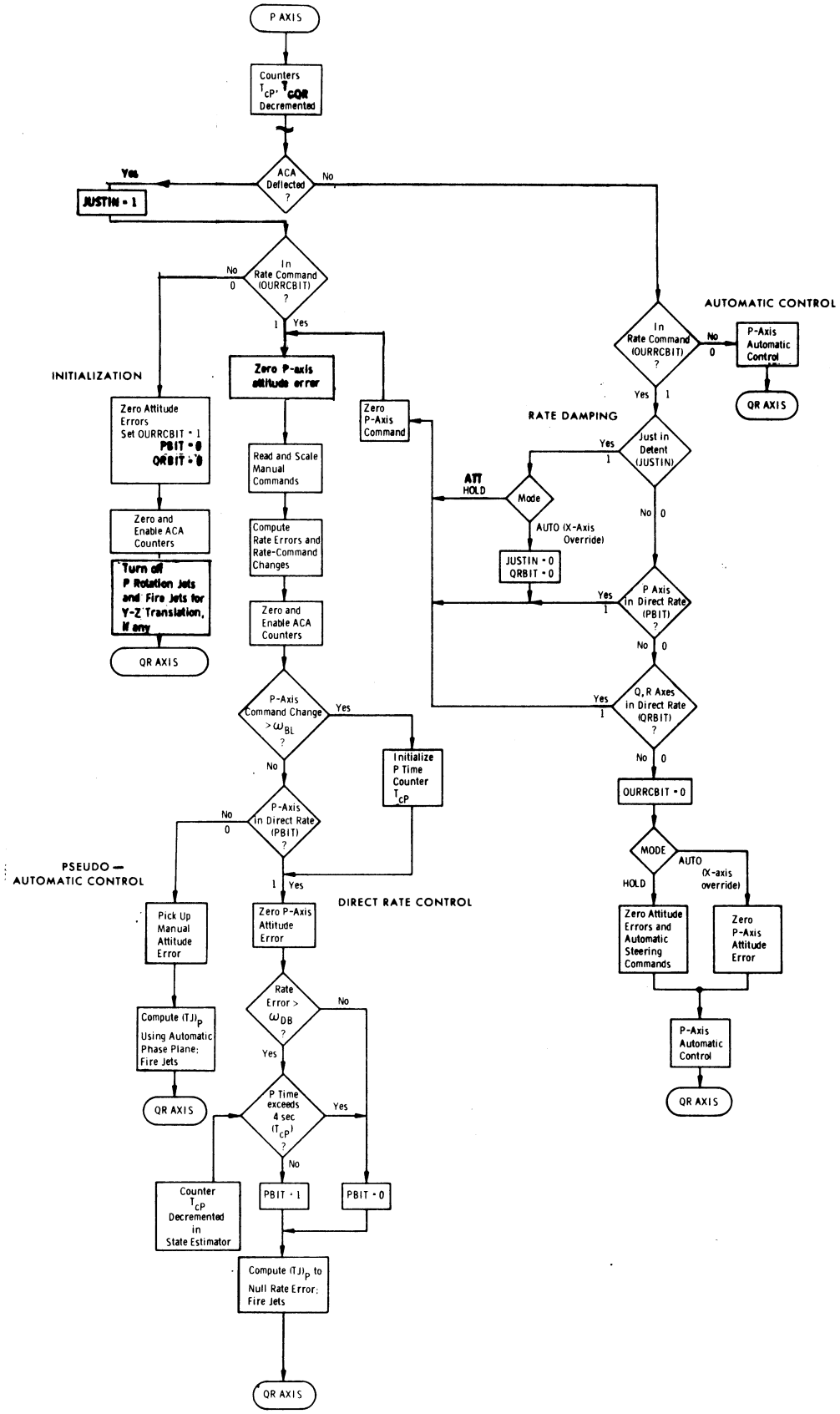

Fig. 3.4-16. Manual rate control logic for the P axis.

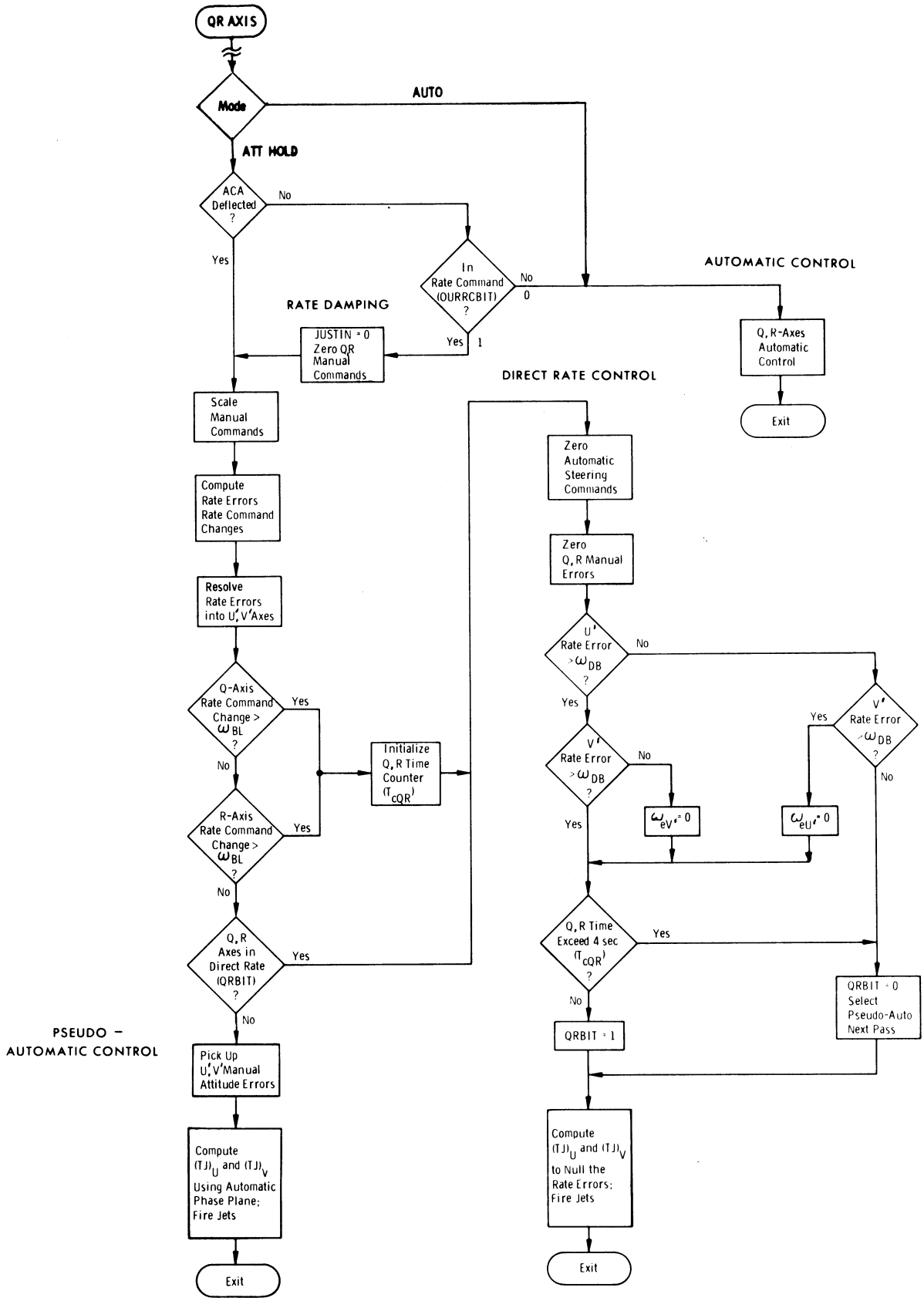

Fig. 3.4-17. Manual rate control logic for the Q,R axes.

P Axis

In the P-axis coding of the autopilot, a check is made to determine if the hand controller is out of detent (bit 15 of channel 31). Each time it is out of detent, the logic sets the JUSTIN bit of the autopilot control flag RCSFLAGS so that rate damping will be initiated when the hand controller is released. When the ACA is first moved out of detent, the DAP must initialize a number of variables and discretes before exercising manual control. In this initialization section, bit 12 of DAPBOOLS (OURRCBIT) is set to 1 to indicate that manual rate control (or X-axis override) is in effect. The bit indicates that rate damping is to be performed when the stick is returned to detent. This bit is also used by the Q, R-axes logic to bypass the calculation of automatic phase-plane errors and to use the manual-control attitude errors (θ_{emP}, θ_{emQ}, θ_{emR}) for the pseudo-automatic control law. These manual errors are computed in the state-estimator section of the P-axis logic and are updated every 0.1 sec according to the following algorithms.

First, a set of incremental body angles is derived from the CDU angle changes in the previous 0.1 sec; that is,

$$\begin{Bmatrix} \Delta A_{X_i} \\ \Delta A_{Y_i} \\ \Delta A_{Z_i} \end{Bmatrix} = [M_{GP}] \begin{Bmatrix} \theta_{o_i} - \theta_{o_{i-1}} \\ \theta_{i_i} - \theta_{i_{i-1}} \\ \theta_{m_i} - \theta_{m_{i-1}} \end{Bmatrix} \qquad (3.4\text{-}1)$$

where $[M_{GP}]$ is the gimbal-rate-to-body-rate transformation matrix, and θ_o, θ_i, and θ_m are the CDU angles. The manual errors are then computed recursively as:

$$\left.\begin{aligned} \theta_{emP_i} &= \theta_{emP_{i-1}} + \Delta A_{X_i} - \omega_{cP_{i-1}} \Delta T \\ \theta_{emQ_i} &= \theta_{emQ_{i-1}} + \Delta A_{Y_i} - \omega_{cQ_{i-1}} \Delta T \\ \theta_{emR_i} &= \theta_{emR_{i-1}} + \Delta A_{Z_i} - \omega_{cR_{i-1}} \Delta T \end{aligned}\right\} \qquad (3.4\text{-}2)$$

where $\omega_{cP_{i-1}}$, $\omega_{cQ_{i-1}}$, $\omega_{cR_{i-1}}$ are the manual rate commands on the previous sample interval and ΔT is the basic autopilot sample interval (0.1 sec). These errors are maintained as double-precision quantities to avoid truncation errors. The higher-order part of the Q, R errors is shared with the Q, R errors generated by the automatic and attitude-hold modes. Thus, in the automatic and attitude-hold modes, they are overwritten by θ_{eQ} and θ_{eR}.

In the initialization section of the manual rate control, both the manual errors (θ_{emP}, θ_{emQ}, and θ_{emR}) as well as the rate commands (ω_{cP}, ω_{cQ}, and ω_{cR}) are

zeroed. The hand-controller counters are also zeroed and the read logic is enabled so that the hand-controller commands can be read on the next autopilot pass. At this point, the logic zeroes the P-axis rotational command, sets up any Y- or Z-axis translation, and transfers control to the Q, R axes.

On the next pass through the P-axis logic, the DAP finds that initialization has been completed (OURRCBIT = 1) and begins its normal control cycle. At this point, CDUXD is set equal to the current CDUX and the P-axis hand-controller channel is read and scaled according to the routine R03 selection. The Q, R-axes commands are read and saved for processing by the Q, R-axes logic. The ACA counters are then zeroed and enabled. The DAP computes the P-axis rate error by differencing the estimated rate, $\hat{\omega}_P$, with the commanded rate, ω_{cP}; that is,

$$\omega_{eP} = \hat{\omega}_P - \omega_{cP} \tag{3.4-3}$$

for use by either the direct rate control logic or the pseudo-automatic logic. The DAP also computes the magnitude of the difference between the rate command and the previous value of the rate command; that is,

$$\Delta\omega_{cP_i} = \left|\omega_{cP_j} - \omega_{cP_{i-1}}\right| \tag{3.4-4}$$

If this difference exceeds the breakout level, ω_{BL}, the direct rate control law is selected. The breakout level is initialized in routine R03 to the following values:

ω_{BL} = 0.6 deg/sec for the ascent and descent configuration

ω_{BL} = 0.3 deg/sec for the CSM-docked configuration

Before entering the direct rate control law, however, a P-axis time counter, T_{cP}, is set to a value corresponding to 4 seconds. This counter is continually diminished in the state-estimator coding and is used to limit the time spent in the direct rate control law. This time limit guarantees that a) the more-efficient pseudo-automatic control law will eventually be utilized to counteract any unmodelled acceleration and b) attitude hold will be established when the ACA is released.

In the direct rate control law, the P-axis phase-plane error, θ_{emP}, is zeroed and CDUXD is set equal to the current value of CDUX. Next, a check is made to determine if the rate error exceeds the target deadband, ω_{DB}; that is, whether $|\omega_{eP}| > \omega_{DB}$. (The target deadband is set equal to the breakout level; that is, ω_{DB} is 0.6 deg/sec for the ascent and descent configurations and is 0.3 deg/sec for the CSM-docked configuration.) If so, the DAP then checks the P-axis time counter, T_{cP}, to determine if the 4-second time limit has been exceeded; that is,

whether $T_{cP} \leqq 0$. If not, a bit is set (PBIT of RCSFLAGS) to indicate that direct rate control will be required on the next pass in order to reduce the rate error further and prevent overshoot when returning to the pseudo-automatic control law.

If, however, the rate errors have been reduced below the target deadband or if the time limit has been exceeded, PBIT is reset to zero to permit the use of the pseudo-automatic control law on the next cycle.

At this point, the DAP computes the jet firing time required to null the rate error:

$$(TJ)_P = - \frac{\omega_{eP}}{2} \frac{1}{a_P} \qquad (3.4\text{-}5)$$

where $(1/a_P)$ is the inverse of the angular acceleration that two P-axis jets are expected to produce. This quantity is computed and stored in the 1/ACCS routine. The firing time is computed on the basis of four jets being used. Four are, in fact, called for in either descent or in the CSM-docked configuration when the magnitude of the rate error is greater than 1.4 deg/sec. When $|\omega_{eP}|$ is smaller, and throughout ascent, two jets are chosen and the firing time $(TJ)_P$ is correspondingly doubled. In the rate command mode, as in the other control calculations, the P-axis offset acceleration is assumed to be zero.

In the CSM-docked configuration, $(1/a_P)$ is set equal to the maximum value (POSMAX), which corresponds to an angular acceleration of approximately 1.4 deg/sec^2. Since the target deadband is relatively large (0.3 deg/sec) in this configuration, undershoot is prevented since the rate increment caused by a 100-millisecond firing is smaller than ω_{DB}. In effect, then, once the P-axis jets are turned on, they will remain on for at least 100 milliseconds – thus preventing chattering, even though $1/a_P$ (and $(TJ)_P$) may be much smaller than the correct value. The width of the target deadband also prevents overshoot even in the most critical case (CSM-LM empty). The same situation exists in computing $(TJ)_U$ and $(TJ)_V$ in the Q, R-axes control logic.

In the direct-rate-control logic, T_{jet} is calculated at 0.1-sec intervals until control reverts to the pseudo-automatic control law. However, when a "skip" request is issued, the T_{jet} calculation interval increases to 0.2 sec. These skips occur when the previously computed T_{jet} is less than 0.150 sec but greater than zero. As long as PBIT is set to 1, the direct rate control law is used.

After $(TJ)_P$ has been computed, the P-axis rotation jets are selected, the firings are initiated, and control is transferred to the Q, R-axes logic.

Selection of the pseudo-automatic control law occurs if $\Delta\omega_{cP} < \omega_{BL}$ and if PBIT is zero. If both conditions exist, the manual attitude and rate errors are stored for the phase-plane computations and control is determined by the same routines that are used for automatic control and attitude hold.

Use of the direct rate control logic assures that both the attitude and rate errors are small when switching to pseudo-automatic control. Thus, there should be little, if any, rate overshoot on switchover. If T_{jet}, as computed in the previous pass through the direct-rate-control logic, happened to be greater than 150 milliseconds, the firing will not be terminated at this time even though the phase point lies within the phase-plane deadband. Either TJETLAW or the simplified CSM-docked control law will continue to fire the jets until the rate error is sufficiently reduced. This feature has been exploited to minimize the effects of the relatively wide target deadbands (ω_{DB}) used in the direct rate control law. This feature is particularly important in the CSM-docked configuration.

When the ACA is returned to detent, the rate damping process begins. This process assures that the spacecraft vehicle rates will be sufficiently reduced so that large transients are avoided on returning to automatic control. In the rate-damping phase, the logic finds that the ACA has been returned to detent but that OURRCBIT = 1. The logic then checks to see if the JUSTIN bit is set to 1. The JUSTIN bit will be set on the first pass through the rate-damping logic. If JUSTIN = 1, the DAP must then determine whether X-axis override, or a three-axis control function is required. For X-axis override control, rate damping is performed about the P axis only. Otherwise, all three axes are rate damped. For X-axis override control, the JUSTIN bit and QRBIT are reset to zero at this point to insure that the automatic mode will be entered as soon as rate damping is completed about the P axis. (For three-axis control, the JUSTIN bit will be reset by the Q, R axes, rather than at this point, to assure that the damping process is also initiated about the Q, R axes when a Q, R-axes skip occurs on the first rate-damping pass.) Next, the command rate, ω_{cP}, is zeroed and the logic returns to the manual rate control laws.

Rate damping is completed when both PBIT and QRBIT are zero. (As indicated above, in X-axis override, QRBIT is automatically zero.) This implies that

$$|\omega_{eP}| < \omega_{DB}$$

$$|\omega_{eU'}| < \omega_{DB} \ *$$

$$|\omega_{eV'}| < \omega_{DB}$$

or that the 4-sec limits have been exceeded. When this is found to be true, OURRCBIT is reset to zero so that on the next and subsequent passes automatic control will be resumed.

At this point, the DAP checks the mode switch to see if X-axis override is in effect. If it is, the desired outer gimbal angle (CDUXD) is set equal to the present gimbal angle (CDUX) and the logic exits to P-axis automatic control. If, however, three-axis manual rate control is in effect, the DAP sets

*Although the discussion in this subsection concerns the P, U', V' axes, it should be noted that in the CSM-docked configuration the U' and V' axes are respectively coincident with the stationary U and V axes.

$$\begin{aligned} \text{CDUXD} &= \text{CDUX} & \theta_{do} &= \theta_o \\ \text{CDUYD} &= \text{CDUY} \quad \text{or} & \theta_{di} &= \theta_i \\ \text{CDUZD} &= \text{CDUZ} & \theta_{dm} &= \theta_m \end{aligned}$$

and zeroes the automatic-steering inputs. The logic then exits to P-axis automatic control.

Q, R Axes

The logic of the Q, R-axes control is similar to that of the P axis, except that the physical coupling and the transformation to U', V' axes requires that both axes utilize the same control law in any given pass. If either the Q or R command exceeds the breakout level, direct rate control is used. Only when both rate errors ($\omega_{eU'}$ and $\omega_{eV'}$) are less than the target deadband – or after the 4-sec limit has elapsed – will the logic return to pseudo-automatic control.

At the beginning of the Q, R-axes manual logic, a check is made to determine if the ACA is out of detent. The DAP does not check the channel bit directly but uses the results of the P-axis check. This procedure eliminates the possibility of exercising Q, R-axes manual control before the P axis has initialized the control variables.

As for the P axis, the control law scales the Q, R commands (ω_{cQ} and ω_{cR}, which are stored by the P axis) and computes the rate errors. Since the DAP controls in U', V' axes, these rate errors are then resolved into U', V' components ($\omega_{eU'}$, $\omega_{eV'}$). A check is then made to determine if either $|\Delta\omega_{cQ}| > \omega_{BL}$ or $|\Delta\omega_{cR}| > \omega_{BL}$. If so, the Q, R-axes direct rate control law is selected. Before entering the direct rate control law, however, the Q, R-axes time counter, T_{cQR}, is set to 4 seconds. This counter has the same function as T_{cP}.

At the beginning of the direct rate control law, the automatic steering inputs are zeroed; that is,

$$\begin{aligned} \omega_{dP} &= 0 \quad & \Delta\theta_{do} &= 0 \quad & \beta_P &= 0 \\ \omega_{dQ} &= 0 \quad & \Delta\theta_{di} &= 0 \quad & \beta_Q &= 0 \\ \omega_{dR} &= 0 \quad & \Delta\theta_{dm} &= 0 \quad & \beta_R &= 0 \end{aligned}$$

and the Q, R manual errors, θ_{emQ} and θ_{emR}, are zeroed. The desired CDU's are also set equal to the current CDU's; that is,

$$\begin{aligned} \text{CDUXD} &= \text{CDUX} & \theta_{do} &= \theta_o \\ \text{CDUYD} &= \text{CDUY} \quad \text{or} & \theta_{di} &= \theta_i \\ \text{CDUZD} &= \text{CDUZ} & \theta_{dm} &= \theta_m \end{aligned}$$

The logic then checks to see if both the U', V' rate errors are within the target deadbands. If so, the QRBIT of RCSFLAGS is reset to zero, allowing pseudo-automatic control on the next cycle, and control is transferred to the jet-on-time calculation.

If $|\omega_{eU'}| > \omega_{DB}$ and $|\omega_{eV'}| \leq \omega_{DB}$, $\omega_{eV'}$ is set to zero so that $(TJ)_V$ is computed to be zero and the V-axis rotational jets are turned off (see below).

If $|\omega_{eU'}| \leq \omega_{DB}$ and $|\omega_{eV'}| > \omega_{DB}$, $\omega_{eU'}$ is set to zero so that $(TJ)_U$ is computed to be zero (see below) and the U-axis rotational jets are turned off. Otherwise, $\omega_{eU'}$ and $\omega_{eV'}$ are left untouched.

If the Q, R timer exceeds the 4-sec limit, QRBIT is reset to zero. Otherwise, QRBIT is set to 1 – indicating that direct rate control will be required on the next pass in order to reduce the rate errors still further.

At this point, the DAP computes the jet firing times $(TJ)_U$ and $(TJ)_V$ required to null the rate errors:

$$(TJ)_U = -\omega_{eU'}\left(\frac{1}{a_{U'}}\right)$$

$$(TJ)_V = -\omega_{eV'}\left(\frac{1}{a_{V'}}\right)$$

The values of $(1/a_{U'})$ and $(1/a_{V'})$, the inverse of the angular acceleration that the jets are expected to produce, are computed and stored in the 1/ACCS routine. They are the "$1/a_{netpos}$" and the "$1/a_{netneg}$" quantities discussed in Subsection 3.4.2 as part of the input to TJETLAW. As mentioned there, the values for the U' and V' axes include any effects of offset acceleration and disabled jets and are stored for both one-jet and two-jet firings. The rate command mode always attempts to use balanced couples (that is, two jets) about the U and V axes, without regard to X-axis translation commands.

In the CSM-docked configuration, both $(1/a_{U'})$ and $(1/a_{V'})$ are set to the maximum value (POSMAX).

After $(TJ)_U$ and $(TJ)_V$ have been computed, the U, V-axes rotation jets are selected, the firing is initiated, and the autopilot pass is terminated.

Selection of the Q, R axes pseudo-automatic control occurs if $|\Delta\omega_{cQ}| < \omega_{BL}$, $|\Delta\omega_{cR}| < \omega_{BL}$, and QRBIT = 0. If these conditions exist, the attitude errors θ_{emQ} and θ_{emR} are resolved into the U', V' axes and stored along with the rate errors $\omega_{eU'}$ and $\omega_{eV'}$ for the phase-plane computations. Control is then transferred to TJETLAW (or the CSM-docked RCS law).

In the rate-damping phase of the Q, R axes, the ACA is returned to detent but OURRCBIT is still set. At this point, the JUSTIN bit is reset to zero, the manual commands ω_{cQ} and ω_{cR} are zeroed, and the manual control laws are executed. The Q, R logic informs the P axis (via QRBIT) when the Q, R rates have been sufficiently damped to permit return to automatic control. The P-axis coding is responsible for terminating the damping phase by resetting OURRCBIT.

The delay time between the deflection of the rotational hand controller and the beginning of the jet firing is made up of the following components:

0 to 100 millisec – to detect that the controller is out of detent, and then zero and enable the counters.

100 millisec – for one command-cycle period to return and read the counters.

30 to 50 millisec (approximately) – for computational delay and jet-thrust on-delay.

Since the checking of the stick position is part of the P-axis coding, an extra 100-millisec delay is introduced immediately following a short P-axis firing (because the control about the P-axis is then skipped).

3.4.4.2 Implementation of the X-Axis Override Mode

Manual rotation control in the X-axis override mode is implemented in a manner similar to that used for the rate command mode, except that the LM DAP will respond only to manual yaw (P-axis) commands. [To avoid interference with the automatic steering, the LM DAP will not alter the pitch (Q-axis) and roll (R-axis) automatic steering commands.] After the ACA controller has been removed from its center (detent) position and during the rate-damping phase subsequent to the controller's return to its detent position, the LM DAP zeroes the yaw phase-plane errors and sets the desired outer gimbal angle equal to the current outer gimbal angle; that is,

$$CDUXD = CDUX \qquad (3.4\text{-}11)$$

For further information, see Subsection 3.4.4.1.

3.4.4.3 Implementation of the Minimum Impulse Mode

During manual rotation control of the minimum-impulse type, the LGC interrogates bits 1 through 6 of channel 31, which interface with the pulse/direct switches of the ACA. The LM DAP interprets these input bits as minimum-impulse commands about the P, Q and R axes.

Each yaw (P-axis) command of the ACA controller will cause a two-jet 14-millisec firing to be commanded about the P axis. The ACA controller must then be returned to its center (detent) position about the yaw axis before another P-axis impulse will be fired.

A pitch (Q-axis) or roll (R-axis) minimum-impulse command will produce a corresponding two-jet firing about the Q axis or the R axis for a duration of 14 millisec in the LM-alone configuration and for a duration of 60 millisec in the CSM-docked configuration. Given simultaneous pitch and roll commands, the LM DAP will honor only the pitch request. As in the case of yaw-axis control, the ACA controller must be returned to its center position about the pitch and roll axis before another Q-axis or R-axis impulse can be fired. When there are no disabled jets,

the two-jet torque couples employed are selected from the fuel system (A or B) that is specified by the astronaut in NOUN 46 by means of routine R03.

Whenever the minimum impulse mode is in effect, the LM DAP zeroes the automatic steering inputs and the phase-plane attitude errors. This means that when the ACA controller is in its center (detent) position, the LM DAP will not attempt to maintain any attitude control and the LM will be in a free-drift condition.

The LM DAP responds to minimum-impulse commands on the first pass during which the controller is found to have moved out from the detent position. However, a move back to detent will not be recorded on the pass immediately following a P-axis impulse, since the check of stick position is a part of the P-axis coding and is therefore skipped over on the cycle subsequent to a short P-axis firing. It is, therefore, theoretically possible to obtain up to 5 pulses per second about the Q and/or R axes and up to 3-1/3 pulses per second about the P axis.

3.4.5 The Jet Select Logic*

In general, each of the attitude control laws produces requirements for some number of jets to be fired about the P, U, and V axes. The astronaut can simultaneously command manual translation of the LM by displacing the tee-handle left-hand controller of his thrust/translation controller assembly (TTCA) from its neutral (detent) position in the same direction he wishes the LM to move.** This action results in the application to the LGC by the TTCA of a discrete for each of the axes commanded. These discretes instruct the LGC to issue commands to the RCS that cause the LM to be accelerated in the desired direction. The acceleration is independent of the magnitude of the displacement of the TTCA from its neutral position. The acceleration stops when the discretes are removed by the return of the controller to its neutral position. These translation commands are monitored by the autopilot during each cycle (except when skips occur), that is, ten times per second.

Ullage is automatically commanded via the LM DAP by the mission programs just prior to ignition of either of the main engines. An internal discrete (the ULLAGER bit in DAPBOOLS) is provided for this purpose. The ACC4OR2X bit of DAPBOOLS indicates whether two or four jets are to be used. The mission programs are responsible for initiating and terminating automatic ullage. For further information, see Section 4 of this GSOP.

---

*By Richard D. Goss and Lowell Hull.

**The two-position selector on the controller must be in the JETS position to obtain control of X-axis translation by means of the RCS jets. With the selector in the THROTTLE position, up-and-down motion of the controller along the X axis results in varying the thrust magnitude of the descent engine.

Given information concerning the desired rotational torque, the desired direction of translation, and the desired numbers of jets to be used for each, the jet select logic determines the jet selection policy – that is, the best jet firing policy, taking any disabled jets into account. The output of the jet select logic consists of LGC data words that are suitable for loading into LGC output channels 5 and 6 to turn the jets on and off. In addition, the jet select logic provides information on the number, and directions, of the U-axis, V-axis, and P-axis firings for use in the recursive state estimator.

When there are no jets available to carry out a required rotation or translation – that is, when all the jets required have been isolated by the crew – the program alarm light on the DSKY is lit and the appropriate alarm code is stored. (The various codes are given in the following discussion.) It should be mentioned that this routine will continue to set up the alarm on every subsequent pass until either the need for the jets is removed or the required jet(s) is (are) re-enabled by the crew or uplink.

Figure 3.4-18 identifies the 16 jets of the RCS and their thrust directions. The RCS employs two independent fuel systems, each of which supplies eight of the jets. The figure also shows this division.

The RCS jets are assigned to channels 5 and 6 in the following order:

Channel 5		Channel 6	
Bit	Jet	Bit	Jet
1	1	1	7
2	2	2	3
3	5	3	15
4	6	4	11
5	9	5	12
6	10	6	8
7	13	7	4
8	14	8	16

3.4.5.1 The Jet Selection Policies for Rotation about the P Axis and for Translation Along the Y and Z Axes

The channel-6 jets are employed both for rotational control about the P axis and for Y-axis and Z-axis translation commands. Selection of jets for P-axis rotational control is made without simultaneously trying to satisfy the Y-axis and Z-axis translation commands. That is, rotation will take priority over translation, and therefore Y-axis and Z-axis translation commands will be executed only when no P-axis rotation commands are present.

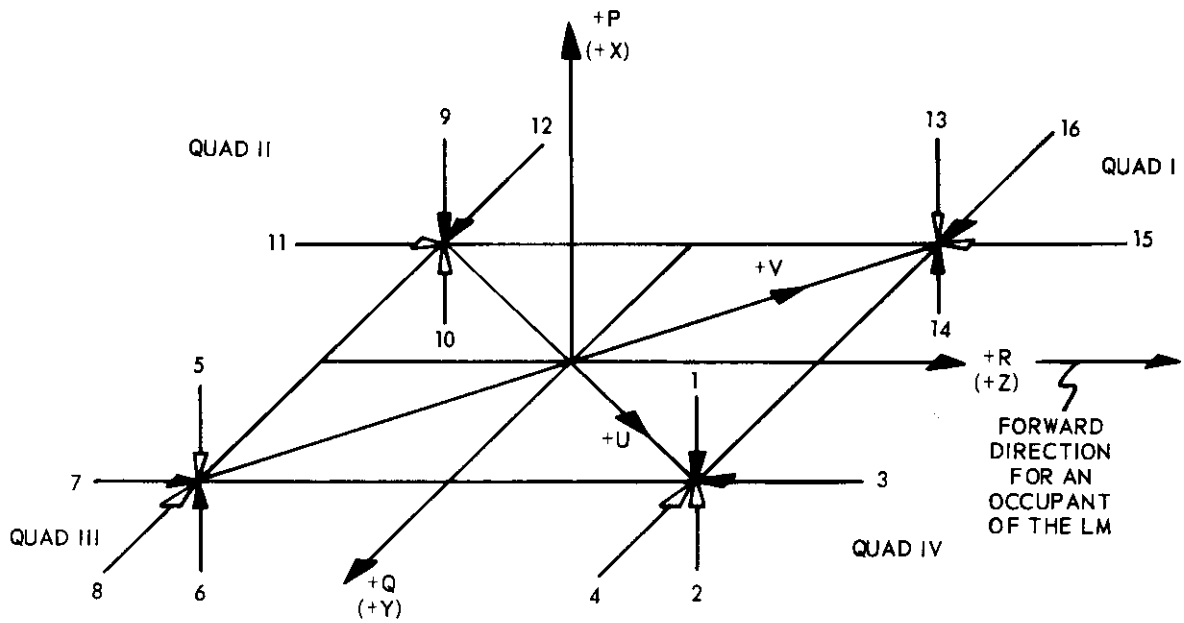

KEY

JETS ASSOCIATED WITH RCS FUEL SYSTEM A (JETS 2, 4, 5, 8, 10, 11, 13, AND 15)

JETS ASSOCIATED WITH RCS FUEL SYSTEM B (JETS 1, 3, 6, 7, 9, 12, 14, AND 16)

NOTES:

1. THE ARROWS INDICATE THRUST DIRECTION, NOT EXHAUST VELOCITY.
2. SEE FIG. 3.1-5 OF SUBSECTION 3.1 FOR THE RELATIONSHIP OF THE RCS JETS AND CONTROL AXES DEPICTED HERE TO THE LM VEHICLE.
3. IN CASE OF FAILED JETS, THE ASTRONAUT DISABLES JETS IN PAIRS AS FOLLOWS:

1,3	5,8	9,12	13,15
2,4	6,7	10,11	14,16

4. THE P, Q, AND R DESIGNATIONS FOR THE CONTROL AXES ARE USED IN CONNECTION WITH ROTATION, WHEREAS THE X, Y, AND Z DESIGNATIONS ARE USED IN CONNECTION WITH TRANSLATION.

Fig. 3.4-18. The 16 jets of the RCS and their thrust directions.

Table 3.4-5 specifies the normal P-axis rotation policies – that is, the jet selection policies for the case in which no jets have been disabled. If any of the rotation policies given in Table 3.4-5 contains a disabled jet, then alternative two-jet rotation policies will be attempted in the following order, starting from the top of the list, until a policy containing nondisabled jets is found:

+P Rotation	-P Rotation
7, 15	8, 16
4, 12	3, 11
4, 7	8, 11
7, 12	11, 16
12, 15	3, 16
4, 15	3, 8

If none of these alternative policies is possible, then the program alarm light is displayed and alarm code 02003 is set up to inform the astronaut that a P-axis rotation failure exists.

Table 3.4-5. The normal jet selection policies for various types of rotation about the P axis.

Type of Rotation Requested	Jet Selection Policy
4-jet, +P rotation	4, 7, 12, 15
2-jet, +P rotation	Alternate pulses between (4, 12) and (7, 15).
4-jet, -P rotation	3, 8, 11, 16
2-jet, -P rotation	Alternate pulses between (3, 11) and (8, 16).
Note: All rotations expressed are to be interpreted in terms of the right-hand rule.	

Table 3.4-6 gives the normal Y-axis and Z-axis translation policies, together with the alternative policies for use in case any disabled jets are present. If, for a given Y-axis or Z-axis translation command, the associated alternative disabled-jet policy is not possible, then the program alarm light is displayed and code 02001 is set up to inform the astronaut of a Y-axis or Z-axis translation failure.

3.4.5.2 The Jet Selection Policies for Rotation about the U and V Axes* and Translation Along the X Axis

The channel-5 jets are used both for rotational control about the U and V axes and for X-axis translation, including automatic ullage. The ACC4OR2X and AORBTRAN bits in DAPBOOLS specify whether X-axis translation is

*For the purposes of this subsection, the discussion will concern the U and V axes rather than the U' and V' axes. It is to be understood that U and V rotational policies refer to torques to be applied about the U and V axes, with control being maintained about the U' and V' axes in the ascent and descent configurations and about the U and V axes in the CSM-docked configuration.

Table 3.4-6. The jet selection policies for various types of translation along the Y and Z axes.

Type of Translation Commanded	Normal Policy	Alternative Disabled-Jet Policy
+Y translation	12, 16	If 16 has been disabled, set up the tacking* policy of alternating between (12, 3) and (12, 11). If 12 has been disabled, set up the tacking policy of alternating between (16, 15) and (16, 7).
-Y translation	4, 8	If 8 has been disabled, set up the tacking policy of alternating between (4, 3) and (4, 11). If 4 has been disabled, set up the tacking policy of alternating between (8, 7) and (8, 15).
+Z translation	7, 11	If 11 has been disabled, set up the tacking policy of alternating between (7, 8) and (7, 16). If 7 has been disabled, set up the tacking policy of alternating between (11, 12) and (11, 4).
-Z translation	3, 15	If 15 has been disabled, set up the tacking policy of alternating between (3, 4) and (3, 12). If 3 has been disabled, set up the tacking policy of alternating between (15, 8) and (15, 16).
(+Z, +Y) translation [+U translation]	7, 11, 12, 16	If either 11 or 12 has been disabled, use (7, 16). If either 7 or 16 has been disabled, use (11, 12).
(-Z, -Y) translation [-U translation]	3, 4, 8, 15	If either 8 or 15 has been disabled, use (3, 4). If either 3 or 4 has been disabled, use (8, 15).
(+Z, -Y) translation [+V translation]	4, 7 8, 11	If either 4 or 11 has been disabled, use (7, 8). If either 7 or 8 has been disabled, use (4, 11).
(-Z, +Y) translation [-V translation]	3, 12 15, 16	If either 15 or 16 has been disabled, use (3, 12). If either 3 or 12 has been disabled, use (15, 16).

*Tacking alternation is done every 0.1 sec.

to be done with two or four jets and, if two, whether system A or system B pairs are to be preferred.

If no conflict exists between the jets required for translation and the jets required for rotation, then both the rotation policies and the translation policies are executed. If a conflict does exist, however, then only the rotation policy is executed – to be followed by the translation policy as soon as the required rotation has been completed. For example, if two jets are desired for positive rotation

about the U axis (that is, jets 5 and 14) and the two B-system jets (6 and 14) are requested for translation, then the translation will be postponed. If, on the other hand, only one jet were desired for +U rotation, then jet 14 would be used to give both rotation and translation.

Table 3.4-7 gives the normal U-axis and V-axis rotational policies, together with the alternative policies for use in case any disabled jets are present. If, for a given U-axis or V-axis rotation request, the associated alternative disabled-jet policy is not possible, then the program alarm light is displayed and code 02004 is set up to inform the astronaut of a U-axis or V-axis rotation failure.

Table 3.4-7. The jet selection policies for various types of rotation about the U and V axes.

Type of Rotation Requested	Normal Policy	Alternative Disabled-Jet Policy
2-jet, +U rotation	5, 14	If 14 has been disabled, use 5 alone. If 5 has been disabled, use 14 alone.
1-jet, +U rotation (+X translational sense desired)	14	If 14 has been disabled, use 5.
1-jet, +U rotation (-X translational sense desired)	5	If 5 has been disabled, use 14.
2-jet, -U rotation	6, 13	If 13 has been disabled, use 6 alone. If 6 has been disabled, use 13 alone.
1-jet, -U rotation (+X translational sense desired)	6	If 6 has been disabled, use 13.
1-jet, -U rotation (-X translational sense desired)	13	If 13 has been disabled, use 6.
2-jet, +V rotation	1, 10	If 10 has been disabled, use 1 alone. If 1 has been disabled, use 10 alone.
1-jet, +V rotation (+X translational sense desired)	10	If 10 has been disabled, use 1.
1-jet, +V rotation (-X translational sense desired)	1	If 1 has been disabled, use 10.
2-jet, -V rotation	2, 9	If 9 has been disabled, use 2 alone. If 2 has been disabled, use 9 alone.
1-jet, -V rotation (+X translational sense desired)	2	If 2 has been disabled, use 9.
1-jet, -V rotation (-X translational sense desired)	9	If 9 has been disabled, use 2.

Note: The +X translational sense is considered "desirable" throughout the powered ascent.

Table 3.4-8 gives the normal X-axis translation policies, together with the alternative policies for use in case any disabled jets are present. If, for a given X-axis translation policy, the associated alternative disabled-jet policy is not possible, then the program alarm light is displayed and code 02002 is set up to inform the astronaut of an X-axis translation failure.

Table 3.4-8. The jet selection policies for various types of translation along the X axis.

Type of Translation Commanded	Normal Policy	Alternative Disabled-Jet Policy
4-jet, +X translation	2, 6, 10, 14	If either 2 or 10 has been disabled, use (6, 14). If either 6 or 14 has been disabled, use (2, 10).
2-jet, +X translation with fuel system A	2, 10	If either 2 or 10 has been disabled, use (6, 14).
2-jet, +X translation with fuel system B	6, 14	If either 6 or 14 has been disabled, use (2, 10).
4-jet, -X translation	1, 5, 9, 13	If either 5 or 13 has been disabled, use (1, 9). If either 1 or 9 has been disabled, use (5, 13).
2-jet, -X translation with fuel system A	5, 13	If either 5 or 13 has been disabled, use (1, 9).
2-jet, -X translation with fuel system B	1, 9	If either 1 or 9 has been disabled, use (5, 13).

REFERENCES FOR SUBSECTION 3.4

1. Goss, R. D., Derivation of TJETLAW Algorithm, Spacecraft Autopilot Development Memorandum No. 2-68, Instrumentation Laboratory, Massachusetts Institute of Technology, Cambridge, Massachusetts, February 1, 1968.

2. Jones, J. E., Modification of ROUGHLAW in Log Section TJETLAW to Stabilize Lightest Ascent Configuration, Spacecraft Autopilot Development Memorandum No. 8-69, Instrumentation Laboratory, Massachusetts Institute of Technology, Cambridge, Massachusetts, February 14, 1969.

3. Kalan, G. R., Improvement of the Bending Stability of the LM Autopilot in the CSM-Docked Configuration, Spacecraft Autopilot Development Memorandum No. 18-69, Instrumentation Laboratory, Massachusetts Institute of Technology, Cambridge, Massachusetts, April 18, 1969.

4. Goss, R. D., Nonorthogonal Axis System for LM DAP, Spacecraft Autopilot Development Memorandum No. 12-69, Instrumentation Laboratory, Massachusetts Institute of Technology, Cambridge, Massachusetts, March 5, 1969.

SUBSECTION 3.5

TRIM-GIMBAL CONTROL LAWS

by

Craig C. Work

3.5.1 Control Objectives

Although the trim-gimbal control system in the LM was originally intended to keep the thrust vector of the descent engine locked onto the shifting center of gravity of the LM, it is also capable of maintaining full attitude control whenever the flight situation imposes only mild requirements on the LM digital autopilot (LM DAP). Some benefits that derive from this latter capability of the trim-gimbal control system are the following:

1. A reduction in the RCS fuel usage, which can result in larger emergency fuel supplies and/or a decrease in the initial lift-off weight.
2. A reduction in the number of RCS jet firings, with a corresponding decrease in the anticipated probabilities of jet failures.

Each of the two trim-gimbal drives rotates the descent-engine bell about its hinge pin at a rate of 0.2 deg/sec. Because the trim-gimbal rate is so slow and because there is no penalty attached to continuous trim-gimbal activity, a control law that minimizes the reaction time required for attitude-error control is the most desirable kind of control law. A law of this type – termed the GTS attitude control law in this report — has been derived and implemented in the LM DAP; see References 1 through 3.

By means of the two trim gimbals, the descent-engine bell can be rotated about either the pitch (Q) axis or the roll (R) axis. The attitude control law is applied to each of these two axes independently. Accordingly, the ensuing discussion generally refers to only one trim gimbal.

A trim gimbal can affect the angular acceleration of the LM about an axis by redirecting the thrust vector, while the RCS jets can add to this angular

acceleration in order to achieve temporary variation. The RCS jets, however, should not be required to fire indefinitely to compensate for an error in the direction of the thrust vector. Therefore, the trim gimbal always has the sole responsibility for controlling the angular acceleration of the LM about an axis, while the RCS jets and the trim gimbal together share the function of controlling the attitude error and the attitude rate about that axis.

Two operational modes are used, therefore, for controlling a trim gimbal. These bear the following designations:

1. The GTS attitude control mode.
2. The GTS acceleration nulling mode.

The GTS attitude control mode defines a switching surface in the attitude-control phase space. Here, the trim-gimbal-drive directions are selected by the LM DAP to zero the attitude error, rate, and acceleration about a given axis simultaneously. When the trim-gimbal control system operates in the GTS attitude control mode, the Q and R RCS jets are ordinarily inactive. When the state estimator shows that the LM is not in the RCS jet "coast zone", the GTS attitude control mode can still continue — provided the RCS jet firings are short (that is, the LM is only slightly outside the coast zone).

The position of the LM in the RCS phase plane is calculated every 0.1 sec, while the GTS attitude control mode is executed every 0.2 sec. This allows for the "shared control" condition. A short RCS jet firing (less than 0.1 sec) can "interlace" with the GTS attitude control mode without mutual interference. A long RCS jet firing (greater than 0.1 sec), however, forces the trim gimbal to drop back into the GTS acceleration nulling mode, where it remains until a) the LM is in a coast zone again and b) the thrust vector is aligned sufficiently close to the LM center of gravity to enable the trim gimbal to null the remaining offset angular acceleration within less than 5 seconds. The interaction of RCS control with trim-gimbal control is discussed in detail in Subsection 3.6.

3.5.2 The GTS Attitude Control Law

The GTS attitude control mode is based on the following modified time-optimal control law:[1, 3]

$$K = 0.3\ FLR/I \tag{3.5-1}$$

$$\Delta = -\mathrm{sgn}\ (\dot{\theta} + \ddot{\theta}\,|\ddot{\theta}|/(2K)) \tag{3.5-2}$$

$$u = -\mathrm{sgn}\ [K\theta + \ddot{\theta}\,(\ddot{\theta}^2/(3K) - \Delta\dot{\theta}) - \Delta K^{1/2}(-\Delta\dot{\theta} + \ddot{\theta}^2/(2K))^{3/2}] \tag{3.5-3}$$

where

K = the assumed control effectiveness*

u = the sign of the commanded change in angular acceleration that is to be induced by driving the trim gimbal about its axis (note that the quantity Δ in the relationship for u is defined by Eq. (3.5-2))

$\theta, \dot{\theta}, \ddot{\theta}$ = the attitude error and its first and second derivatives with respect to time

F = the descent-engine thrust

L = the distance from the hinge pin of the descent-engine bell to the center of gravity of the LM

R = 0.2 deg/sec, the rotation rate at which the descent-engine bell can be gimballed

I = the moment of inertia of the LM

The output of the GTS attitude control law is u, the sign of the commanded change in angular acceleration that is to be induced by driving each trim gimbal about its axis. The GTS attitude control law is executed separately for rotation about the pitch axis and for rotation about the roll axis.

During steady-state trim-gimbal control, the computation of the sign of the trim-gimbal drives is repeated every 0.2 second. The drives are then commanded at the beginning of the next DAP pass, about 80 millisec later. This delay between control determination and execution was introduced in order to allow a short quiescent period to be forced whenever a drive reversal is required, thus avoiding a false trim-gimbal failure indication that could be triggered in a very tight GTS limit cycle. When the drive direction is not reversed, no off-time is inserted and the gimbal drive continues smoothly from one control pass to the next. This solution to the false-failure-indication problem is in conformity with the technical requirements specified by GAEC.[4] It was not necessary to reduce the actuator switching frequency as authorized in PCR 141, so there should be no significant degradation in the system closed-loop performance.

The gain reduction of 0.3 in the assumed control effectiveness, K, is introduced to compensate for the effects of missing the optimum switching time by as much as 0.2 sec.[2] Without the gain reduction, the closed-loop performance of the LM DAP would exhibit unacceptable overshoot in the transient response and an unacceptably large limit cycle about the desired attitude.

To prevent an uncontrolled drive of a trim gimbal, a drive-timing mechanism is implemented to shut off the trim-gimbal drive. The drive timers – one for the

*K for each axis is actually computed in the 1/ACCS routine, rather than in the control determination, as a function of the mass and the linear acceleration.

pitch axis and one for the roll axis — are always set at 0.3 sec each time the GTS attitude control law is executed. Thus, if the use of the trim gimbals is disallowed, execution of the attitude control law is bypassed and the drives will stop within 0.3 sec.

The algorithm given for the GTS attitude control law [Eqs. (3.5-1) through (3.5-3)] is mathematically equivalent to the algorithm implemented in both SUNDANCE 306 and LUMINARY 069; that is, u as a function of K, θ, $\dot{\theta}$, and $\ddot{\theta}$ is unchanged. However, the magnitudes of the arguments of the signum functions have been altered by dividing these arguments by K. This change eliminates the computational underflow problem that existed for small values of K.[5, 6] The improved performance will be most noticeable in the CSM-docked configuration.

3.5.3 The GTS Acceleration Nulling Control Law

When the trim gimbals are to be used only to trim the thrust direction so as to null the offset angular accelerations, the desired drive times are calculated for the Q and R axes (see Fig. 3.1-5) to be

$$T = 0.4 \left| \frac{\ddot{\theta}}{FLR/I} \right| \qquad (3.5\text{-}4)$$

where T is the trim-gimbal drive time and the other symbols are defined in Subsection 3.5.2.* The damping factor of 0.4 was chosen to ensure that overshooting will not occur — even if the estimated offset angular acceleration should be double the true value. (This is an error that could be readily caused by an undetected jet-off failure.)

The LM DAP is executed once every 0.1 sec; during each execution, the drive timers are decremented by one. The desired trim-gimbal drive time for each axis is expressed as a number of deciseconds and that number is entered into the appropriate drive timer. Whenever a drive timer is found to be zero, the related trim gimbal is stopped.

The drive direction is redetermined at 2-second intervals. The trim gimbal is therefore driving constantly as long as T exceeds 2 seconds (or the undamped time exceeds 5 seconds). In order to provide for stopping these long drives in case control of the gimbal is locked out between executions of the GTS acceleration nulling control law, the drive timers are set to 2.5 seconds whenever T is greater than 2 seconds.

*As for the previous case, the control authority, FLR/I, is computed in 1/ACCS.

REFERENCES FOR SUBSECTION 3.5

1. Widnall, W., Derivation of the Optimal Control Program for Steering the LEM Using the Gimballed Descent Engine, Space Guidance Analysis Memorandum No. 3-66, Instrumentation Laboratory, Massachusetts Institute of Technology, Cambridge, Massachusetts, January 14, 1966.

2. Informal memorandum dated January 22, 1966 from W. Widnall to G. W. Cherry (both of the Instrumentation Laboratory, Massachusetts Institute of Technology) titled "Increasing the Stability of Nonlinear Bang-Bang Control Programs Through Gain Reduction".

3. Cherry, G. W., Controlling the Attitude and Attitude Rate of the LEM with the Gimballed Descent Propulsion System, Space Guidance Analysis Memorandum No. 4-66, Instrumentation Laboratory, Massachusetts Institute of Technology, Cambridge, Massachusetts, January 20, 1966.

4. Coursen, J. W., "Requirements for Primary Guidance, Navigation, and Control System (PGNCS) Digital Autopilot (DAP) Gimbal Drive Actuator Malfunction Detection Logic Interface," GAEC letter to MSC LLR-500-228, June 13, 1968.

5. Weissman, P. S., Engine Mistrim due to GTS Underflow, Spacecraft Autopilot Development Memorandum No. 9-68, Instrumentation Laboratory, Massachusetts Institute of Technology, Cambridge, Massachusetts, June 14, 1968.

6. Work, C. C., Elimination of GTS Computation Underflow, Spacecraft Autopilot Development Memorandum No. 3-69, Instrumentation Laboratory, Massachusetts Institute of Technology, Cambridge, Massachusetts, January 20, 1969.

SUBSECTION 3.6

LOGICAL STRUCTURE OF THE LM DAP

by

Peter S. Weissman

3.6.1 How the LM DAP Is Set Up; Parameter Determination

3.6.1.1 Fresh Start and Restart

A "fresh start" is a programmed sequence that brings all the programs in the LGC to a "ground zero state" as a response to either a crew command (Verb 36) or to a detected chronic hardware problem in the LGC (that is, multiple restarts). Generally speaking, a fresh start puts the LGC in a state suitable for the beginning of the mission and discontinues any program or routine that may be running when the fresh start occurred.

A "restart" is a combination of hardware functions and computer coding that occurs in response to various apparent malfunctions within the LGC, such as an over-long interrupt or an endless loop.* An entire mission may very well pass without any restarts other than the trivial one when the computer is first switched on. When a restart occurs, the outputs of the LGC are momentarily nulled and – as far as is possible – all the programs that are active are restored to states which they were in shortly before the restart. LGC operation should therefore continue almost as though there had been no interruption. Under some (unfortunate) conditions, however, a restart triggers a fresh start.

It was found desirable to design the LM DAP's response to fresh starts and restarts somewhat differently from that of other programs because of the following considerations:

1. The frequency at which the entire LM DAP sequence is executed.
2. The rather clean interface between the LM DAP and other programs and the lack of any necessity to maintain synchronization between them.
3. The existence of a panel switch that allows the crew to turn off the LM DAP when necessary.

*A restart can be triggered by the crew by means of Verb 69.

When a fresh start occurs, all of the erasables used by the LM DAP are initialized (or recomputed from initialized values) with the exception only of a few quantities, such as present mass, for which it would be difficult to choose "nominal" values.* The initialization covers not only the interface quantities, such as desired attitude and jet firing commands, but also internal registers, such as the state estimate and the switches that control the usage of the two control systems (RCS and GTS). The flag word DAPBOOLS is set to indicate the following state (octal value 21322):

1. A 2-deg/sec rate for automatic (KALCMANU) maneuvers.
2. Outputs of 1/ACCS are suspect.
3. A wide (5 deg) deadband was selected by the crew.
4. No ullage.
5. 20-deg/sec maximum commanded rate for the rotational hand controller.
6. Zero offset acceleration to be assumed.
7. X-axis override is permitted.
8. X-axis translation is to be done with two B-system jets.
9. The LM is not docked to the CSM.
10. The trim gimbal may not be used (the engine is off).
11. The manual inputs are rate commands, rather than minimum impulse commands.

A restart, rather than attempting to resume LM DAP operation at the point in its cycle where it was cut off, simply reinitializes the LM DAP in much the same way that a fresh start does. The differences between the two sequences arise from the restriction that a restart can make no assumption regarding the current state of the mission. Thus, a restart does not turn off the main engine or change most bits of DAPBOOLS** or the deadband. In other words, all the internal quantities of the LM DAP are initialized by a restart, but the inputs which control the state of the LM DAP are left unchanged. A restart also causes the present attitude to be taken as the desired attitude and the commanded rates to be set to zero. If a maneuver was in progress, it is interrupted until the maneuver routine is executed again.

---

*Note that mass is, however, checked against a maximum and minimum; see Subsection 3.6.1.5.

**The exception is the clearing of the ACCSOKAY bit, a momentary and essentially clerical change that serves to ensure that the 1/ACCS routine is executed before the LM DAP resumes operation.

The following steps are carried out in the fresh start and restart routines in order to accomplish the functions that have been described:

1. The channel bits that command on the RCS jets and trim-gimbal drives are cleared. (This is done by the hardware in a restart.)
2. In a fresh start, various parameters and flags related to the mission phase are initialized and values for the highest ascent mass (HIASCENT) and the state-estimator filter gains are assumed for use until an erasable load is performed.
3. The ACCSET flag is cleared to force a 1/ACCS call on the first pass through DAPIDLER, so that all the outputs of 1/ACCS will be recomputed before the LM DAP becomes active.
4. A TIME5 interrupt is set up to do DAPIDLER (see description below).

A restart may be triggered by either the hardware or the program. The former turns on the DSKY "restart" light; the latter turns on the "program alarm" light.* Otherwise, the two sequences are almost identical. A change in major mode, Verb 37, is similar to a restart in that it drastically alters the configuration of the mission-oriented programs. However, it leaves the LM DAP almost untouched – merely ensuring that it is set up for non-powered flight using the deadband last selected by the crew and zero desired rate, and that X-axis override is enabled.

3.6.1.2 DAP Idling and Start-Up (see Fig. 3.6-1)

When the LM DAP is switched off or when it cannot function because its inputs are not available, a program named DAPIDLER is called to monitor the conditions which turn the LM DAP off. Until these conditions disappear, DAPIDLER keeps the output commands to the RCS and the trim gimbal systems nulled and employs TIME5 to recycle itself every 0.1 sec. When all of the inhibitions are removed, DAPIDLER initiates the STARTDAP sequence.

The conditions that can cause the LM DAP to idle are the following:

1. The IMU CDU's are not usable.
2. The mode select switch has been turned to OFF by the crew.
3. The use of the abort guidance system (AGS) has been selected by the crew.
4. The 1/ACCS routine has not been executed since the last fresh start or restart. (A job to do 1/ACCS is set up in the first DAPIDLER pass after a fresh start or a restart.)

At the beginning of every normal LM DAP pass, the first three conditions listed above are checked for and DAPIDLER is entered if any of them exists.

*Not all program alarms, however, cause restarts.

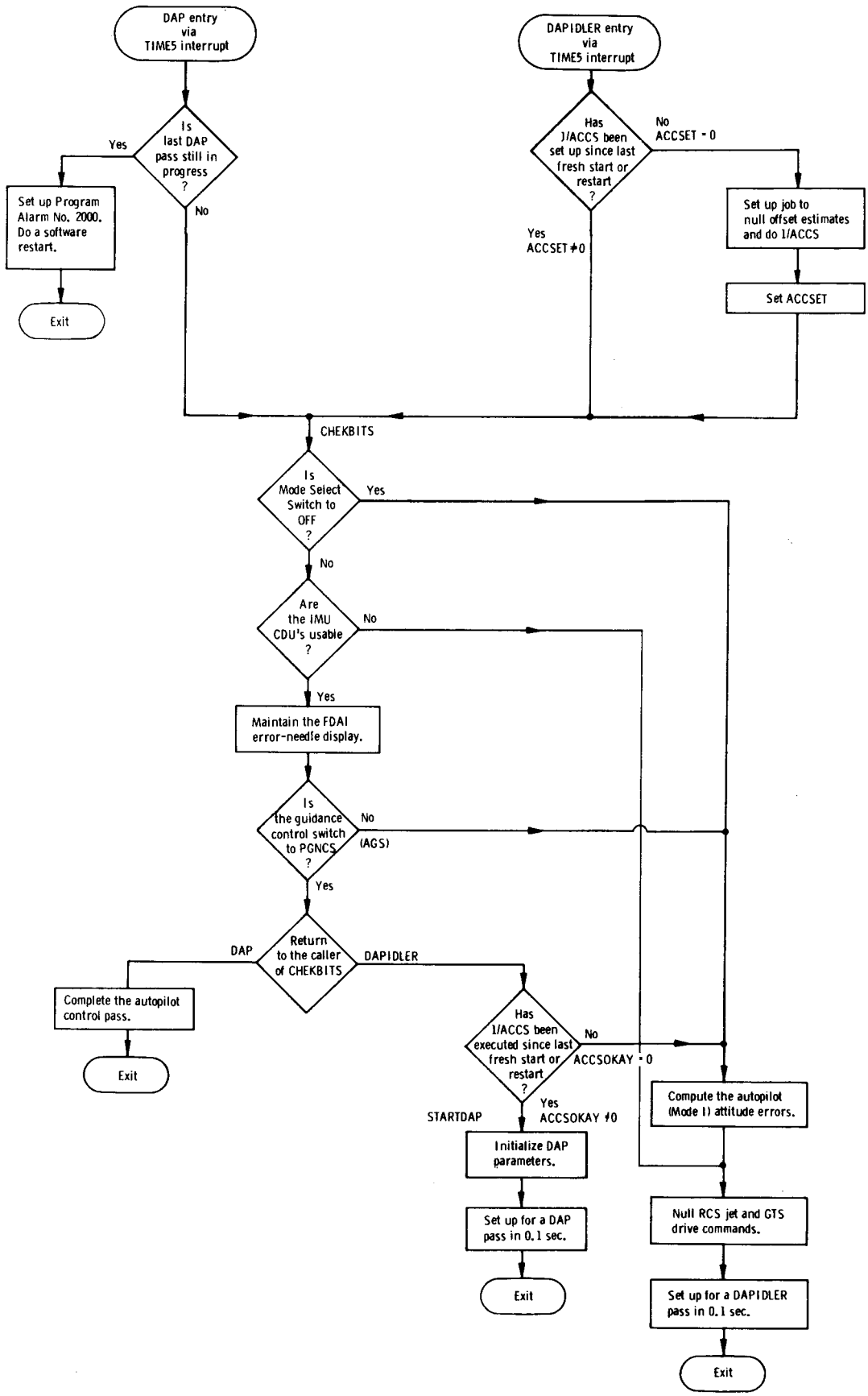

Fig. 3.6-1. Autopilot readiness checks.

Fresh start and restart also set up DAPIDLER (to be the next TIME5 interrupt) so that the LM DAP will initialize itself via STARTDAP.

One function of the LM DAP is carried on even when idling — the display of attitude errors or DAP-estimated rates on the FDAI needles. This is done whenever the IMU CDU's are usable and the PGNCS mode select switch is not in the OFF position. It should be noted, however, that the display is meaningless if the last computed "desired attitude" or the outputs of the IMU CDU's are wrong. Also, a STARTDAP zeroes a Mode 1 display because it sets the "desired attitude" equal to the present attitude. Since the DAP does not estimate rates while idling, the rate displays are also meaningless in this mode.

The sequence STARTDAP, which is executed by DAPIDLER when the LM DAP is to resume operation, performs the following functions:

1. It initializes the state estimator; in particular, it
   a) nulls the offset-acceleration estimate,
   b) nulls the attitude-rate estimate,
   c) nulls the accumulated unexplained attitude estimates, and
   d) reads the IMU CDU's.
2. It nulls the attitude error and commanded rate.
3. It disallows trim-gimbal control (until the next 1/ACCS execution).
4. It zeroes the jet-inhibition counters for the CSM-docked autopilot.
5. It prevents a possible TIME6 interrupt from turning on jets before the LM DAP is actually in operation.
6. It sets up TIME5 to start a normal DAP pass in 0.1 sec. The delay is required by the rate filter in order that the time interval between attitude measurements will be nominal.

3.6.1.3 Routine 3: DAP Data Load

The crew loads data for use by the LM DAP by means of Verb 48, which calls up Routine 3. The relationship of this data to autopilot control is discussed in Subsection 3.2.5. The crew procedure is described in detail in Section 4 of this document (separate volume).

3.6.1.4 Monitoring of Jet Failures and Trim-Gimbal Failures

RCS Jet Failure Monitor

The crew is warned of jet failures by lamps lit by the Grumman failure-detection circuitry and by off-nominal patterns of control behavior. They may respond by operating panel switches that isolate pairs of jets from the propellant tanks and set bits in channel 32.

The RCS failure monitor is attached to the TIME4 interrupt and is entered every 480 milliseconds. Its function is to examine channel 32 to see if any isolation-valve closure bits have appeared or disappeared. In the event that any of these bits differ from PVALVEST, the record of actions taken by this routine, the appropriate bits in CH5MASK and CH6MASK are updated, as is PVALVEST. CH5MASK and CH6MASK are used in the LM DAP jet-selection logic and in 1/ACCS, where the available control torque is computed. To speed up and shorten the routine,no more than one change is accepted per cycle. The highest-numbered bit in channel 32 that requires action is the one processed.

The coding in the failure monitor routine has been written so as to have almost complete restart protection. For example, no assumption is made when setting a CH5MASK bit to 1 that the previous state is 0, although it of course should be. One case that may be seen to evade protection is the occurrence of a restart after updating one or both DAP mask-words but before updating PVALVEST, coupled with a change in the valve-bit back to its former state. The consequence of this is that the next entry would not see the change incompletely incorporated by the last pass (because it went away at just the right time), but the DAP mask-words will be incorrect. This combination of events seems quite remote, but not impossible unless the crew operates the switches at half-second intervals or longer. In any event, a disagreement between reality and the DAP masks will be cured if the misinterpreted switch is reversed and then restored to its correct position (slowly).

Trim-Gimbal Monitor

The USEQRJTS bit of DAPBOOLS indicates to the LM DAP whether the trim gimbal may be used (in any mode). It is cleared (to allow gimballing) when, and only when, the following set of conditions exists:

1. The thrust monitor (DVMON) of the SERVICER program is cycling; this generally occurs before and during a burn.
2. The measured thrust is above the threshold.
3. APSFLAG is clear, indicating the LM is unstaged.
4. The gimbal-fail bit (bit 9/channel 32) has not been set by the crew.

3.6.1.5 Adaptive Loop; the 1/ACCS Routine

Mass Initialization and Tracking

The masses of the LM and the CSM are initialized as part of the preflight erasable load. They may be subsequently updated by the crew by means of Routine 03 (Verb 48). Routine 03 does not accept values that are below fixed limits. During LM powered flight, the mass is decremented in the SERVICER program to correct for the loss of main-engine fuel.* The amount subtracted is a function of the measured change in velocity, ΔV, over the last sample period (2 sec) and the exhaust velocity, V_e, of the engine being used. Specifically,

$$(\text{Mass})_t = (\text{Mass})_{t-2} - \frac{\Delta V}{V_e}(\text{Mass})_{t-2} \qquad (3.6\text{-}1)$$

In an "RCS burn", the exhaust velocity of the main engine of the current stage is employed. No account is taken of RCS fuel used for attitude control.

The mass value that is tracked in this way is the total mass, that is, the one- or two-vehicle mass value that was last set in Routine 03.

*SERVICER, which also includes the PIPA-read routine, is executed on a two-second cycle during the appropriate portions of the following programs: 12, 40, 41, 42, 47, 63, 64, 66, 70 and 71.

[x] Revised LUMINARY 1C
[ ] Added GSOP # R-567 PCR # 988 Rev. 4 Date 3/70

The 1/ACCS Routine

Another part of the SERVICER program is the 1/ACCS routine, the primary function of which is to compute the control effectiveness of the LM DAP as a function of the vehicle mass, the unfailed jets, the configuration, and other such factors. In addition to being executed as part of the SERVICER program every 2 seconds during powered-flight mission phases, 1/ACCS is called several times during a mission when certain discrete events occur, such as restarts, fresh starts, detection of disabled jets, data load by crew (Routine 03), resetting of the attitude deadband, and the turning-off of the main engine. Also, prior to lunar lift-off, the ignition logic of the powered-ascent program (P12) loads the bias angular accelerations of the state estimator from the prior estimates given in pad-loaded erasables IGNAOSQ and IGNAOSR. This is followed by an execution of 1/ACCS that establishes the proper ascent control effectiveness.

The first thing done in 1/ACCS is a determination of the vehicle configuration on the basis of APSFLAG and CSMDOCKD. The LM mass limits and the mass-to-inertia coefficients to be used in 1/ACCS itself are selected on this basis.

Next, the mass of the LM alone is separated out as follows:

a) For the LM-alone case, LM mass = total mass.

b) For the CSM-docked case, LM mass = total mass - CSM mass.

The LM mass, which is displayed and loaded in Routine 03, is therefore kept updated during burns as though it were maintained directly in the SERVICER program.

There is a check on the LM mass in the 1/ACCS routine that serves to keep this critical parameter within a reasonable range despite any possible error in the initialization, in the Routine 03 load, or in SERVICER maintenance. It also results in an automatic correction of the mass when staging occurs, since the old, descent value is too high for the ascent stage alone.

The following limits on the LM mass have been implemented:

Highest descent mass = 33,730 lb

Lowest descent mass = 3858 lb + HIASCENT

Highest ascent mass = HIASCENT

Lowest ascent mass = 4850 lb

HIASCENT was made a pad-loaded erasable quantity so that it can reflect the ascent fuel loading used in each particular flight. Its value for a fully loaded ascent stage is about 11,133 lb, and it is so initialized in a fresh start (to be over-written by the erasable load shortly thereafter). HIASCENT should not be less than 7265 lb, in order that the minimum descent mass will not be too low. When the LM mass is found to violate a limit, its value is changed to equal the limit (maximum or minimum); the total mass is changed correspondingly.

After the mass value has been thus guaranteed to be within acceptable limits, the control effectiveness of the RCS jets about each axis and, when the descent stage is attached, the control effectiveness of the trim-gimbal drives are computed as described in Subsection 3.3.1.

Various functions of the control effectiveness, the estimated offset acceleration, the deadband and the vehicle configuration are computed and stored at this point so that they need not be determined each time they are needed in the LM DAP.*

During descent powered flight, when the trim gimbal is usable and the third-order trim-gimbal control system is not maintaining attitude control, 1/ACCS sets up offset-nulling drives. This function of 1/ACCS is discussed in Subsections 3.5 and 3.6.2.3.

3.6.2 How the LM DAP Sequences

The following paragraphs attempt to present a fairly detailed look at how the various functions of the LM DAP that have been described individually relate to one another from the point of view of both information flow and the selection of the appropriate modes of control.

An overview of the LM DAP sequencing is followed by descriptions of the interface between the various manual modes and automatic control. The interaction between the RCS and the trim gimbal system is then examined.

This information should prove useful both as an introduction to the actual coding and as an explanation of how the components described in Subsections 3.3 through 3.5 are used to accomplish the functions of the LM DAP mentioned in Subsections 3.1 and 3.2.

3.6.2.1 Information Flow in the LM DAP

Figure 3.6-2 shows the overall sequencing of the LM DAP. Figures 3.6-3 and 3.6-4 illustrate the data used in RCS jet selection (see Subsection 3.4.5). Note that a clean separation exists between the handling of "horizontal" jets (which lie in the Y-Z plane) and "vertical" jets (which are perpendicular to the Y-Z plane).

The following points will aid in reading Figs. 3.6-2 through 3.6-4:

1. The trapezoidal blocks indicate major functions of the LM DAP that are described elsewhere in this document, together with their associated inputs and outputs.
2. The symbols θ, ω and α denote estimated attitude, angular rate, and bias angular acceleration, respectively.

*Most of these functions are described in Subsection 3.4.2.

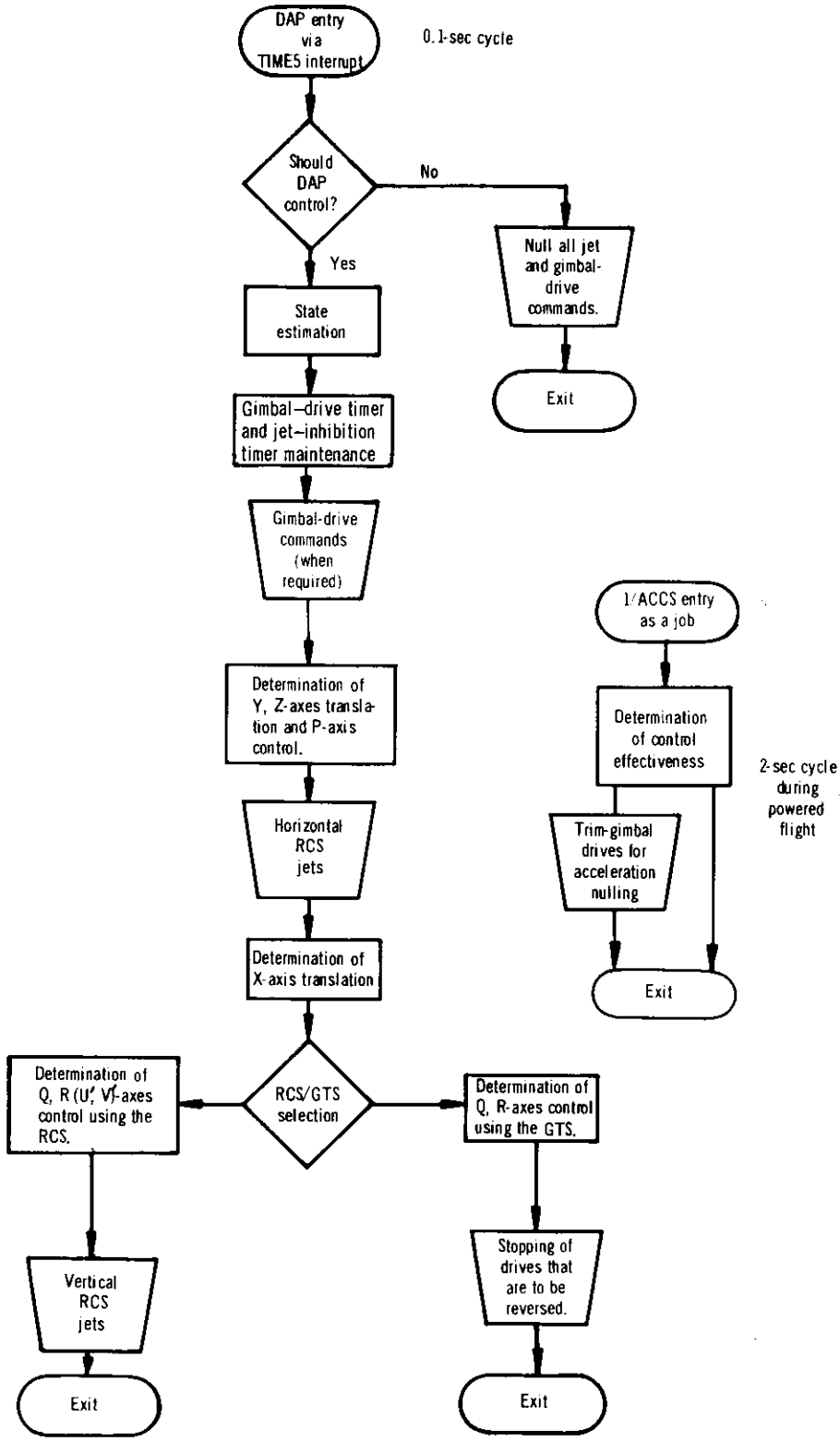

Fig. 3.6-2. Control sequencing of the LM DAP.

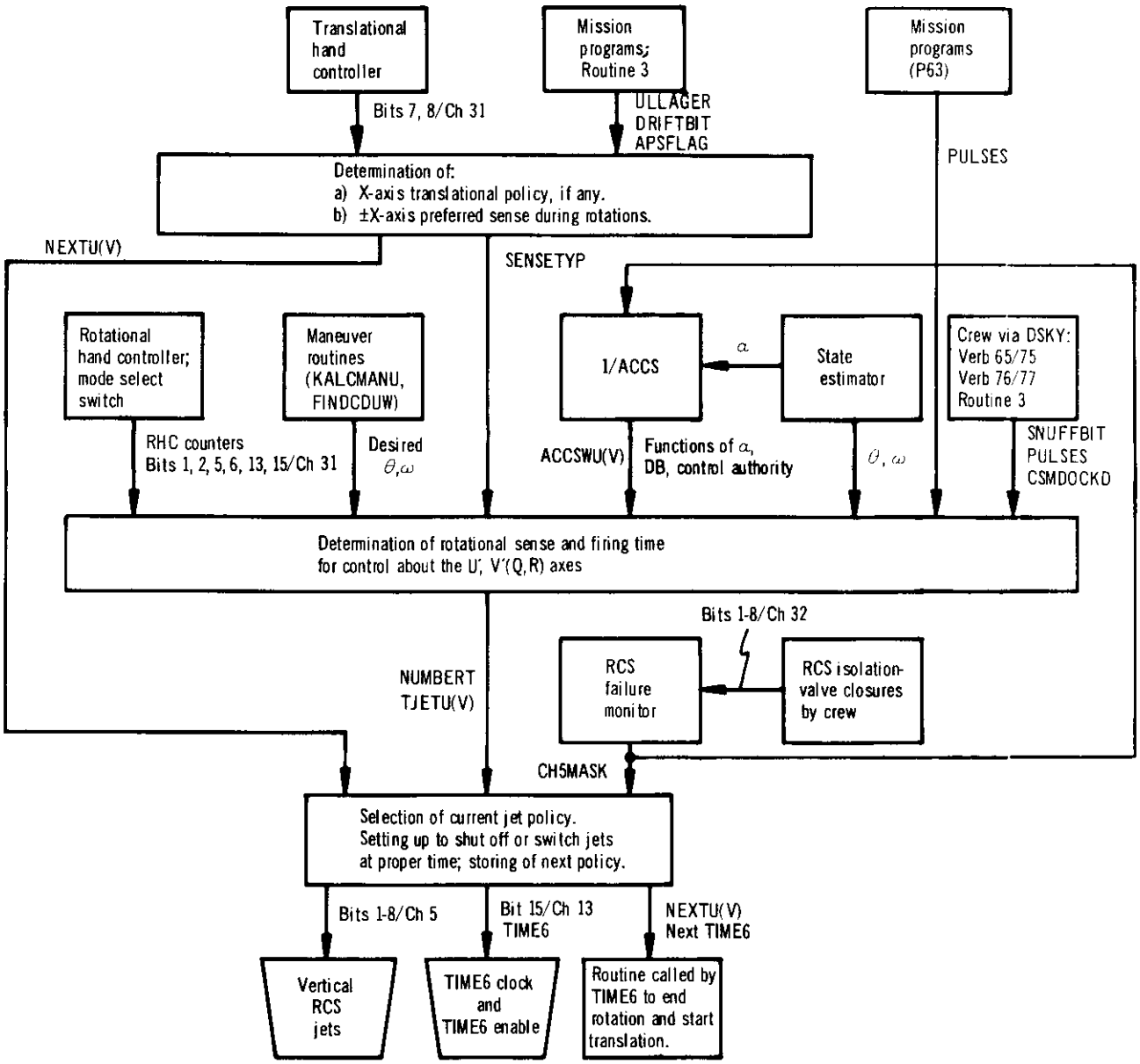

Fig. 3.6-3. Data flow in the selection of jets for U'-axis and V'-axis rotation and for X-axis translation.

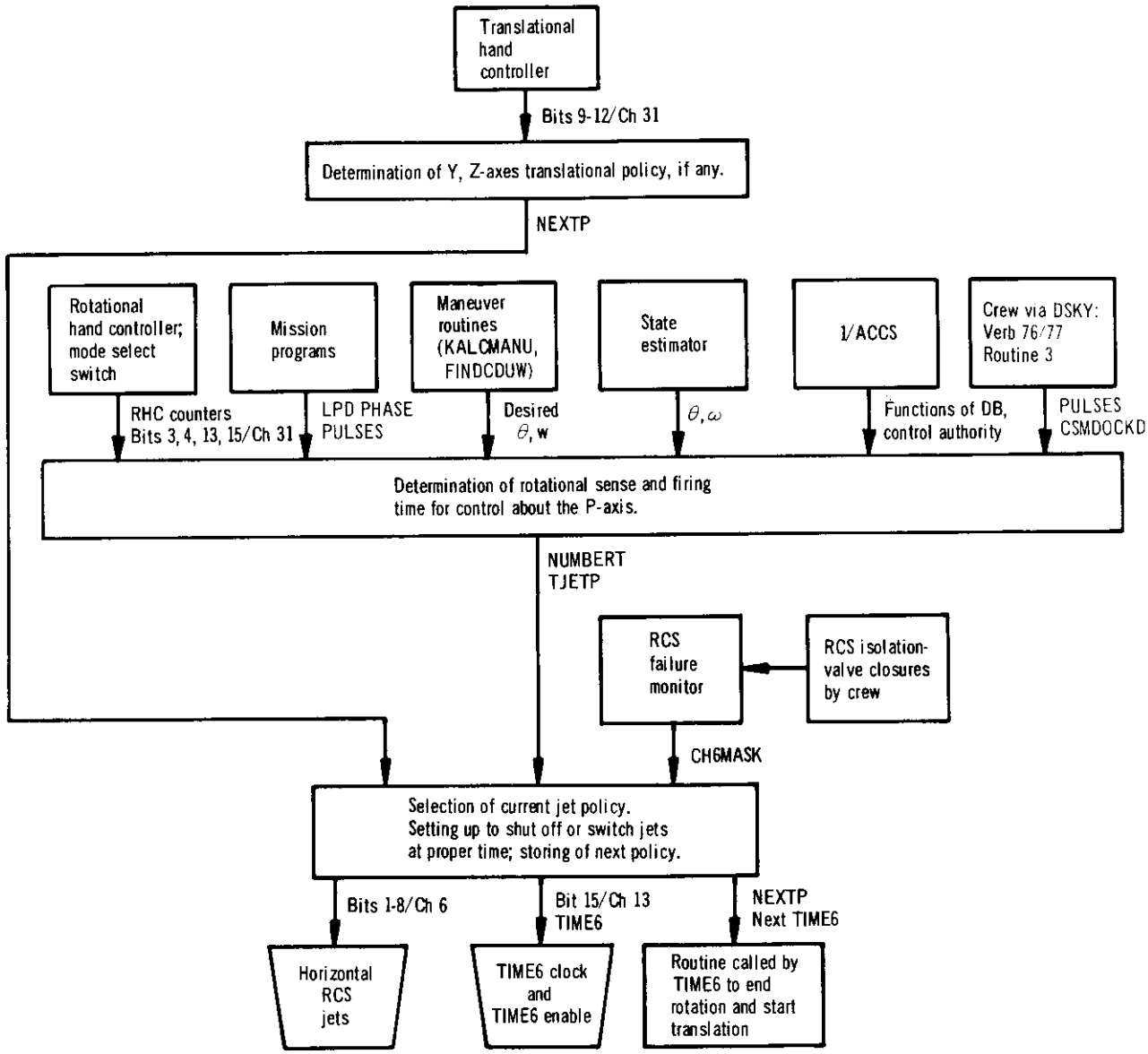

Fig. 3.6-4. Data flow in the selection of jets for P-axis rotation and for Y-axis and Z-axis translation

3. The capitalized switch names are defined in the glossary presented in Subsection 3.6.3.

3.6.2.2 Manual Modes – Automatic Modes Interface

The rather complex flow chart of Fig. 3.6-5 shows all of the switches that are tested in each LM dap pass in order to determine the appropriate source of control commands. The first part of the figure deals with the "horizontal" jets; the second part deals with the "vertical" jets.

3.6.2.3 RCS – Trim Gimbal System Interface; LM-Alone Case

During powered descent, it is desirable to have an interface between the RCS and the trim gimbal system that allows control within the specified deadbands and is not wasteful of RCS fuel. To accomplish this objective, it is necessary during trim-gimbal operation to continually check the vehicle's state in the RCS phase plane. The RCS – trim gimbal system interface has been designed so that the vehicle's state in the RCS phase plane is examined (and the RCS control law applied) at least every 200 millisec. The time line of RCS – trim gimbal system operation is set up as follows:

t	t + 100 ms	t + 200 ms	t + 300 ms
RCS control law	Test requirements to use GTS attitude control law. If requirements are met, exercise GTS attitude control; otherwise, return to RCS control (either directly or after setting up GTS acceleration nulling drives).	RCS control law	Test requirements to use GTS attitude control law. If requirements are met, exercise GTS attitude control; otherwise, return to RCS control (either directly or after setting up GTS acceleration nulling drives).

The complete logic for the RCS – trim gimbal system interface is shown in the flow charts of Figs. 3.6-6 and 3.6-7. From Fig. 3.6-6, it can be seen that in the TRYGTS section there are three requirements that must be met before the GTS attitude control law can be used. These requirements are:

1. USEQRJTS bit of DAPBOOLS = 0.
2. ALLOWGTS = 1.
3. All U-V RCS jets are off.

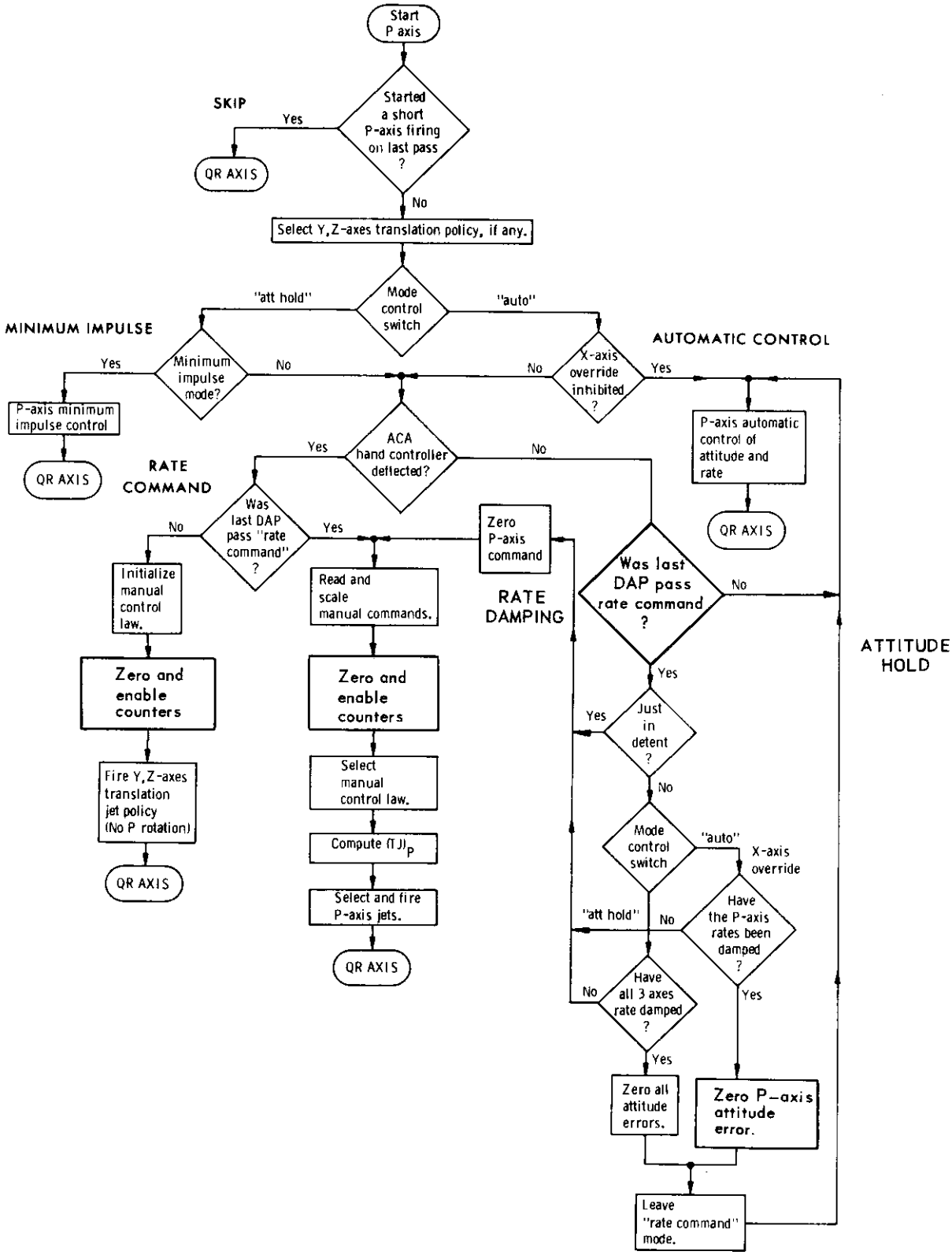

a) P-axis control

Fig. 3.6-5. Selection of manual and automatic modes (page 1 of 3).

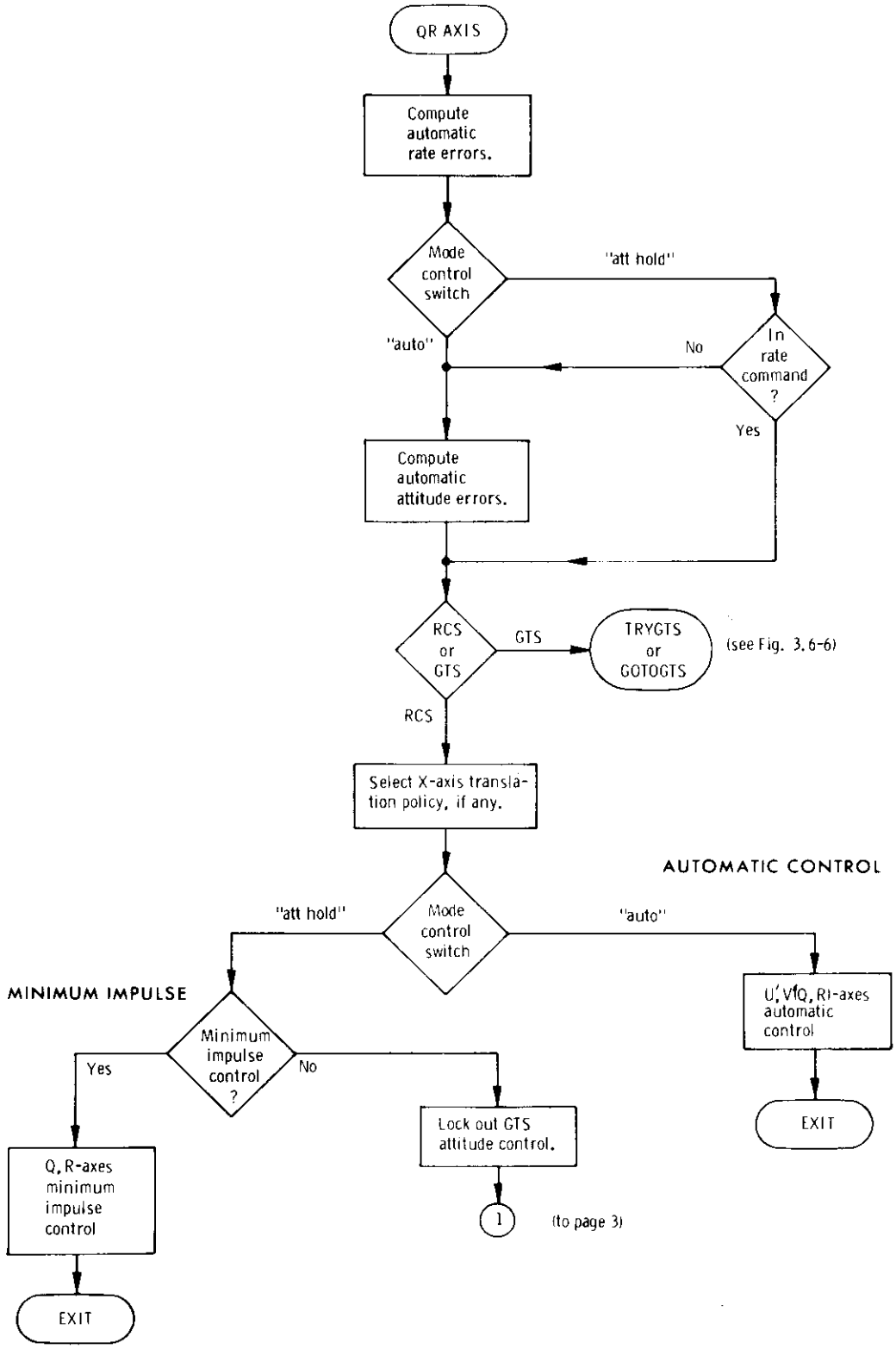

b) Q, R(U', V')-axes control

Fig. 3.6-5. Selection of manual and automatic modes (page 2 of 3).

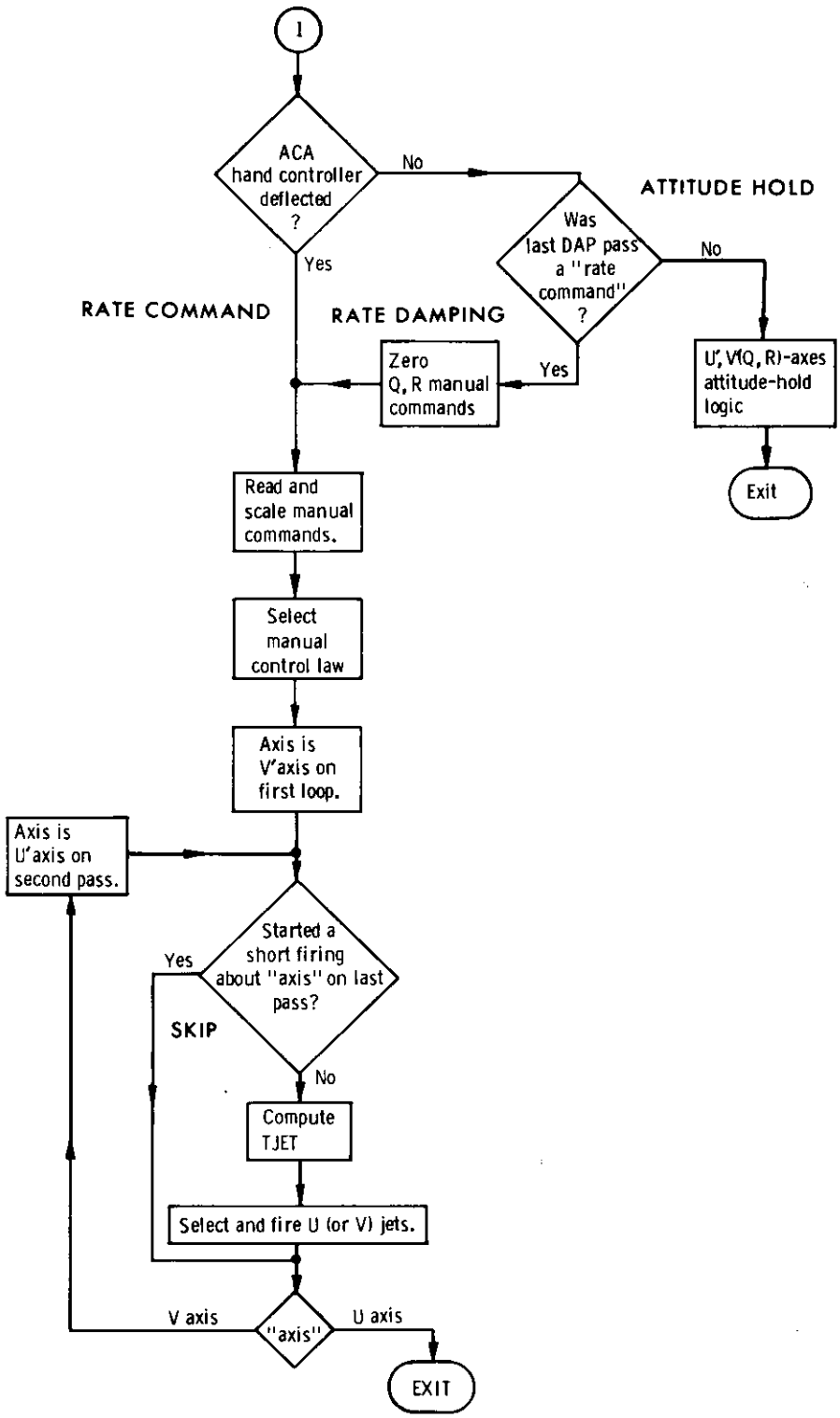

b) Q,R(U',V')-axes control

Fig. 3.6-5. Selection of manual and automatic modes (page 3 of 3).

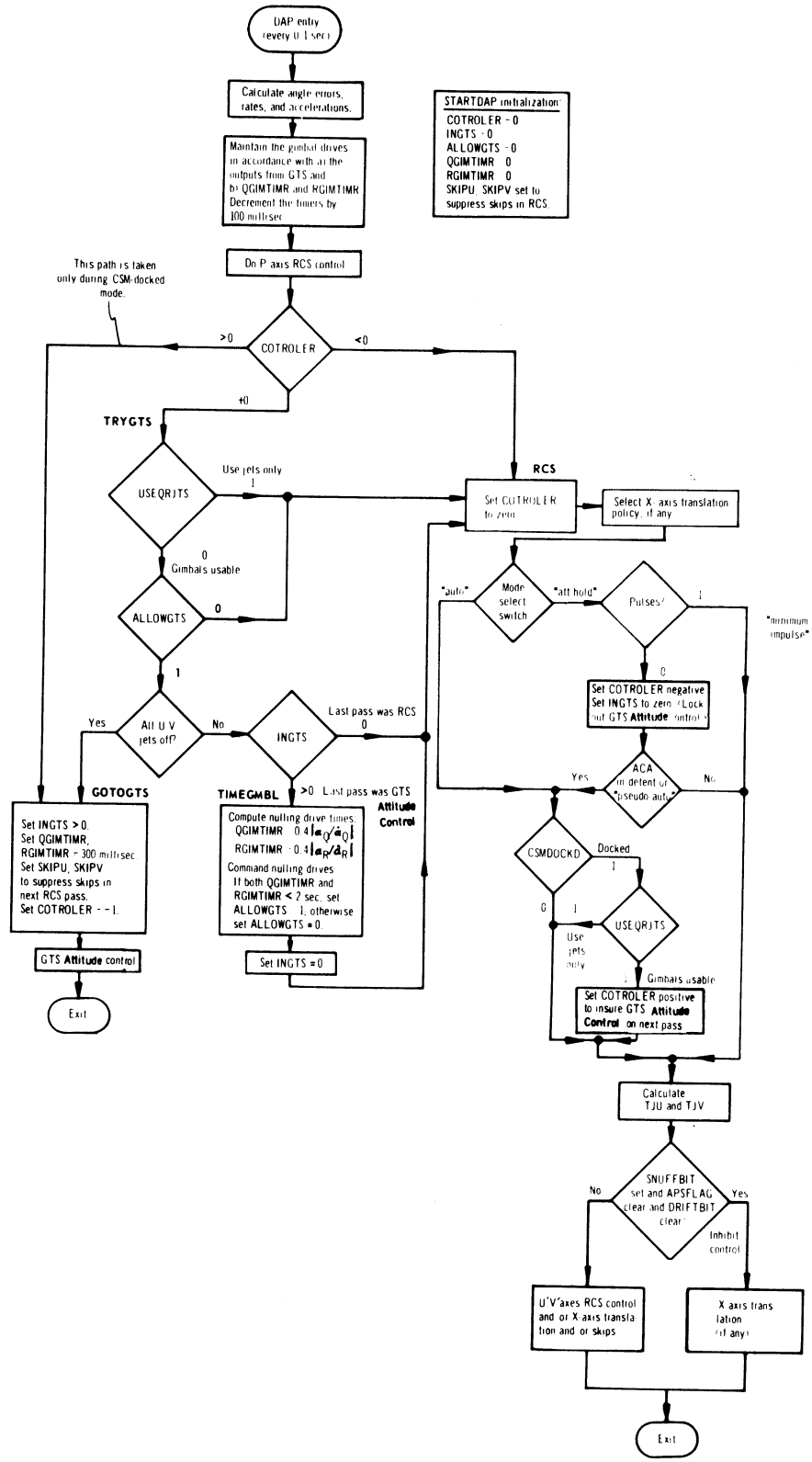

Fig. 3.6-6. Selection of RCS/GTS control.

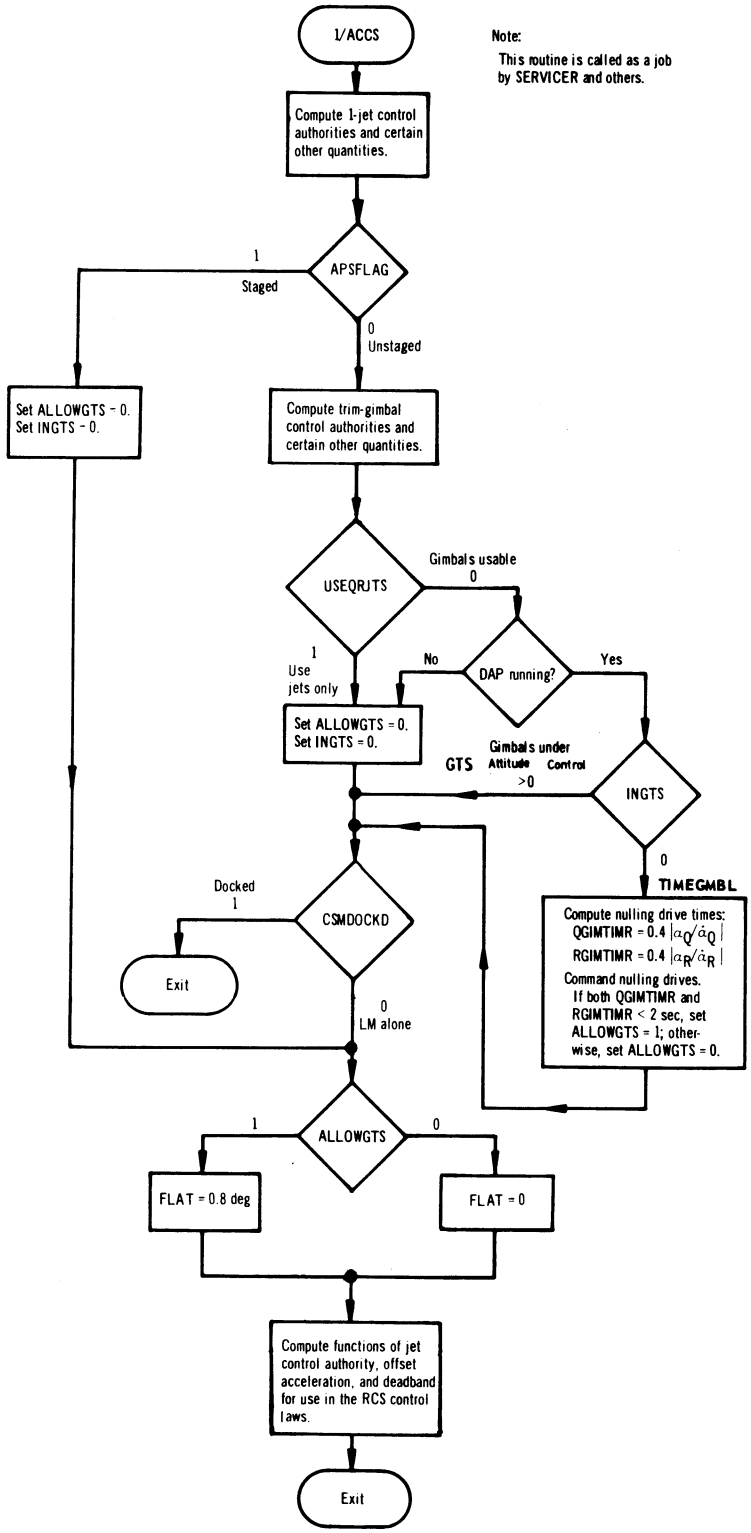

Fig. 3.6-7. The functioning of 1/ACCS in the RCS-GTS interface.

The USEQRJTS bit of DAPBOOLS is set to zero and in general will remain zero during powered descent. It will be set to 1 only when a decision is made that the use of the trim gimbal is not permissible (see Subsection 3.6.1.4).

ALLOWGTS is initialized to be zero and can be set to 1 only by the TIMEGMBL routine. TIMEGMBL is a routine that commands the trim gimbal to drive toward the null position (that is, to put the thrust vector through the vehicle center of gravity for both Q-axis and R-axis rotations). After determining the drive times, TIMEGMBL sets ALLOWGTS. ALLOWGTS is set to 1 if both drive times are less than two seconds; otherwise, ALLOWGTS is set to zero.*

From the preceding discussion, it follows that if requirement 2 for using the GTS attitude control law is satisfied, the gimballed engine will be close to the null position and therefore will not produce a large acceleration. Similarly, if requirement 3 is satisfied, the vehicle angular error and rate error will, in general, not be large. The purpose of these requirements is to have the trim-gimbal control laws be presented with errors in angle, rate, and acceleration that are small enough to allow a limit cycle within the coast region of the RCS phase plane to be achieved.

From Figs. 3.6-6 and 3.6-7 and the previous discussion, it can be seen that there are two ways in which the trim-gimbal drive direction is determined during trim gimbal — RCS operation. One way is by the GTS attitude control law, which attempts to drive the vehicle angle error, rate and acceleration simultaneously to zero (for both the Q and R axes). The other way is by the TIMEGMBL routine (the GTS acceleration nulling control law), which attempts to drive acceleration to zero but does not control angle and rate. The requirements for using the GTS attitude control law have already been discussed. In the following discussion, a more complete description of TIMEGMBL and the conditions under which it is used in powered descent is given.

The TIMEGMBL routine can be called both in the trim gimbal — RCS 100-millisec loop and in the 1/ACCS job, which is executed every two seconds. In either of these cases, the decision to use TIMEGMBL will depend on a test of whether or not the trim gimbal is presently under the control of the GTS attitude control law. The definition of being under GTS attitude control is that the existing trim-gimbal drive direction was determined by the GTS attitude control law. The quantity that specifies whether or not the trim gimbal is under GTS attitude control is INGTS. It will be positive (having been set each time the GTS attitude control law is used) whenever the trim gimbal is under GTS attitude control and will be zero otherwise. In the 1/ACCS job, the TIMEGMBL routine is used during DPS burns if, and only if, the trim gimbal is <u>not</u> under GTS attitude control (that is, INGTS = 0) and the gimbal is usable (that is, USEQRJTS = 0). The initial control of the trim

*The drive times include a damping factor of 0.4; the branch is on an undamped time of five seconds.

gimbal at the beginning of powered descent will not occur until 1/ACCS is first called. During this first 1/ACCS job, the TIMEGMBL routine will be entered and will command the trim-gimbal nulling drives. If at least one of the commanded drive times is greater than two seconds, then the trim gimbal cannot be put under GTS attitude control before the 1/ACCS job is called again. 1/ACCS will continue to use the TIMEGMBL routine every two seconds until both times are less than two seconds. When this occurs, TIMEGMBL sets the quantity ALLOWGTS to 1 — thereby satisfying requirement 2 for entering GTS attitude control. Once all three requirements for GTS attitude control are tested and satisfied, the trim gimbal will remain under GTS attitude control until one of the requirements is not met. In general, this will be requirement 3 — that all U-V RCS jets must be off. (Note that, as previously mentioned, control of the trim gimbal cannot be transferred from GTS attitude control to TIMEGMBL control in the 1/ACCS job.)

When the trim gimbal has been under GTS attitude control but cannot continue under GTS attitude control because U-V RCS jets are on, then control of the trim gimbal is immediately transferred to TIMEGMBL. After the nulling drives are set up and ALLOWGTS is determined, INGTS is set to zero to indicate that the trim gimbal is no longer under GTS attitude control. In this trim gimbal — RCS loop, the TIMEGMBL routine is entered only if the trim gimbal is currently under GTS attitude control (that is, INGTS > 0). Therefore, it is used only in the transition between GTS attitude control and TIMEGMBL control of the trim gimbal. Subsequent entries into TIMEGMBL are made in the 1/ACCS job.

The drive times that are computed in TIMEGMBL for the two trim gimbals are written into the registers QGIMTIMR and RGIMTIMR, respectively. The actual timing of the drives is then achieved by the cycling of the LM DAP. As part of each DAP pass, the timers are decremented by 0.1 sec. When one of the timers is zero, the appropriate gimbal drive is stopped. This mechanism is used to guard against a run-away of the gimbals that could otherwise occur when trim-gimbal control is suddenly locked out by the USEQRJTS bit being restored to 1 (as part of the engine-off routine, for example). The timers are set up in each pass of the trim-gimbal system to a value such that they will not be counted down to zero before the next trim-gimbal-system pass; the drives therefore continue from one pass to the next. If, however, the "next" trim-gimbal-system pass never occurs, the timers will reach zero and the drives will be stopped. Note that the LM DAP must be ON for this drive termination to function.

In the manual rate command and attitude hold modes, the LM DAP uses the gimbal drives only in the GTS acceleration nulling mode, rather than attempting to follow the manual commands with the trim gimbal system.

3.6.2.4 RCS — Trim Gimbal System Interface; CSM-Docked Case

The sequencing within the LM DAP is the same for the CSM-docked and the LM-alone configurations, with the exception of the RCS — trim gimbal system interfacing. Thus, the functions and interdependence of 1/ACCS, the state estimator, the jet select logic, the RCS and trim-gimbal control laws, the data-load routine, etc. do not depend upon the configuration, although some of the parameters employed within these sections do. The manner in which control is shared by the jets and the trim gimbals must, however, be quite different in order to deal with the two distinct control problems. The inertia about the Y- and Z-axes increases by an order of magnitude when the CSM is attached. Naturally, the jet control authority decreases proportionately. On the other hand, the center of gravity shifts so far from the LM main engine that the control effectiveness of the trim gimbals is almost unchanged. The GTS attitude control is therefore roughly on a par with RCS control and is in fact required to maintain reasonable attitude errors in the CSM-docked case. (When U, V-axes RCS control is disabled by Verb 65, which sets SNUFFBIT, control of the spacecraft by the trim gimbal system is, of course, even more important.) This is in direct contrast with the undocked situation, when the jets can bring about error corrections quite rapidly and the gimbals are used for attitude control only as a fuel-saving measure when the errors are small enough not to require RCS activity.

The two, relatively equal control systems are simultaneously utilized by the CSM-docked autopilot by the simple expedient of alternation between the RCS and GTS attitude control laws on successive DAP passes. As shown in Figs. 3.6-6 and 3.6-7, GTS-attitude-control-law gimbal drives are computed every 0.2 second when USEQRJTS is zero. When USEQRJTS is set, and the gimbals may not be used, RCS control is re-evaluated for the U and V axes every DAP pass. In the minimum impulse mode, either the GTS acceleration nulling control law or the GTS attitude control law is used.

3.6.3 Glossary of Key Flags and Parameters

Tables 3.6-1, 3.6-2, and 3.6-3 describe some of the more important internal switches, inputs, and outputs of the LM DAP. While this list is not complete by any means, it should serve as an aid to the reader of this document, and of the listing itself, by helping to clarify how communication is accomplished between the various sections of the LM DAP and between the LM DAP and the outside world.

Tag	Bit/Location	Meaning	
		Set	Cleared
ACC4OR2X	11/DAPBOOLS	X-axis translation to use 4 jets.	X-axis translation to use 2 jets.
ACCSOKAY	3/DAPBOOLS	Control-authority values from 1/ACCS usable.	Restart or fresh start since last 1/ACCS; outputs suspect.
ACCSWU ACCSWV	—— ——	+1 or -1 indicates 1-jet net acceleration less than $\pi/2^7$ rad/sec^2 in rotational sense corresponding to sense of flag.	0 indicates 1-jet control authority in both directions exceeds the minimum.
ALLOWGTS	—	Thrust offset small enough to use GTS attitude control law.	Thrust offset too large to use GTS attitude control law.
AORBSYST*	5/FLAGWRD5	Prefer P-axis jet couples 7, 15 and 8, 16.	Prefer P-axis couples 4, 12 and 3, 11.
AORBTRAN	10/DAPBOOLS	Prefer B-system jets for X translation.	Prefer A-system jets for X translation.
APSFLAG	13/FLGWRD10	LM staged or on lunar surface.	LM unstaged and not on lunar surface.
AUTRATE1 AUTRATE2	1/DAPBOOLS 2/DAPBOOLS	KALCMANU maneuver rates chosen by crew: 00 indicates 0.2 deg/sec 01 indicates 0.5 deg/sec 10 indicates 2.0 deg/sec 11 indicates 10.0 deg/sec	
CH5MASK CH6MASK	—— ——	Jets which have been disabled by crew; in channel 5(6) format.	
COTROLER	—	Indicator of control system employed in current DAP pass: = 0 indicates GTS; LM-alone case. > 0 indicates GTS; CSM-docked case. < 0 indicates RCS.	

*Not related to fuel systems; bit is automatically alternated between set and cleared.

Table 3.6-1. Selected flag definitions.

Tag	Bit/Location	Meaning	
		Set	Cleared
CSMDOCKD	13/DAPBOOLS	CSM docked to LM.	CSM not attached to LM.
DAPBOOLS	——	Autopilot flag word containing the following bits: Bit 1 – AUTRATE1 Bit 2 – AUTRATE2 Bit 3 – ACCSOKAY Bit 4 – DBSELECT Bit 5 – DBSLECT 2 Bit 6 – ULLAGER Bit 7 – RHCSCALE Bit 8 – DRIFTBIT Bit 9 – LPDPHASE (XOVINHIB) Bit 10 – AORBTRAN Bit 11 – ACC4OR2X Bit 12 – OURRCBIT Bit 13 – CSMDOCKD Bit 14 – USEQRJTS Bit 15 – PULSES	
DAPFLAGS	————	Autopilot flag word containing a number of internal autopilot switches (see Table 3.6-3).	
DBSELECT DBSLECT 2	4/DAPBOOLS 5/DAPBOOLS	Phase-plane deadbands selected by crew: 00 indicates minimum (0.3 deg) deadband 01 indicates 1.0-deg deadband 10 indicates maximum (5.0 deg) deadband 11 indicates maximum (5.0 deg) deadband (not normally selected)	
DRIFTBIT	8/DAPBOOLS	Null offset acceleration estimate.	Use offset acceleration estimate.
INGTS	——	GTS attitude control law presently controlling attitude.	RCS presently controlling attitude.
LPDPHASE	9/DAPBOOLS	X-axis override locked out (Landing Point Designation phase).	X-axis override permitted.
NEXTP NEXTU NEXTV	—— —— ——	Jets to be turned on (for translation) at the end of the corresponding rotation; in channel 5(6) format.	

Table 3.6-1. Selected flag definitions (continued).

Tag	Bit/Location	Meaning	
		Set	Cleared
NUMBERT	——	Type of rotational or translational jet policy; input to, and output from, the jet-selection routine.	
OURRCBIT	12/DAPBOOLS	Current DAP pass is rate command.	Current DAP pass is not rate command.
PULSES	15/DAPBOOLS	Minimum impulse command mode in "Att hold" (Verb 76).	Not minimum-impulse command mode (Verb 77; P63).
RHCSCALE	7/DAPBOOLS	Normal (20 deg/sec) rotational-hand-controller scaling selected by crew.	Fine (4 deg/sec) rotational-hand-controller scaling selected by crew.
SENSETYP	——	X-translational sense desirable during U and V rotations: 0 indicates balanced couples 1 indicates -X translational sense 2 indicates +X translational sense TJETLAW requires SENSETYP = 0 for P axis	
SKIPU SKIPV	—— ——	4 indicates control about the corresponding axis is to be exercised in the current DAP pass.	0 indicates control about the corresponding axis is not to be re-evaluated in the current DAP pass because a short (<150 millisec), non-zero firing was started in the last pass.
SNUFFBIT	13/FLAGWRD5	Inhibit RCS control about the U, V axes during unstaged powered flight.	Exercise normal RCS control.
ULLAGER	6/DAPBOOLS	Ullage requested by mission program.	No internal ullage request.
USEQRJTS	14/DAPBOOLS	Trim gimbal unusable; use jets only.	Gimbals may be used.
XOVINHIB	9/DAPBOOLS	(Same as LPDPHASE)	

Table 3.6-1. Selected flag definitions (concluded).

Tag	Scaling	Meaning
ABDELV	2^{14} cm/sec, 2^{13} cm/sec^2	Absolute value of change in velocity over last two seconds; computed in SERVICER from PIPA readings.
CSMMASS	2^{16} kg	Mass of the CSM, as loaded by crew.
DB	45 deg	Current attitude deadband for use in TJETLAW: 0.3, 1.0 or 5.0 degrees.
HIASCENT	2^{16} kg	Anticipated mass of LM immediately after staging; pad-loaded erasable.
LEMMASS	2^{16} kg	Current mass of the LM: LEMMASS = MASS for the LM-alone case LEMMASS = MASS - CSMMASS for the CSM-docked case
MASS	2^{16} kg	Current mass of the LM or LM and CSM together. Initialized via external load and maintained in SERVICER during burns.
QGIMTIMR RGIMTIMR	0.1 sec/bit	Trim-gimbal drive timers; drive stopped in DAP pass when timer is zero.
TJP TJU TJV	10.24 sec (as TIME6)	Rotational jet firing time. Values above 0.150 sec cause re-evaluation in 0.100 sec; values below 0.014 sec cause minimum impulse.

Table 3.6-2. Selected parameter definitions.

BIT	NAME	SET	CLEARED
1	———	First leg of tacking pattern for Y or Z translation with a jet failure.	Second leg of tacking pattern.
2	———	Enable IMU error counters. DAC's have been zeroed. Used in conjunction with bit 3 in attitude-error display routine.	Counters presumed OK.
3	———	IMU error counters should be disabled in order to zero DAC's. Used in conjunction with bit 2 in attitude-error display routine.	Counters presumed OK.
4	DSPLYALT	Display attitude errors.	Compute total attitude errors when needed.
5	CALLGMBL	Requests setting of gimbal-drive bits in Channel 12 (i.e., perform ACDT + C12).	Do not set gimbal-drive bits in channel 12 (i.e., do not perform ACDT + C12).
6, 7, 8	———	——— Unused ———	———
9	JUSTIN	RHC stick out of detent on last pass.	RHC stick not out of detent on last pass.
10	PBIT	Direct rate mode of manual rate command required in P axis.	Direct rate not required in P axis.
11	QRBIT	Direct rate mode of manual rate command required in Q, R axes.	Direct rate not required in Q, R axes.
12	———	Perform control of P axis in next pass.	Skip control of P axis in next pass.
13	ACCSET	A job to do 1/ACCS has been set up since the last fresh start or restart.	Set up a job in DAPIDLER to do 1/ACCS.
14, 15	———	——— Unused ———	———

Table 3.6-3. RCSFLAGS Description

SUBSECTION 3.7

COASTING-FLIGHT ATTITUDE MANEUVER ROUTINE

by

Donald W. Keene

3.7.1 Introduction

The purpose of the attitude maneuver routine (R60) is to automatically reorient the spacecraft during coasting flight. This maneuver process is illustrated in Fig. 3.7-1. The desired attitude to which the spacecraft is to be aligned can be specified in one of two ways:

a) By a set of terminal desired gimbal angles, $\underline{\theta}_c$.

b) By two unit vectors, $\underline{u}_{DSM}$ and $\underline{u}_{ANB}$.

$\underline{\theta}_c$ is the set of desired (or commanded) gimbal angles defined by

$$\underline{\theta}_c = \begin{Bmatrix} \theta_{co} \\ \theta_{ci} \\ \theta_{cm} \end{Bmatrix} = \begin{Bmatrix} \text{desired outer gimbal angle} \\ \text{desired inner gimbal angle} \\ \text{desired middle gimbal angle} \end{Bmatrix}$$

$\underline{u}_{ANB}$ is a body-fixed axis vector, $\underline{u}_A$, with components in navigation-base coordinates. $\underline{u}_{DSM}$ is a desired-direction vector, $\underline{u}_D$, with components in stable-member coordinates. $\underline{u}_{DSM}$ specifies the direction in inertial space to which $\underline{u}_{ANB}$ is to be aligned. A flag switch, FL_{3AXIS}, is provided to specify which of the two types of inputs is to be used.

If the vector type of input is chosen, the routine known as VECPOINT is used to compute a set of desired gimbal angles, $\underline{\theta}_c$, based on the values of $\underline{u}_{DSM}$, $\underline{u}_{ANB}$ and the current gimbal angles, $\underline{\theta}$. In routine 60, these desired gimbal angles are converted to the corresponding FDAI angles and displayed to the crew. The crew then has the option of performing the maneuver either manually or automatically. If the automatic option is selected, R60 calls a routine known as KALCMANU which computes a set of parameters ($\underline{u}_r$, A) that determine how the reorientation is to be performed. The maneuver is performed by rotating the spacecraft about the axis

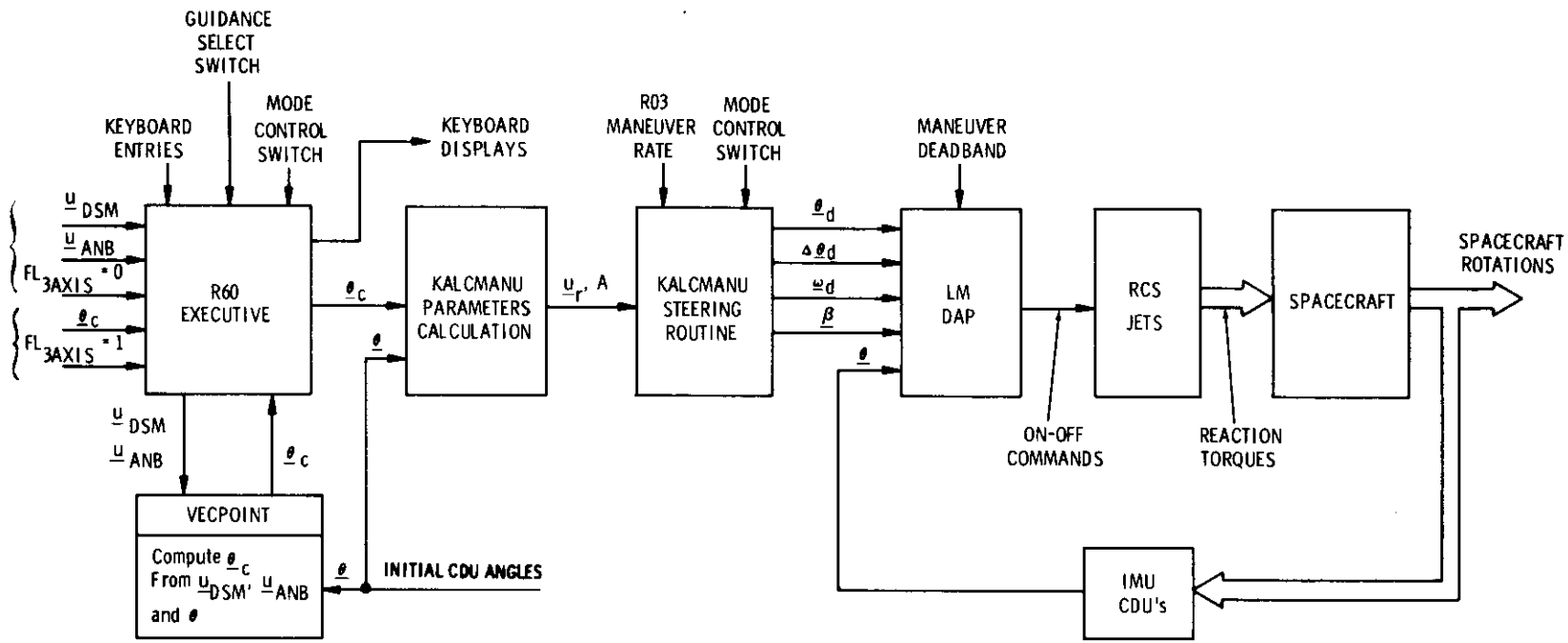

Fig. 3.7–1. R60 information flow.

of single equivalent rotation, $\underline{u}_r$, by the angle A. $\underline{u}_r$ and A are completely determined by the initial orientation, $\underline{\theta}$, and the desired terminal orientation, $\underline{\theta}_c$. The rate at which the maneuver is performed is specified by the crew in R03.

The KALCMANU steering routine computes four sets of quantities for use by the digital autopilot in following the angular path defined by $\underline{u}_r$, A. The first of these is a set of autopilot reference angles, $\underline{\theta}_d$ (or intermediate desired CDU angles), which are updated once every second during the maneuver. To achieve a smoother sequence of commands between successive updates, the program also generates a set of incremental CDU angles, $\Delta\underline{\theta}_d$, to be added to $\underline{\theta}_d$ by the digital autopilot. The steering routine also computes the component maneuver rates, $\underline{\omega}_d$ (in spacecraft axes), and a set of bias angles, $\underline{\beta}$, to be used by the autopilot to prevent fuel-consuming overshoot when starting and stopping an automatic maneuver.

The aforenoted procedure allows the autopilot to establish and maintain a spacecraft rotation about the vector $\underline{u}_r$ at a fixed rotation rate $\underline{\omega}_d$. The maneuvers are timed in open-loop fashion so that after a predetermined interval $\Delta\underline{\theta}_d$, $\underline{\omega}_d$, and $\underline{\beta}$ are set to zero and the autopilot reference angles, $\underline{\theta}_d$, are set equal to the terminal angles, $\underline{\theta}_c$. Thus, upon completion of the maneuver, the spacecraft will finish up in a limit cycle about $\underline{\theta}_c$.

3.7.2 R60 Executive

The R60 Executive section of the attitude maneuver routine is illustrated in Fig. 3.7-2. The keyboard displays indicate the total FDAI ball-angle attitude required for the reorientation. If the vector option is selected by the calling program, the routine VECPOINT is used to compute the terminal desired gimbal angles $\underline{\theta}_c$. The FDAI-IMU transformation routine is used to compute the required ball angles. The crew has the option of either manually reorienting the spacecraft or having the maneuver performed automatically. Mode 2 total-attitude-error displays are automatically selected when R60 is called. If the automatic option is to be used, the guidance select switch must be in PGNCS and the mode select switch in AUTO. During the maneuver, the crew should monitor the FDAI for gimbal lock since KALCMANU has no provisions for avoiding gimbal lock. If the spacecraft attitude is approaching the gimbal-lock zone, the crew should stop the maneuver by switching to ATT HOLD and manually steer the spacecraft around gimbal lock. The maneuver may then be completed either automatically or manually.

The desired gimbal angles, $\underline{\theta}_c$, computed by VECPOINT are determined on the basis of minimizing the rotation angle required to align $\underline{u}_{ANB}$ with $\underline{u}_{DSM}$. In general, this procedure will reduce the fuel required for the maneuver by not

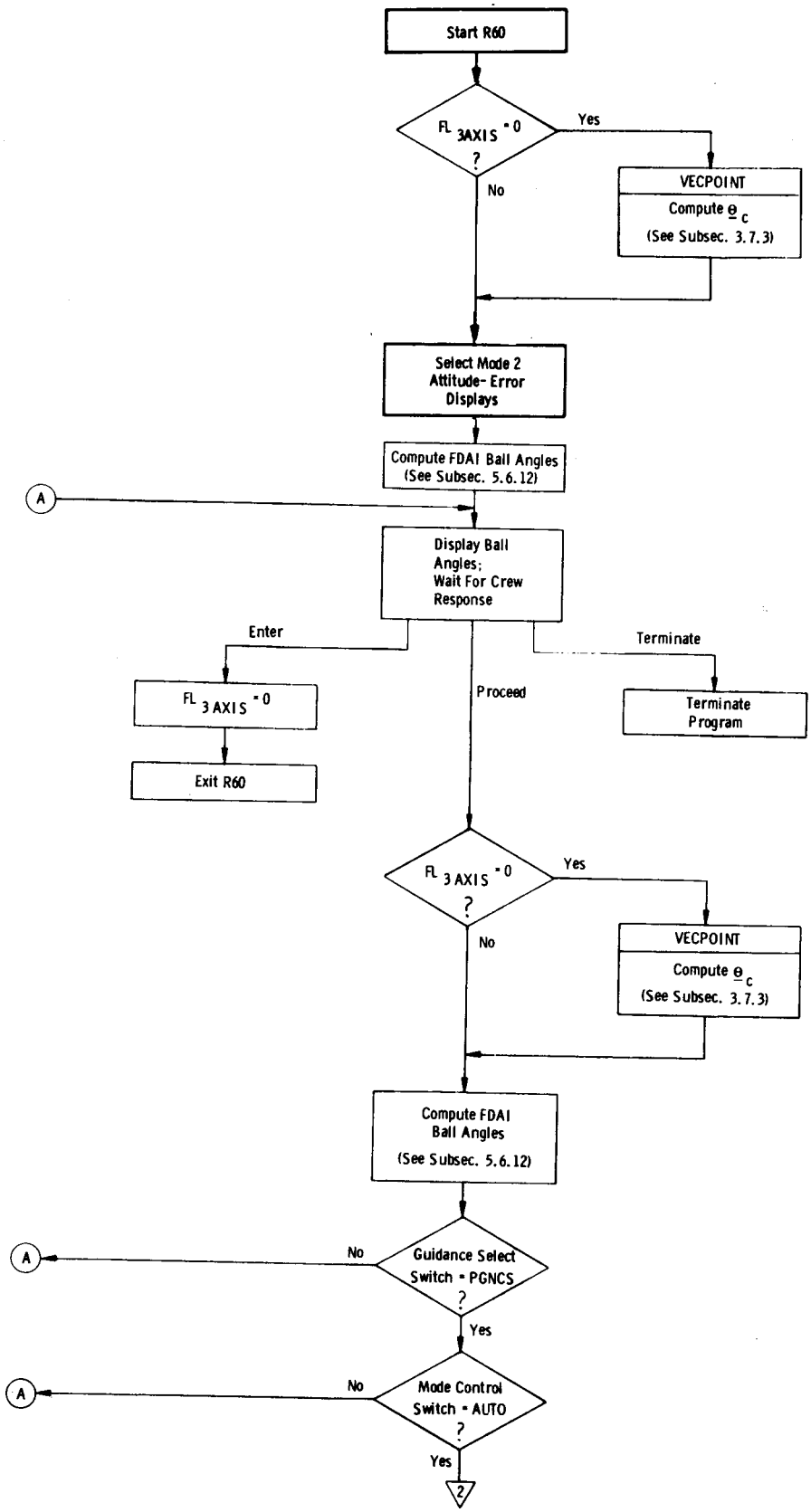

Fig. 3.7–2. R60 Executive (Sheet 1 of 2)

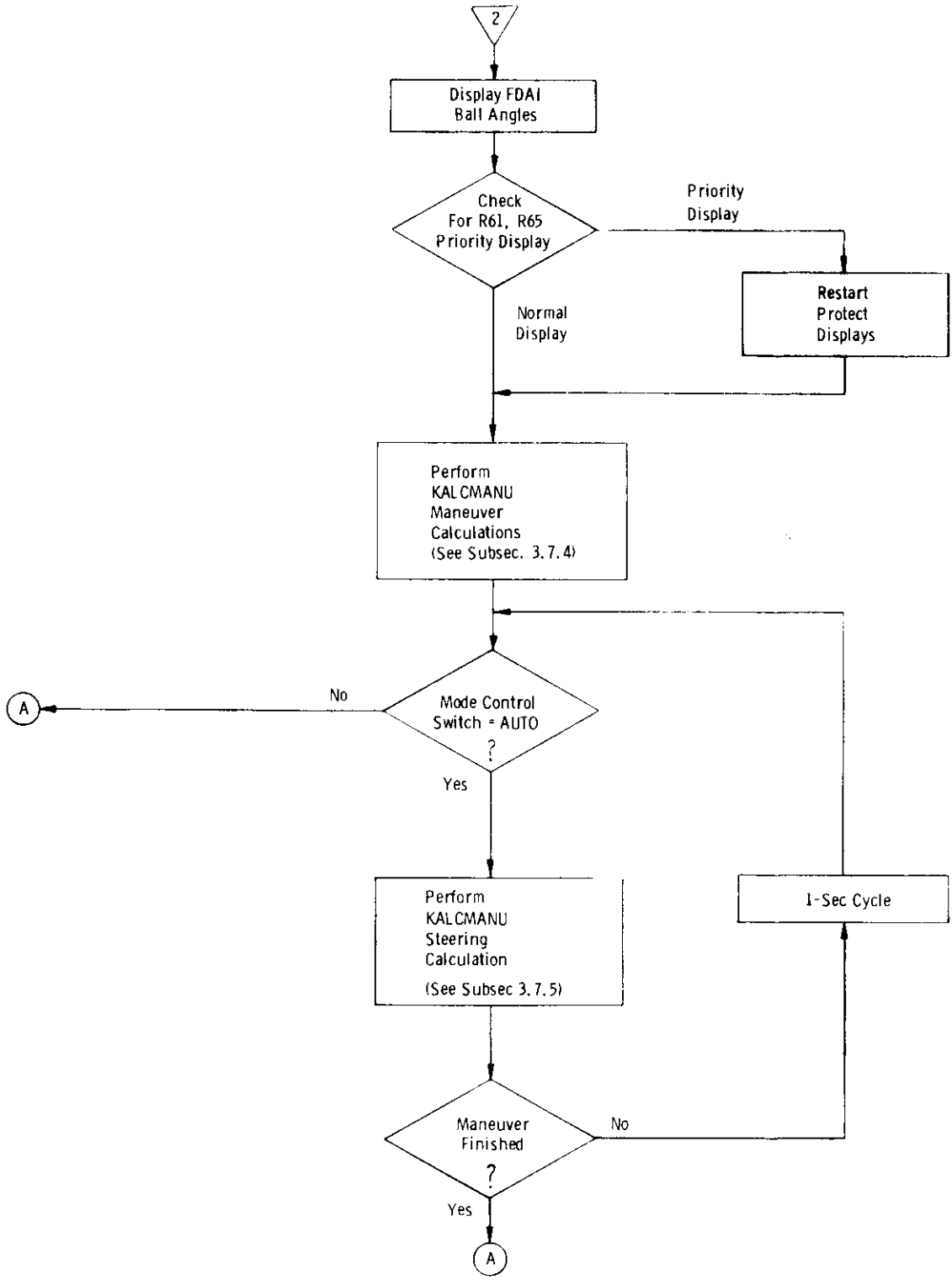

Fig. 3.7–2. R60 Executive (Sheet 2 of 2)

constraining the orientation of the spacecraft about the pointing axis*, defined by $\underline{u}_{DSM}$. Additionally, the attitude about $\underline{u}_{DSM}$ will be left unchanged. Consequently, the crew may specify the attitude about the pointing axis to satisfy additional communication, visibility, or thermal constraints, if desired. This is done by manually reorienting the spacecraft about the pointing axis either prior to or after the maneuver. If this procedure is done after the automatic maneuver, a final trim will usually be required to assure that $\underline{u}_{ANB}$ is aligned with $\underline{u}_{DSM}$. If the trim is to be done manually, the crew should leave the mode switch in ATT HOLD and proceed with the maneuver request so that the VECPOINT solution is recomputed from the new attitude.

3.7.3 VECPOINT

As mentioned in the preceding subsections, the VECPOINT routine is used to compute the desired gimbal angles, $\underline{\theta}_c$, based upon the values of $\underline{u}_{DSM}$, $\underline{u}_{ANB}$ and the current gimbal angles, $\underline{\theta}$. VECPOINT, in turn, uses a number of subroutines in its computations. These subroutines will be described first.

a) CDUTODCM Subroutine

This subroutine converts three gimbal angles, $\underline{\theta}$, to a direction-cosine matrix, $\overset{*}{C}$, that relates the corresponding spacecraft navigation-base orientation to the stable-member frame. The formulas for this conversion are

$$\overset{*}{C} = \begin{bmatrix} C_1 & C_2 & C_3 \\ C_4 & C_5 & C_6 \\ C_7 & C_8 & C_9 \end{bmatrix}$$

$$C_1 = \cos\theta_i \cos\theta_m$$

$$C_2 = -\cos\theta_i \sin\theta_m \cos\theta_o + \sin\theta_i \sin\theta_o$$

$$C_3 = \cos\theta_i \sin\theta_m \sin\theta_o + \sin\theta_i \cos\theta_o$$

$$C_4 = \sin\theta_m$$

$$C_5 = \cos\theta_m \cos\theta_o$$

$$C_6 = -\cos\theta_m \sin\theta_o$$

$$C_7 = -\sin\theta_i \cos\theta_m$$

*See exception noted in Subsection 3.7.3.

$$C_8 = \sin\theta_i \sin\theta_m \cos\theta_o + \cos\theta_i \sin\theta_o$$

$$C_9 = -\sin\theta_i \sin\theta_m \sin\theta_o + \cos\theta_i \cos\theta_o$$

where

θ_o = outer gimbal angle

θ_i = inner gimbal angle

θ_m = middle gimbal angle

The interpretation of this matrix is as follows: If a_x, a_y, a_z represent the components of a vector in navigation-base axes, then the components of the same vector in stable-member axes (b_x, b_y, b_z) are

$$\begin{Bmatrix} b_x \\ b_y \\ b_z \end{Bmatrix} = \overset{*}{C}(\underline{\theta}) \begin{Bmatrix} a_x \\ a_y \\ a_z \end{Bmatrix}$$

b) DCMTOCDU Subroutine

This subroutine extracts the CDU angles from a direction-cosine matrix, $\overset{*}{C}$, that relates the navigation-base axes to the stable-member axes. The formulas for this conversion are

$$\theta_m = \arcsin C_4$$

$$\theta_i = \arcsin(-C_7/\cos\theta_m)$$

[If C_1 is negative, θ_i is replaced by π SGN $\theta_i - \theta_i$]

$$\theta_o = \arcsin(-C_6/\cos\theta_m)$$

[If C_5 is negative, θ_o is replaced by π SGN $\theta_o - \theta_o$]

c) ROTCOMP Subroutine

This subroutine computes the direction-cosine matrix, $\overset{*}{R}$, that relates one coordinate frame to another frame that is rotated with respect to the first by an angle A about a unit vector $\underline{u}_r$. The formula for this matrix is

$$\overset{*}{R}(\underline{u}_r, A) = \overset{*}{I} \cos A + \underline{u}_r \underline{u}_r^T (1 - \cos A) + \overset{*}{U}X_r \sin A$$

where

$$\overset{*}{I} = \begin{bmatrix} 1 & 0 & 0 \\ 0 & 1 & 0 \\ 0 & 0 & 1 \end{bmatrix}$$

$$\underline{u}_r \, \underline{u}_r^T = \begin{bmatrix} u_{rx}^2 & u_{rx}\,u_{ry} & u_{rx}\,u_{rz} \\ u_{ry}\,u_{rx} & u_{ry}^2 & u_{ry}\,u_{rz} \\ u_{rz}\,u_{rx} & u_{rz}\,u_{ry} & u_{rz}^2 \end{bmatrix}$$

$$\overset{*}{UX}_r = \begin{bmatrix} 0 & -u_{rz} & u_{ry} \\ u_{rz} & 0 & -u_{rx} \\ -u_{ry} & u_{rx} & 0 \end{bmatrix}$$

$\underline{u}_r$ = unit rotation vector resolved into spacecraft axes

A = rotation angle

The interpretation of $\overset{*}{R}$ is as follows: If a_x, a_y, a_z represent the components of a vector in the rotated frame, then the components of the same vector in the original frame (b_x, b_y, b_z) are

$$\begin{Bmatrix} b_x \\ b_y \\ b_z \end{Bmatrix} = \overset{*}{R}(\underline{u}_r, A) \begin{Bmatrix} a_x \\ a_y \\ a_z \end{Bmatrix}$$

The process used by VECPOINT in determining the terminal desired angles, $\underline{\theta}_c$, is illustrated schematically in Fig. 3.7-3. VECPOINT uses three frames of reference: the L frame, the M frame, and the N frame – as well as the stable-member (SM) frame. The L frame is simply a base frame used as the starting

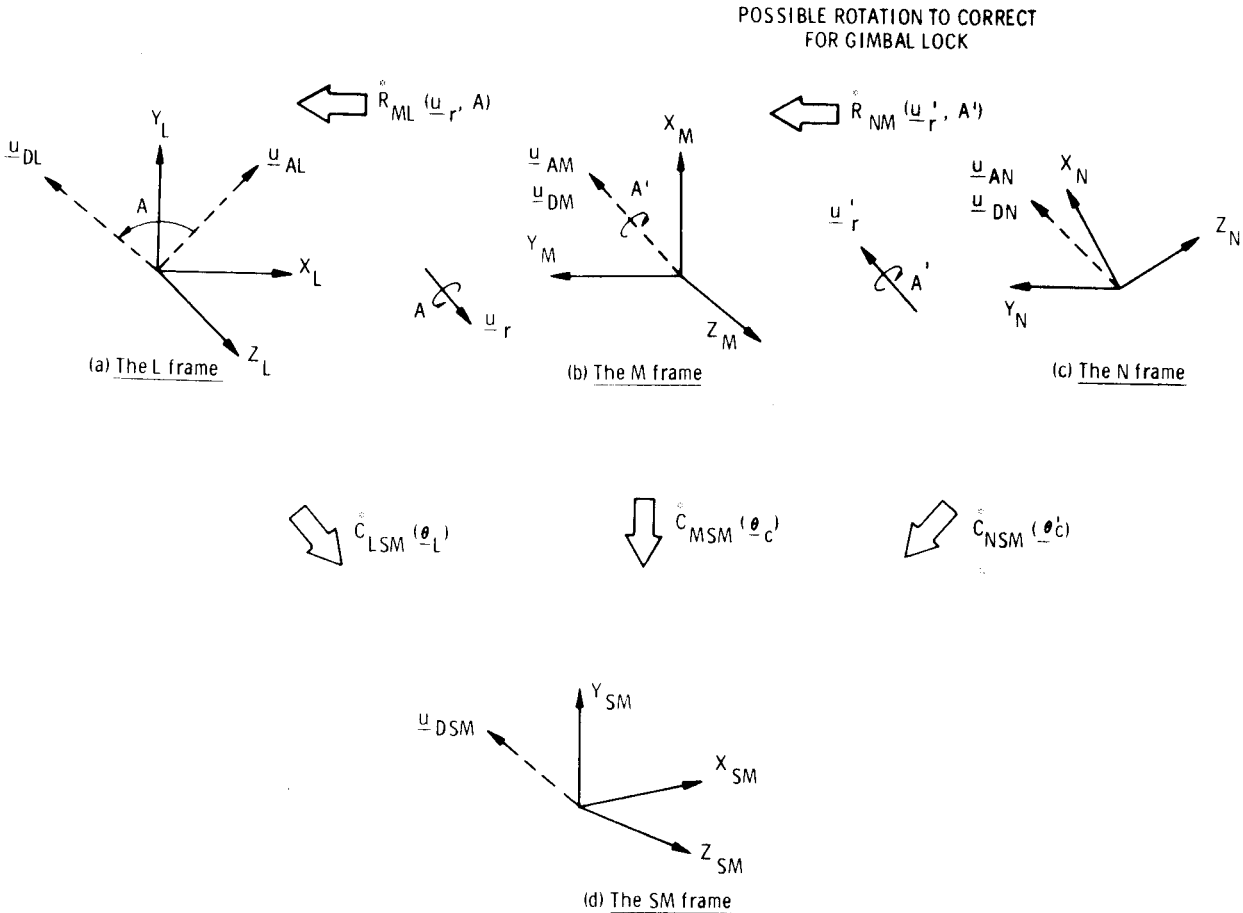

Fig. 3.7–3. The coordinate frames and transformations used in VECPOINT.

point for subsequent rotations. In R60 VECPOINT computations, the L frame is the initial navigation-base frame computed from the initial gimbal angles, $\underline{\theta}$. For R65, the preferred axis-tracking routine, the L frame is computed on the basis of the autopilot reference angles, $\underline{\theta}_d$ (see Fig. 3.7-4). The vector $\underline{u}_D$ is resolved from the stable-member frame into this frame as $\underline{u}_{DL}$ † using the transformation $\overset{*}{C}{}^T_{LSM}$. †† The L frame is then rotated so that $\underline{u}_{AL}$ and $\underline{u}_{DL}$ are coincident. The rotation vector, $\underline{u}_r$, is defined by the cross product between $\underline{u}_{AL}$ and $\underline{u}_{DL}$. If the two vectors are either parallel or antiparallel, a special computation of $\underline{u}_r$ is performed (see below). Rotation about the cross-product vector will assure that spacecraft maneuvering will be minimized and that the rotation vector will have no component in the $\underline{u}_{AL}$ or $\underline{u}_{DL}$ directions.

In the M frame, $\underline{u}_A$ is aligned with $\underline{u}_D$ and normally the desired terminal angles can be extracted directly from the matrix $\overset{*}{C}_{MSM}$ that relates this frame to the stable-member frame. If, however, the M frame corresponds to a gimbal-lock orientation, an extra rotation about $\underline{u}_{DM}$ (or $\underline{u}_{AM}$) will be necessary to correct for the gimbal-lock condition. For VECPOINT, gimbal lock is defined when $\underline{u}_{XM}$ is within 31 deg of the $\pm y$ stable-member axis direction ($\pm \underline{u}_{YSM}$), that is, when the magnitude of the desired terminal middle gimbal angle, $|\theta_{cm}|$, exceeds 59 deg. This situation is illustrated in Fig. 3.7-5, in which the shaded area represents the gimbal-lock region. As can be seen, $\underline{u}_{XM}$ can be rotated out of gimbal lock by a sufficiently large rotation about $\underline{u}_{AM}$. Under some circumstances, however, no amount of rotation about $\underline{u}_{AM}$ will correct for gimbal lock. This possibility may occur if the angle between $\pm \underline{u}_{XM}$ and $\underline{u}_{AM}$ is less than 31 deg. Whether or not gimbal lock can be corrected in such a case depends on the geometry of the problem In order to simplify the VECPOINT calculations, however, it was decided that gimbal lock would be unavoidable under these circumstances. In fact, no correction will be made in VECPOINT if

$$\left|\underline{u}_{AM} \cdot \underline{u}_{XM}\right| \geq \cos 40.6 \text{ deg}$$

and $\underline{u}_{XM}$ falls within the gimbal-lock region. Note that this criterion includes the thrust vector for P40 pre-burn alignments. In such cases, a platform realignment would be required before reorienting the spacecraft.

---

† The subscript L appended to the vector indicates the frame of reference into which the vector is resolved. Note that the components of $\underline{u}_{ANB}$, $\underline{u}_{AL}$, $\underline{u}_{AM}$ and $\underline{u}_{AN}$ are all numerically equal since they represent the same body-fixed vector.

†† $\overset{*}{C}_{LSM}$ is defined as the transformation from the L frame (or first subscript) to the stable-member frame (or second subscript). $\overset{*}{C}{}^T_{LSM}$ is its transpose.

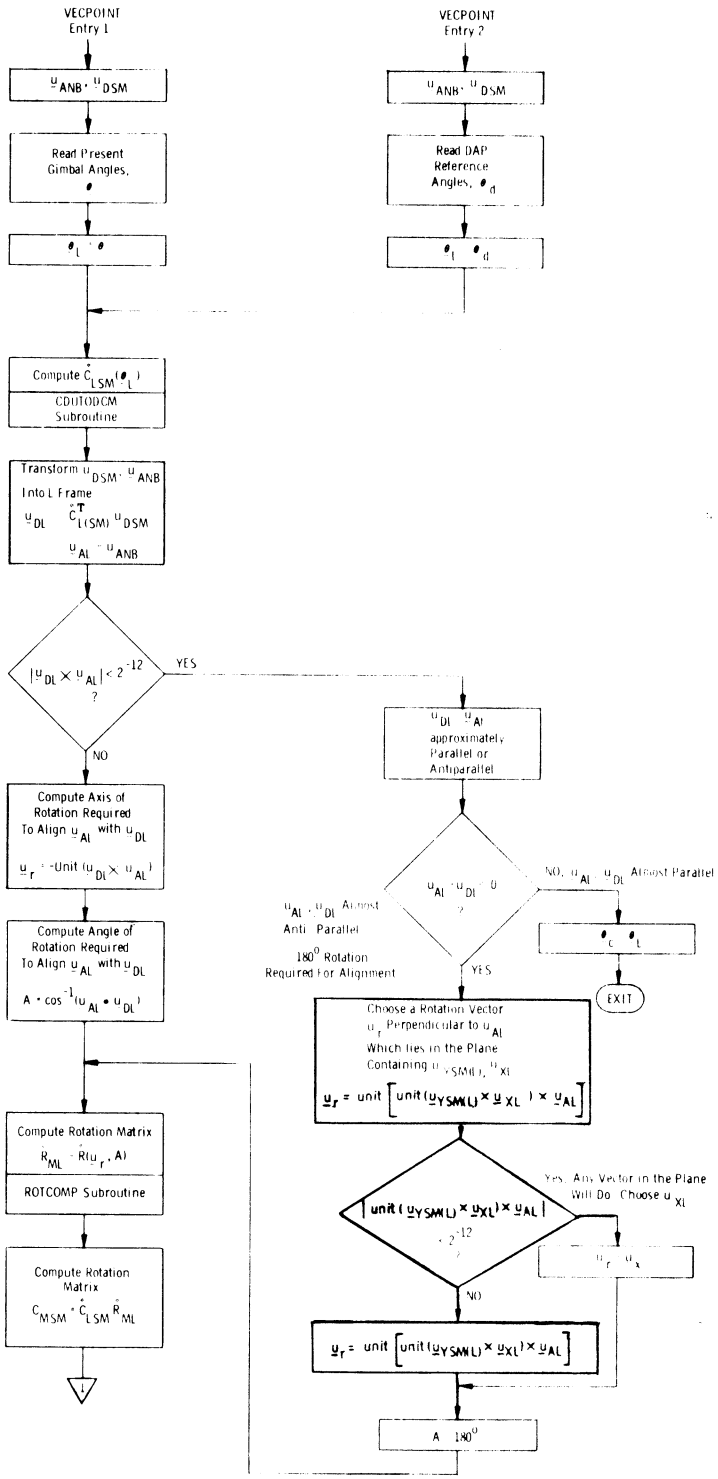

Fig. 3.7–4. VECPOINT logic flow (Sheet 1 of 2)

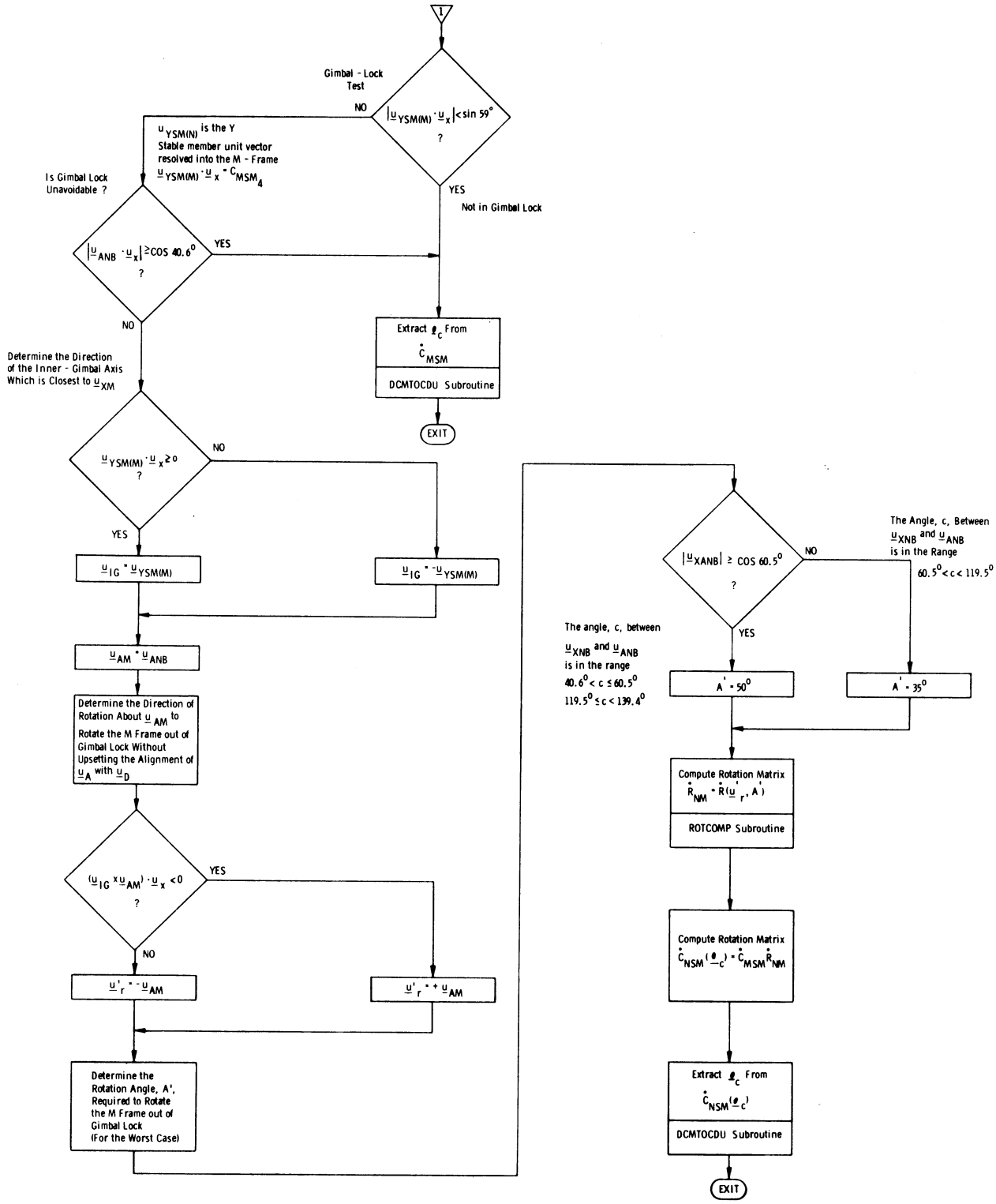

Fig. 3.7–4. VECPOINT logic flow (Sheet 2 of 2)

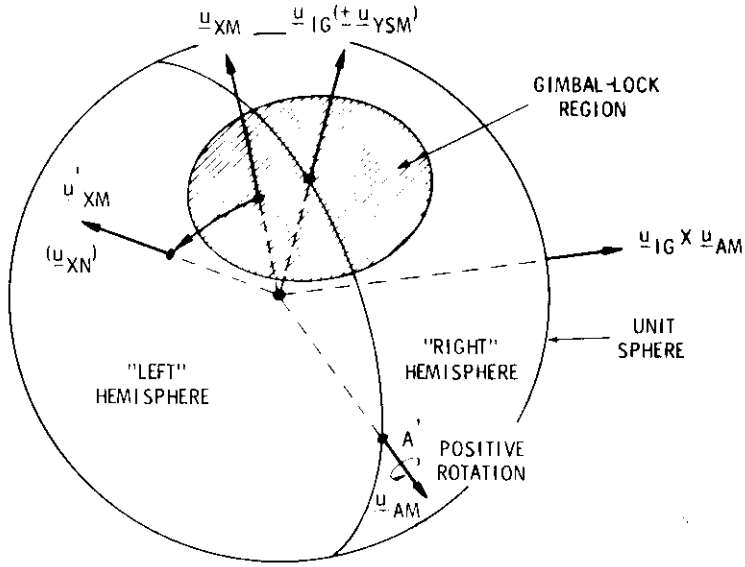

a) A' Positive

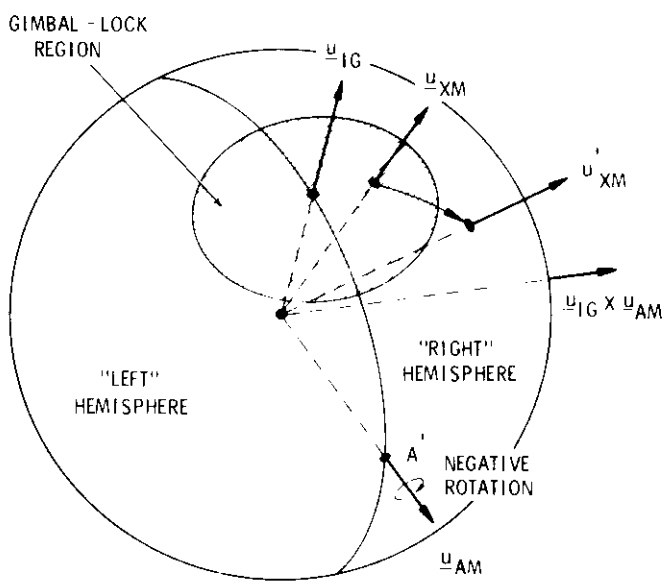

b) A' Negative

Fig. 3.7–5. Rotation to correct for gimbal lock.

If it is found that the M frame can be reoriented to correct for gimbal lock, then the next step in the logic is to determine the direction of rotation about $\underline{u}_{AM}$ and the magnitude of the rotation, A', required for this reorientation. It is desirable to find the direction that minimizes the angular excursion through the gimbal-lock region. This is found by first locating the direction $\underline{u}_{IG}$ of the inner gimbal axis ($+\underline{u}_{YSM}$ or $-\underline{u}_{YSM}$) that is closest to $\underline{u}_{XM}$. Referring to Fig. 3.7-5, if $\underline{u}_{XM}$ lies to the "left" of the plane defined by $\underline{u}_{IG}$ and $\underline{u}_{AM}$, then A' is positive. If, on the other hand, $\underline{u}_{XM}$ lies to the "right" of the plane defined by $\underline{u}_{IG}$ and $\underline{u}_{AM}$, then A' is negative. Note that if $\underline{u}_{XM}$ lies in the plane of $\underline{u}_{IG}$ and $\underline{u}_{AM}$ then A' can be either positive or negative. For this case, $|A'|$ is greatest for any fixed angular relation between $\underline{u}_{IG}$ and $\underline{u}_{AM}$.

The remaining part of the problem is to determine the magnitude of the rotation required to correct for gimbal lock. Theoretically, one could determine the minimum rotation required to place $\underline{u}'_{XM}$ exactly on the boundary of the gimbal-lock region. To simplify the problem, however, VECPOINT uses a predetermined set of angles that will assure that, even in the worst case, $\underline{u}'_{XM}$ will always lie outside the gimbal-lock region. To define the worst-case conditions, examine the spherical triangle ABC shown in Fig. 3.7-6. The problem is to find the maximum value of the rotation angle, A, required to rotate $\underline{u}_{XM}$ to the gimbal-lock boundary (point B), given the angle c between $\underline{u}_{AM}$ and $\underline{u}_{XM}$. Clearly, the maximum value of A occurs when $\underline{u}_{XM}$ falls in the "middle" of the gimbal-lock region, that is, when $\underline{u}_{XM}$ lies in the plane of $\underline{u}_{IG}$ and $\underline{u}_{AM}$. The following relationship holds for any spherical triangle:

$$\sin A = \sin a \frac{\sin C}{\sin c}$$

The maximum value of A, A_{max}, occurs when

$$\frac{dA}{dC} = \frac{\sin a}{\sin c} \frac{\cos C}{\cos A} = 0$$

or when $\cos C = 0$, that is, $C = 90°$.

Thus,

$$A_{max} = \sin^{-1} \frac{\sin a}{\sin c}$$

Note that the required rotation angle depends directly on the angle between $\underline{u}_{XM}$ and $\underline{u}_{AM}$. If c is less than a, then A_{max} is indeterminate; that is, gimbal lock may be unavoidable. To avoid calculating A_{max} explicitly, VECPOINT divides the problem into three zones as defined in the following table.

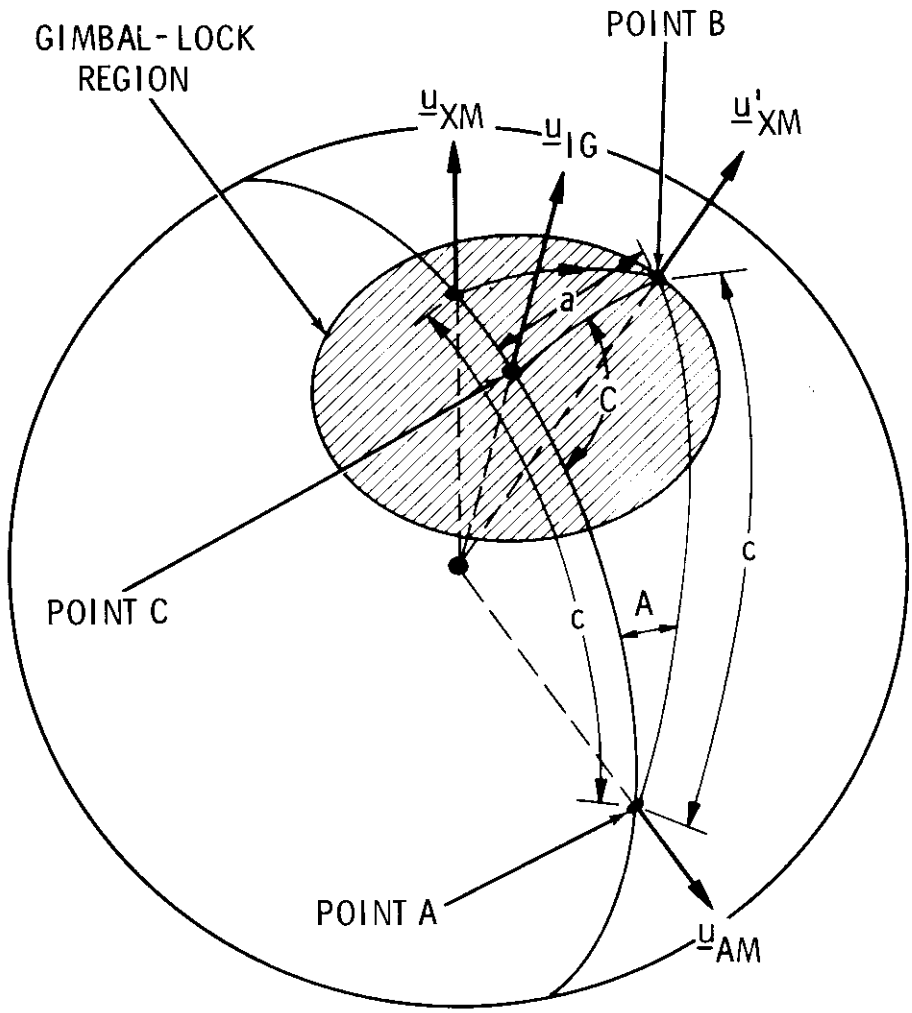

Fig. 3.7–6. Geometry for computing the maximum value of the angle A.

c	A_{max} ($a \simeq 30°$)
$60.5° < c < 119.5°$	35°
$40.6° < c \leq 60.5°$ $119.5° \leq c < 139.4°$	50°
$0 \leq c \leq 40.6°$ $139.4° \leq c \leq 180°$	INDETERMINATE

Note that the correction for gimbal lock will override the desire to minimize the rotation about the $\underline{u}_A$ axis. If during R65 Z-axis tracking the M frame encounters gimbal lock, VECPOINT will call for an automatic 35-deg rotation about the pointing axis. Unfortunately, R65 may not sense this relatively large rotation and therefore not call for an R60-supervised maneuver. However, the additional rotation, A', is usually large enough so that subsequent tracking should not encounter gimbal lock.

The one remaining item to be discussed concerning VECPOINT is the case when $\underline{u}_{AL}$ and $\underline{u}_{DL}$ are almost parallel or antiparallel. If $\underline{u}_{AL}$ and $\underline{u}_{DL}$ are almost parallel, then $\underline{\theta}_c$ is set equal to $\underline{\theta}_L$. If the two vectors are almost antiparallel, then a 180-deg rotation is required for the alignment. In this case, the rotation vector is chosen so that $\underline{u}_r$ is perpendicular to $\underline{u}_{AL}$ and lies in the plane that contains $\underline{u}_{YSM(L)}$ and $\underline{u}_{XL}$. If, however, $\underline{u}_{AL}$ happens to be perpendicular to the plane, then any vector in the plane may be used for $\underline{u}_r$. In this event, the X axis is chosen. The computation of the M frame, the check for gimbal lock, and the extraction of the desired angles, $\underline{\theta}_c$, are then performed in the manner already described.

3.7.4 KALCMANU Maneuver-Parameters Calculation

The KALCMANU routine is designed to generate commands for the LM autopilot to reorient the spacecraft from an initial attitude to some desired attitude specified by $\underline{\theta}_c$. Although a number of authors have discussed optimal solutions to this problem, the task is a formidable one because of the nonlinear nature of rigid-body dynamics and the kinematics of rotational motion. Optimal solutions for a particular class of spacecraft configurations are treated in Reference 1. In this reference, the criterion for optimality is based upon the product of maneuver duration and fuel expenditure. Using the same criterion, previous design studies based upon a number of suboptimal approaches [2] have shown that a reasonable design compromise is to rotate the spacecraft about a single inertially fixed axis. This technique is employed in KALCMANU.

The process used by KALCMANU in computing the rotation axis, $\underline{u}_r$, and the rotation angle, A_m, is illustrated in Fig. 3.7-7. If the magnitude of the commanded middle gimbal angle, $|\theta_{cm}|$, exceeds 70 deg, program alarm 401 is issued and the logic returns to the R60 Executive. No automatic maneuver is permitted in this case.* However, the crew may manually reorient the spacecraft to the required attitude if desired. If the gimbal-lock test is passed, KALCMANU then proceeds to compute the transformation between the initial spacecraft axes (at the time the KALCMANU routine begins) and the stable-member axes, $\overset{*}{C}_{BSM}$. The program also computes the matrix relating the desired terminal spacecraft attitude and the stable-member axes, $\overset{*}{C}_{CSM}$. The transformation between the desired and the initial attitude is $\overset{*}{R}_{CB}$, where

$$\overset{*}{R}_{CB} = \overset{*}{C}^{T}_{BSM}\ \overset{*}{C}_{CSM}$$

$\overset{*}{R}_{CB}$ can be partitioned into its symmetric and antisymmetric components as follows. For the symmetric part,

$$\overset{*}{R}_S = (1/2)(\overset{*}{R}_{CB} + \overset{*}{R}^{T}_{CB})$$

By comparing this with the equations described in the ROTCOMP subroutine (see Subsection 3.7.3) it can be seen that

$$\overset{*}{R}_S = \overset{*}{I} \cos A_m + \underline{u}_r \underline{u}_r^{T} (1-\cos A_m)$$

For the antisymmetric part,

$$\overset{*}{R}_A = (1/2)(\overset{*}{R}_{CB} - \overset{*}{R}^{T}_{CB})$$

or

$$\overset{*}{R}_A = \begin{bmatrix} 0 & -u_{rz} & u_{ry} \\ u_{rz} & 0 & -u_{rx} \\ -u_{ry} & u_{rx} & 0 \end{bmatrix} \sin A_m$$

The maneuver angle can easily be obtained from $\overset{*}{R}_{CB}$ as

$$A_m = \cos^{-1}\left(\frac{\text{Trace}\,(\overset{*}{R}_{CB}) - 1}{2}\right)$$

The rotation vector, $\underline{u}_r$, is normally extracted from the antisymmetric part of $\overset{*}{R}_{CB}$; that is,

$$\underline{u}_r = \text{unit}\ (-R_{A6},\ R_{A3},\ -R_{A2})$$

*Note that while there is logic in VECPOINT and KALCMANU to avoid a final middle gimbal angle causing gimbal lock, there is no logic in the KALCMANU calculation of maneuver parameters which ensures that the computed maneuver will not carry the vehicle attitude through gimbal lock during the maneuver.

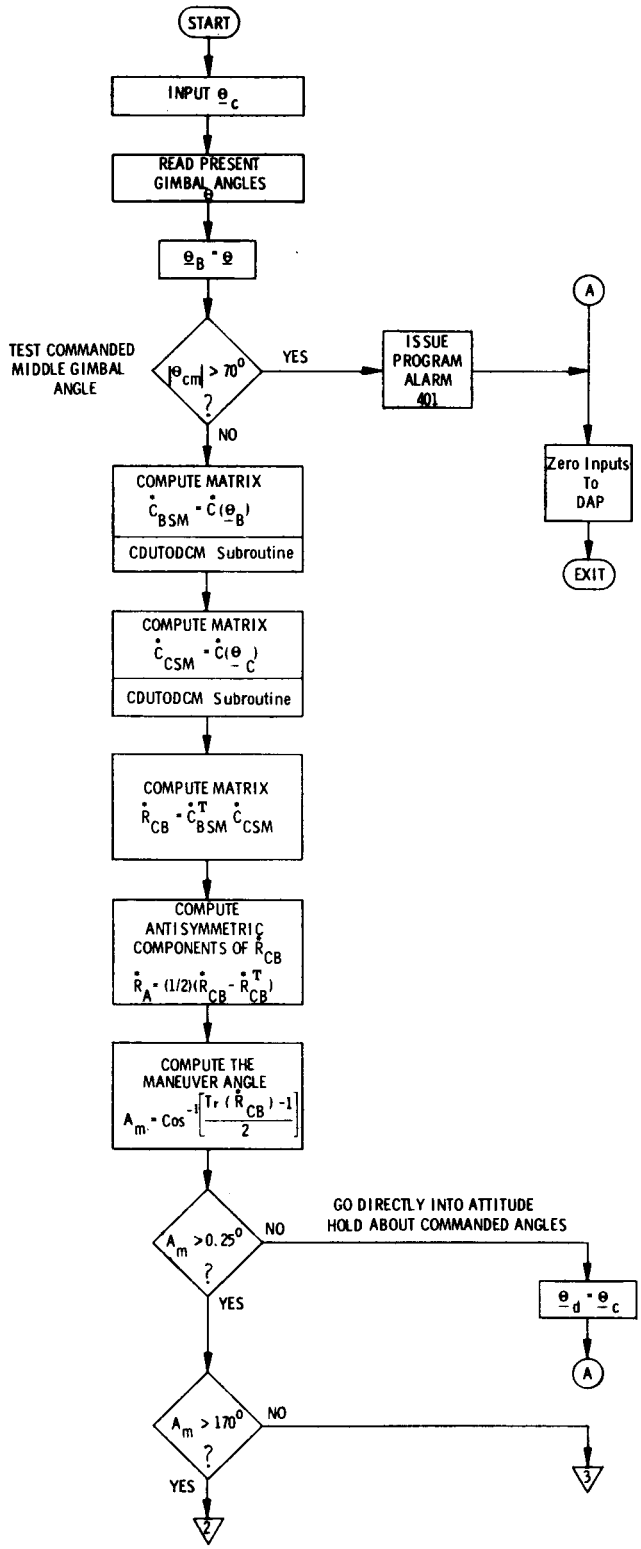

Fig. 3.7–7. Calculation of KALCMANU maneuver parameters (Sheet 1 of 3).

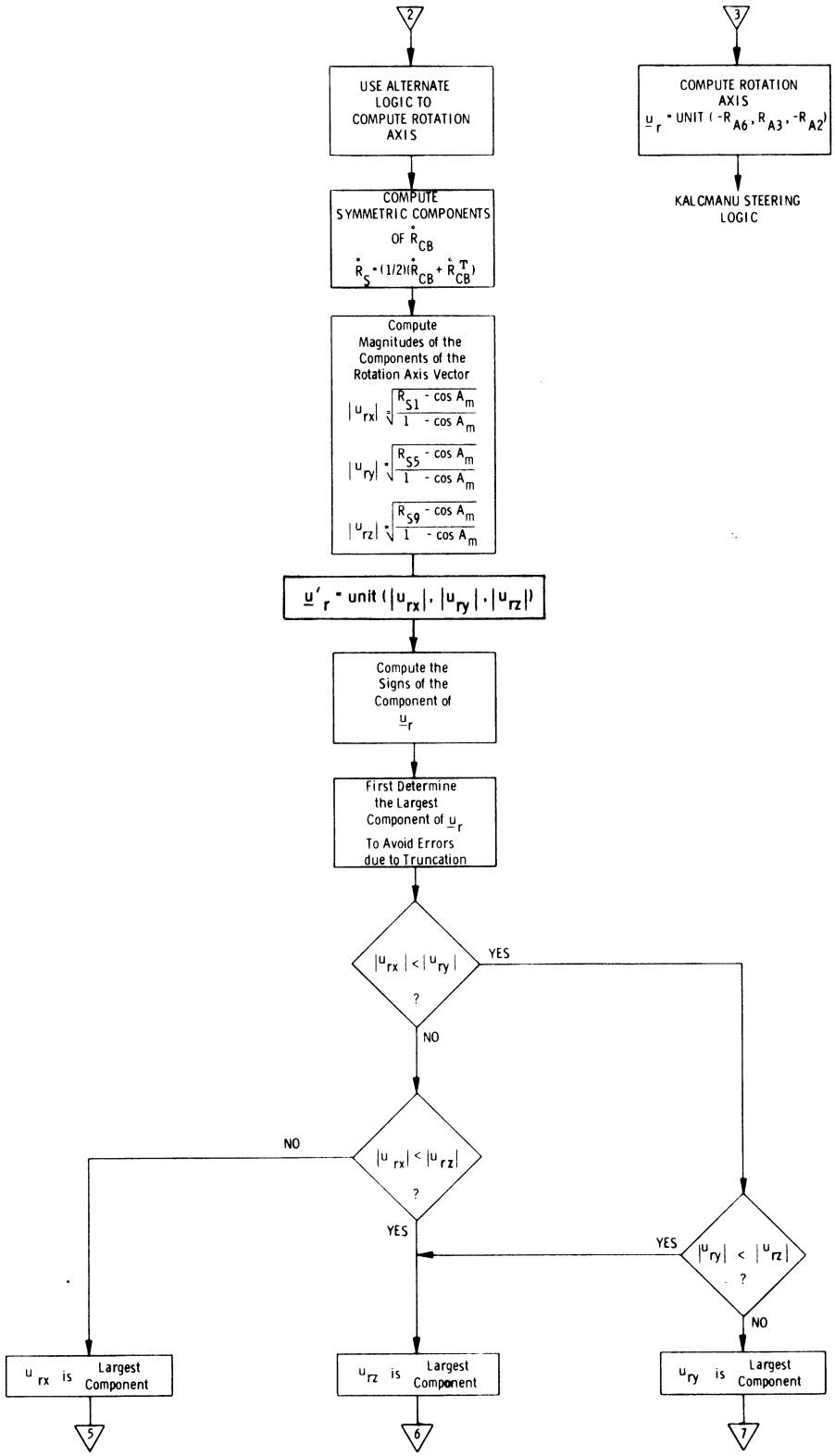

Fig. 3.7–7. Calculation of KALCMANU maneuver parameters (Sheet 2 of 3).

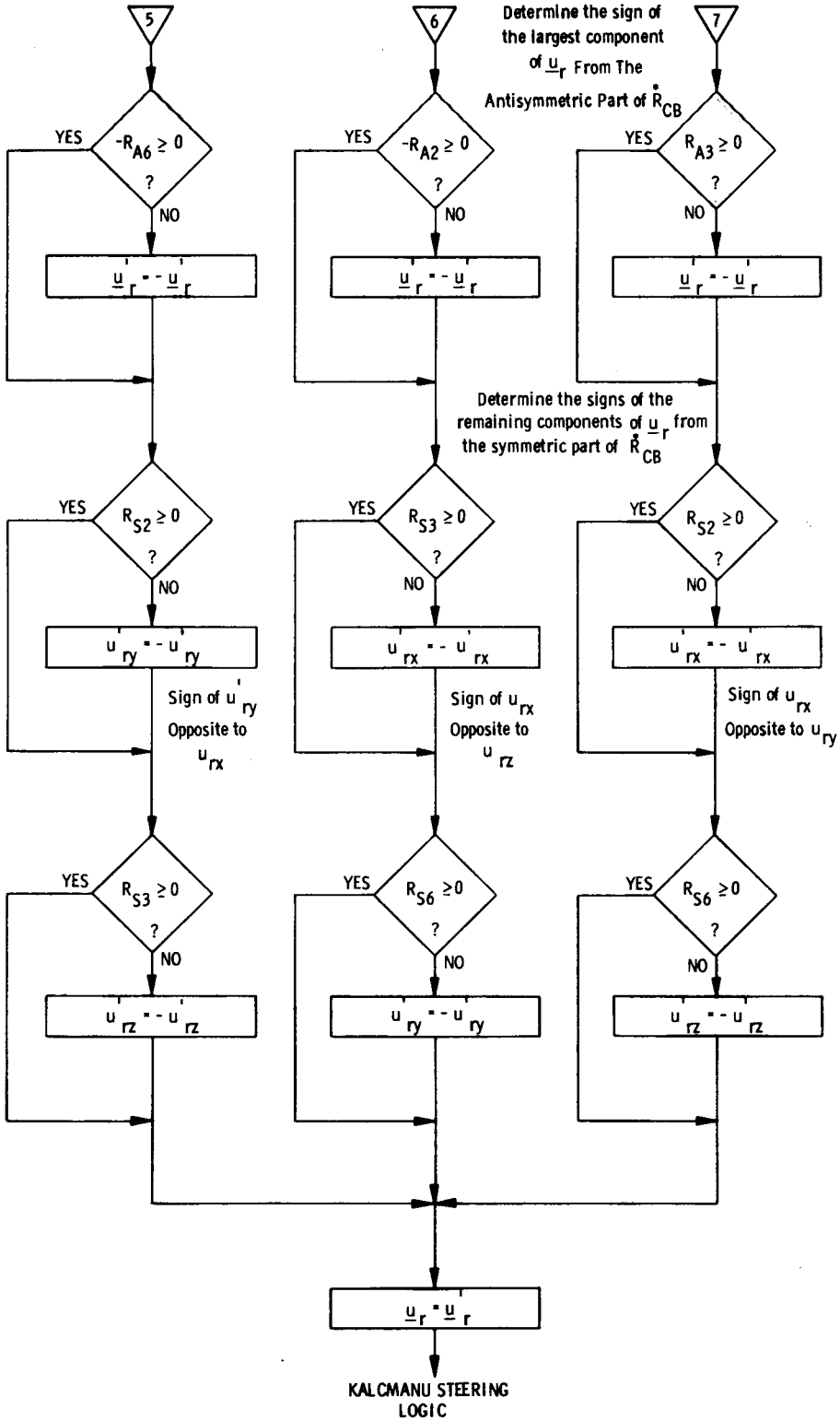

Fig. 3.7–7. Calculation of KALCMANU maneuver parameters (Sheet 3 of 3).

As $\sin A_m$ approaches zero, however, the unit operation becomes indeterminate and an alternative calculation must be performed. If the maneuver angle is less than 0.25 deg, then no complicated automatic maneuvering is necessary and therefore one can simply set the autopilot reference angle, $\underline{\theta}_d$, equal to the terminal desired angles $\underline{\theta}_c$ and exit. If $A_m > 170$ deg, a method employing the symmetric part of $\overset{*}{R}_{CB}$ is used to determine $\underline{u}_r$, as illustrated in Fig. 3.7-7. The magnitudes of the components of $\underline{u}_r$ are easily determined as

$$|u_{rx}| = \sqrt{\frac{R_{S1} - \cos A_m}{1 - \cos A_m}}$$

$$|u_{ry}| = \sqrt{\frac{R_{S5} - \cos A_m}{1 - \cos A_m}}$$

$$|u_{rz}| = \sqrt{\frac{R_{S9} - \cos A_m}{1 - \cos A_m}}$$

To obtain the signs of each component, it is first necessary to determine the sign of the largest component by referring to the values of $\overset{*}{R}_A$. This is done to avoid the problem caused by truncation as $\sin A_m$ approaches zero. If A_m is equal to 180 deg, then the sign of the largest component may be arbitrarily chosen. The signs of the remaining components may be determined by examining the off-diagonal terms in $\overset{*}{R}_S$.

3.7.5 KALCMANU Steering

The KALCMANU parameter calculations described in the preceding subsection solve the problem of what angular path to take in order to reorient the spacecraft without excessive fuel expenditure. However, the problem of how to steer the spacecraft along this path must now be considered. One solution is to iteratively solve for $\underline{u}_r$ and A_m explicitly as a function of the current spacecraft attitude and to control the spacecraft angular velocity, $\underline{\omega}$, by firing the RCS jets so that $\underline{\omega}$ is parallel to $\underline{u}_r$. This approach, however, leads to several problems. First of all, because of the deadband requirements of the autopilot, and control inaccuracies, explicit guidance can lead to excessive changes in control commands as the spacecraft approaches the terminal attitude. This problem of terminal guidance is characteristic of explicit guidance schemes unless special consideration is given to the terminal-control problem. Secondly, there is a timing problem since the computation of $\underline{u}_r$ and A_m is somewhat lengthy and would require an excessive amount of computer time. Instead, it is better to formulate the problem in terms of perturbations from a smooth reference trajectory that satisfies the end-point constraints. The procedure is to solve the global problem once via KALCMANU in order to establish a reference trajectory (defined by $\underline{u}_r$, A_m) and then have the autopilot solve

the micro-problem of controlling the spacecraft deviations from this reference trajectory, using small-angle approximations. This approach not only avoids the terminal-guidance problem and the timing problem but also provides "tighter" path control for satisfying other boundary conditions that may be placed upon the selection of the reference trajectory.

In order to determine the required steering interface between KALCMANU and the autopilot, it is first necessary to define the nature of the autopilot control variables. To simplify the discussion, the two-dimensional problem of rotation in a plane is considered first. There are two state variables of interest; namely, the attitude error, θ_e, defined by

$$\theta_e = \theta - \theta_d$$

where

θ = actual vehicle attitude

θ_d = desired vehicle attitude (constant)

and the angular velocity of the vehicle, ω. The "state" equations are

$$\dot{\theta}_e(t) = \omega(t)$$

and

$$\dot{\omega}(t) = f(\theta_e, \omega)$$

where

$f(\theta_e, \omega)$ is the control acceleration (applied by the jets) as determined by nonlinear phase-plane switching logic. The control law is defined so that θ_e and ω will be nulled to within the control-law deadbands so as to maintain attitude hold about the reference attitude, θ_d.

New state variables can be defined as follows:

$$\phi_e(t) = \theta(t) - \phi_d(t) + \beta$$

and

$$\omega_e(t) = \omega(t) - \omega_d$$

where

$$\phi_d(t) = \phi_d(t_o) + \omega_d \left[t - t_o\right]$$

ω_d = a constant

β = a constant

$\phi_d(t_o) \triangleq \theta(t_o)$ = constant

The state equations for the new variables are

$$\dot{\phi}_e = \omega_e$$

$$\dot{\omega}_e = f(\phi_e, \omega_e)$$

With these control variables, the autopilot will attempt to null the rate error, ω_e, thus forcing the spacecraft to rotate at a constant rate. With this simple transformation of variables, using the same control law as used for attitude hold, the autopilot can be converted to a constant-rate-command system. Note that at the beginning of the maneuver the desired angle $\phi_d(t_o)$ is set equal to the initial angle $\theta(t_o)$. The constant, β, is added to the attitude error to prevent overshoot when starting and stopping the maneuver. β is computed as

$$\beta = \frac{|\omega_d|\omega_d}{2\alpha}$$

where

α = magnitude of the control acceleration

To interpret the effect of β, refer to Fig. 3.7-8a. This figure shows a simplified phase-plane logic and a typical phase-point trajectory. The maneuver starts at point A with $\theta_e = 0$ and $\omega = 0$. With the application of steering commands, the phase point instantaneously jumps to a biased condition at B where $\phi_e = \beta$ and $\omega_e = -\omega_d$ (ω_d is negative for the case illustrated). The phase point drifts to point C, where the control jets are turned on to reduce the rate error toward zero at point D. The trajectory then traverses a limit cycle DEFG until the maneuver finishes at point H, where the biases β and ω_d are removed. At this point, the trajectory jumps to an unbiased condition at point I. Note that the actual rate is approximately equal to the desired rate and the phase point drifts to point J, where the jets decelerate the vehicle back into a limit cycle around the desired attitude. The situation without the angular bias, β, is illustrated in Fig. 3.7-8b. Note the fuel-consuming overshoot in this case. The inclusion of the bias term is based on the assumption that the initial rates are small and that the desired rates are achievable during the maneuver. For the three-dimensional problem, it must also be assumed that β is small enough so that the small-angle assumptions are not violated. For these reasons, CSM-docked automatic maneuvers should not exceed rates of more than 2 deg/sec.

The logic flow for KALCMANU steering is shown in Fig. 3.7-9. The basic inputs are

a) $\underline{u}_r$, the unit rotation vector.

b) A_m, the rotation angle.

c) $|\omega_d|$, the magnitude of the desired angular velocity as specified in R03.

d) The auto-stabilization discrete in channel 31.

The steering logic works on a cyclic basis. Every ΔT_c (= 1 sec), the program issues new steering commands to the autopilot. On the first pass, a number of

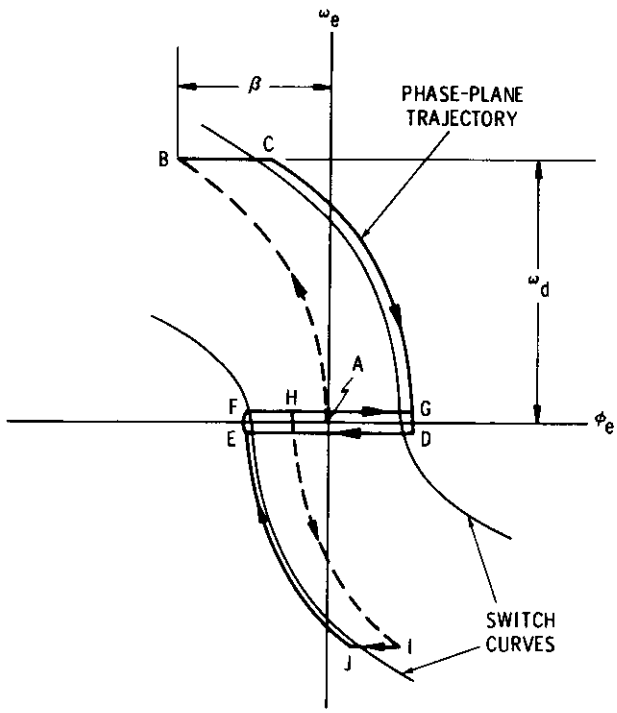

a) Typical phase-plane trajectory with β

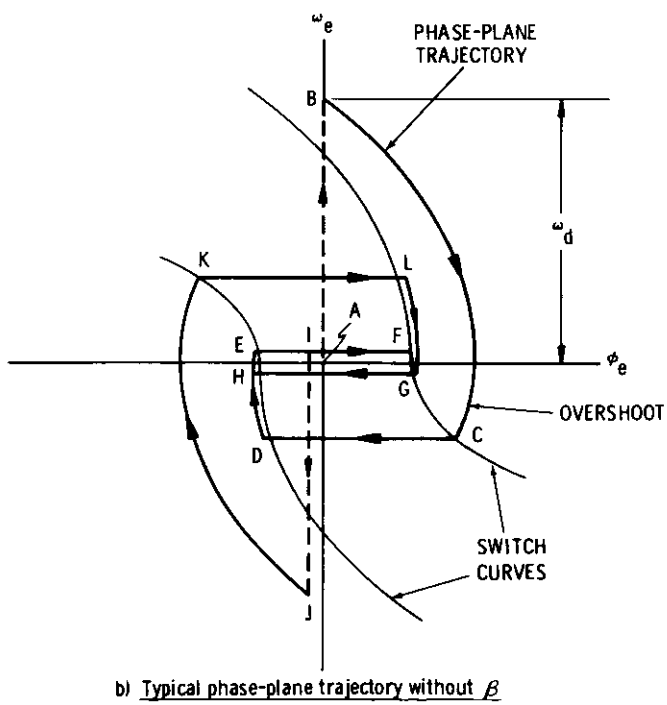

b) Typical phase-plane trajectory without β

Fig. 3.7–8. Maneuver phase–plane trajectories.

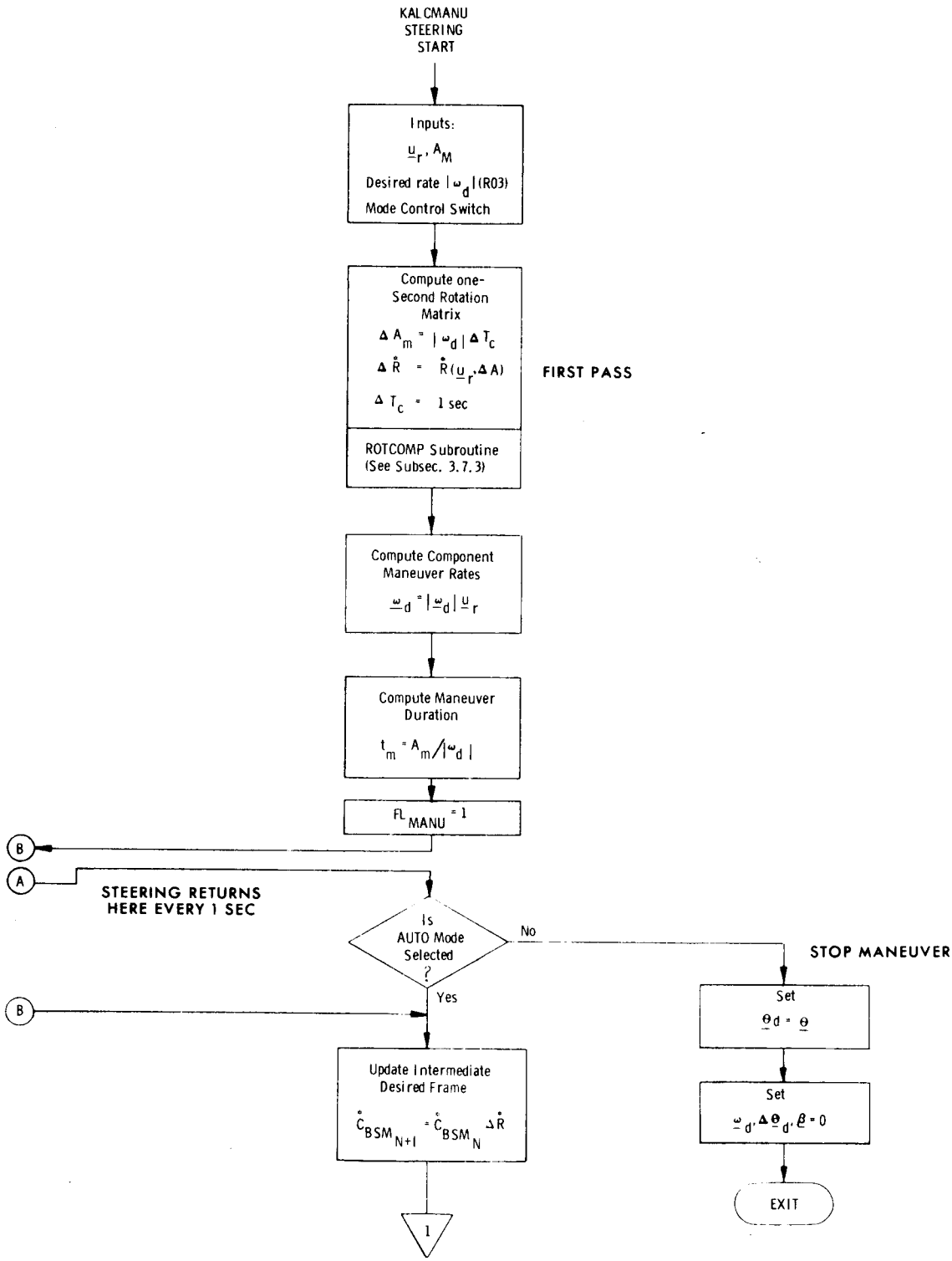

Fig. 3.7–9. KALCMANU steering logic (Sheet 1 of 4).

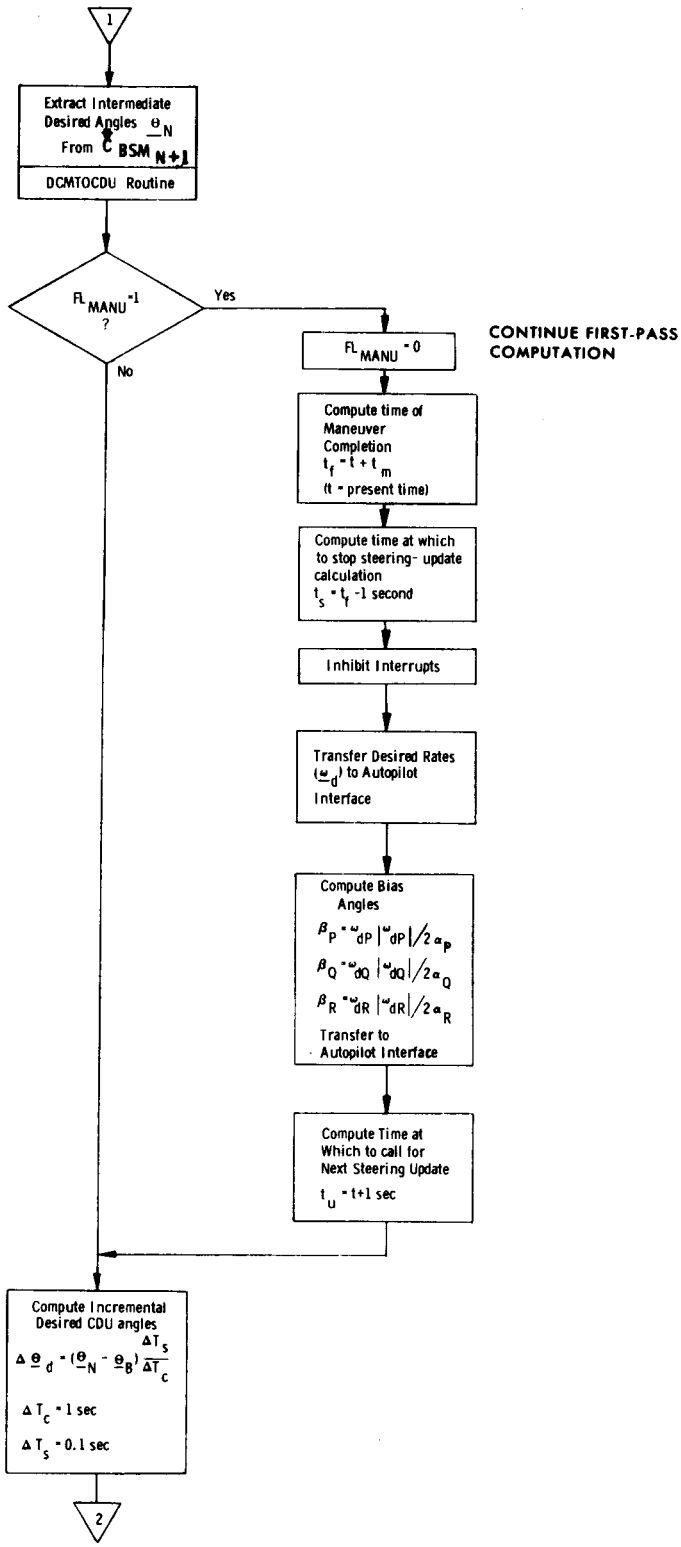

Fig. 3.7–9. KALCMANU steering logic (Sheet 2 of 4).

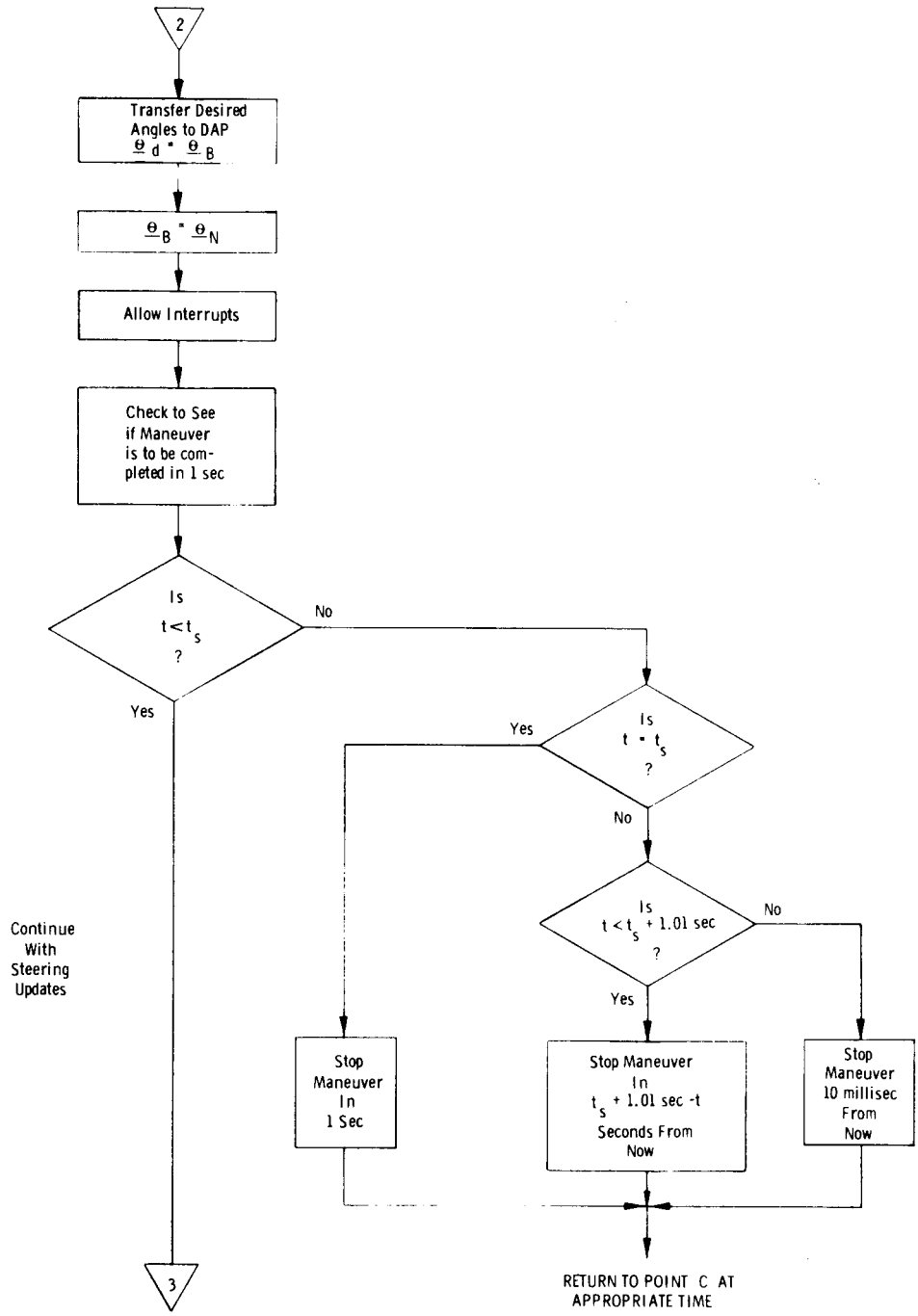

Fig. 3.7–9. KALCMANU steering logic (Sheet 3 of 4).

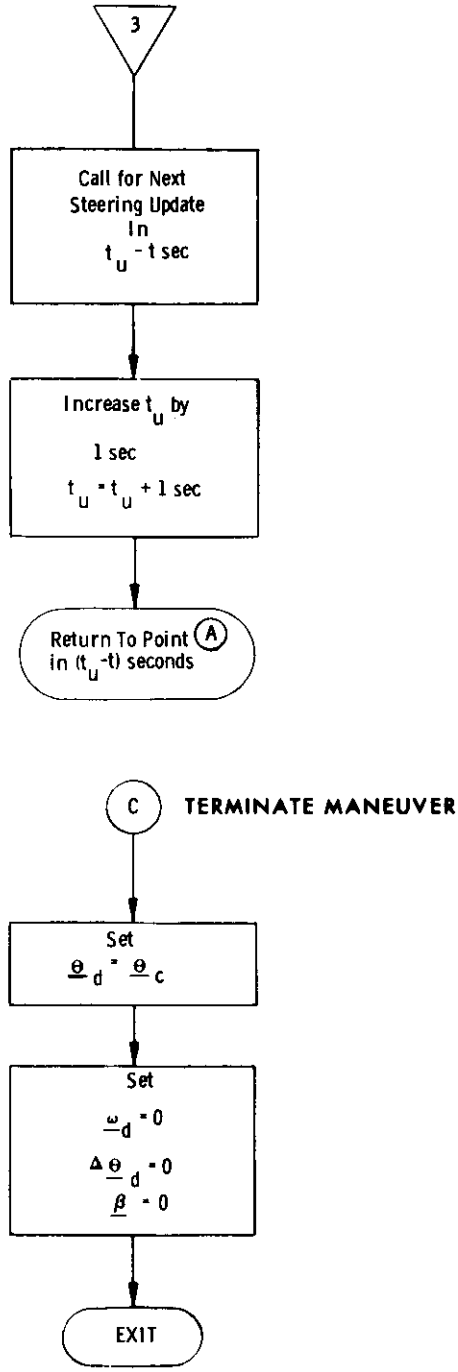

Fig. 3.7–9. KALCMANU steering logic (Sheet 4 of 4).

parameters are computed once and used during subsequent passes. One of these is the incremental rotation matrix, $\Delta\overset{*}{R}$. This matrix corresponds to a one-second rotation of $\overset{*}{C}_{BSM}$, the intial spacecraft orientation, about the rotation axis, $\underline{u}_r$. The magnitude of the rotation ΔA_m is determined as

$$\Delta A_m = |\omega_d| \Delta T_c$$

For the first and all subsequent passes through the steering logic, $\overset{*}{C}_{BSM}$ is rotated by the angle ΔA_m, and the autopilot reference angles $\underline{\theta}_d$ are extracted from this matrix. The new desired reference matrix is simply

$$\overset{*}{C}_{BSM_{N+1}} = \overset{*}{C}_{BSM_N} \Delta\overset{*}{R}$$

This iterative process generates the required reference trajectory $\underline{\theta}_d(t)$, which begins at the initial spacecraft attitude, $\underline{\theta}_B$, and terminates at $\underline{\theta}_c$. The desired rate is simply

$$\underline{\omega}_d = |\omega_d| \ \underline{u}_r$$

and remains constant throughout the maneuver. The bias (or lag) angles are computed as

$$\beta_P = \omega_{dP} |\omega_{dP}| / 2\alpha_P$$

$$\beta_Q = \omega_{dQ} |\omega_{dQ}| / 2\alpha_Q$$

$$\beta_R = \omega_{dR} |\omega_{dR}| / 2\alpha_R$$

where α_P, α_Q, α_R are the two-jet RCS control accelerations as computed by the autopilot. These also remain constant during the maneuver and are added to the attitude errors by the autopilot.

As mentioned in Subsection 3.7.1, the maneuver is timed in open-loop fashion and, for this reason, the first pass also computes the maneuver duration, t_m, as

$$t_m = \frac{A_m}{|\omega_d|}$$

The logic then sets a flag (FL_{MANU}) to identify this as the first pass and, utilizing a section of coding common to both the first and subsequent passes, updates the desired reference angles $\underline{\theta}_N$ (= $\underline{\theta}_d$ projected 1 sec in advance) as described above.

With coding still unique to the first pass, the steering logic computes the time at which the maneuver will be completed as

$$t_f = t + t_m$$

where

t = present time

and the time at which to stop the steering-update process as

$$t_s = t_f - 1 \text{ sec}$$

The logic also computes the time t_u, at which the next update is to occur. Note that all the initial commands are issued simultaneously to the autopilot with interrupt inhibited so that the maneuver will be started properly.

Returning to the common section of the coding, the logic then computes a set of incremental angles, $\Delta\underline{\theta}_d$, for interpolation of the $\underline{\theta}_d$ reference angles between successive updates. This interpolation is required because the autopilot operates at a much higher sample rate, ΔT_s (= 0.1 sec), than the steering (ΔT_c = 1 sec). $\Delta\underline{\theta}_d$ is computed as

$$\Delta\underline{\theta}_d = (\underline{\theta}_N - \underline{\theta}_B) \frac{\Delta T_s}{\Delta T_c}$$

where

$\underline{\theta}_N$ = desired reference angle projected 1 sec in advance

$\underline{\theta}_B$ = present desired reference angles

These incremental angles are subsequently added to $\underline{\theta}_d$ by the autopilot. $\underline{\theta}_d$ is then then set equal to $\underline{\theta}_B$, and $\underline{\theta}_B$ is replaced by $\underline{\theta}_N$ for use on the subsequent pass.

The logic then checks to see if the maneuver is to be completed within 1 sec. If not, the next steering cycle is called for in 1 sec, compensating for any delays between updates. If the maneuver is to be terminated, further updates are suspended and the program stops the maneuver at the appropriate time*. To stop the maneuver, the program simply sets

$$\underline{\omega}_d = 0$$

$$\Delta\underline{\theta}_d = 0$$

$$\underline{\beta} = 0$$

and sets $\underline{\theta}_d = \underline{\theta}_c$ to eliminate any steering error. The crew can also intervene and stop the maneuver at any time by simply switching out of AUTO stabilization.

*Actually delayed by approximately 10 millisec.

REFERENCES FOR SUBSECTION 3.7

1. Dixon, M., "Fuel-Time Optimal Spacecraft Reorientation," Ph. D. Thesis T-502, Instrumentation Laboratory, M. I. T., May 1968.

2. Crisp, R. and Keene, D., "Attitude Maneuver Optimization to Conserve Reaction Control Propellants," Report E-1832, Instrumentation Laboratory, M. I. T., August, 1965.

3. Crisp, R. and Keene, D., "Apollo Command and Service Module Reaction Control by the Digital Autopilot," Report E-1964, Instrumentation Laboratory, M. I. T., May 1966.

4. Keene, D., "Block II LGC Attitude Maneuver Routine: KALCMANU For Flight 206," Group 23 Internal Memo #8, Instrumentation Laboratory, M. I. T., November 1966.

5. Gorman, S. and Kimball, G., Apollo Software Information Memo 5-68-9, "VECPOINT Automatic Maneuvers for Program SUNDISK," U. S. Government Memorandum, May 1968.

Internal Distribution List

R-567

Luminary 1C

Section 3 (Rev 3)

Group 23A	S. MacDougall	IL7-205	15
	Gustafson	Philliou	
	Kachmar	Pickford	
	Klumpp	Pippenger	
	Kriegsman	Pu	
	Levine (4)	Reber	
	Muller	Robertson	
Group 23B	J. Flaherty	IL7-238A	9
	Barnert	Kirven	
	Berman	McCoy	
	Eyles	Millard	
	Finkelstein	Moore	
	Gilson		
Group 23B	J. Kaloostian	IL7-221L	5
	Bernikowich	Volante	
	Dunbar	White	
	Ostanek		
Group 23B	D. Lutkevich	IL7-228	40
	Allen	Hubbard	
	Babicki	Klawsnik	
	Beck	Maher	
	Danforth	Nayer	
	Daniel	Pope	
	DeCain	Reed (20)	
	Entes	Seiler	
	Fisher	Sprague	
	Flaherty	Williams	
	Glendenning	Wolff	
	Good		
Group 23P	A. Tucholke	IL7-203	1
	Battin		
Group 23B	C. Taylor	IL7-221L	5
	Densmore	Rye	
	Hamilton	Stoppleman	
	Rosenberg		
Group 33	J. Hargrove	IL7-111	4
	Drane	Johnson (23P)	
	Glick	Mimno	
Group 23H	B. Lynn	IL7-234A	3
	Cook	OConnor	
	Kossuth		

Group 23C	T. Carlton	IL11-102	12
	Bairnsfather	Penchuk	
	Fraser	Pope	
	Goss	Schlundt	
	Jones	Stengel	
	Kalan	Widnal	
	Keene	Work	
Group 23D	S. Prangley	IL7-209	1
	Nevins		
Group 23P	J. Sutherland	IL7-266	2
	Greene	Stubbs	
Group 23D	F. McGann	IL7-332	14
	Davis	Olsson	
	Dimock	Schroeder	
	Drake	Schulte	
	Dunbar	Sewall	
	Johnson	Siarniche	
	Kiburz	Walsh	
	Metzinger	Woolsey	
Group 23P	C. Mitaris	IL7-213	3
	Cherry	Larson	
	Copps		
Group 23S	P. Amsler	IL7-240	10
	Adams	McOuat	
	Aiyawar	Petrillo	
	Day	Strunce	
	Felleman	Werner	
	Johnston	White	
Group 23T	J. Grinnel	IL7-140	11
	Edmonds	Lones	
	Goodwin	McKern	
	Grace	Megna	
	Kido	Sarda	
	Laats	Sheridan	
	Lawrence		
Group 23N	G. Grover	IL7-202	5
	Blanchard	Parr	
	Johnson	Tanner	
	Ogletree		
Group 23P	A. Rubin	IL7-252	2
	Hoag	Larson	
Group 23P	E. Johnson	IL7-248	2
	Ragan	Stameris	
APOLLO Library			2
MIT/IL Library			6

External Distribution List

MIT Instrumentation Laboratory (5)
P.O. Box 21025
Kennedy Space Center, Florida 32815
Attn: Mr. Robert O'Donnell

MIT Instrumentation Laboratory (3)
Code EG/MIT Building 16
NASA Manned Spacecraft Center
Houston, Texas 77058
Attn: Mr. Thomas Lawton

NASA MSC HW (10)
Building M7-409
Kennedy Space Center, Florida 32815
Attn: Mr. Frank Hughes

Mr. A. Metzger (NASA/RASPO at MIT/IL) (1)

AC Electronics Division (15)
General Motors Corporation
Milwaukee, Wisconsin
Attn: Mr. J. Stridde, Dept. 32-31 (13)
Attn: Mr. Reino Karell (2)

Kollsman Instrument Corporation (1)
575 Underhill Boulevard
Syosset, Long Island
Attn: Mr. F. McCoy

Raytheon Company (6)
Boston Post Road
Sudbury, Massachusetts 01776
Attn: Mr. R. Zazrodnick

NASA/MSFC: National Aeronautics and Space Administration (10)
George C. Marshall Space Flight Center
Huntsville, Alabama
Attn: J. Mack R-ASTR-5 (1)
Attn: V. Buckelew S&E-AERO-MFG (1)
A. Deaton R-AERO-DG (1)
F. Moore R-ASTR-N (1)
H. Hosenthien R-ASTR-F (1)
A. McNair I-MO-R (1)
D. Germany I-I/IB-E (1)
R. Barraza I-V-E (1)
W. Chubb R-ASTR/NG (1)
J. McCullough I-VE/T (1)

NASA/MSC National Aeronautics and Space Administration 300 + 2R
Manned Spacecraft Center
APOLLO Document Control Group (PA 2)
Houston, Texas 77058
Attn: A. Alber, FS5 (letter of transmittal only)

BELLCOMM:	Bellcomm, Inc. 1100 17th Street N.W. Washington, D.C. 20036 Attn: Info. Analysis Section	(6)
LINK:	LINK Group, GPSI SIMCOM 1740 A NASA Boulevard Houston, Texas 77058 Attn: Mr. D. Klingbell	(3)
TRW	H.V. Kienberger Bldg 82 Room 2045 TRW Systems Group One Space Park Redondo Beach, Calif 90278	(1)
NASA/GSFC:	National Aeronautics and Space Administration Goddard Space Flight Center Greenbelt, Maryland Attn: Mr. Paul Pashby, Code 813	(2)
GA:	Grumman Aerospace LEM Crew Systems Bethpage, Long Island, New York 11714 Attn: Mr. J. Marino (1R) Mr. C. Tillman (13) Mr. F. Wood (1) Mr. H. Sherman (Attn: W. Webster) (3) Mr. R. Pratt (4) Mr. B. Sidor (1) Mr. R. Kress (1)	(23 + 1R)
NAR:	North American Rockwell, Inc. Space and Information Systems Division 12214 Lakewood Boulevard Downey, California 90241 Attn: APOLLO Data Requirements Dept. 096-340 Building 3, CA 99	(1 + 1R)
NASA/RASPO GA:	National Aeronautics and Space Administration Resident APOLLO Spacecraft Program Officer Grumman Aerospace LEM Crew Systems Bethpage, Long Island, New York 11714	(1)
NASA/WSMR:	National Aeronautics and Space Administration Post Office Drawer MM Las Cruces, New Mexico Attn: RH4 Documentation	(2)
NASA/RASPO NAR	National Aeronautics and Space Administration Resident APOLLO Spacecraft Program Office North American Rockwell, Inc. Space and Information Systems Division 12214 Lakewood Boulevard Downey, California	(1)

NASA-KSC:	National Aeronautics and Space Administration John F. Kennedy Space Center J.F. Kennedy Space Center, Florida 32899 Attn: Technical Document Control Office	(3)
NASA/RASPO GE:	NASA Daytona Beach Operation P.O. Box 2500 Daytona Beach, Florida 32015 Attn: Mr. A.S. Lyman	(1)
NASA/HDQ:	NASA Headquarters 600 Independence Avenue S.W. Washington, D.C. 20546 Attn: MAP-2 (4) Attn: Mission Director, Code MA (1) Attn: Robert Aller, Code MAO (1)	(6)
NASA/LEWIS:	National Aeronautics and Space Administration Lewis Research Center Cleveland, Ohio Attn: Library	(2)
NASA/FRC:	National Aeronautics and Space Administration Flight Research Center Edwards AFB, California Attn: Research Library	(1)
NASA/LRC:	National Aeronautics and Space Administration Langley Research Center Langley AFB, Virginia Attn: Mr. A.T. Mattson	(2)